

132902  
132902

(NASA-CR-132902) ATTITUDE DYNAMIC OF  
SPIN-STABILIZED SATELLITES WITH FLEXIBLE  
APPENDAGES Final Report (Carnegie-Mellon  
Univ.) 266 p HC \$15.50

N74-15517

CSCL 22B

Unclassified

G3/31 15646



CARNEGIE-MELLON UNIVERSITY

Applied Space Sciences Program

FINAL REPORT

NASA Grant NGR-39-087-026

"ATTITUDE DYNAMICS OF SPIN-STABILIZED  
SATELLITES WITH FLEXIBLE  
APPENDAGES"

Marc L. Renard

(Principal Investigator)

Pittsburgh, September 1973

*Marc L. Renard*

Dr. Marc L. Renard  
Associate Professor of  
Applied Space Sciences and  
Electrical Engineering

#### ACKNOWLEDGEMENTS

The author of this report wishes to gratefully acknowledge the support of this work by the NATIONAL AERONAUTICS and SPACE ADMINISTRATION.

Of particular value to him were discussions held with Drs. J.V. Fedor, T. Flatley, R. Montgomery and S.J. Paddack of GSFC, on the subject of satellite IMP-I, and with Dr. D.L. Blanchard on UK-4.

Contributing to this project as Research Engineers were, in chronological order and for various lengths of time: J.E. Rakowski, P. Stakem, W. Keksz, R. Sridharan, J. Russial and N. Winowich. We are also indebted to Miss Cheryll Conaway, formerly of the Applied Space Sciences Program, for her help in typing and editing the present report.

TABLE OF CONTENTS

	<u>Page No.</u>
Cover Page	
Acknowledgements	
Table of Contents	
Chapter 1                   Object of the Study	1-1 to 1-2
Chapter 2                   A Study of Modal Shapes and Eigen-frequencies of Flexible Appendages on a Spin-Stabilized Satellite	2-1 to 2-69
Chapter 3                   Application to Some Problems of Satellite Dynamics	3-1 to 3-23
Chapter 4                   Simulation of the Motion of the Central Rigid Body and its Elastic Appendages	4-1 to 4-46
Chapter 5                   Simulation of the Satellite Attitude Motion and Stability Studies	5-1 to 5-47
Chapter 6                   Other Topics	6-1 to 6-6
Chapter 7                   General Conclusions	7-1

## CHAPTER 1

Object of the Study

In recent years, the study of the attitude dynamics of a space-craft considered as a partly rigid, partly elastic or articulated body has become of increasing importance<sup>[1-1]</sup>. At first, such work did not present such a degree of urgency, as many investigations concentrated on rotational and librational dynamics of essentially rigid spacecraft, as is apparent from the reviews of D.B. De Bra<sup>[1-2]</sup> and R.E. Robertson<sup>[1-3,1-4]</sup>. Any elastic body effects are conspicuously absent of V.V. Beletskii's classic book on the "Motion of an artificial satellite about its center of mass" who writes at the outset that "the discussion is confined to problems which fall within the scope of the dynamics of rigid bodies".

Satellites became increasingly "elastic", as booms were extended tens and hundreds of meters from the central body<sup>[1-5, 1-6, 1-7]</sup> or as large solar panels or manned toroidal space stations are considered<sup>[1-8]</sup>. Three methods are most commonly used in the study of the dynamics of the elastic spacecraft: discretization by modeling the continuous system by finite elements; modal representation; and the Likin's<sup>[1-9]</sup> method of hybrid coordinates.

The present work uses the modal approach. It is a study of the relevant equations and parameters in the dynamical analysis of the attitudes motion of a spin-stabilized spacecraft having flexible appendages. It is principally aimed at developing working tools, such as stability diagrams, tables or simulation analyses by means of computer

programs. These programs are of low time-consumption, and their use is quite easy to learn. As such, it is hoped that they will prove valuable to the engineer engaged in the design of spin-stabilized elastic spacecraft.

## CHAPTER 2

A Study of Modal Shapes and Eigenfrequencies of  
Flexible Appendages on a Spin-Stabilized Satellite

## 2.1 Introduction

In order to study the dynamics of the spin-stabilized satellite with flexible appendages, by the methods of generalized dynamics, the continuum of the elastic parts should be represented by generalized coordinates  $q_i$  ( $i = 1, 2, \dots$ ). The  $q_i$  are functions of time describing the amplitude of the non-dimensional displacements,  $\frac{w_k}{\ell}$ , of boom k at abscissa  $\xi \equiv \frac{x}{\ell}$ , in terms of modes  $\phi_i(\xi)$

$$w_k(\xi) \frac{1}{\ell} = \sum_i q_i(t) \phi_i(\xi) \quad (2.1-1)$$

$w_k$  will be (in the assumption of small displacements) along y for equatorial displacements (E) and along z for meridional displacements (M) (See Fig. 2.1).

$\xi$ ,  $\eta$ ,  $\zeta$  are the geometric coordinates x, y, z non-dimensionalized by  $\ell$ , undeflected length of the boom.  $\xi_0 = \frac{x_0}{\ell}$  is the non-dimensional radius of the central hub.

The system of mode shapes,  $\phi_i$ , adopted here are the modes of the rotating structure corresponding to the boom's Etkin number [2-1]

$$\bar{\lambda} = \frac{\rho \ell^4}{EI} \omega_s^2 \quad \text{and non-dimensional radius } \xi_0 = \frac{x_0}{\ell} : \rho \text{ is the (uniform)}$$

lineal density of the boom, in units of mass/length.  $E$  is the boom's Young modulus, in units of force/unit area,  $I$  is the geometric moment of inertia of the boom's cross section, in units of length<sup>4</sup>, and  $\omega_s$  is the spin rate, in rad./sec. Thus  $\bar{\lambda}$  is non-dimensional. Finally,  $\infty$  is the radius of the central hub, at which distance the elastic boom is assumed to be cantilevered. As will be seen, these significantly depart in shape and frequency from those of the non-rotating structure corresponding to  $\bar{\lambda} = 0$  and  $\xi_0 = 0$ .

In the following, it is assumed that only antisymmetric motions are considered, or that the motion of the CM away from the origin is negligible. The latter amounts, as has been shown by F. Vigneron<sup>[2-2]</sup>, to assuming that the central mass  $M_c$  is sufficiently large for terms of order

$$\rho \ell \left( \frac{\rho \ell}{M_c} \right)^2 \left[ \int_{\text{boom}} w^2 dx \right]^2$$

to be neglected in comparison with terms like

$$\rho \int_{\text{boom}} w^2 dx$$

Typically, for the ALOUETTE and ISIS satellites, Ref. [2-2] gives the values:  $\frac{\rho \ell}{M_c} = 0.005$  to  $0.01$  (copper-beryllium booms)

## 2.2 Equations of Motion: equatorial vibrations

### 2.2.1 Basic equation

We shall first consider motions in the "equatorial" plane of the satellite, i.e.  $(x,y)$  or  $(\xi,\eta)$ . These were the first type of vibrations considered by this author and J.E. Rakowski<sup>[2-3]</sup>.

Any section of boom located at  $\rho$ , of abscissa  $x$ , is in rotational equilibrium under the action of (Fig. 2.1).

- bending moment from the left, which for pure flexure in the equatorial plane, is

$$dM_{el} = -EI \frac{\partial^2 w(x)}{\partial x^2} \vec{l}_z \quad (2.2-1)$$

in which  $w(x)$  is the assumed small displacement of the boom element in the  $y$ -direction, and  $\vec{l}_z$  is the unit vector along the  $z$ -direction.

- the moment about  $\rho$  of inertia forces

$$d\vec{F}_{in} = -\rho dx_1 \ddot{\vec{r}}_Q \quad (2.2-2)$$

imparted by the particles of the boom to the right of  $\rho$ , i.e. having abscissa between  $x$  and  $\ell$ .

Therefore,

$$EI \frac{\partial^2 w(x)}{\partial x^2} = - \int_x^\ell \rho dx_1 \left\{ [\vec{\pi}_Q - \vec{\pi}_r] \wedge \ddot{\vec{\pi}}_Q \right\}_z$$

In terms of their components, we have

$$\begin{aligned} \vec{\pi}_{\rho Q} &= \vec{\pi}_Q - \vec{\pi}_r = (x_1 - x) \vec{i}_x + (w(x_1) - w(x)) \vec{i}_y = \begin{bmatrix} x_1 - x \\ w(x_1) - w(x) \\ 0 \end{bmatrix} \\ \vec{\pi}_Q &= (x_0 + x_1) \vec{i}_x + w(x_1) \vec{i}_y = \begin{bmatrix} x_0 + x_1 \\ w(x_1) \\ 0 \end{bmatrix} \end{aligned}$$

Thus

$$\begin{aligned} \dot{\vec{\pi}}_Q &= \dot{w}(x_1) + \vec{\omega} \wedge \vec{\pi}_Q \\ &= \begin{bmatrix} -w(x_1) \omega_z \\ \dot{w}(x_1) + \omega_z (x_0 + x_1) \\ \omega_x w(x_1) - \omega_y (x_0 + x_1) \end{bmatrix} \end{aligned}$$

Also

$$\begin{aligned}
 \ddot{\vec{n}}_Q &= \frac{\partial}{\partial t} (\dot{\vec{n}}_Q) + \vec{\omega} \wedge \dot{\vec{n}}_Q = \begin{bmatrix} -\dot{\omega}_z w(x_1) - \omega_z \dot{w}(x_1) \\ \dot{\omega}_z (x_0 + x_1) + \ddot{w}(x_1) \\ \dot{\omega}_x w(x_1) + \omega_x \dot{w}(x_1) - \dot{\omega}_y (x_0 + x_1) \end{bmatrix} \\
 &+ \begin{vmatrix} \omega_x & \omega_y & \omega_z \\ -w(x_1) \omega_z & \dot{w}(x_1) + \omega_z (x_0 + x_1) & \omega_x w(x_1) - \omega_y (x_0 + x_1) \end{vmatrix} \\
 &= \begin{bmatrix} (\omega_x \omega_y - \dot{\omega}_z) w(x_1) - (\omega_y^2 + \omega_z^2)(x_0 + x_1) - 2\omega_z \dot{w}(x_1) \\ (\ddot{w}(x_1) - \omega_z^2 w(x_1)) - \omega_x^2 w(x_1) + (\dot{\omega}_z + \omega_x \omega_y)(x_0 + x_1) \\ (\omega_x \omega_z - \dot{\omega}_y)(x_0 + x_1) + (\dot{\omega}_x + \omega_y \omega_z) w(x_1) + 2\omega_x \dot{w}(x_1) \end{bmatrix}
 \end{aligned}$$

Under the assumption of small displacements and transverse angular rates, terms of order  $w^2$ ,  $\omega_x \omega_y$ ,  $\omega_x^2$ ,  $\omega_y^2$ ... are neglected, and  $\ddot{\vec{r}}_Q$  reduces to

$$\ddot{\vec{r}}_Q = \begin{bmatrix} -\dot{\omega}_z w(x_1) - \omega_z^2 (x_0 + x_1) - 2\omega_z \dot{w}(x_1) \\ (\ddot{w}(x_1) - \omega_z^2 w(x_1)) + \dot{\omega}_z (x_0 + x_1) \\ (\omega_x \omega_z - \dot{\omega}_y) (x_0 + x_1) \end{bmatrix} \quad (2.2-3)$$

Finally, along  $\vec{l}_z$

$$[(\vec{r}_Q - \vec{r}_P) \wedge \ddot{\vec{r}}_Q]_z = \begin{bmatrix} x_1 - x & w(x_1) - w(x) \\ -\dot{\omega}_z w(x_1) - \omega_z^2 (x_0 + x_1) & \ddot{w}(x_1) - \omega_z^2 w(x_1) + \dot{\omega}_z (x_0 + x_1) \\ -2\omega_z \dot{w}(x_1) & \end{bmatrix}$$

and neglecting quantities of smaller order

$$[(\vec{r}_Q - \vec{r}_P) \wedge \ddot{\vec{r}}_Q]_z = (x_1 - x) [\ddot{w}(x_1) - \omega_z^2 w(x_1) + \dot{\omega}_z (x_0 + x_1)] + (w(x_1) - w(x)) \omega_z^2 (x_0 + x_1)$$

With the same notation as above, let  $\xi_1 = \frac{x_1}{l}$ ,  $\eta_1 = \frac{w(x_1)}{l}$ ,  $\alpha = \frac{\rho l^4}{EI}$ ; this becomes

$$\frac{EI}{l} \frac{\partial^2 \eta}{\partial \xi^2} = -l^3 \int_{\xi_0}^{\xi_1} \{ (\xi_1 - \xi) [(\ddot{\eta}_1 - \omega_z^2 \eta_1) + \dot{\omega}_z (\xi_0 + \xi_1) + \omega_z^2 (\eta_1 - \eta)] \\ + (\xi_0 + \xi_1) \] d\xi$$

With the abbreviated notation  $\underbrace{\eta_{\xi \dots \xi}}_k = \frac{\partial^k \eta}{\partial \xi^k}$ , we obtain

$$\eta_{\xi \xi} = -\alpha \int_{\xi}^1 \left[ (\eta_1 - \eta) \omega_z^2 (\xi_0 + \xi_1) + (\xi_1 - \xi) (\dot{\omega}_z (\xi_0 + \xi_1) + \ddot{\eta}_1 - \omega_z^2 \eta_1) \right] d\xi_1 \quad (2.2-4)$$

Taking the derivative of (2.2-4) with respect to  $\xi$ , and using Leibniz's formula,  $f(\xi_1, \xi)$  being the integrand,

$$\begin{aligned} \eta_{\xi \xi \xi} &= \alpha \int_{\xi}^1 (\xi_1 = \xi, \xi) - \alpha \int_{\xi}^1 \left[ -\eta_{\xi} \omega_z^2 (\xi_0 + \xi_1) - (\ddot{\eta}_1 - \omega_z^2 \eta_1) - \dot{\omega}_z (\xi_0 + \xi_1) \right] d\xi_1 \\ &\quad - \alpha \int_{\xi}^1 \left[ -\eta_{\xi} \omega_z^2 (\xi_0 + \xi_1) - (\ddot{\eta}_1 - \omega_z^2 \eta_1) - \dot{\omega}_z (\xi_0 + \xi_1) \right] d\xi_1 \end{aligned}$$

Finally

$$\begin{aligned} \eta_{\xi \xi \xi \xi} &= -\alpha \eta_{\xi} \omega_z^2 (\xi_0 + \xi) - \alpha \dot{\omega}_z (\xi_0 + \xi) - \alpha (\ddot{\eta} - \omega_z^2 \eta) + \alpha \\ &\quad \int_{\xi}^1 \eta_{\xi \xi} \omega_z^2 (\xi_0 + \xi_1) d\xi_1, \quad (2.2-5) \\ &= -\alpha \eta_{\xi} \omega_z^2 (\xi_0 + \xi) - \alpha \dot{\omega}_z (\xi_0 + \xi) - \alpha (\ddot{\eta} - \omega_z^2 \eta) + \alpha \omega_z^2 \eta_{\xi \xi} \left[ \frac{1}{2} (1 - \xi^2) + \xi_0 (1 - \xi) \right] \end{aligned}$$

The non-dimensionalization is completed by introducing the non-dimensional Etkin's number<sup>[2-1]</sup>

$$\bar{\lambda} = \alpha \omega_z^2 = \frac{\ell \ell^4}{EI} \omega_z^2 \div \left( \frac{\omega_z}{\omega_{CRNT, NR}} \right)^2$$

where  $\omega_{cant}$  is the first cantilever frequency of the non-rotating boom.

It is to be stressed that  $\bar{\lambda}$  is a constant only if  $\omega_z$ , the satellite spin-rate, may be considered such. Equation (2.2-5) is rewritten in the form

$$\begin{aligned} \eta_{\xi \xi \xi \xi} - \bar{\lambda} \eta_{\xi \xi} \left[ \frac{1}{2} (1 - \xi^2) + \xi_0 (1 - \xi) \right] + \bar{\lambda} \eta_{\xi} (\xi + \xi_0) \\ + \alpha \ddot{\eta} - \bar{\lambda} \eta = -\alpha \dot{\omega}_z (\xi + \xi_0) \quad (2.2-6) \end{aligned}$$

So far, quantities which have been neglected were of order  $\epsilon^2$  of smallness, or smaller. Now  $\alpha \dot{\omega}_z$  itself is of order  $\epsilon^2$ , i.e. with

$$d\phi = \omega_z dt \quad \frac{\bar{\lambda}}{\omega_z^2} \dot{\omega}_z \approx \bar{\lambda} \frac{d\omega_z / \omega_z}{d\phi}$$

if the product  $\bar{\lambda} \times$  the percentage change of  $\omega_z$  per unit angle of rotation is very much smaller than quantities assumed to be of order  $\epsilon$ .

Assuming that such is the case, we are then left with the homogeneous Equation (2.2-6) with a r.h. side equal to zero.

$$\begin{aligned} \eta_{\xi\xi\xi\xi} - \bar{\lambda} \eta_{\xi\xi} & \left[ \frac{1}{2} (1-\xi^2) + \xi_0 (1-\xi) \right] + \bar{\lambda} \eta_{\xi} (\xi + \xi_0) \\ - \bar{\lambda} \eta_j + \alpha \eta_j & = 0 \end{aligned} \quad (2.2-7)$$

### 2.2.2 Solution of the basic equation

Using separation of variables, with  $\tau = \frac{d}{dt} = \frac{d}{d(\omega_z t)} ;$

$$\tau = \omega_z t ,$$

$$\eta_j = \Phi_j(\xi) T_j(\tau) \quad (2.2-8)$$

Hence

$$\Phi_j^{(IV)} - \bar{\lambda} \Phi_j^{(2)} \left[ \frac{1}{2} (1-\xi^2) + \xi_0 (1-\xi) \right] + \bar{\lambda} \Phi_j^{(1)} (\xi + \xi_0) - \bar{\lambda} (1 + \bar{\omega}_j^2) \Phi_j = 0$$

yielding

$$T_j = \frac{\sin(\bar{\omega}_j \tau)}{\cos(\bar{\omega}_j \tau)} = \frac{\sin(\omega_j t)}{\cos(\omega_j t)}$$

where  $\omega_j$  is the jth eigenfrequency of the equatorial vibrations associated with  $(\xi_0, \bar{\lambda})$ . This equation is in agreement with that obtained by Etkins and Hughes [2-1], in the special case  $\xi_0 = 0$ .

Determination of  $\omega_j$  (or  $\bar{\omega}_j$ ) from Equation (2) proceeds as follows. Equation (2) is linear, with  $\xi$  varying coefficients. Thus any linear combination of solutions of (2) is a solution of (2).

Let  $\delta_{3,j}$  be the solution satisfying the b.c.

$$\begin{matrix} \xi=0 : & 0 & 0 & 1 & 0 \\ & \phi_j & \phi_j^{(1)} & \phi_j^{(2)} & \phi_j^{(3)} \end{matrix} \quad (2.2-9)$$

and  $\delta_{4,j}$  be the solution satisfying

$$\begin{matrix} \xi = 0 : & 0 & 0 & 0 & 1 \\ & \phi_j & \phi_j^{(1)} & \phi_j^{(2)} & \phi_j^{(3)} \end{matrix} \quad (2.2-10)$$

Therefore, the desired solution, which satisfies the "built-in, free" boundary conditions

$$\begin{matrix} \xi = 0 & \phi_j & \phi_j^{(1)} & \phi_j^{(2)} & \phi_j^{(3)} \\ & 0 & 0 & 0 & 0 \end{matrix} \quad (2.2-11)$$

$$\xi = 1 \quad 0 \quad 0 \quad 0 \quad 0 \quad (2.2-12)$$

is of the form

$$C_3 \delta_{3,j} + C_4 \delta_{4,j} \quad (2.2-13)$$

with  $C_3, C_4$  unknown. (2.2-11) is automatically satisfied by (2.2-13).

Expressing (2.2-12)

$$C_3 \left[ \delta_{3,j}^{(2)} \right]_{\xi=1} + C_4 \left[ \delta_{4,j}^{(2)} \right]_{\xi=1} = 0 \quad (2.2-14)$$

$$C_3 \left[ \delta_{3,j}^{(3)} \right]_{\xi=1} + C_4 \left[ \delta_{4,j}^{(3)} \right]_{\xi=1} = 0 \quad (2.2-15)$$

In order to be satisfied for non-zero values of  $c_3, c_4, \bar{\omega}_j$  should be such that the determinant

$$D(\bar{\omega}_j) = \left[ \begin{matrix} \delta_{3,j}^{(2)} & \delta_{4,j}^{(3)} \\ \delta_{3,j}^{(3)} & \delta_{4,j}^{(2)} \end{matrix} \right] \frac{1}{\bar{\omega}_j, \xi=1} = 0 \quad (2.2-16)$$

The successive eigenfrequencies,  $\bar{\omega}_j$ , are determined to any prescribed accuracy by iteration.  $\delta_{1,j}, \delta_{2,j}$  are determined by numerical integration of differential equation (2), subject to b.c. (9) and (10.) respectively.

The modal shapes,  $\Phi_j(\xi)$ , which as expected are defined only to an arbitrary multiplicative constant, are determined, once  $\bar{\omega}_j$  is known, as

$$\bar{\Phi}_j(\xi) = C_3 \left[ \delta_{3,j} - \frac{\delta_{3,j}^{(2)}}{\delta_{4,j}^{(2)}} \delta_{4,j} \right] \frac{1}{\bar{\omega}_j} \quad (2.2-17)$$

### 2.23 Orthogonality of the mode shapes

It is now proven, that given  $\bar{\lambda}, \xi_0 \geq 0$ , the modes  $\phi_j, \phi_k$  are orthogonal, i.e.

$$\langle \phi_j, \phi_k \rangle = \int_0^1 \bar{\Phi}_j(\xi) \bar{\Phi}_k(\xi) d\xi = 0 \quad j \neq k$$

Note that  $\langle \bar{\Phi}_j, \bar{\Phi}_j \rangle = \int_0^1 \bar{\Phi}_j^2 d\xi \stackrel{\text{def}}{=} m_{1,j} > 0$

Let  $\mathcal{L}$  be the operator

$$\frac{d^4}{d\xi^4} - \bar{\lambda} \left[ \frac{1}{2} (1-\xi^2) + \xi_0 (1-\xi) \right] \frac{d^2}{d\xi^2} + \bar{\lambda} (\xi + \xi_0) \frac{d}{d\xi} - \bar{\lambda}$$

Now

$$\mathcal{L}(\bar{\Phi}_j) = \bar{\lambda} \bar{\omega}_j^2 \bar{\Phi}_j$$

$$\text{and } \mathcal{L}(\bar{\Phi}_k) = \bar{\lambda} \bar{\omega}_k^2 \bar{\Phi}_k \quad (2.2-18)$$

Then, from multiplying by  $\phi_k$  and  $\phi_j$  respectively, and subtracting

$$\begin{aligned} \Phi_j^{(4)} \bar{\Phi}_k - \bar{\Phi}_k^{(4)} \Phi_j &= \bar{\lambda} \left[ \frac{1}{2} (1-\xi^2) + \xi_0 (1-\xi) \right] \left[ \Phi_j^{(2)} \bar{\Phi}_k - \bar{\Phi}_k^{(2)} \Phi_j \right] \\ &\quad + \bar{\lambda} (\xi + \xi_0) \left( \Phi_j^{(1)} \bar{\Phi}_k - \bar{\Phi}_k^{(1)} \Phi_j \right) = \bar{\lambda} (\bar{\omega}_j^2 - \bar{\omega}_k^2) \bar{\Phi}_j \bar{\Phi}_k \end{aligned} \quad (2.2-19)$$

Integrate with respect to  $\xi$ , from  $\xi = 0$  (root) to  $\xi = 1$  (tip),

$$\begin{aligned} \int_{\text{boom}} \Phi_j^{(4)} \bar{\Phi}_k d\xi &= \left[ \Phi_j^{(3)} \bar{\Phi}_k \right]_{\text{root}}^{\text{tip}} - \int_{\text{boom}} \Phi_j^{(3)} \bar{\Phi}_k^{(1)} d\xi \\ &= - \left[ \Phi_j^{(2)} \bar{\Phi}_k^{(1)} \right]_{\text{root}}^{\text{tip}} + \int_{\text{boom}} \bar{\Phi}_j^{(2)} \bar{\Phi}_k^{(2)} d\xi \\ &= \int_{\text{boom}} \bar{\Phi}_k^{(4)} \bar{\Phi}_j d\xi \end{aligned}$$

Thus

$$\int_{\text{boom}} \left\{ \Phi_j^{(4)} \bar{\Phi}_k - \bar{\Phi}_k^{(4)} \Phi_j \right\} d\xi = 0$$

Next compute

$$\int_{\text{boom}} \frac{1}{2} (1-\xi^2) \Phi_j^{(2)} \bar{\Phi}_k d\xi = \left[ \frac{1}{2} (1-\xi^2) \Phi_j^{(1)} \bar{\Phi}_k \right]_{\text{root}}^{\text{tip}} + \int_{\text{boom}} \bar{\Phi}_k^{(1)} \left[ -\frac{1}{2} \bar{\Phi}_k^{(1)} (1-\xi^2) + \xi \bar{\Phi}_k \right] d\xi \quad (1) \quad (2)$$

$$\int_{\text{boom}} \frac{1}{2} (1-\xi^2) \bar{\Phi}_k^{(2)} \bar{\Phi}_j d\xi = \left[ \frac{1}{2} (1-\xi^2) \bar{\Phi}_k^{(1)} \bar{\Phi}_j \right]_{\text{root}}^{\text{tip}} + \int_{\text{boom}} \bar{\Phi}_k^{(1)} \left[ -\frac{1}{2} \bar{\Phi}_j^{(1)} (1-\xi^2) + \xi \bar{\Phi}_j \right] d\xi \quad (3) \quad (4)$$

Terms corresponding to (1) and (3) will cancel in the difference. Terms (2) and (4) will cancel the terms resulting from the last term in  $\xi$ , in (2.2-19).

in the l.h. side of (2.2-19). Finally

$$\int_{\xi_0}^{\xi_0 + \xi} (\xi - \xi_0) \bar{\Phi}_j^{(2)} \bar{\Phi}_k d\xi = \xi_0 \bar{\Phi}_j^{(1)} (\xi - \xi_0) \bar{\Phi}_k \Big|_{root}^{\text{tip}} - \xi_0 \int_{\xi_0}^{\xi_0 + \xi} \bar{\Phi}_j^{(1)} \left[ -\bar{\Phi}_k + (\xi - \xi_0) \bar{\Phi}_k^{(1)} \right] d\xi \quad (5) \quad (7)$$

$$\int_{\xi_0}^{\xi_0 + \xi} (\xi - \xi_0) \bar{\Phi}_k^{(2)} \bar{\Phi}_j d\xi = \xi_0 \bar{\Phi}_k^{(1)} (\xi - \xi_0) \bar{\Phi}_j \Big|_{root}^{\text{tip}} - \xi_0 \int_{\xi_0}^{\xi_0 + \xi} \bar{\Phi}_k^{(1)} \left[ -\bar{\Phi}_j + (\xi - \xi_0) \bar{\Phi}_j^{(1)} \right] d\xi \quad (6) \quad (8)$$

Again, terms (7) and (8) will cancel in the difference. Terms (5) and (6) will cancel the terms resulting from the last term in  $\xi_0$ , in the l.h. side of (2.2-19). We are left with

$$\bar{\lambda} (\bar{\omega}_j^2 - \bar{\omega}_k^2) \int_{\xi_0}^{\xi_0 + \xi} \bar{\Phi}_j(\xi) \bar{\Phi}_k(\xi) d\xi = 0$$

$$\int_{\xi_0}^{\xi_0 + \xi} \bar{\Phi}_j \bar{\Phi}_k d\xi = 0 \quad (j \neq k) \quad (2.2-20)$$

The modal mass,  $m_j(\bar{\lambda}, \xi_0)$ , is defined, for  $j=k$ , as

$$m_{j,j} \underset{\text{def}}{=} \int_{\xi_0}^{\xi_0 + \xi} \bar{\Phi}_j^2 d\xi \quad (2.2-21)$$

in which  $\bar{\Phi}_j(\xi)$  is normalized to correspond to a unit deflection at the boom's tip,  $\xi = 1$ . The following quantity, to appear later, is also of interest

$$m_{j,1} \underset{\text{def}}{=} \int_{\xi_0}^{\xi_1} \xi_1 \bar{\Phi}_j(\xi) d\xi \quad (2.2-22)$$

with  $\xi_1 = \xi_0 + \xi$ , varying between  $\xi_0$  (root) and  $\xi_0 + 1$  (tip). It is readily determined when the modal shape,  $\bar{\Phi}_j(\xi)$ , is known.

Also, for later use, two identities are given here, which are obtained by multiplying Eq. (2.2-19) written for  $\phi_j$ , by  $\phi_k$ , and integrating over the boom,

$$\begin{aligned}
\frac{1}{\lambda} \int_{\text{boom}} \bar{\Phi}_j^{(4)} \bar{\Phi}_k d\xi &= \frac{1}{\lambda} \int_{\text{boom}} \bar{\Phi}_j^{(2)} \bar{\Phi}_k^{(2)} d\xi = \int_{\text{boom}} \frac{1}{2} [ (1-\xi^2) + 2\xi_0(1-\xi) ] \\
&\quad \bar{\Phi}_j^{(2)} \bar{\Phi}_k d\xi - \int_{\text{boom}} (\xi + \xi_0) \bar{\Phi}_j^{(1)} \bar{\Phi}_k d\xi \\
&\quad + (\bar{\omega}_s^2 + \bar{\omega}_j^2) \int_{\text{boom}} \bar{\Phi}_j \bar{\Phi}_k d\xi \\
&= - \int_{\text{boom}} \bar{\Phi}_j^{(1)} \bar{\Phi}_k^{(1)} \frac{1}{2} [ (1-\xi^2) + 2\xi_0(1-\xi) ] d\xi \\
&\quad + \int_{\text{boom}} \bar{\Phi}_j^{(1)} \bar{\Phi}_k (\xi + \xi_0) d\xi - \int_{\text{boom}} \bar{\Phi}_j^{(1)} \bar{\Phi}_k \\
&\quad (\xi + \xi_0) d\xi + (\bar{\omega}_s^2 + \bar{\omega}_j^2) \int_{\text{boom}} \bar{\Phi}_j \bar{\Phi}_k d\xi.
\end{aligned}$$

Thus, for  $j \neq k$

$$\frac{1}{\lambda} \int_{\text{boom}} \bar{\Phi}_j^{(2)} \bar{\Phi}_k^{(2)} d\xi + \int_{\text{boom}} \bar{\Phi}_j^{(1)} \bar{\Phi}_k^{(1)} \frac{1}{2} [ (1-\xi^2) + 2\xi_0(1-\xi) ] d\xi = 0. \quad (2.2-23)$$

and for  $j = k$

$$\frac{1}{\lambda} \int_{\text{boom}} \bar{\Phi}_j^{(2)} \bar{\Phi}_j^{(2)} d\xi + \int_{\text{boom}} \bar{\Phi}_j^{(1)} \bar{\Phi}_j^{(1)} \frac{1}{2} [ (1-\xi^2) + 2\xi_0(1-\xi) ] d\xi = (\bar{\omega}_s^2 + \bar{\omega}_j^2) m_{jj}. \quad (2.2-24)$$

### 2.3 Equations of motion: meridional vibrations

The developments in the case of motions in the  $(x, z)$  plane, of a boom located along axis  $+x$  in its undeflected position, or "meridional" vibrations, closely parallels those for equatorial vibrations, given in Section 2.2. In the following, only those terms which depart from the ones in Section 2.2 will be given in detail.

#### 2.3.1 Basic equation

The equation expressing the equilibrium, at any section "x" of the boom, at point P, between the flexure moment from the left and the

moment , about P, of inertia forces imparted by the particles Q of the boom to the right of P (i.e. those having an abscissa x, between x and l , reads

$$EI \frac{\partial^2 w(x)}{\partial x^2} = \int_x^l \rho dx_1 [(\vec{r}_Q - \vec{r}_P) \wedge \ddot{\vec{r}}_Q]_y \quad (2.3-1)$$

Now  $w(x)$  is an elastic displacement parallel to z. Computing the relevant quantities,

$$\begin{aligned}\vec{r}_{PQ} &= (x_1 - x) \vec{i}_x + (w(x_1) - w(x)) \vec{i}_z \\ \vec{r}_Q &= (x_0 + x_1) \vec{i}_x + w(x_1) \vec{i}_z\end{aligned}$$

Thus

$$\ddot{\vec{r}}_Q = \begin{bmatrix} \omega_y w(x_1) \\ \omega_z (x_0 + x_1) - \omega_x w(x_1) \\ \dot{w}(x_1) - \omega_y (x_0 + x_1) \end{bmatrix}$$

Also

$$\begin{aligned}\ddot{\vec{r}}_Q &= \frac{\partial}{\partial t} (\dot{\vec{r}}_Q) + \vec{\omega} \wedge \dot{\vec{r}}_Q \\ \ddot{\vec{r}}_Q &= \begin{bmatrix} \ddot{\omega}_y w(x_1) + 2\omega_y \dot{w}(x_1) - (x_0 + x_1)(\omega_y^2 + \omega_z^2) + \omega_x \omega_z w(x_1) \\ -\ddot{\omega}_x w(x_1) - 2\omega_x \dot{w}(x_1) + (x_0 + x_1)(\omega_x \omega_y + \ddot{\omega}_z) + \omega_y \omega_z w(x_1) \\ \ddot{w}(x_1) - w(x_1)(\omega_x^2 + \omega_y^2) + (x_0 + x_1)(\omega_x \omega_z - \ddot{\omega}_y) \end{bmatrix}\end{aligned}$$

Again, under the assumption of small displacements and transverse angular rates, terms of order  $w^2$ ,  $\omega_x \omega_y$ ,  $\omega_x^2, \omega_y^2 \dots$  are neglected.  $\vec{r}_Q$  reduces to

$$\ddot{\vec{r}}_a = \begin{bmatrix} -(x_0 + x_i) \omega_z^2 \\ (x_0 + x_i) \dot{\omega}_z \\ \ddot{w}(x_i) + (x_0 + x_i) (\omega_x \omega_z - \dot{\omega}_y) \end{bmatrix}$$

Along  $\vec{l}_y$ ,

$$[(\vec{r}_a - \vec{r}_p) \wedge \vec{r}_a]_y = \begin{vmatrix} w(x_i) - w(x) & x_i - x \\ \ddot{w}(x_i) + (x_0 + x_i) (\omega_x \omega_z - \dot{\omega}_y) & -(x_0 + x_i) \omega_z^2 \end{vmatrix}$$

Substituting into (2.3-1), and non-dimensionalizing

$$\frac{EI}{l} \frac{\partial^2 \eta}{\partial \xi^2} = -\rho l^3 \int_{\xi}^l \{(\xi_i - \xi) (\ddot{\eta}_i + (\xi_o + \xi_i) (\omega_x \omega_z - \dot{\omega}_y)) + \omega_z^2 (\eta_i - \eta) \\ (\xi_o + \xi_i)\} d\xi$$

or

$$\eta_{\xi\xi} = -\alpha \int_{\xi}^l \{(\eta_i - \eta) \omega_z^2 (\xi_o + \xi_i) + (\xi_i - \xi) (\xi_o + \xi_i) (\omega_x \omega_z - \dot{\omega}_y) \\ + (\xi_i - \xi) \ddot{\eta}_i\} d\xi, \quad (2.3-2)$$

Comparing (2.3-2) to (2.2-4), it is seen that terms (b) and (c) in (2.3-2) differ in the following way from the corresponding ones in (2.2-4)

(b) here has a factor  $(\omega_x \omega_z - \dot{\omega}_y)$  instead of  $\dot{\omega}_z$

(c) here has a factor  $\ddot{\eta}_i$  instead of  $\ddot{\eta}_i - \omega_z^2 \eta_i$

Therefore, with these changes, the equation analogous to (2.2-6) which describes the meridional vibrations should be

$$\ddot{\eta}_{\xi\xi\xi\xi} - \bar{\lambda} \eta_{\xi\xi} [\frac{1}{2} (1 - \xi^2) + \xi_o (1 - \xi)] + \bar{\lambda} \eta_{\xi\xi} (\xi + \xi_o) + \alpha \ddot{\eta} = -\alpha (\omega_x \omega_z - \dot{\omega}_y) (\xi + \xi_o) \quad (2.3-3)$$

So far, quantities neglected have been of order  $\epsilon^2$  of smallness, or smaller. Now, in order for the r.h. side of (2.3-3) to be of order  $\epsilon^2$ , we should have

$$\alpha \omega_z^2 \frac{\omega_x}{\omega_z} = \bar{\lambda} \frac{\omega_x}{\omega_z}$$

$$\alpha \frac{d\omega_y}{dt} = \bar{\lambda} \frac{d\omega_y/\omega_z}{d\phi}$$

very small compared to quantities assumed to be of order E. If such is the case, we are left with homogeneous equation

$$\eta_{\xi\xi\xi\xi} - \bar{\lambda} \eta_{\xi\xi} \left[ \frac{1}{2} (1-\xi^2) + \xi_0 (1-\xi) \right] + \bar{\lambda} \eta_\xi (\xi + \xi_0)$$

$$+ \alpha \eta'' = 0 \quad (2.3-4)$$

(2.3-4) differs from (2.2-7) only in that term  $- \bar{\lambda}\eta$  of (2.2-7) is not present.

### 2.3.2 Solution of the basic equation

After separation of variables and non-dimensionalizing time by  $\tau = \omega_z t$ , the solution to (2.3-4) will be

$\eta_j = \Phi_j(\xi) T_j(\tau)$   
in which  $T_j = \frac{\sin \bar{\omega}_j \tau}{\cos \bar{\omega}_j \tau} = \frac{\sin \tilde{\omega}_j t}{\cos \tilde{\omega}_j t}$ , and  $\Phi_j$  satisfies the differential equation

$$\Phi_j^{(iv)} - \bar{\lambda} \Phi_j^{(2)} \left[ \frac{1}{2} (1-\xi^2) + \xi_0 (1-\xi) \right] + \bar{\lambda} \Phi_j^{(1)} (\xi + \xi_0)$$

$$- \bar{\lambda} \bar{\omega}_j^2 \Phi_j = 0 \quad (2.3-5)$$

As expected, this equation is the same as that obtained in (2.2-8) for equatorial vibrations provided the substitution of

$$\bar{\omega}_j^2 \text{ in (2.3-5) is made for } \left[ \left( \frac{1}{2} + \bar{\omega}_j^2 \right) \right] \text{ in [2.2-8]} \quad (2.3-6)$$

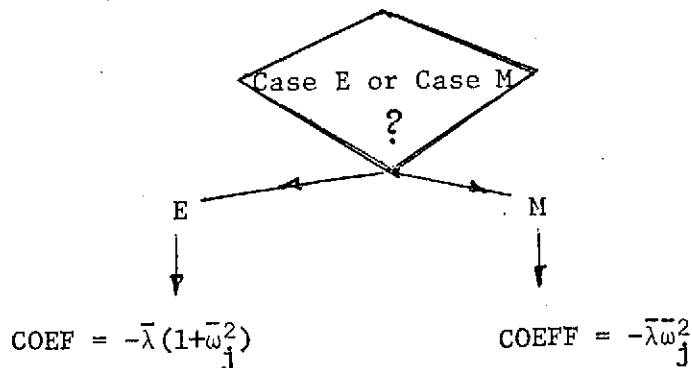
Therefore, the method outlined in Section (2.2.2) to solve for  $\bar{\omega}_j$  can be adopted and followed without any other modification than that specified by (2.3-6). In fact, program SEARCH DP, which obtains the first three eigenvalues

$$\omega_1, \omega_2, \omega_3$$

given a pair  $(\bar{\lambda}, \xi_0)$ , iteratively solves an equation such as (2.3-5),

$$\begin{aligned} \bar{\Phi}_j^{(n)} - \bar{\lambda} \bar{\Phi}_j^{(2)} & [ \frac{1}{2} (1 - \xi^2) + \xi_0 (1 - \xi) ] + \bar{\lambda} \bar{\Phi}_j^{(1)} (\xi + \xi_0) \\ & + COEF * \bar{\Phi}_j = 0 \end{aligned} \quad (2.3-7)$$

in which the coefficient "COEF" is determined as follows:



### 2.3.3 Orthogonality of the mode shapes

Modes  $\phi_j(\xi)$  ( $j = 1, 2, \dots$ ) for meridional vibrations can be proven to be orthogonal, as in Section (2.2-3), since Equation (2.2-19) holds equally well in the present case. Thus

$$\int_{\text{boom}} \phi_j \phi_k d\xi = 0 \quad j \neq k \quad (2.3-8)$$

and we define, for case M,

$$m_{1,j} \stackrel{\text{def}}{=} \int_{\text{boom}} \phi_j^2 d\xi > 0 \quad (2.3-9)$$

$$m_{2,j} \stackrel{\text{def}}{=} \int_{\text{boom}} \phi_j \xi_1 d\xi \quad (2.3-10)$$

with  $\xi_1 = \xi_0 + \xi$ .

With the substitution  $\bar{\omega}_s^2 + \bar{\omega}_j^2$  in (2.2-8)  $\rightarrow \bar{\omega}_j^2$  in (2.3-5), the following relations, valid for meridional vibrations, are deduced straightforwardly from Equations (2.2-23) and (2.2-24)

for  $j \neq k$

$$\frac{1}{\lambda} \int_{\text{boom}} \Phi_j^{(2)} \bar{\Phi}_k^{(2)} d\xi \int_{\text{boom}} \Phi_j^{(1)} \bar{\Phi}_k^{(1)} \frac{1}{2} [ (1-\xi^2) + 2\xi_0 (1-\xi) ] d\xi = 0. \quad (2.3-11)$$

and for  $j=k$

$$\frac{1}{\lambda} \int_{\text{boom}} \Phi_j^{(2)} \bar{\Phi}_j^{(2)} d\xi + \int_{\text{boom}} \Phi_j^{(1)} \bar{\Phi}_j^{(1)} \frac{1}{2} [ (1-\xi^2) + 2\xi_0 (1-\xi) ] d\xi = m_j \bar{\omega}_j^2. \quad (2.3-12)$$

It should be noted here that for the same pair of values  $(\bar{\lambda}, \xi_0)$ , if  $(\text{COEF})_j$  is the value to be given to COEF in (2.3-7), in order for the determinant (2.2-16) to vanish, then

$$(\text{COEF})_{j,E} = (\text{COEF})_{j,M} = \text{COEF}$$

or

$$\bar{\omega}_{j,E}^2(\bar{\lambda}, \xi_0) + 1 = \bar{\omega}_{j,M}^2(\bar{\lambda}, \xi_0) \quad (2.3-13)$$

whereas the modal shapes determined from (2.3-7) with the value

$(\text{COEF})_j$  of COEF have to be the same in cases E and M

$$\bar{\Phi}_{j,E}(\bar{\lambda}, \xi_0, \bar{\omega}_{j,E}) = \bar{\Phi}_{j,M}(\bar{\lambda}, \xi_0, \bar{\omega}_{j,M})$$

In (2.3-13), if it is found more convenient to non-dimensionalize

by a quantity proportional to the 1st eigenfrequency of the non-rotating cantilever boom, namely

$$\omega_{NR}^* = (EI/\rho l^4)^{1/2}$$

then (2.3-13) becomes

$$\left( \frac{\omega_{d,E}}{\omega_{NR}^*} \right)^2 + \left( \frac{\omega_z}{\omega_{NR}^*} \right)^2 = \left( \frac{\omega_{d,E}}{\omega_{NR}^*} \right)^2 + \bar{\lambda} = \left( \frac{\omega_{d,M}}{\omega_{NR}^*} \right)^2 \quad (2.3-14)$$

as illustrated in some examples of Section (2.8)

## 2.4 Program determining the modal frequencies for equatorial or meridional vibrations: SEARCH DP.

Program SEARCH DP, listed at the end of the present chapter, is written in FORTRAN V and implements the developments of Section 2.2 and 2.3.

The calculations are carried out in double precision, which suffices for values of  $\bar{\lambda}$  up to about 5,000. For higher values of  $\lambda$ , an arbitrary N-precision, scheme had to be used: this is described in Section 2.7.

### 2.4.1 Description of the program

Number of statements (including comment cards): about 270

Input: - 1 card giving  $Q = E$  or  $M?$ ;  $\bar{\lambda}$ ;  $\xi_0$  in format (A1, F6.5, G5.4)

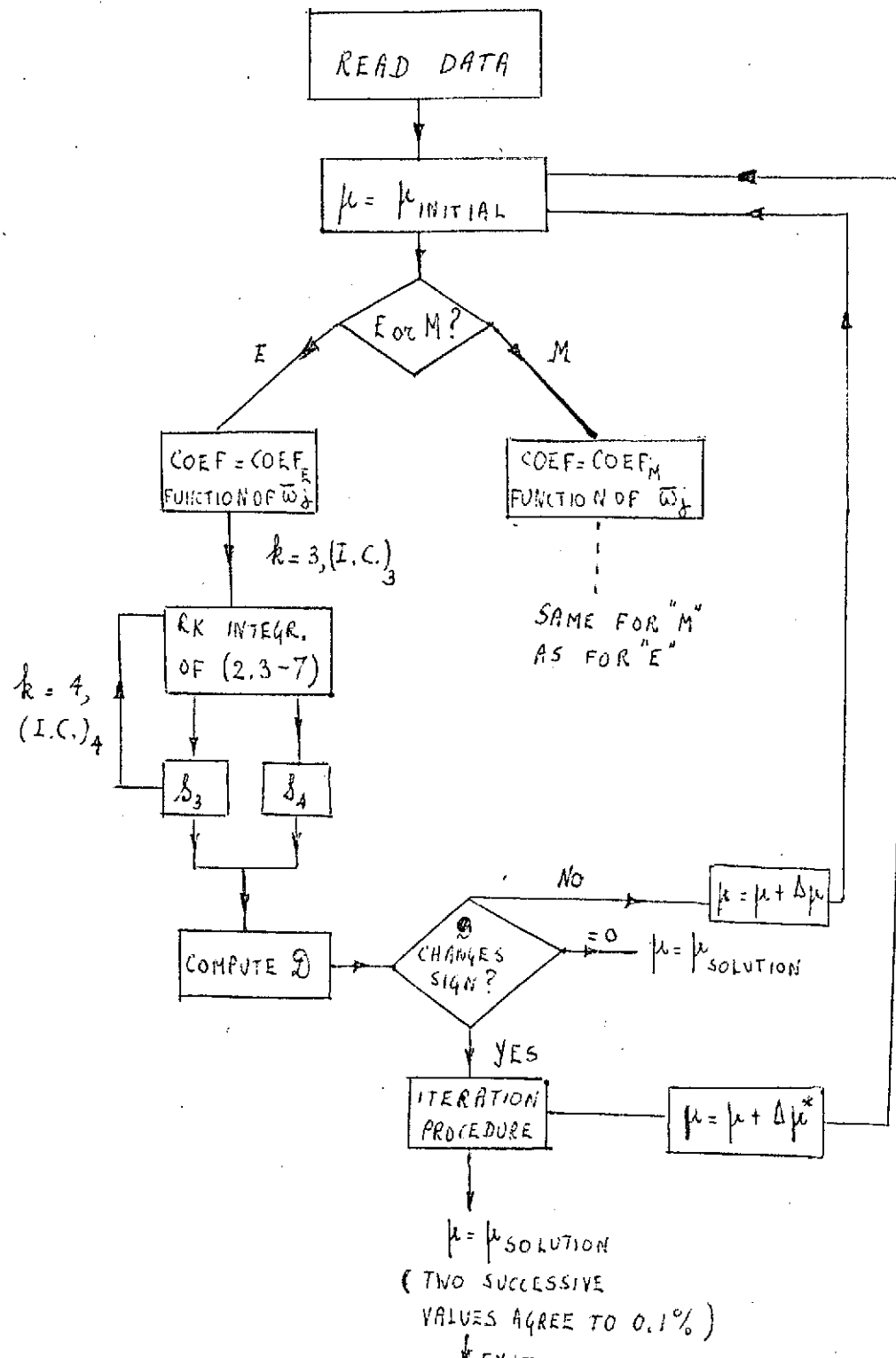
Output: 1) - A heading, specifying "Equatorial case" or "Meridional case"

2) - The values of a "frequency" number defined as  $\sqrt{\bar{\lambda}}$

- Lines giving the value of determinant of Equation (2.2-16), called here FE<sup>34</sup>; the value of  $\sqrt{COFF}$ , the value of index U, number of trials in  $\mu$  before converging to the root of  $\mathcal{O}(\bar{\omega}_j) = 0$
  - Lines labeled KKK number of iterations, giving the successive values of the determinant as  $\mu$  is changed to obtain convergence of the determinant to zero. The iteration stops when  $\mu_{k+1}$  differs from  $\mu_k$  by less than  $10^{-4}$ .
  - A statement that "MU converged" giving the value of FE34 and  $\mu$ .
  - A print-out of FE34,  $\mu$ ,  $\lambda$ , and NATFRQ, defined as  $\frac{\omega_1}{\omega_N}$
  - The value of the step in  $\mu$ , DLT, and the value of the order of the eigenvalue, j or NOR
- 3) same for  $j = 2, 3$ , in that order.

#### 2.4.2 Schematic flow chart:

The following flow chart schematically describes the main control flow in SEARCH DP.



SEARCH - DP

#### 2.4.3 Comments

- a) It has been numerically determined<sup>[2-4]</sup> that 100 steps across the boom's length would suffice, over the range of  $\bar{\lambda}$  and  $\xi_0$  investigated, to obtain eigenvalues agreeing up to the 5<sup>th</sup> digit with those obtained with 200 steps across the boom's length. The "100-steps" are therefore incorporated as a "fixed" feature in program SEARCH DP.
- b) A method of linear interpolation is used for finding the roots of  $(\tilde{\omega}_j) = 0$ . The iteration on  $\mu$  (or equivalently the eigenvalue to be found) stops when two successive values of  $\mu$ , in the iteration process, agree to at least 0.1%.
- c) The integration method is a simple Runge-Kutta with fixed step, having a per step error of the order of  $\Delta x^5$ .
- d) Using double-precision arithmetic, the number of significant digits retained in the two terms in  $\mathcal{D}$ , in Equation 2.2-16, does not suffice for values of  $\bar{\lambda}$  larger than about 5,000, and an arbitrary precision package ("NP" - package, N > 0 integer) had to be developed and is described in Section 2.7.

#### 2.4.4 Listing and sample output

A listing and a sample output of program SEARCH DP are given at the end of this chapter.

## 2.5 Program Determining the Modal Shapes $\phi_j$ and "Masses" $m_{1,j}$ , $m_{2,j}$ :

### MODE

MODE is a Fortran-V, double precision program determining the modal shapes, normalized to unit deflection at the boom's tip,

$$\phi_j(\xi) \quad j = 1, 2, 3$$

which are solutions of Equation 2.3-7, in which

$\bar{\omega}_j$  is the  $j$ th eigenvalue determined by SEARCH DP

$$\text{COEF} = (\text{COEF})_{j,E} = (\text{COEF})_{j,M}$$

$$(\text{COEF})_{j,E} = 1 + \bar{\omega}_{j,E}^2$$

$$(\text{COEF})_{j,M} = \bar{\omega}_{j,M}^2$$

#### 2.5.1 Description of program MODE

Number of statements (including comment cards): 158

Input: - 1 card giving IE - E or M?;  $j$ ;  $\bar{\lambda}$ ;  $\xi_0$ :

$\mu = \text{COEF}$  (to be used in Equation 2.3-7)

in (A1, I1, 3G12.6 format)

Output: 1) - A heading, specifying "Equatorial Case" or "Meridional Case"

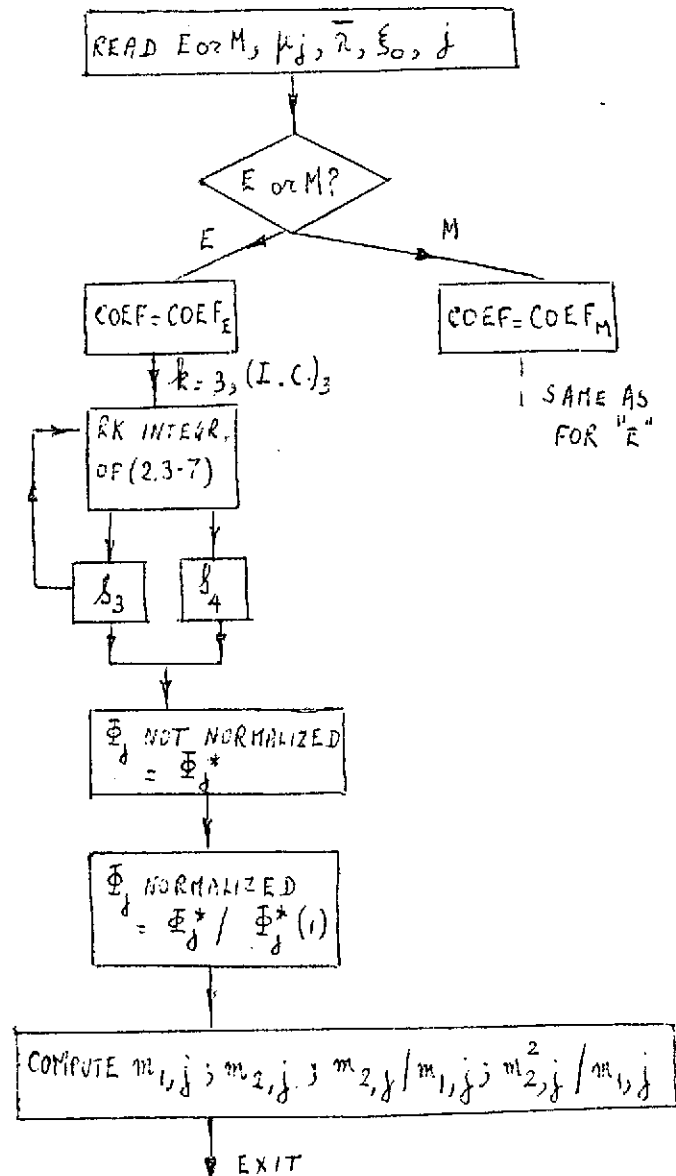
2) - The values of  $\mu_j = \text{COEF}_j$  (as obtained from SEARCH DP),  $\bar{\lambda}$ ,  $\xi_0$ ,  $j$  (1, 2 or 3)

- The values of  $m_{1,j} = \int_{\text{boom}} \phi_j^2 d\xi$ ;  $m_{2,j} = \int_{\text{boom}} (\xi_0 + \xi) \phi_j^2 d\xi$ ;  
 $\frac{m_{2,j}}{m_{1,j}}$ ,  $\frac{m_{2,j}}{m_{1,j}}$  which are of interest in the dynamical

simulation of the evolution in time of the space-craft angular rates ( $\omega_x$ ,  $\omega_y$ ,  $\omega_z$ ) and modal coordinates ( $q_j$ )

- The deflection  $\Phi_j(\xi)$  as a function of  $\xi$ ;  $I$ , the station index, varying from  $I = 1$  (at the root)  $I = 101$  (at the tip), in steps of 2.

2.5.2 Schematic flow diagram. The main control flow in MODE is as follows:



### 2.5.3 Comments

- a) The number of steps of integration, experimentally determined to give values of  $\mu$  agreeing up to the 5th digit when solving the step size, was found to be 100. As in 2.4.3 and SEARCH DP, the the 100 steps are a fixed feature incorporated in the program.
- b) The method of integration is Runge-Kutta with fixed step.
- c) The calculations are carried out in double-precision, which should suffice for values of  $\bar{\lambda}$  of up to 10,000. The data  $\mu_j$ , however, might have had to be determined with the use of "NP" arbitrary precision package.

### 2.5.4 Listing and sample output.

A listing and a sample output of program MODE are given at the end of this chapter.

## 2.6 Parametric Study of Eigenfrequencies and Modal Shapes as a Function of $\bar{\lambda}$ (Etkin's Number) and $\xi_0$ (Non-Dimensional Radius of the Hub)

Given the design parameters  $\bar{\lambda}$  and  $\xi_0$ , the study of the eigenfrequencies  $\omega_j$ , (which normalized to  $\omega_s$ , are noted  $\bar{\omega}_j$ , and to  $\omega_{NR}^* = \left(\frac{EI}{\rho l^4}\right)^{1/2}$ , are noted  $\frac{\omega_j}{\omega_{NR}^*}$ ) will be made easier by using several programs described hereunder.

### 2.6.1 Preliminary Comment

First of all, it should be emphasized here that there is no point in comparing mode shapes  $\phi_j$  for "E" and "M", since they are the same solutions to Equation (2.3-7), for  $COEF_j = COEF_{j,E} = COEF_{j,M}$ , once  $j$  has been chosen and  $\bar{\lambda}$  and  $\xi_0$  have been given. Any slight

numerical departure, such as described in Ref. [2-4], 2-5] could only result from the inaccuracy in determining the eigenfrequency (0.1% relative accuracy on  $\mu$ , in program SEARCH DP). Only the eigenfrequencies  $\bar{\omega}_{j,E}$ ,  $\bar{\omega}_{j,M}$  corresponding to these modal shapes will be different.

### 2.6.2 Program computing dynamical parameters, given $\bar{\lambda}, \xi_0$ : PARAM.

Program PARAM, written in FORTRAN-V, will permit to get a quick look at various relevant dynamical parameters, given  $Q = E$  or  $M$ ,  $\bar{\lambda}$  and  $\xi_0$ , namely

$$m_{1,j}$$

$$m_{2,j}$$

$$(m_2/m_1)_j \quad \text{and } j = 1, 2, 3$$

$$(m_2^2/m_1)_j$$

and also the sum over one, two, three modes

$$\sum_j \frac{m_{2,j}^2}{m_{1,j}}$$

a quantity to be used later in this work. It will also plot the mode shapes (up to  $j = 3$ ) in the computer printout.

The data entered are

$$\bar{\omega}_{j,M} \quad (j = 1, 2, 3) \quad \text{obtained from SEARCH DP, case M (NDS = 0)}$$

$$\bar{\lambda}$$

$$\xi_0$$

The program basically computes  $\Phi_j(\xi)$  and

the relevant integrals,  $m_{1,j}$ ,  $m_{2,j}$  etc... as defined before.

A listing and a sample output of program PARAM is given at the end of this chapter.

2.7 Arbitrary Precision Package: MP (for use on OS) and P (N-Precision Package), in Fortran.

#### 2.7.1 Motivation

An earlier version of SEARCH DP had been written<sup>[2-4]</sup> to alleviate a problem of numerical stability at large values of  $\bar{\lambda}$  (higher than about 5,000). This version used on IBM-library multiple precision (MP package). It was found, however, that this package was unavailable in a TSS environment. Therefore, an arbitrary precision package (NP) was written in Fortran V, and used for finding the eigenvalues  $\bar{\omega}_j$  at values of  $\bar{\lambda}$ , and the accuracy of determinant  $\mathcal{D}$  in Equation (2.2-16) will be critically affected when taking differences of very large numbers.

MPAP (Multiple Precision Arithmetic Package) is present in the Internal Library of the IBM-360. The routine calls on specialized subroutines to perform floating point calculations with precision to be specified by the programmer (typically, here, quadruple precision was required).

MP-SEARCH, as used in Ref. [2-4], and MP-MODE, are thus basically MPAP versions of SEARCH and MODE. Their one disadvantage, as expected, is

an increased running time, of the order of 1.5 minutes for eigenvalue (IBM/360). For this reason, it is important that the eigenvalues or modal quantities of MP-MODE obtained for high  $\bar{\lambda}$  be stored for later use in the simulation (Option MG1V = 1 in program FLEXAT, see Chapter 5), and that interpolation be used whenever possible.

### 2.7.3 Multiple precision in TSS: MP-package

Written in FORTRAN for case of conversion to any machine, N-PRES is a multiple-precision arithmetic system for scientific calculation. It may be used on any machine which stores one integer per word, where a word is  $\geq 31$  bits long.

#### 2.7.3.1 Short description of the program

##### 2.7.3.1.1 Representable numbers.

Let  $N, M$  be integers

$$2 \leq N \leq 16$$

All numbers in the program are considered floating point constants of  $+ N$  precision, expressed in scientific notation. Thus, for  $N = 3$ , or precision  $4N = 12$ , we could have

.371246875003\*10\*\*8371

The exponent must always be an integer, positive, negative or zero and less than or equal to 4 decimal digits long. Thus a number such as  $\pm d_1 d_2 \dots d_{60} * 10^{+D_1 D_2 D_3 D_4}$

##### 2.7.3.1.2 Internal Storage (Multiple-point, floating)

The mantissa is stored 4 digits to a word, in "N" digits.

The exponent takes up the  $N+1$  . tition (Any  $1 \leq N \leq 16$ )

Example: for M = 3, N = 2

$$8.4326 \times 10^4 = .84326000 \times 10^5$$

$$6.0 \times 10^4 = .6 \times 10^2$$

represented as

NUMBER 1	NUMBER 2	
8	6	
4	0	Word 1
3	0	
2	0	
<hr/>	<hr/>	
6	0	
0	0	Word 2
0	0	
0	0	
<hr/>	<hr/>	
EXPO+	0	
0	0	
0	0	
5	2	

All operations are designed to handle such units, called N-CONS (for N constant).

#### 2.7.3.1.3 Quick guide to operations and subroutines

Name	Subroutine Function (all operating with N cons)
INIT	Initialize the N-precision system
INPUT	Input
OUTPUT	Output
CIN	Convert integer to N-CON
CNI	Convert N-CON to integer
CFN	Convert floating point to N-CON
CNF	Convert N-CON to floating point
NABS	Mem(Add) $\leftarrow$ ABS[Mem(Add)]
NPWR	Mem(Add) $\leftarrow$ [Mem(Add)]**P with P a parameter to NPWR
NSCL	Mem(Add) $\leftarrow$ [Mem(Add)]*10**S with S a parameter to NSCL

Name	Subroutine function (all operating with N cons)
NCMPR	if Mem(Add 1) = Mem(Add 2), A = B if Mem(Add 1) > Mem(Add 2), A > B if Mem(Add 1) < Mem(Add 2), A < B with A, B, parameters to NCMPR
COPY	Mem(Add 2) $\leftarrow$ Mem(Add 1)
RENORM }	
SHIFT	Internal use only
PUNCH	Output to punch
IMUL	Mem(Add) $\leftarrow$ Mem(Add)*I $I =  \text{integer}  \leq \text{limit}$
FDIV	Mem(Add) $\leftarrow$ Mem(Add)/F $F = \text{floating point}$
MADD	Mem(Add 3) $\leftarrow$ Mem(Add 1) + Mem(Add 2)
MSUB	Mem(Add 3) $\leftarrow$ Mem(Add 1) - Mem(Add 2)
MMUL	Mem(Add 3) $\leftarrow$ Mem(Add 1) * Mem(Add 2)
MDIV	Mem(Add 3) $\leftarrow$ Mem(Add 1) / Mem(Add 2)

### 2.7.3.2 Some examples of N-precision programming

#### 2.7.3.2 Square root

##### A. Algorithm: Newton-Raphson

Let  $B = \sqrt{A}$ , with old  $B = 1$

$$\text{the } B = \frac{1}{2} \left( \frac{A}{\text{old } B} + \text{old } B \right)$$

If  $\text{Abs}(\text{old } B - B) > B * 10^{** \text{ limit}}$

Old  $B = B$

Else done

B. Fortran Program:

```

Limit = - 12

Read (5,1)A

1 Format (F10.2)

Old B = 1.

2 B = (A/Old B + Old B)/2

X = ABS(Old B-B)

Y = B*10**Limit

If (X, LE, Y) G0 T0 3

Old B = B

GO TO 2

3 WRITE (6,4)B,A

4 FORMAT ('' , F10.2, '' IS SQUARE ROOT OF, F10.2)

STOP

END

```

C. N-Precision ProgramComments

IMPLICIT INTEGER (A-Z)	(all N-cons.)
CALL INIT(1,4)	(16 digits of precision, N=4)
CON V = -12	(limit)
A = 1	
B = 2	(Allocation of variable names to N-con addresses)
Old = 3	
TWO = 4	
X = 5	
Y = 6	
HALF = 7	
CALL Input(A)	
Call NSCL(A,1)	
CALL CIN(TWO,2)	(N-con at address TWO contains the value 2)

```

Call CIN(Old B,1)           (N-con. at address 'Old B'
                           contains the value 1)

Call CFN(HALF,.5)          (Half contains 0.5)

Call Output(HALF)           (Conversion OK; print
                           and check)

Call Output(A)              (Print input number)

Q = 1                       (Iteration Counter)

Call MDIV(A, OldB,B)        (B = A/Old B)

Call MADD(B,Old B,B)         (B = B+Old B)

Call MMUL(B,HALF,B)          (B = B*.5)

Call Output(B)              (write partial answer)

Call HM                      (How many subroutines called
                           so far. Print it out)

Call MSUB(B,Old B,X)         (X = B-Old B)

Call NABS(X)                (X = Abs X)

Call COPY (B,Y)              (Y = (B))

Call NSCL (Y,CONV.)          (Y = (Y)*10** CONV )

Call NCMPR(X,Y,I,J)          (Result:

If X > Y, I > J
X < Y, I < J
X = Y, I = J)
(IF(ABS(B-Old B).LE.
B*10**CONV) GO TO 2
(Old B = (B))

Call COPY(B, Old B)           (Done!)

GO TO 1                      (How many calls)

CONTINUE                     (Write out results)

```

#### 2.7.3.2.2 Conversion of a statement from SEARCH DP

Consider the FORTRAN statement of SEARCH DP:

IF(FE34\*DECID) 52, 51, 50

The N-PREC. translation would be

CALL MMUL(DECID, FE34, TEMP)

CALL NCMPR(TEMP,ZERO,I,J)

If(I.LT. J) GO TO 52

If(J.EQ. J) GO TO 51

50 CONTINUE

### 2.8 Results from programs SEARCH DP, MP and NP

The frequencies  $\bar{\omega}_j$  (normalized to  $\omega_s = 1$ ) for  $j = 2$ , are given for case M. Those for case E are immediately obtained from

$$\bar{\omega}_{E,j}^2 = \bar{\omega}_{M,j}^2 - 1$$

Also given below is the quantity  $\sum_{j=1}^3 \frac{m_{2,j}}{m_{1,j}}$ , which will be of special

importance in Chapters 4 and 5. The first non-dimensional frequency  $x$

$\omega_1 \sqrt{\rho \ell^4 / EI}$  is also represented, for cases E and M, and various values of  $\xi_0$ , on Fig. 2.2.

## CASE M - FIRST NONDIMENSIONAL NATURAL FREQUENCY

	0.00	0.10	0.25	0.50
0	3.681	3.703	3.734	3.787
5	1.913	1.953	2.013	2.107
10	1.555	1.605	1.675	1.788
20	1.339	1.395	1.476	1.601
30	1.256	1.316	1.401	1.531
50	1.183	1.246	1.335	1.469
100	1.120	1.186	1.278	1.417
200	1.081	1.148	1.242	1.385
500	1.050	1.118	1.214	1.358
1000	1.034	1.104	1.201	1.346
3000	1.021	1.091	1.188	1.339
7000	1.016	1.087	1.184	1.329
10000	1.013	1.083	1.181	1.327

NOTE:  $\bar{\omega}_E = \left( \bar{\omega}_M^2 - 1 \right)^{1/2}$   
 $(\omega_1)_{\bar{\lambda}=0} = 3.518 \left( \frac{EI}{\rho l^4} \right)^{1/2}$

CASE M - SECOND NONDIMENSIONAL NATURAL FREQUENCY  $\bar{\omega}_2 = \omega_2 / \omega_s$ 

	0.00	0.10	0.25	0.50
1	22.18	22.20	22.23	22.78
5	10.236	10.276	10.339	10.447
10	7.419	7.476	7.561	7.703
20	5.546	5.624	5.736	5.921
30	4.760	4.849	4.981	5.191
50	4.023	4.128	4.281	4.523
100	3.364	3.488	3.665	3.941
200	2.976	3.113	3.308	3.606
500	2.707	2.855	3.060	3.373
1000	2.603	2.754	2.964	3.282
3000	2.520	2.673	2.886	3.195
7000	2.490	2.644	2.857	3.178
10000	2.482	2.635	2.849	3.171

NOTE:  $\bar{\omega}_E = (\bar{\omega}_M^2 - 1)^{1/2}$   
 $(\omega_2)_{\bar{\lambda}=0} = 21.91 \left( \frac{EI}{\rho l^4} \right)^{1/2}$

$m_{2,1}^2/m_{1,1}$ 

(ONE NODE)

$\frac{\xi_0}{\lambda}$	0.00	0.10	0.25	0.50
0	0.3233	0.4190	0.5810	0.9250
10	0.3249	0.4212	0.5893	0.9325
20	0.3260	0.4231	0.5929	0.9400
30	0.3268	0.4246	0.5957	0.9457
50	0.3280	0.4268	0.5997	0.9538
100	0.3297	0.4301	0.6056	0.9652
200	0.3311	0.4330	0.6111	0.9757
500	0.3323	0.4357	0.6165	0.9861
1000	0.3328	0.4371	0.6194	0.9916
3000	0.3331	0.4385	0.6224	0.9950
10000	0.3332	0.4392	0.6241	1.001
	$\Delta =$ 0.3333	$\Delta =$ 0.4433	$\Delta =$ 0.6458	$\Delta =$ 1.0833

## NONDIMENSIONAL DYNAMICAL PARAMETERS

SUM OVER 3 NODES

$\frac{\xi_0}{\lambda}$	0.0	0.10	0.25
10	0.3328	0.4401	0.6336
100	0.3329	0.4404	0.6343
1000	0.3332	0.4413	0.6366
$\Delta = 0.3333$		$\Delta = 0.4433$	$\Delta = 0.6458$

 $m_{2,1}^2/m_{1,1}$  (ONE MODE)

$\frac{\xi_0}{\lambda}$	0.00	0.10	0.25	0.50
0	0.3233	0.4190	0.5810	0.9250
10	0.3249	0.4212	0.5893	0.9325
20	0.3260	0.4231	0.5929	0.9400
30	0.3268	0.4246	0.5957	0.9457
50	0.3280	0.4268	0.5997	0.9538
100	0.3297	0.4301	0.6056	0.9652
200	0.3311	0.4330	0.6111	0.9757
500	0.3323	0.4357	0.6165	0.9861
1000	0.3328	0.4371	0.6194	0.9916
3000	0.3331	0.4385	0.6224	0.9950
10000	0.3332	0.4392	0.6241	1.001
$\Delta =$		$\Delta =$	$\Delta =$	$\Delta =$
0.3333		0.4433	0.6458	1.0833

REFERENCES - Chapter 2

- [2-1] ETKIN, B. and HUGHES, P.C.: "Explanation of the anomalous spin behavior of satellites with long flexible antennae," Jour. of Spacecraft and Rockets, 4, 9, 1139-1145.
- [2-2] VIGNERON, F.R.: "Stability of a Freely Spinning Satellite of Crossed-Dipole Configuration." CASI Trans., 3, 1, 8-9, March 1970.
- [2-3] RENARD, M.L. and RAKOWSKI, J.E.: "Equatorial Vibrations of a Long Flexible Boom on a Spin-Stabilized Satellite of Non-Zero Radius," Proc. of the Astronautical Congress, October 1969. Vol. 1, pp. 35-53, E. Lunc (Editor), Pergamon Press, 1971.
- [2-4] RAKOWSKI, J.E.: "A Study of the Attitude Dynamics of a Spin-Stabilized Satellite Having Flexible Appendages," Ph.D. Thesis, Mech. Engrg., Carnegie-Mellon University, December 1970.
- [2-5] RAKOWSKI, J.E. and RENARD, M.L.: "A Study of the Nutational Behavior of a Flexible Spinning Satellite Using Natural Frequencies and Modes of the Rotating Structure," Paper 70-1046, presented at the AAS/AIAA Astrodynamics Conference, Santa Barbara, August, 1970.

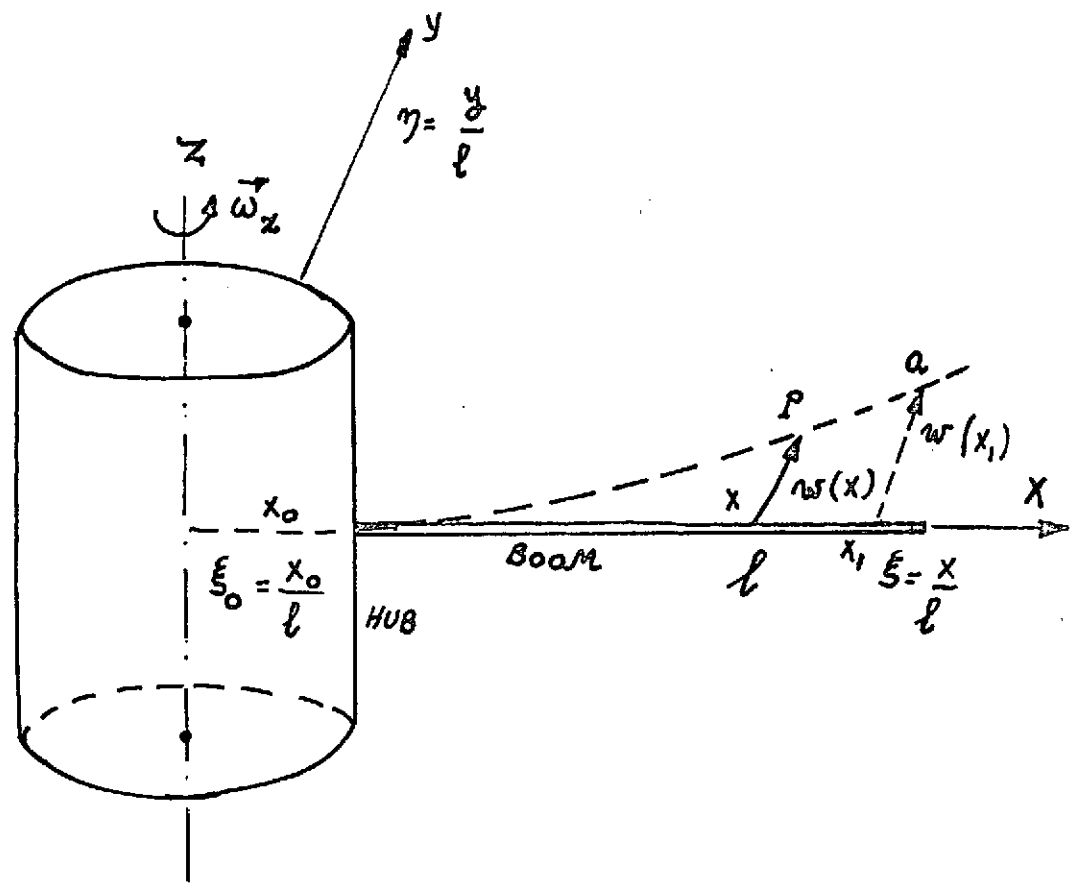
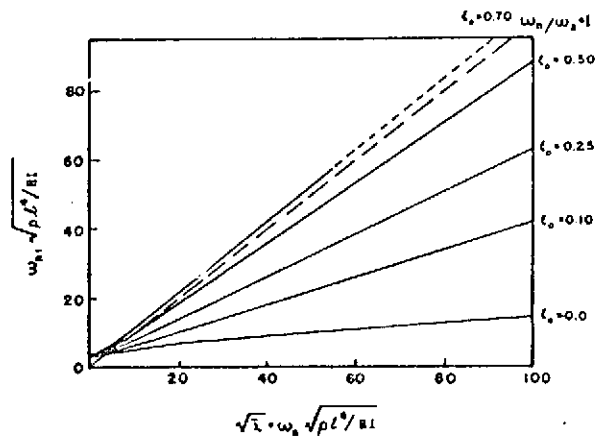
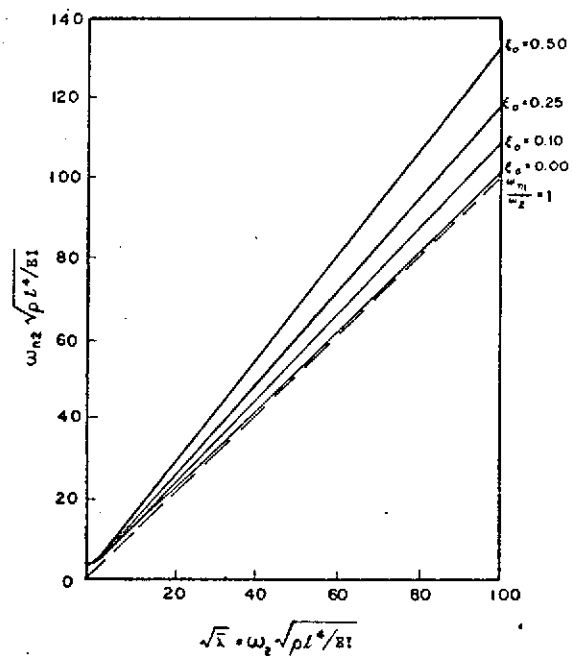


FIG. 2-1. GEOMETRY OF SPINNING SATELLITE WITH FLEXIBLE APPENDAGE.



Equatorial vibrations.



Meridional vibrations.

FIG. 2-2. FREQUENCY OF FUNDAMENTAL MODE VS  $\lambda$ .

PROGRAM LISTING

AND

SAMPLE OUTPUT

SEARCH DP

```

C THIS PROGRAM FINDS THE FIRST THREE EIGENVALUES (MU) FOR THE ROTATING
4* C BOOM IN EITHER EQUATORIAL OR MERIDIONAL FLEXURE.
5* C
6* C IT WILL COMPUTE THESE ACCURATELY FOR VALUES OF LAMBDA UP TO
7* C APPROXIMATELY 5000
8* C
9*     DOUBLE PRECISION P(4),K(4),M(4),L(4),E3(101),E31P(101),E32P(101),
0*     1FE34,DECID,TVAL,HY,EM0N3,EM0M4,ES,IR3,ESHR4,FEPRV,
1*     1E33P(101),E34P(101),E4(101),E41P(101),E42P(101),E43P(101),
2*     3E44P(101),A,B,C,E,A0,B0,C0,E0,MU1,MU,EPSC,EPSB,LAS,LASS,
3*     4 DLT,UP,DWN,SIO,SI
4*     1 REAL H,NN,LAM,NATFRQ
5*     INTEGER I,DIN,Z, NINT,INTER,W,R,U,NOR,KKK,Q
6*     DATA/LM/1HM
7* C
8* C INPUT DATA IS E OR M,LAMBDA,PSI=ZERO
9* C
10*    18 READ(S,20,END=220),LAM,SIO
11*    20 FORMAT(A1,F6.5,G5.4)
12*    NDS=1
13*    IF(Q.EQ.LM)NDS=0
14*    IF(NDS.EQ.1)WRITE(6,16)
15*    IF(NDS.EQ.0)WRITE(6,17)
16*    16 FORMAT(' EQUATORIAL CASE'//)
17*    17 FORMAT(' MERIDIONAL CASE'//)
18*    WRITE(6,21) LAM,SIO
19*    21 FORMAT(1H , 'LAM=' ,F12.6,3X,'SIO=' ,D9.3/)
20*    KKK#1
21*    R#0
22*    U#1
23*    FE34#0.
24*    MU#1.0D-6
25*    EPSB#1.0D-14
26*    W#0
27*    FEPRV#0.
28*    EPSB#10.*#-14
29* C
30* C SET NOPT = 1 FOR REVERSED INTEGRATION (TIP TO ROOT)
31* C
32*    NOPT#1
33* C
34* C NDS = DIRECTION SWITCH
35* C WHEN NDS = 1, SEARCH FOR EQUATORIAL ROOTS,
36* C WHEN NDS = 0, SEARCH FOR MERIDIAN ROOTS
37* C
38* C
39* C NORE#1
40* C N#1
41* C DLT#1.
42* C IA#0
43* C NINT#100
44* C INTER#NINT+1
45* C ANFRQ#SORT(LAM)
46* C WRITE(6,60) ANFRQ
47* C 60 FORMAT(1H , 'NFRQ=SORT(LAM)' ,F10.5)
48* C 99 SI#0.
49* C TVAL#FE34
50* C JU#0
51* C
52* C CLEAR ARRAYS
53* C DO 31 I#1,4

```

```

62*      K(I)=0.
63*      L(I)=0.
64*      M(I)=0.
65*      31 P(I)=0.
66*      00 1. I=1,101
67*      E34P(1)=0.
68*      E44R(1)=0.
69*      E33P(1)=0.
70*      E43P(1)=0.
71*      E32P(1)=0.
72*      E42P(1)=0.
73*      E31P(1)=0.
74*      E41P(1)=0.
75*      E4(I)=0.
76*      1 E3(I)=0.
77*      H=1./FLOAT(NINT)
78*      C
79*      C SET INITIAL CONDITIONS ON THE S3 AND S4 SOLUTIONS
80*      C
81*      D=3
82*      8 IF(D.EQ.4) GO TO 2
83*      EO=0.
84*      BO=0.
85*      IF(NOPT.GT.0) GO TO 12
86*      E32P(1)=1.
87*      BO=E32P(1)
88*      GO TO 13
89*      12 E3(I)=1.
90*      EO=E3(I)
91*      13 CO=0.
92*      AO=0.
93*      GO TO 3
94*      2 AO=0.
95*      CO=0.
96*      IF(NOPT.GT.0)GO TO 14
97*      E43P(1)=1.
98*      CO=E43P(1)
99*      GO TO 15
100*      14 E41P(1)=1.
101*      AO=E41P(1)
102*      15 BO=0.
103*      EO=0.
104*      3 A=AO
105*      B=BO
106*      C=CO
107*      E=EO
108*      C
109*      C BEGIN RUNGA KUTTA INTEGRATION
110*      C
111*      N=1
112*      4 I=1
113*      NN=N
114*      S1=(NN-1.)*H
115*      5 K(I)=H*A
116*      L(I)=H*B
117*      M(I)=H*C
118*      MU1=1.+MU*MU
119*      IF(NDS.EQ.1) GO TO 40

```

```

100*      MU1=MU1-1.
121*      40 P(I)=((1.-SI*SI+2.*SI0*(1.-SI))/2.*B-(S1+SI0)*A+MU1)*E)*LAM*H
122*      IF(NOPT.GT.0) P(I)=((-SI*SI+2.*SI*(1.+SI0))/2.*B-
123*          1+(1.-SI+SI0)*A+MU1*E)*LAM*H
124*      S1=(NN-1.)*II.
125*      I=I+1
126*      IF(I.GT.3) GO TO 6
127*      Z=I-1
128*      E=E0+K(Z)/2.
129*      A=A0+L(Z)/2.
130*      B=B0+M(Z)/2.
131*      C=C0+P(Z)/2.
132*      S1=SI+H/2.
133*      GO TO 5
134*      6 IF(I.GT.4) GO TO 7
135*      E=E0+K(3)
136*      A=A0+L(3)
137*      B=B0+M(3)
138*      C=C0+P(3)
139*      S1=SI+H
140*      GO TO 5
141*      7 IF(D.EQ.4) GOTO 9
142*      S1=NN*H
143*      Z=N+1
144*      E3(Z)=E3(N)+(K(1)+2.*K(2)+2.*K(3)+K(4))/6.
145*      E31P(Z)=E31P(N)+(L(1)+2.*L(2)+2.*L(3)+L(4))/6.
146*      E32P(Z)=E32P(N)+(M(1)+2.*M(2)+2.*M(3)+M(4))/6.
147*      E33P(Z)=E33P(N)+(P(1)+2.*P(2)+2.*P(3)+P(4))/6.
148*      E34P(Z)=LAM*((SI0+1.)**2-(SI+SI0)**2)*E32P(Z)/2.
149*      1-(SI+SI0)*E31P(Z)+MU1*E3(Z))
150*      IF(NOPT.GT.0) E34P(Z)=LAM*((SI0+1.)**2-(1.-SI+SI0)**2)
151*      1*E32P(Z)/2.+((1.-SI+SI0)*E31P(Z)+MU1*E3(Z))
152*      E=E3(N+1)
153*      A=E31P(N+1)
154*      B=E32P(N+1)
155*      C=E33P(N+1)
156*      E0=E
157*      AO=A
158*      BO=B
159*      CO=C
160*      N=N+1
161*      IF(N.LT.INTER) GO TO 4
162*      EMOM3=E32P(INTER)
163*      ESHR3=E33P(INTER)
164*      IF(NOPT.GT.0) EMOM3=E3(INTER)
165*      IF(NOPT.GT.0) ESHR3=E31P(INTER)
166*      D=4
167*      GO TO 8
168*      9 SI=NN*H
169*      Z=N+1
170*      E4(Z)=E4(N)+(K(1)+2.*K(2)+2.*K(3)+K(4))/6.
171*      E41P(Z)=E41P(N)+(L(1)+2.*L(2)+2.*L(3)+L(4))/6.
172*      E42P(Z)=E42P(N)+(M(1)+2.*M(2)+2.*M(3)+M(4))/6.
173*      E43P(Z)=E43P(N)+(P(1)+2.*P(2)+2.*P(3)+P(4))/6.
174*      E44P(Z)=LAM*((SI0+1.)**2-(SI+SI0)**2)*E42P(Z)/2.
175*      1-(SI+SI0)*E41P(Z)+MU1*E4(Z))
176*      IF(NOPT.GT.0) E44P(Z)=LAM*((SI0+1.)**2-(1.-SI+SI0)**2)
177*      1*E42P(Z)/2.+((1.-SI+SI0)*E41P(Z)+MU1*E4(Z))

```

```

178*      E=E4(N+1)
179*      A=E41P(N+1)
180*      B=E42P(N+1)
181*      C=E43P(N+1)
182*      EO=E
183*      AO=A
184*      BO=B
185*      CO=C
186*      N=N+1
187*      IF(N.LT.INTER) GO TO 4
188*      EMOM4=E42P(INTER)
189*      ESHR4=E43P(INTER)
190*      IF(NOPT.GT.0) EMOM4=E4(INTER)
191*      IF(NOPT.GT.0) ESHR4=E41P(INTER)
192*      C
193*      C RUNGA KUTTA FINISHED
194*      C NOW BEGIN LINEAR INTERPOLATION
195*      C FE34 IS THE VALUE OF THE DETERMINANT (S3 AND S4)
196*      C
197*      FE34=EMOM3*ESHR4-ESHR3*EMOM4
198*      IF(K.EQ.1) GO TO 51
199*      IF(U.EQ.1) GO TO 50
200*      IF(FE34*DEC1D)52,51,50
201*      50 DEC1D=FE34
202*      LAS=MU
203*      LASS=LAS
204*      WRITE(6,85)FE34,MU,U
205*      85 FORMAT(1H , 'FE34',D12.6,5X,'MU=' ,D12.6,5X,'U=' ,I3)
206*      MU=MU+DLT
207*      U=U+1
208*      GO TO 99
209*      52 UP=MU
210*      DWN=LAS
211*      HY=FE34
212*      TVAL=FE34
213*      51 IF(ABS(FE34).LE.EPSG) GO TO 53
214*      IF(ABS(DEC1D).LE.EPSB) GO TO 42
215*      WRITE(6,86)KKK,FE34,MU
216*      86 FORMAT(1H , 'KKK',13,3X,'FE34',D12.6,3X,'MU',D12.6)
217*      R=1
218*      IF(FE34*DEC1D)55,51,56
219*      55 UP=MU
220*      MU=DWN-(DWN-UP)*DEC1D/(DEC1D-FE34)
221*      KKK=KKK+1
222*      EPSC=ABS(ABS(MU)-ABS(LASS))
223*      IF(EPSC.LT.MU*10.**-4)GO TO 10
224*      LASS=MU
225*      GO TO 58
226*      56 DWN=MU
227*      DEC1D=FE34
228*      MU=DWN-(DWN-UP)*DEC1D/(DEC1D-HY)
229*      KKK=KKK+1
230*      EPSC=ABS(ABS(MU)-ABS(LASS))
231*      IF(EPSC.LT.MU*10.**-4)GO TO 10
232*      LASS=MU
233*      58 FE1=ABS(FEPRV)-ABS(FE34)
234*      IF(ABS(FE1).GT.1.0D-14)GOTO 82
235*      IA=IA+1

```

```

254* .. IF(IA.LT.5) GO TO 82
255* .. WRITE(6,85)FE34
256* .. 83 FORMAT(1H,,!STUCK ON THIS FE34!,D12.6)
257* .. IA=0
258* .. FEPRV=0.
259* .. GO TO 53
260* .. 82 FEPRV=FE34
261* .. GO TO 99
262* .. 42 WRITE(6,43)DECID
263* .. 43 FORMAT(1H , 'NO GOOD DECIDE!',D12.6)
264* .. GO TO 53
265* .. 10 WRITE(6,11) FE34,MU
266* .. 11 FORMAT(1H0, 'MU CONVERGED.FE34=',D24.18,3X,'MU=',D12.6)
267* .. 53 NATFRQ=MU*SQRT(LAM)
268* .. WRITE(6,54) FE34,MU,LAM,NATFRQ,W
269* .. 54 FORMAT(1H0, 'FE34',D12.6,5X,'MU=',D12.6,5X,'LAM=',F12.6,
270* .. 15X,'NATFRQ=',E12.6,5X,'W=',I,13)
271* .. WRITE(6,86) DLT,NOR
272* .. 86 FORMAT(1H0, 'DLT=',09.3,5X,'NOR=',I,13)
273* .. IF(NOR.EQ.3) GO TO 57
274* .. NOR=NOR+1
275* .. R=0
276* .. U=1
277* .. KKK=1
278* .. MU=MU+DLT
279* .. GO TO 99
280* .. 57 MU=1.0D-6
281* .. WRITE(6,100)
282* .. 100 FORMAT('1')
283* .. NOR=1
284* .. KKK=1
285* .. DLT=1.
286* .. R=0
287* .. U=1
288* .. GOTO 18
289* .. 22 CALL EXIT
290* .. END

```

END OF UNIVAC 1108 FORTRAN V COMPILED. 0 \*DIAGNOSTIC\* MESSAGE(S)

## QUATORIAL CASE

A= 10.00000 S10= .100+000

P=SQRT LAM= 3.16228  
E<sub>34</sub> .170180+001 MU= .100000-005 U= 1  
E<sub>34</sub> .607250+000 MU= .100000+001 U= 2  
K<sub>1</sub> 1 FE34=.239548+001 MU=.200000+001  
K<sub>1</sub> 2 FE34=.134973+000 MU=.120223+001  
K<sub>1</sub> 3 FE34=.258975-001 MU=.124479+001  
K<sub>1</sub> 4 FE34=.482325-002 MU=.125286+001  
K<sub>1</sub> 5 FE34=.893275-003 MU=.125436+001  
K<sub>1</sub> 6 FE34=.165264-003 MU=.125464+001

U CONVERGED FE34= .165264106829071666-003 MU= .125469+001

E<sub>34</sub> .165264-003 MU= .125469+001 LAM= 10.00000 NATFRQ= .396769+01

L= .100+001 NOR= 1  
E<sub>34</sub> -.337822+001 MU= .225469+001 U= 1  
E<sub>34</sub> -.756432+001 MU= .325469+001 U= 2  
E<sub>34</sub> -.111908+002 MU= .425469+001 U= 3  
E<sub>34</sub> -.126038+002 MU= .525469+001 U= 4  
E<sub>34</sub> -.100439+002 MU= .625469+001 U= 5  
E<sub>34</sub> -.165669+001 MU= .725469+001 U= 6  
K<sub>1</sub> 1 FE34=.132765+002 MU=.825469+001  
K<sub>1</sub> 2 FE34=.395210+000 MU=.737738+001  
K<sub>1</sub> 3 FE34=.798063-001 MU=.740274+001  
K<sub>1</sub> 4 FE34=.159426-001 MU=.740785+001  
K<sub>1</sub> 5 FE34=.317792-002 MU=.740685+001

U CONVERGED FE34= -.317791832175018385-002 MU= .740905+001

E<sub>34</sub> -.317792-002 MU= .740905+001 LAM= 10.00000 NATFRQ= .234295+02

L= .100+001 NOR= 2  
E<sub>34</sub> .162358+002 MU= .840905+001 U= 1  
E<sub>34</sub> .403199+002 MU= .940905+001 U= 2  
E<sub>34</sub> .718355+002 MU= .104091+002 U= 3  
E<sub>34</sub> .109783+003 MU= .114091+002 U= 4  
E<sub>34</sub> .151555+003 MU= .124091+002 U= 5  
E<sub>34</sub> .193483+003 MU= .134091+002 U= 6  
E<sub>34</sub> .230505+003 MU= .144091+002 U= 7  
E<sub>34</sub> .266265+003 MU= .154091+002 U= 8  
E<sub>34</sub> .263256+003 MU= .164091+002 U= 9  
E<sub>34</sub> .243054+003 MU= .174091+002 U= 10  
E<sub>34</sub> .186657+003 MU= .184091+002 U= 11  
E<sub>34</sub> .849254+002 MU= .194091+002 U= 12  
K<sub>1</sub> 1 FE34=.708675+002 MU=.204091+002  
K<sub>1</sub> 2 FE34=.722558+001 MU=.199542+002  
K<sub>1</sub> 3 FE34=.519382+000 MU=.199963+002  
K<sub>1</sub> 4 FE34=.368619-001 MU=.199993+002

U CONVERGED FE34= .368618862557834587-001 MU= .199495+002

E<sub>34</sub> .368619-001 MU= .199495+002 LAM= 10.00000 NATFRQ= .632439+02

## PERIODICAL CASE

LAM= 10.000000 S10= .100+000

NR QESORT LAM= 13.16228

FE34 .284392+001	MU= .100000-005	UE 1
FE34 .170179+001	MU= .100000+001	UE 2
KR 1 FE34-.144094+001	MU .200000+001	
KR 2 FE34 .207673+000	MU .154150+001	
KR 3 FE34 .173932-001	MU .159926+001	
KR 4 FE34 .140389-002	MU .160404+001	
KR 5 FE34 .112971-003	MU .160442+001	

U CONVERGED FE34= .112970857023636517-003 MU= .160446+001

E34 .112971-003 MU= .160446+001 LAM= 10.000000 NATFPO= .507373+01

L1= .100+001 NOR= 1

E34-.398435+001	MU= .260446+001	UE 1
E34-.841747+001	MU= .360446+001	UE 2
E34-.117975+002	MU= .460446+001	UE 3
E34-.123912+002	MU= .560446+001	UE 4
E34-.842668+001	MU= .660446+001	UE 5
KR 1 FE34 .160603+001	MU .760446+001	
KR 2 FE34-.483714+000	MU .743773+001	
KR 3 FE34-.175355-001	MU .747490+001	
KR 4 FE34-.623739-003	MU .747623+001	

U CONVERGED FE34=-.623739425547498172-003 MU= .747628+001

E34-.623739-003 MU= .747628+001 LAM= 10.000000 NATFPO= .236421+02

L1= .100+001 NOR= 2

E34 .164506+002	MU= .847628+001	UE 1
E34 .407204+002	MU= .947628+001	UE 2
E34 .725760+002	MU= .104763+002	UE 3
E34 .110735+003	MU= .114763+002	UE 4
E34 .152709+003	MU= .124763+002	UE 5
E34 .194697+003	MU= .134763+002	UE 6
E34 .231551+003	MU= .144763+002	UE 7
E34 .256871+003	MU= .154763+002	UE 8
E34 .263048+003	MU= .164763+002	UE 9
E34 .241608+003	MU= .174763+002	UE 10
E34 .183506+003	MU= .184763+002	UE 11
E34 .795076+002	MU= .194763+002	UE 12
KR 1 FE34-.780630+002	MU .204763+002	
KR 2 FE34 .732752+001	MU .199786+002	
KR 3 FE34 .578262+000	MU .200209+002	
KR 4 FE34 .450579-001	MU .200242+002	

U CONVERGED FE34= .450578704412691877-001 MU= .200245+002

E34 .450579-001 MU= .200245+002 LAM= 10.000000 NATFPO= .633229+02

L1= .100+001 NOR= 3

PROGRAM LISTING

AND

SAMPLE OUTPUT

MØDE

C MODE

C THIS PROGRAM CALCULATES THE MODE SHAPES  
C GIVEN THE EIGENVALUES, LAMBDA, AND PSI-ZERO  
C REVERSED INTEGRATION METHOD ONLY. CASE E OR CASE M -SPECIFY ON INPUT

C IMPLICIT DOUBLE PRECISION(A-H,O-Z)

C INTEGER D,ZI

C DOUBLE PRECISION MU,LAM,MU1

C DOUBLE PRECISION K(4),L(4),M(4),P(4)

C DIMENSION EG3(101),EG4(101),NBPT(101),BPT(101)

C DATA/LE/1HE

C NPR1=1 FOR PRINTED OUTPUT/NPR1=0 FOR PUNCHED OUTPUT

C READ(5,180) NPR1

C IAO FORMAT(11)

C MAKE SURE MU IS THE CORRECT ONE FOR EITHER THE E OR H CASE.

C READ(5,93) IE,JZ,LAM,SIO,MU

```

93 FORMAT(A1,11,3G12.6)
WRITE(6,101) IE
101 FORMAT(IHI,'CASE',2X,A1//)
WRITE(6,95) MU,LAM,S10,JZ
95 FORMAT(' MU=',D12.6,' LAM=',D12.6,' S10=',D12.6,' J=',I2)
NDS=0
IF(LE.EQ.IE)NDS=1
NINT=100
HH=1./FLOAT(NINT)
INTER=NINT+1
H=HH
ANFRQ=DSQRT(LAM)
WRITE(6,1)ANFRQ
FORMAT(' ANFREQ='D10.5)

```

D=3 I.C.

```

E0=1.
A0=0.
C0=0.
B0=0.
E=1.
A=0.
B=0.
C=0.
EV=1.
ER3(1)=1.

```

### D=3 INTEGRATION

```

D=3
N=1
I=1
NN=FLOAT(N)
S1=(NN-1.)*HH
K(I)=H*A
L(I)=H*B
M(I)=H*C
MU1=MU*NU+I.
IF(NDS.EQ.1)GOTO 40
MU1=MU1-1.
P1=(S1+S1)/2.
P1=B*(P1+S1*(S10+I.))
P3=A*((S10-S1)+I.)
P4=E*MU1
P(I)=H*LAM*(P4+P1+P3)
S1=(NN-1.)*HH
I=I+1
IF(I.GT.3)GOTO 61
ZI=I-1
E=E0+K(ZI)/2.
A=A0+L(ZI)/2.
B=B0+M(ZI)/2.
C=C0+P(ZI)/2.
S1=S1+H/2.
GOTO 5
IF(I.GT.4)GOTO 7
E=K(3)+E0

```

```

A=A0+L(3)
B=B0+M(3)
C=C0+P(3)
S1=SI+H
GOTO 5
SI=NN*HH
EV=EV+(K(1)+K(4)+2.0*(K(2)+K(3)))/4.
EV1=EV1+(L(1)+L(4)+2.0*(L(2)+L(3)))/6.
EV2=EV2+(M(1)+M(4)+2.0*(M(2)+M(3)))/6.
EV3=EV3+(P(1)+P(4)+2.0*(P(2)+P(3)))/6.
P1=-SI*SI/2.
P1=(S10+1.)*SI+P1)*EV2
P3=(S10-SI+1.)*EV1
P4=MU1*EV
EV4=(P1+P3+P4)*LAM
E=EV
A=EV1
B=EV2
C=EV3
E0=E
A0=A
B0=B
C0=C

```

### C RUNGA KUTTA FINISHED

```

N=N+1
IF(D.EQ.4)GOTO 70
EG3(N)=EV
GOTO 71
70 EG4(N)=EV
71 IF(N.LT.INTER)GOTO 4
IF(D.EQ.4)GOTO 9
EMOM3=EV.

```

### C RESET FOR D=4 INTEGRATION

```

D=4
CASE D=4 I.C.
A0=1.
E0=0.
B0=0.
C0=0.
A=1.
E=0.
B=0.
C=0.
EV=0.
EV2=0.
EV3=0.
EV4=0.
EV1=A0
N=1
GOTO 4
9 EMOM4=EV
ALF=EMOM3/EMOM4
DO 72 LB=1,101
LL=102-LB

```

72 BAPT(LL)=EG3(LB)=ALF+EG4(LB)  
CONTINUE  
BET=BBPT(101)  
DO 73 LC=1,101  
BPT(LC)=BBPT(LC)/BET  
73 CONTINUE  
SM=0.000  
DO 216 I=2,101  
SM=SM+(BPT(I)\*BPT(I-1))/2.0\*((FLOAT(I)-1.5)\*HH+S10)\*HH  
216 CONTINUE  
AM2=SM  
SM=0.000  
DO 218 I=2,101  
SM=SM+(BPT(I)\*BPT(I)+BPT(I-1)\*BPT(I-1))/2.0\*HH  
218 CONTINUE  
AM1=SM  
COR=AM2\*AM2/AM1  
SQOT=AM2/AM1  
WRITE(6,74) AM1,AM2,SQOT,COR  
74 FORMAT(' M1= ',D15.6,3X,' M2= ',D15.6,3X,' M2/M1= ',D15.6,  
13X,' M2\*\*2/M1= ',D15.6)  
IF(NPR1) 181,181,182  
182 CONTINUE  
WRITE(6,75) (BPT(I),I,I=1,101,2)  
GO TO 75  
181 PUNCH 77,(BPT(I),I=1,101,2)  
75 CONTINUE  
76 FORMAT(' BPT= ',D12.6,3X,' I= ',I,13)  
77 FORMAT(G11.5)  
STOP  
END

APPLICATION: NO DIAGNOSTICS.

CASE E

MU= .200245+002 LAM= .100000+002 SJ0= ,100000+000 J= 3

ANFREQ=.31623+001

M1= .248946+000 M2= .282874+001 M2/M1= .113628+000

BPT= .888178+015 I= 1

BPT= .110301+001 I= 3

BPT= .430495+001 I= 5

BPT= .920902+001 I= 7

M2+2/M1= .321424+002

BPT= .154254+000 I= 9

BPT= .225733+000 I= 11

BPT= .302842+000 I= 13

BPT= .382053+000 I= 15

BPT= .460035+000 I= 17

BPT= .533701+000 I= 19

BPT= .600246+000 I= 21

BPT= .657190+000 I= 23

BPT= .702417+000 I= 25

BPT= .734203+000 I= 27

BPT= .751246+000 I= 29

BPT= .752680+000 I= 31

BPT= .738089+000 I= 33

BPT= .707505+000 I= 35

BPT= .661400+000 I= 37

BPT= .600672+000 I= 39

BPT= .524613+000 I= 41

BPT= .440877+000 I= 43

BPT= .345438+000 I= 45

BPT= .242535+000 I= 47

BPT= .134621+000 I= 49

BPT= .243010+001 I= 51

BPT= .857352+001 I= 53

BPT= .1927775+000 I= 55

BPT= .294150+000 I= 57

BPT= .387303+000 I= 59

BPT= .469844+000 I= 61

BPT= .539613+000 I= 63

BPT= .594726+000 I= 65

BPT= .633625+000 I= 67

BPT= .655103+000 I= 69

BPT= .658338+000 I= 71

BPT= .642905+000 I= 73

BPT= .608779+000 I= 75

BPT= .556327+000 I= 77

BPT= .486292+000 I= 79

BPT= .399758+000 I= 81

BPT= .298114+000 I= 83

BPT= .182998+000 I= 85

BPT= .562353+001 I= 87

BPT= .802290+001 I= 89

BPT= .224411+000 I= 91

BPT= .374373+000 I= 93

BPT= .528312+000 I= 95

BPT= .684655+000 I= 97

BPT= .842156+000 I= 99

BPT= .100000+001 I= 101

PROGRAM LISTING

AND

SAMPLE OUTPUT

PARAM

```
TEST OF SUBROUTINE PARAM
INTEGER PLOTS
REAL LAM
DOUBLE PRECISION MU(3),S10
COMMON/ONE/LAM,S10
COMMON/T10/MU
COMMON/FIVE/NAUX2,LH,AUX1
COMMON/NINE/MODE
COMMON/GRAF/PLOTS
READ(5,201) MODE,LAM,S10,PLOTS
201 FORMAT(15,F12.6,G12.6,A3)
READ(5,202) (M1(K),K=1,MODE)
202 FORMAT(3D12.6)
CALL PARAM
STOP
END
```

#### SUBROUTINE PARAM

SUBROUTINE PARAM IS DESIGNED TO COMPUTE AND OUTPUT PARAMETERS M1, M2, M2/M1, AND M2SQUARED/M1 AND THEIR SUMS THROUGHOUT THE FIRST THREE MODES. ALSO WILL PLOT OUT THE FIRST THREE MODES IF DESIRED. CALLED THRU MAIN JUST AS CASEM.

C MODE IS ENTERED IN COMMON

```

COMMON/ONE/LAM,S10
COMMON/T30/MU
COMMON/FIVE/NAUX2,LB,AUX1
COMMON/NINE/MODE
COMMON/GRAF/PLOTS
REAL NN,LAM
INTEGER I,D,N,Z,NINT,INTER,PLOTS
DIMENSION OUTPUT(23),ZHU(3)
DOUBLE PRECISION P(4),K(4),M(4),L(4),E3(101),E31P(101),E32P(101),
1 E33P(101),E34P(101),E4(101),E41P(101),E42P(101),E43P(101),
1 E44P(101),A,B,C,E,AD,BD,CO,EO,MUL,M(3),S10,S1
DOUBLE PRECISION AM1(4),AM2(4),SM

```

NAUX2 IS A PLOT CONTROL PARAMETER  
NDS=0 FOR MERIDIONAL CASE/NDS=1 FOR EQUATORIAL CASE

```

NAUX2=101
347 WRITE(6,347) PLOTS
FORMAT(1H1,*PARAM           PLOT=*,AA//)
NORT=1
NDS=0
MODES=3
NINT=100
INTER=NINT+1
DO 34 MODE=1,MODES
  S1=0.
  N=1
  D=1./FLOAT(NINT)

```

CLEAR ARRAYS

```

D0 31 I=1,4
  K(I)=0.
  L(I)=0.
  M(I)=0.
  P(I)=0.
D0 1 I=1,101
  E34P(I)=0.
  E44P(I)=0.
  E33P(I)=0.
  E43P(I)=0.
  E32P(I)=0.
  E42P(I)=0.
  E31P(I)=0.
  E41P(I)=0.
  E4(I)=0.
  E3(I)=0.

```

C THIS SECTION COMPUTES THE FIRST MODE SHAPE AND THEN THE NINE SHAPE  
PARAMETERS A1 AND A2 FOR CASE N

```

3 D=3
  IF(D>F9.4) GO TO 2
  CO=0.
  BO=0.

```

```

1 IF(INOPT.GT.0) GO TO 12
E32P(1)=1.
B0=E32P(1)
GO TO 13
12 E3(1)=1.
E0=E3(1)
13 C0=0.
A0=0.
GO TO 3
2 A0=0.
C0=0.
IF(INOPT.GT.0) GO TO 14
E43P(1)=1.
C0=E43P(1)
GO TO 15
14 E41P(1)=1.
A0=E41P(1)
15 B0=0.
E0=B.
3 A=A0
B=B0
C=C0
E=E0
N=1
4 I=1
NN=N
SI=(NN-1.)*4
5 K(1)=H*A
L(1)=H*B
M(1)=H*C
MU1=1.+MU(MODE)+MU(NOISE)
IF(NDS.EQ.1) GO TO 40
MU1=MU1+1.
40 P(1)=((1.-SI*SI+2.*SI0*(1.-SI))/2.+(-(SI+SI0)*A+MU1*E)*LAM*H
IF(INOPT.GT.0) P(1)=(-SI*SI+2.*SI*(1.+SI0))/2.+B
I+(1.-SI+SI0)*A+MU1*E)*LAM*H
SI=(NN-1.)*H
I=I+1
IF(I.GT.3) GO TO 6
Z=1+1
E=E0+K(Z)/2.
A=A0+L(Z)/2.
B=B0+M(Z)/2.
C=C0+P(Z)/2.
SI=SI+H/2.
GO TO 5
6 IF(I.GT.4) GO TO 7
E=E0+K(3)
A=A0+L(3)
B=B0+M(3)
C=C0+P(3)
SI=SI+H
GO TO 5
7 IF(D.EQ.4) GOTO 9
SI=NN*H
Z=N+1
E3(Z)=E3(N)+(K(1)+2.*K(2)+2.*K(3)+K(4))/6.
E31P(Z)=E31P(N)+(L(1)+2.*L(2)+2.*L(3)+L(4))/6.

```

```

E32P(Z)=E32P(N)+(M(1)+2.*M(2)+2.*M(3)+M(4))/6.
E33P(Z)=E33P(N)+(R(1)+2.*P(2)+2.*P(3)+P(4))/6.
E34P(Z)=LAM*((SI0+1.)*2-(SI+SI0)*2)*E32P(Z)/2.
1*(SI+SI0)*E31P(Z)+MU1*E3(Z))
1F(NOPT.GT.0) E34P(Z)=LAM*((SI0+1.)*2-(1.-SI+SI0)*2)
1*E32P(Z)/2+(1.-SI+SI0)*E31P(Z)+MU1*E3(Z))
E=E3(N+1)
A=E31P(N+1)
B=E32P(N+1)
C=E33P(N+1)
E0=E
AO=A
BO=B
CO=C
N=N+1
1F(N.LT.INTER) GO TO 4
EMOM3=E32P(INTER)
1F(NOPT.GT.0) EMOM3=E3(INTER)
DO 30 I=1,INTER
30 MMX3(I)=E3(I)
D=4
GO TO 6
9 SI=NN*H
Z=N+
E4(Z)=E4(N)+(K(1)+2.*K(2)+2.*K(3)+K(4))/6.
E41P(Z)=E41P(N)+(L(1)+2.*L(2)+2.*L(3)+L(4))/6.
E42P(Z)=E42P(N)+(M(1)+2.*M(2)+2.*M(3)+M(4))/6.
E43P(Z)=E43P(N)+(P(1)+2.*P(2)+2.*P(3)+P(4))/6.
E44P(Z)=LAM*((SI0+1.)*2-(SI+SI0)*2)*E42P(Z)/2.
1*(SI+SI0)*E41P(Z)+MU1*E4(Z))
1F(NOPT.GT.0) E44P(Z)=LAM*((SI0+1.)*2-(1.-SI+SI0)*2)
1*E42P(Z)/2+(1.-SI+SI0)*E41P(Z)+MU1*E4(Z))
E=E4(N+1)
A=E41P(N+1)
B=E42P(N+1)
C=E43P(N+1)
E0=E
AO=A
BO=B
CO=C
N=N+1
1F(N.LT.INTER) GO TO 4
EMOM4=E42P(INTER)
1F(NOPT.GT.0) EMOM4=E4(INTER)
DO 32 I=1,INTER
32 MMX4(I)=E4(I)
ALFA=EMOM3/EMOM4
BETA=MMX3(101)+ALFA*MMX4(101)
1F(NOPT.GT.0) BETA=MMX3(1)-ALFA*MMX4(1)
DO 102 LB=1,101
LL=LB
1F(NOPT.GT.0) LL=102-LB
102 BPT(LL,MODE)=(MMX3(LB)-ALFA*MMX4(LB))/BETA
DO 512 LB=1,101
AUX1=BPT(LB,MODE)
1FPLOTS.EQ.'YES') CALL PLOT
2 CONTINUE
SM=0.

```

```

216  DO 216 I=2,101
      SM=SM+(BPT(I,MODE)+BPT(I-1,MODE))/2.*I*(FLOAT(I)-1)*S)*H
      AM2(MODE)=SM
      SM=0.
218  DO 218 I=2,101
      SM=SM+(BPT(I,MODE)*PPT(I,MODE)+BPT(I-1,MODE)*BPT(I-1,MODE))/2.*H
      AM1(MODE)=SM
      CONTINUE
34

```

END OF MODE SHAPE AND MODE PARAMETER CALCULATION

```

OUTPUT( 1 )=S10
OUTPUT( 2 )=LAM
OUTPUT( 3 )=MU(1)
OUTPUT( 4 )=MU(2)
OUTPUT( 5 )=MU(3)
ZMU(1)=SQRT(OUTPUT(3)*OUTPUT(3)-1.)
ZMU(2)=SQRT(OUTPUT(4)*OUTPUT(4)-1.)
ZMU(3)=SQRT(OUTPUT(5)*OUTPUT(5)-1.)
OUTPUT( 6 )=AM1(1)
OUTPUT( 7 )=AM1(2)
OUTPUT( 8 )=AM1(3)
OUTPUT( 9 )=AM2(1)
OUTPUT(10)=AM2(2)
OUTPUT(11)=AM2(3)
OUTPUT(12)=AM2(1)/AM1(1)
OUTPUT(13)=AM2(2)/AM1(2)
OUTPUT(14)=AM2(3)/AM1(3)
OUTPUT(15)=OUTPUT(12)*AM2(1)
OUTPUT(16)=OUTPUT(13)*AM2(2)
OUTPUT(17)=OUTPUT(14)*AM2(3)
OUTPUT(18)=OUTPUT(12)
OUTPUT(19)=OUTPUT(18)+OUTPUT(13)
OUTPUT(20)=OUTPUT(19)+OUTPUT(14)
OUTPUT(21)=OUTPUT(15)
OUTPUT(22)=OUTPUT(21)+OUTPUT(16)
OUTPUT(23)=OUTPUT(22)+OUTPUT(17)
WRITE(6,501) OUTPUT
FORMAT(1H),*K51-ZERO.....*,F4.3/1H ,*LAMBDA...
******,F6.0///,1H ,*MU*,1H ,*S ARE FOR CASE M*,1H
*NUM1******,F8.4/1H ,*NUM2******,F8.4/1H ,
*****,F3.4/1H ,*NUM3******,F8.4/1H ,*M 1 MODE 1*****,F11.8/1H ,*M 1 MODE 2*****,F11.8/1H ,*M 1 MODE 3*****,F11.8/1H ,*M 2 MODE 1*****,F11.8/1H ,*M 2 MODE 2*****,F11.8/1H ,*M 2 MODE 3*****,F11.8/1H ,*M2 OVER M1 MODE 1*****,F11.8/1H ,*M2 OVER M1 MODE 2*****,F11.8/1H ,*M2 OVER M1 MODE 3*****,F11.8/1H ,*M2 SQUARED OVER M1 MODE 1*****,F11.8/1H ,*M2 SQUARED OVER M1 MODE 2*****,F11.8/1H ,*M2 SQUARED OVER M1 MODE 3*****,F11.8/1H ,*SUM OVER 1 MODE 0*****,F11.8/1H ,*SUM OVER 2 MODES OF M2/M1*****,F11.8/1H ,*SUM OVER 3 MODES OF M2/M1*****,F11.8/1H ,*SUM OVER 1 MODE OF M2*M2/M1*****,F11.8/1H ,*SUM OVER 2 MODES OF M2*M2/M1*****,F11.8/1H ,*SUM OVER 3 MODES OF M2*M2/M1*****,F11.8/1H

```

```

TM2=M2/M1.*',F11.6/1H ,////
WRITE(6,S02) (ZNU(I),I=1,3)
S02 FORMAT(1H ,*MUE1*****,*' ,*MUE2*****,*' ,FB.4/1H ,
E* MUE2*****,*' ,FB.4/1H ,
X* MUE3*****,*' ,FB.4)
RETURN
END

```

IMPLANTATION: NO DIAGNOSTICS.

AN V LEVEL 2206 0026 (EXEC8 LEVEL E1201-0011)  
 IS DONE ON 06 SEP 73 AT 19:35:03

ENTRY POINT 000341

CODE(1) 000347; DATA(0) 000425; BLANK COMMON(2) 00000n

00006  
0003  
00001

FILES (BLOCK, NAME)

RENT (BLOCK, TYPE, RELATIVE LOCATION, NAME)

	0001	00013	121G	0000	000402	14F	00n1	000320	15L	0
14L	0001	000131	171G	0001	000137	177G	00n1	000022	2L	0
1646	0001	000265	223G	0001	000213	230G	00n1	000220	235G	0
256	0000	000347	4F	0000	000370	7F	00n0	000377	9F	0
3	0000 R	000323	AP	0000 R	000344	A1	00n0 R	000334	BLANK	0
AN	0003	000003	GAMA	0000	000414	INPS	00n0 I	000342	II	0
DOT	0003 R	000000	LAM	0000 R	000001	LTHE	00n0 R	000000	MAX	0
KP	0000 I	000346	M1	0004 I	000001	N	00n0 I	000340	NI	0
MODE	0000 R	000157	SAVE	0003 D	000001	S10	00n0 R	000343	S10R	0

### SUBROUTINE PLOT

THIS SUBROUTINE PLOTS NUTATION ANGLE VS N  
 COMMON/GHE/LAM,S10,GAMA,PKX,PKY

COMMON/FIVE/MK,N,CA

COMMON/NINE/MODE

DOUBLE PRECISION S10

REAL MAX,LAM,LINE

DIMENSION SAVE(100),LINE(110),AP(5),AH(5)

DATA BLANK,STAR,DOT/1H ,1H#,1H#/

IF(N.E.1) GO To 2

N1=(MK+50)/100

DO 1 J1=1,100

SAVE(J1)=0.

J1=0

MAX=0.

11=C

S10R=S10

1F(L/N1+N1-N) GO To 3

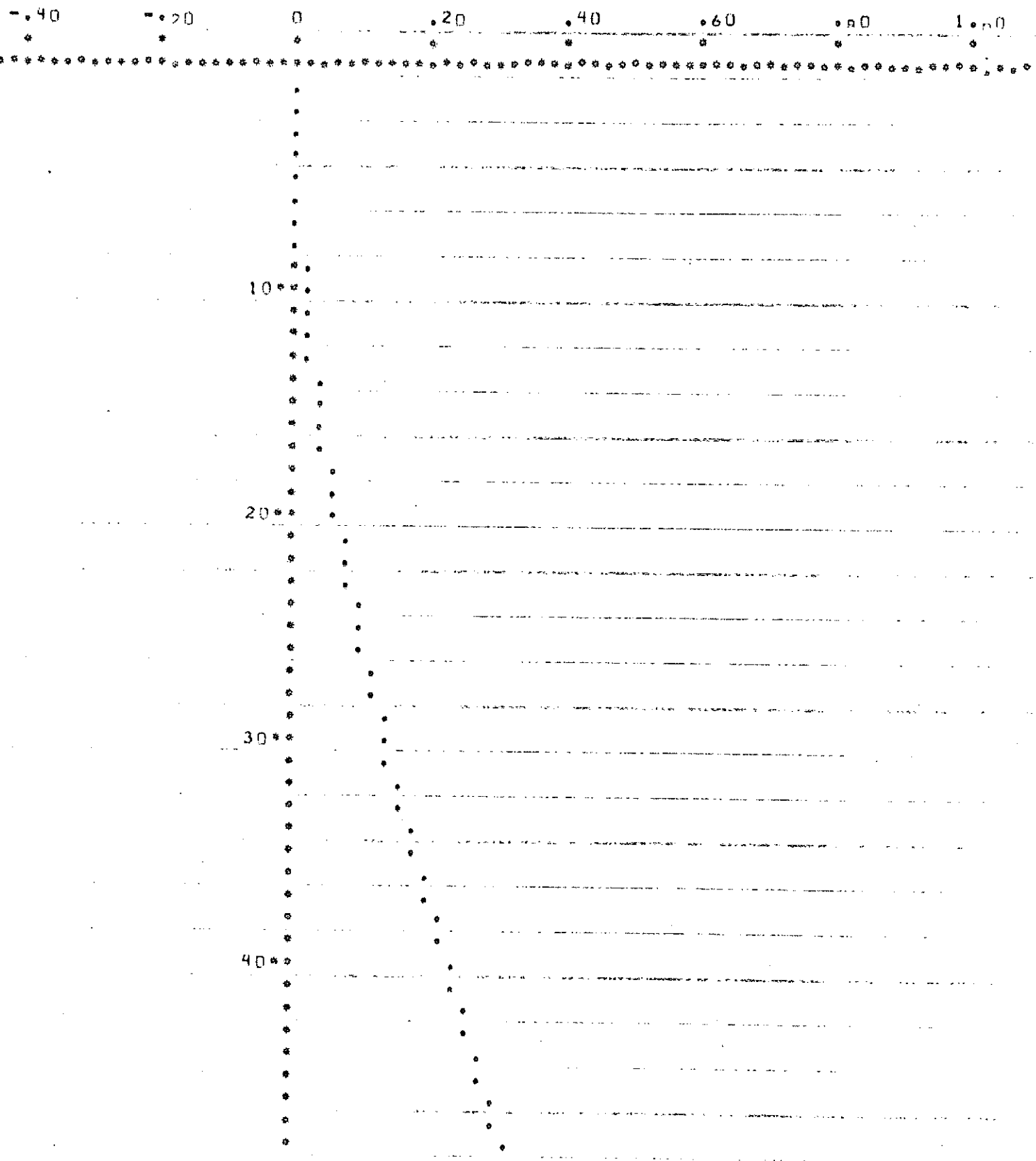
```

J1=J1+1
SAVE(J1)=CA
3 IF(ABS(CA).GT.MAX) MAX=ABS(CA)
IF(N.NE.0K) RETURN
WRITE(6,4)
4 FORMAT(1H,*PLOT OF MODESHAPE FOR*)
WRITE(6,95) LAN,S10R,MODE
95 FORMAT(1H,*LAMBDA=*,F6.0,Z1H,*SI=ZERO=*,F4.2,Z1H,*Mode=*,I2//)
A1=MAX/S0,
DO 6 I1=1,5
AN(I1)=-A1*(60.-+10.*+I1)
AP(6-I1)=-AN(I1)
I1=0
6 WRITE(6,7) AII,I1,AP
7 FORMAT(1H,14X,5(F6.2,4X),3X,I1,2X,E15X,F5.2))
DO 8 J1=1,110
LINE(J1)=BLANK
8 IF((J1+4)/10*10.EQ.(J1+4)) LINE(J1)=STAR
WRITE(6,9) LINE
9 FORMAT(1H,12X,110A1)
DO 10 J1=1,110
LINE(J1)=STAR
10 WRITE(6,9) LINE
DO 11 J1=1,110
LINE(J1)=BLANK
11 DO 13 K1=1,100
J1=SAVE(K1)/A1+S6+S
LINE(S6)=STAR
12 IF(K1/10*10.NE.K1) GO TO 12
LINE(S5)=STAR
LINE(J1)=DOT
WRITE(6,9) LINE
13 IF(K1/10*10.NE.K1) GO TO 15
IF(J1.GE.S0.AND.J1.LE.S4) GO TO 10 15
M1=N1*K1
14 WRITE(6,14) M1
FORMAT(1H+,6IX,15)
LINE(J1)=BLANK
LINE(S5)=BLANK
15 RETURN
END

```

LOCATION: NO DIAGNOSTICS.

PLOT OF MODESHAPE FOR  
LAMBDA = 10.  
SI-ZERO = .10  
MODE = 1

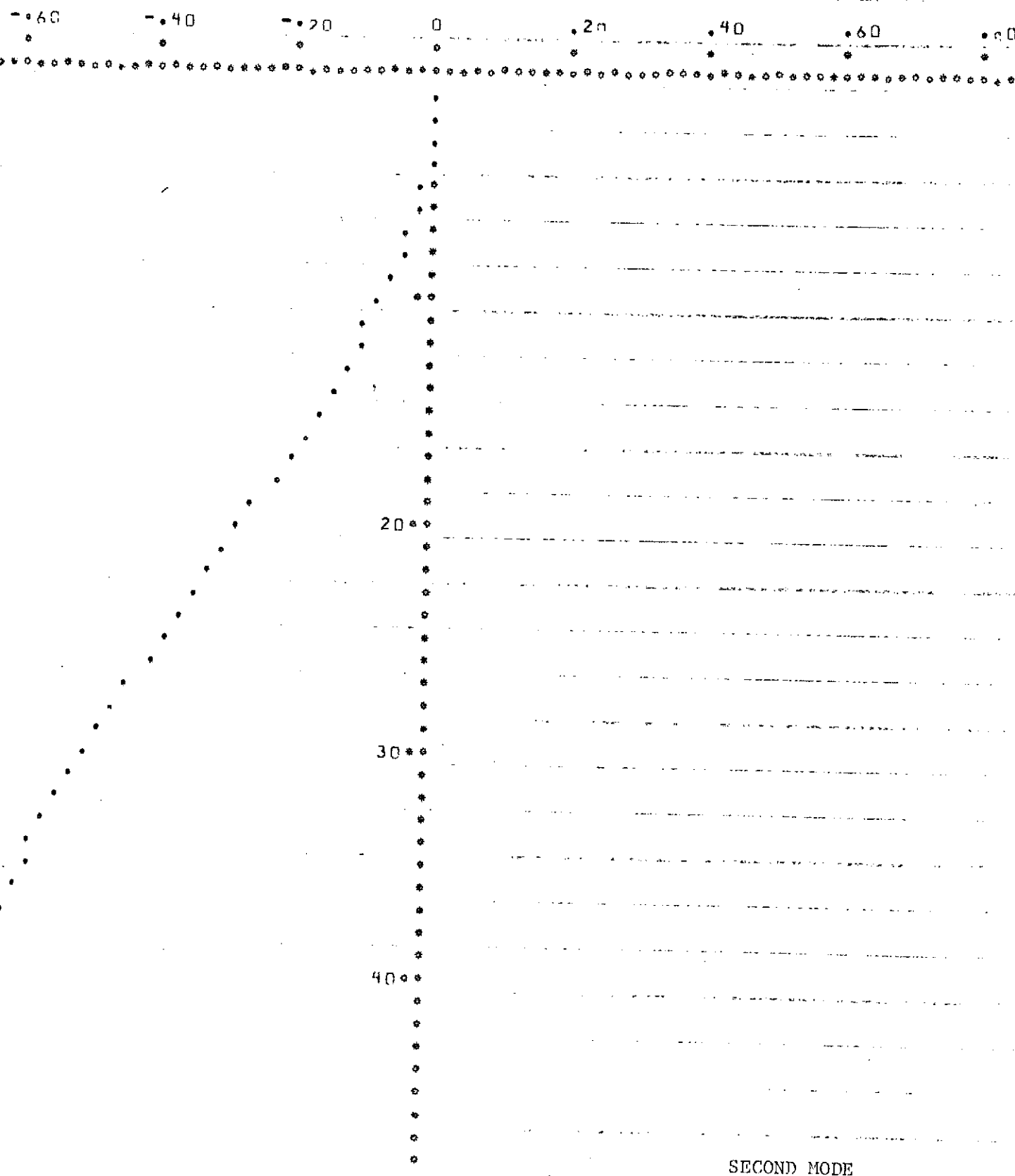


FIRST MODE

50°  
60°  
70°  
80°  
90°  
100°

FIRST MODE (CONTINUED)

PLOT OF MODESHAPE FOR  
LAMBDA = 10.  
S1-ZERO = .10  
MODE = 2



50

2-66

60

70

80

90

100

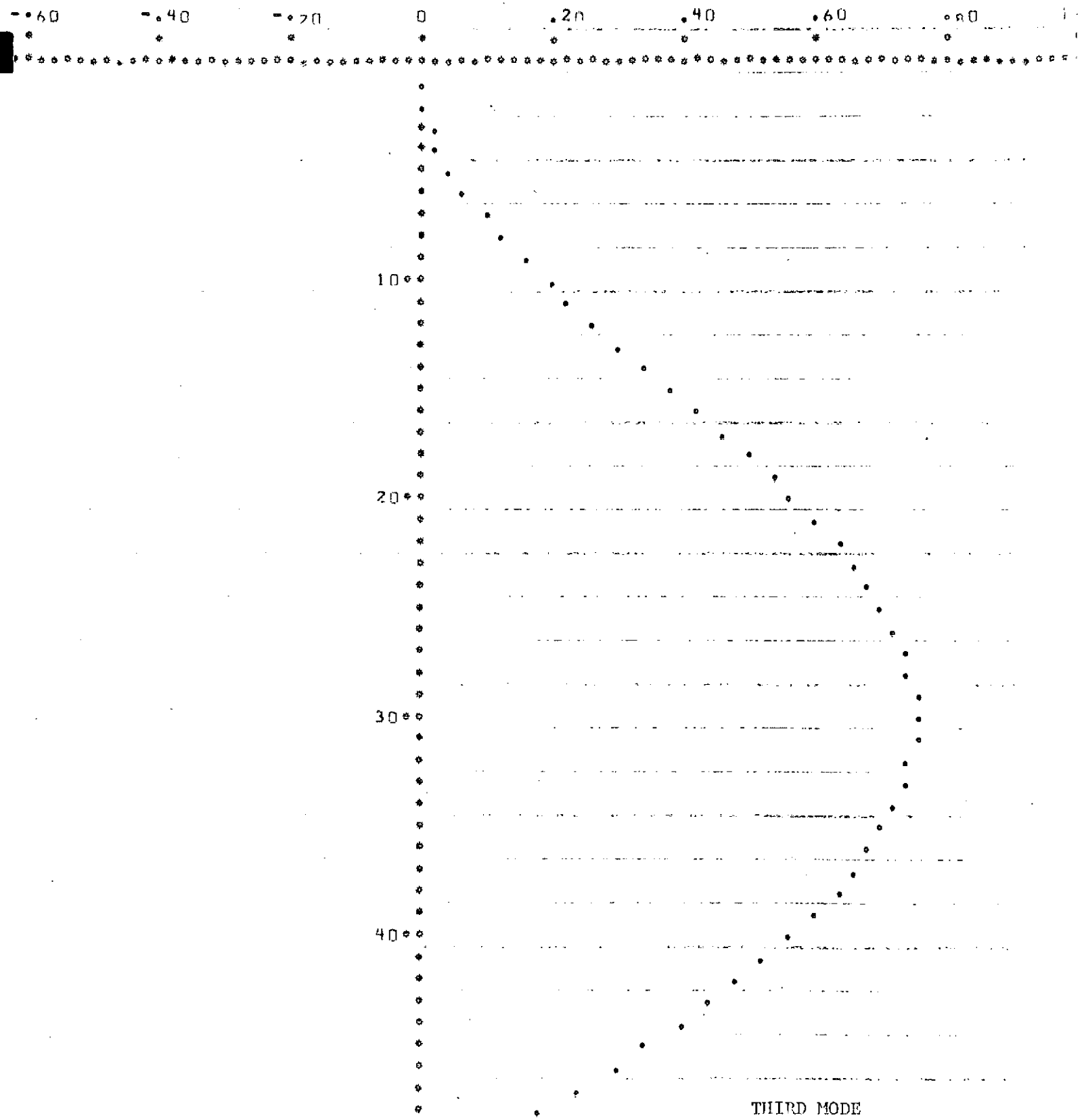
SECOND MODE (CONTINUED)

## PLOT OF MODESHAPE FOR

LAMBDA = 10.

SI-ZERO = .10

MODE = 3



THIRD MODE

50°  
60°  
70°  
80°  
90°  
100°

THIRD MODE (CONTINUED)

KSI-ZERO..... 100  
 LAMBDA..... 10.

MUS ARE FOR CASE M

MUM1..... 1.6045  
 MUM2..... 7.4763  
 MUM3..... 20.0245

M 1 MODE 1..... 25606434  
 M 1 MODE 2..... 24199705  
 M 1 MODE 3..... 24910518

M 2 MODE 1..... 32841758  
 M 2 MODE 2..... -06161919  
 M 2 MODE 3..... .02823317

M2 OVER M1 MODE 1..... 1.28255880  
 M2 OVER M1 MODE 2..... -2.28462787  
 M2 OVER M1 MODE 3..... -1.1333833

M2 SQUARED OVER M1 MODE 1..... -42121486  
 M2 SQUARED OVER M1 MODE 2..... -01566996  
 M2 SQUARED OVER M1 MODE 3..... -00319990

SUM OVER 1 MODE OF M2/M1..... 1.28255880  
 SUM OVER 2 MODES OF M2/M1..... 1.02793093  
 SUM OVER 3 MODES OF M2/M1..... 1.14126925

SUM OVER 1 MODE OF M2\*M2/M1.... -42121486  
 SUM OVER 2 MODES OF M2\*M2/M1.... -43650482  
 SUM OVER 3 MODES OF M2\*M2/M1.... -44010472

MUE1..... 1.2547  
 MUE2..... 7.4091  
 MUE3..... 19.9995

## CHAPTER 3

Application to Some Problems of Satellite Dynamics

The present chapter considers the use that can be made of the results of the previous chapter in some problems of interest in satellite dynamics<sup>[3-1]</sup>. A first field of application is in studying the nutational divergence of a satellite equipped with flexible appendages, but this is the topic of Chapter 4 and 5. We shall be considering here some other problems, such as the simulation of free oscillations, thermal flutter and variation of the spin rate due to the booms motion.

## 3.1 Simulation of free oscillations

## 3.1.1 Generalities

In a motion of type E (equatorial) or M (meridional), the free oscillations can be simulated in the following manner. Given N modes,  $\phi_j(\xi)$ ,  $\xi = 1, \dots, N$ , with associated frequencies  $\bar{\omega}_j$ , and given an initial distribution of displacements and velocities ( $t = \frac{t_{\text{dim}}}{1/\omega_s}$ )

$$\eta(\xi, 0) = \eta_0(\xi) ; \eta_t(\xi, 0) = \left( \frac{\partial \eta}{\partial t} \right)_{t=0} = \eta_{t,0}(\xi)$$

the displacement is written as a sum of modes

$$\begin{aligned} \eta &= \sum_{j=1}^N \phi_j(\xi) (c_j \cos \bar{\omega}_j t + s_j \sin \bar{\omega}_j t) \\ \eta_t &= \sum_{j=1}^N \phi_j(\xi) \bar{\omega}_j (-c_j \sin \bar{\omega}_j t + s_j \cos \bar{\omega}_j t) \end{aligned}$$

Then

$$c_j = \frac{1}{m_{j,j}} \int_{\text{boom}} \eta_0 \phi_j(\xi) d\xi$$

$$s_j = \frac{1}{m_{j,j} \bar{\omega}_j} \int_{\text{boom}} \eta_{t,0} \phi_j(\xi) d\xi$$

As an example, Figures 3.1 and 3.2 are meant to illustrate that

starting with an initial shape identical to the first mode at  $\bar{\lambda} = 10$ ,  $\xi_0 = 0.1$ , with no initial velocities, the stationary wave which exists in this case cannot be maintained if  $\bar{\lambda}$  is changed to 100. Not only has the frequency changed appreciably ( $\tau_1$  is the period of the first mode oscillation for  $\bar{\lambda} = 10$ ,  $\xi_0 = 0.1$ ), but the second mode is present to an appreciable extent.

### 3.1.2 Application to Satellite UK-4

From data received through NASA GSFC on satellite UK-4, we computed the eigenfrequencies and modal shapes for satellite UK-4. This satellite has the following physical characteristics:

#### UK-4 Computations

$$\begin{aligned}\omega_s &= 30 \text{ rpm; } 15 \text{ rpm; } 6 \text{ rpm.} \\ \rho &= 0.00058 \text{ lb mass/in} \\ &= \frac{5.8 \times 10^{-4}}{2.54} \times 10^2 \times .45359 \text{ kg/m} \\ &= 1.036 \times 10^{-2} \text{ kg/m}\end{aligned}$$

$$EI = 10^3 \text{ lbf in}^2$$

$$= 10^3 \times 4.448 \text{ newton in}^2$$

$$= 10^3 \times 4.448 \times 2.54^2 \times 10^{-4} \text{ newton m}^2$$

$$= 2.869 \text{ newton m}^2$$

$$x_0 = 11.6 \text{ inches}$$

$$l = 276 \text{ inches} = 7.01 \text{ m}$$

$$\xi_0 = \frac{x_0}{l} = .042$$

$$I_{zh} = 18.348 \text{ slug ft}^2$$

$$1 \text{ slug} = 14.5938 \text{ kg mass}$$

$$I_{zh} = 18.348 \times 32.1741 \times .4539 \text{ kg ft}^2$$

$$= 24.876 \text{ kgm}^2$$

$$I_{xh} = 17.41 \text{ slug ft}^2$$

$$I_{yh} = 16.54 \text{ slug ft}^2$$

$$\text{ETKIN'S NUMBER: } \bar{\lambda} = \omega_s^2 \frac{\rho l^4}{EI}$$

$$\bar{\lambda}_{30 \text{ rpm}} = \left( \frac{30 \times 2\pi}{60} \right)^2 \times 1.036 \times 10^{-2} \times \frac{(7.01)^4}{2.869}$$

$$= (3.141592)^2 \times 1.036 \times 10^{-2} \times 7.01^4 / 2.869$$

$$= 86.06$$

$$\bar{\lambda}_{15\text{rpm}} = \frac{1}{4}(\bar{\lambda})_{30\text{rpm}} = \frac{86.06}{4} = 21.515$$

$$\bar{\lambda}_{6\text{rpm}} = \frac{86.06}{25} = 3.44$$

Data for programs:

$$\bar{\lambda} = 1; 3.44; 10; 16.8; 21.515; 50; 86.06; 100$$

$$\xi_0 = .042$$

$\bar{I}_p$  determined from

$$[(\frac{I_{zh}}{I_{xh}} - 1)(\frac{I_{zh}}{I_{yh}} - 1)]^{1/2} = \frac{I_z}{\bar{I}_p} - 1$$

giving

$$\frac{I_{zh}}{\bar{I}_p} = 1.0767$$

Results (see graphs)

Graph 1: Resonance on thermal flutter at  $\sqrt{\bar{\lambda}} = .4$  or  $\bar{\lambda} = 16.$ , i.e. at spin rate

$$\omega_s = \omega_{1,\text{rot}} = 1.35 \text{ rad/sec} = 12.9 \text{ rpm}$$

Graph 2 : Mode shapes

$$\omega_s = 6; 15; 30 \text{ r.p.m.}$$

## SATELLITE UK4: ATTITUDE STABILITY

Table I: Case M

$\omega$ (rpm)	6	10.2	13.25	15	22.8	30	32.3
$\bar{\lambda}$	3.44	10.0	16.8	21.515	50	86.06	100.0
$\sqrt{\bar{\lambda}}$	1.84	3.162	4.1	4.64	7.07	9.28	10.0
$\omega_{n_1} \sqrt{\rho \ell^4 / EI}$	4.08	4.98	5.76	6.24	8.56	10.75	11.48
$\omega_{n_1}$	1.38	1.685	1.945	2.11	2.895	3.63	3.88

Table III: Case E

$\omega$ (rpm)	3.23	6.0	10.2	13.25	15	22.8	30	32.3
$\bar{\lambda}$	1.0	3.44	10.0	16.8	21.515	50	86.06	100.0
$\sqrt{\bar{\lambda}}$	1.0	1.84	3.162	4.1	4.64	7.07	9.28	10.0
$\omega_{n_1} \sqrt{\rho \ell^4 / EI}$	3.55	3.64	3.85	4.05	4.18	4.82	5.44	5.64
$\omega_{n_1}$ (Hz)	1.2	1.23	1.30	1.37	1.415	1.63	1.84	1.905

$$\sqrt{\rho \ell^4 / EI} = \sqrt{8.715} = 2.96$$

Resonance on Thermal Flutter at  $\sqrt{\bar{\lambda}} = 4.00$ ,  $\bar{\lambda} = 16.0$

$$\omega_s = \omega_n = 4.0 / 2.96 = 1.35 \text{ (Hz)}$$

$$= 12.90 \text{ rpm.}$$

$K_p > 1$  No posigrade resonance  
No nutational instability

Var. of spin rate for 10% defl.

.57%	30 RPM
.785%	15 RPM

Fig. 3.3 represents the first mode of vibration for the three values of the spin rate being contemplated. Centrifugal effects are noted as Etkin's number  $\bar{\lambda}$  is increased.

### 3.2 Resonant thermal flutter

#### 3.2.1 Determination of resonant frequency

It has been shown by Etkins and Hughes<sup>[3-2]</sup> that assuming a relatively simple model for the boom's thermal curvature  $\bar{E}_{T_0}$  (independent of  $\xi$ ) due to the sun's heat input during the spinning motion, the steady-state oscillation of the booms would be described by

$$\eta = \bar{E}_{T_0} \cos \omega_s (t - t_0)$$

In order to find for which spin rate  $\omega_s$  the motion will diverge (have an amplitude tending to infinity), these authors solved equation for boundary conditions,

$$E(0) = 0 \quad E'(0) = 0 \quad E''(0) = \bar{E}_{T_0} \quad E'''(0) = 0$$

and very  $\bar{\lambda}$  until very large values of  $\Phi(l)$  are observed. The analysis was limited to satellites of zero radius.

An alternative approach was proposed<sup>[3-1]</sup>, which is recalled here. If in Equation (2.2-8), we let  $\omega_1$  tend continuously to  $\omega_s$  along the eigenfrequencies curves  $\bar{\omega}_1(\bar{\lambda}, \xi_0)$ ; the spatial part of a solution to Equation (2.2-7), normalized to unity at the tip, satisfies b.c.

$$\phi(0) = 0 \quad \phi'(0) = 0 \quad \phi''(0) = 0 \quad \phi''(l) = 0$$

In order to also admit boundary conditions 0,0 for the zeroth and first

derivatives at  $\xi = 0$ ,  $\bar{\lambda}_{T0}$ , 0 for the second the third derivatives at  $\xi = 1$ ,  $\phi(\bar{\lambda}, \xi_0)$  should be scaled up by an infinite factor, i.e., the amplitude at the tip tends to infinity. Thus, resonance on thermal flutter will correspond to the intersection of the curve, for given  $\xi_0$

$$\omega_i \left( \frac{p^4}{EI} \right)^{1/2} = f(\sqrt{\bar{\lambda}})$$

with the bisectrix of the first quadrant (Fig. 3.4)

$$\frac{\omega_i}{\omega_s} = 1$$

No thermal flutter resonance can occur for

a)  $\xi_0 > 0.7$

b) second or higher modes

as is shown on Fig. 2.2.

### 3.2.2 Application to UK-4

Using the above data for UK-4, the thermal flutter resonance point was found at (Fig. 3.5)

$$\bar{\lambda} = 16.0 \quad (\xi_0 = 0.042)$$

and for the physical characteristics of the satellite, this translates to

$$\omega_{s, \text{critical}} = 1.35 \text{ Hz} = 12.90 \text{ rad/m.}$$

a spin rate to be avoided for steady-state operation.

## 3.3 Variation of the spin rate due to the free oscillations

### 3.3.1 Method of calculation

It is often of interest to satellite users to know what amount of spin rate variation can be expected, due to the vibrations of

the boom. The equatorial vibrations will cause a very slight variation of the spin rate described by

$$I_{\text{hub}} \frac{d\omega_s}{dt} = T$$

where  $T$  is a torque due to the moment at the root of the boom and to the shear force acting through the central hub radius. This is described in non-dimensional form by ( $\bar{\tau} \equiv \omega_* t$ )

$$\begin{aligned} \frac{d\bar{\omega}}{d\bar{\tau}} &= \frac{1}{I_{\text{hub}} \omega_*^2} \frac{\xi I}{\ell} \eta_{\max} [\eta_{\xi\xi} - \xi_0 \eta_{\xi\xi\xi}]_{\xi=0} \\ &= \frac{\rho \ell^3}{I_{\text{hub}}} \frac{1}{\sqrt{\lambda}} \eta_{\max} \bar{T} \\ \bar{T} &\stackrel{\text{def}}{=} [\eta_{\xi\xi} - \xi_0 \eta_{\xi\xi\xi}]_{\xi=0} \\ \text{or, after integration, and with } \Gamma &\stackrel{\text{def}}{=} \frac{\rho \ell^3}{I_{\text{hub}}}, \end{aligned}$$

$$\left[ \frac{\Delta \omega_s}{\omega_s} \right]_{\max} \frac{1}{\Gamma \eta_{\max}} = \frac{1}{\sqrt{\lambda}} \int_0^{\bar{\tau}_*} \bar{T} d\bar{\tau} \quad (3.3-1)$$

in which  $\bar{\tau}_*$  is the value of  $\bar{\tau}$  maximizing the integral. This value can be obtained using a program such as SIM, which is listed at the end of this chapter.

### 3.3.2 Application to UK-4

Using the above data for satellite UK-4, the maximum variation of the spin rate for an assumed 10% deflection of the boom was determined to be

$$0.57\% \text{ at } \omega_s = 30 \text{ r.p.m.}$$

$$0.755\% \text{ at } \omega_s = 15 \text{ r.p.m.}$$

REFERENCES - Chapter 3

- [3-1] RENARD, M.L. and RAKOWSKI, J.E.: "Equatorial Vibrations of a Long Flexible Boom on a Spin-Stabilized Satellite of Non-Zero Radius," Proc. of the Astronautical Congress, October 1969. Vol. 1, pp. 35-53, E. Lunc (Editor), Pergamon Press, 1971.
- [3-2] ETKIN, B. and HUGHES, P.C.: "Explanation of the anomalous spin behavior of satellites with long flexible antennae," Jour. of Spacecraft and Rockets, 4, 9, 1139-1145.

DISPLACEMENT

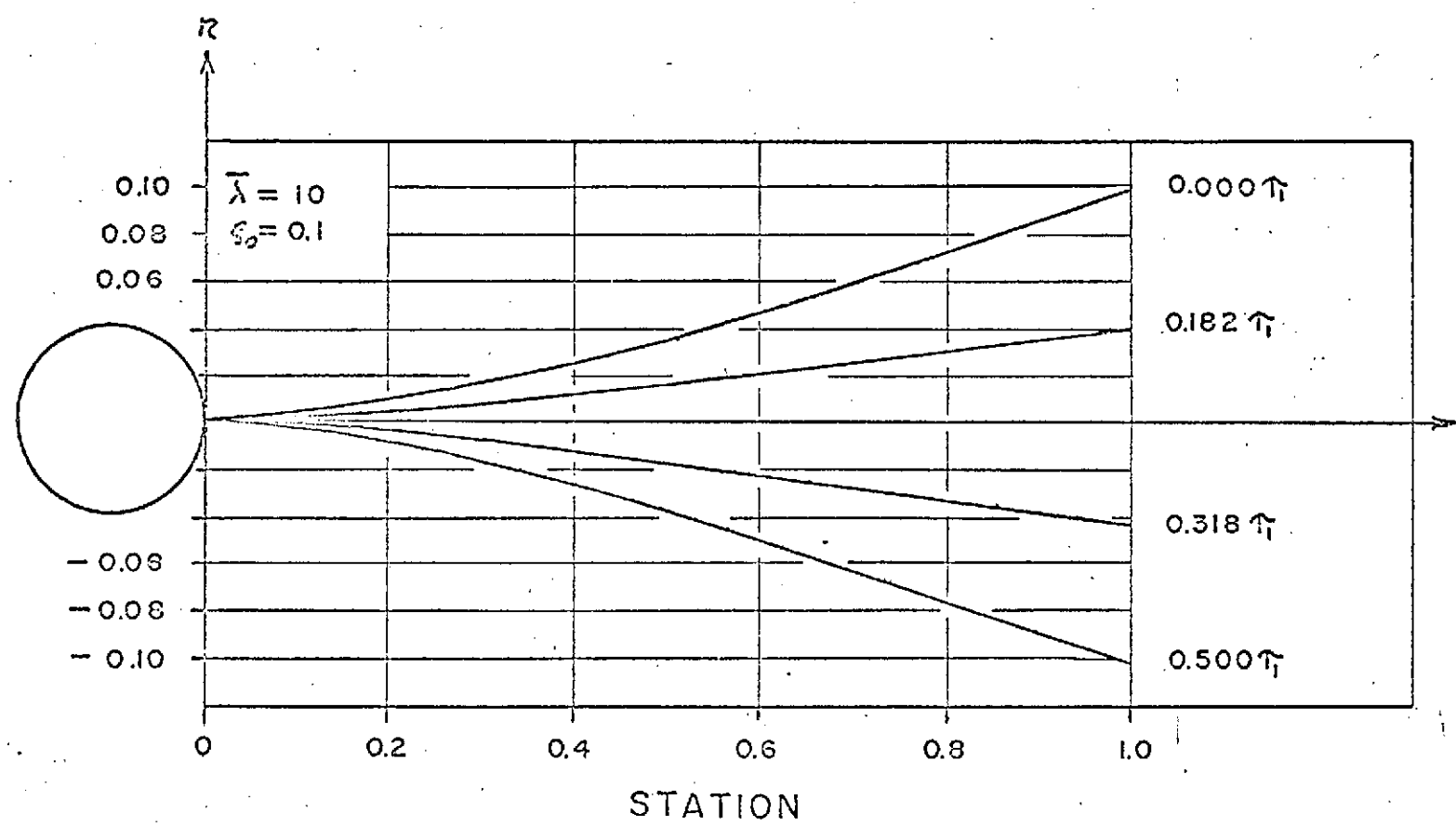


FIG. 3-1. FIRST MODE VIBRATION IN ROTATING AXES  
FOR THE REFERENCE CASE

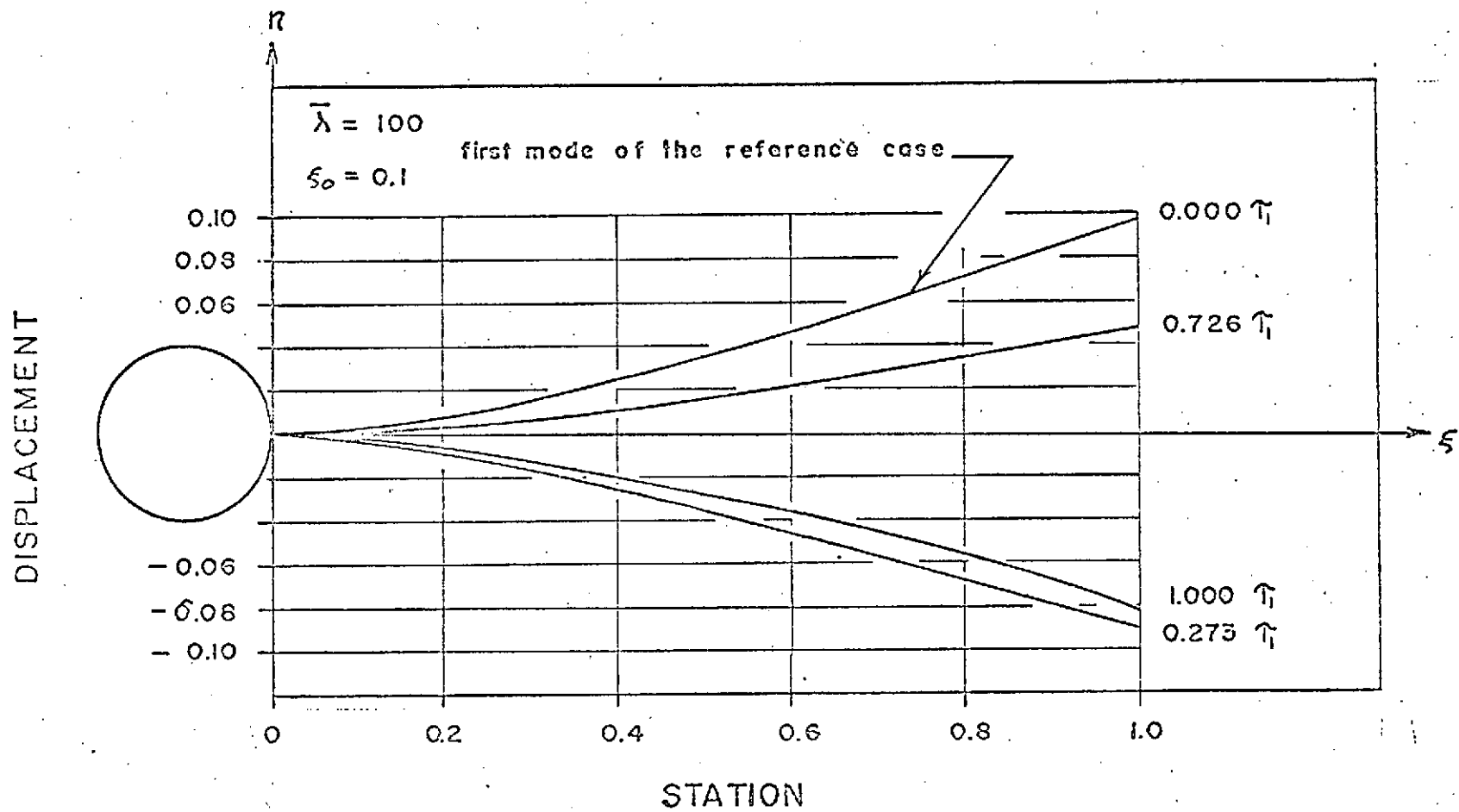


FIG. 3-2.

VIBRATION IN ROTATING AXES WITH THE REFERENCE CASE FIRST MODE AS INITIAL SHAPE

SATELLITE UK-4 : MODE SHAPES

$$\xi_0 = 0.042$$

- I -:  $\bar{\lambda} = 3.44$ ,  $\mu = 2.202$ , spin = 6 rpm  
 II -:  $\bar{\lambda} = 21.515$ ,  $\mu = 1.34594$ , spin = 15 rpm  
 III -:  $\bar{\lambda} = 86.06$ ,  $\mu = 1.15914$ , spin = 30 rpm

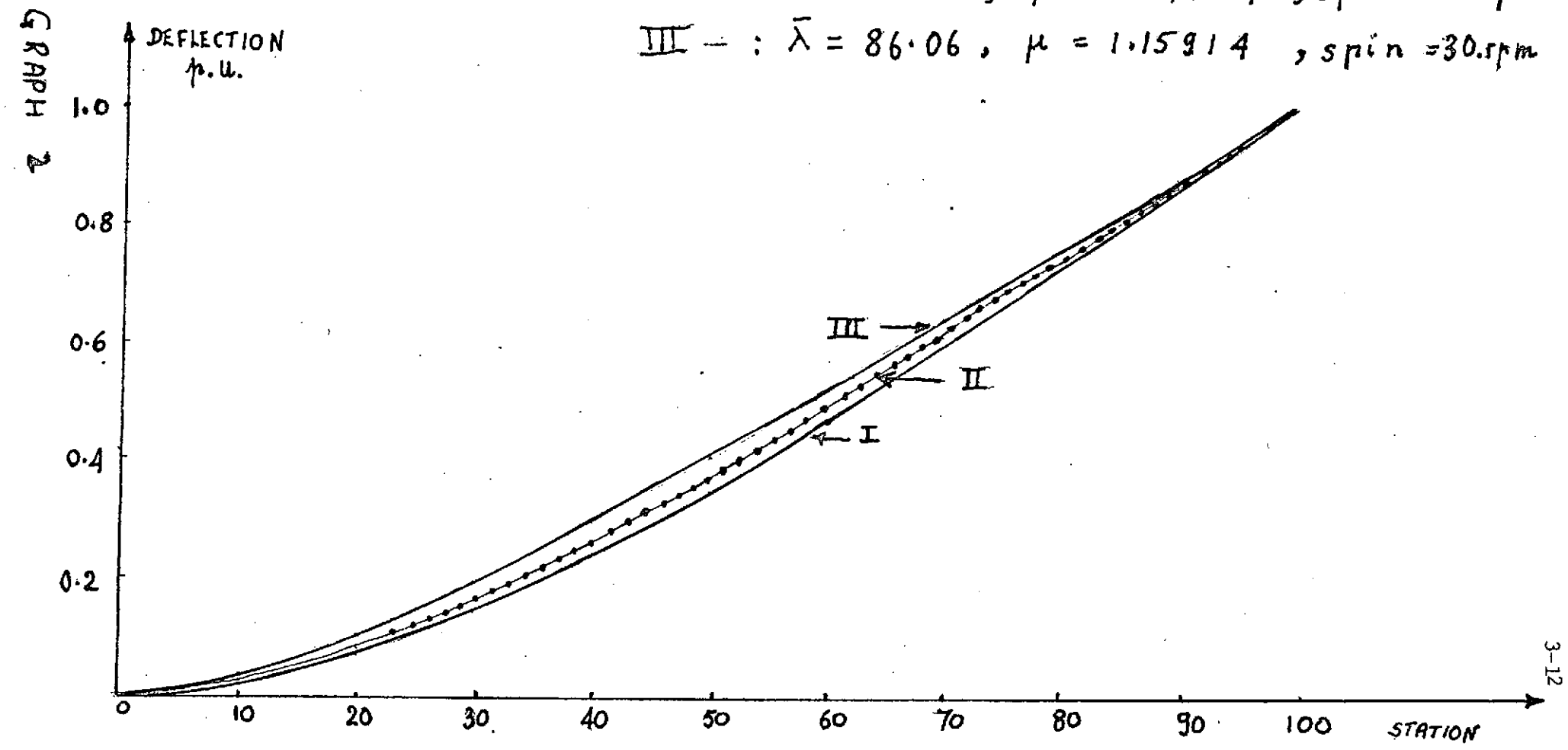


FIG. 3-3. FIRST MODE SHAPE FOR UK-4.

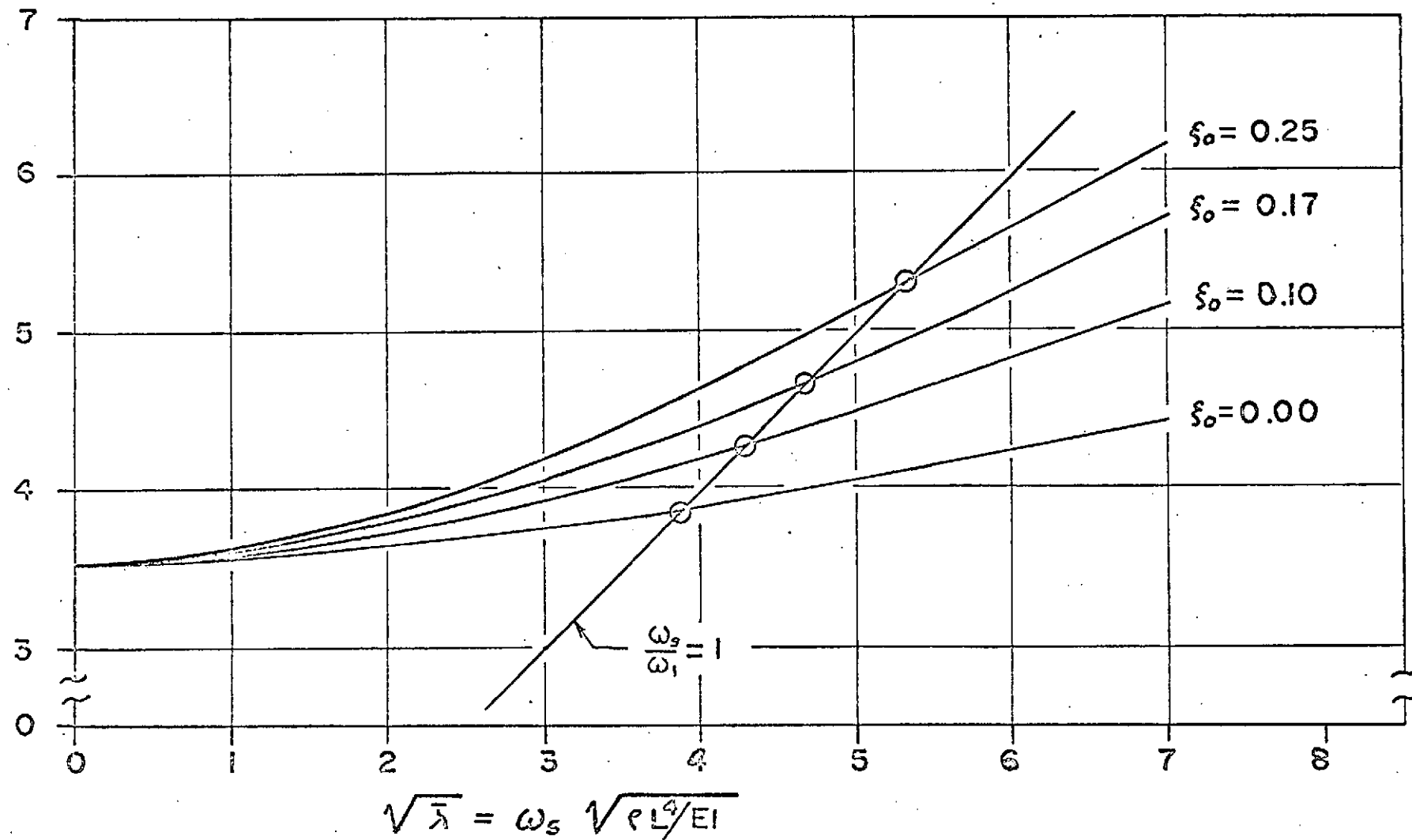


FIG.3-4 RESONANT VALUES OF THE FUNDAMENTAL FREQUENCY

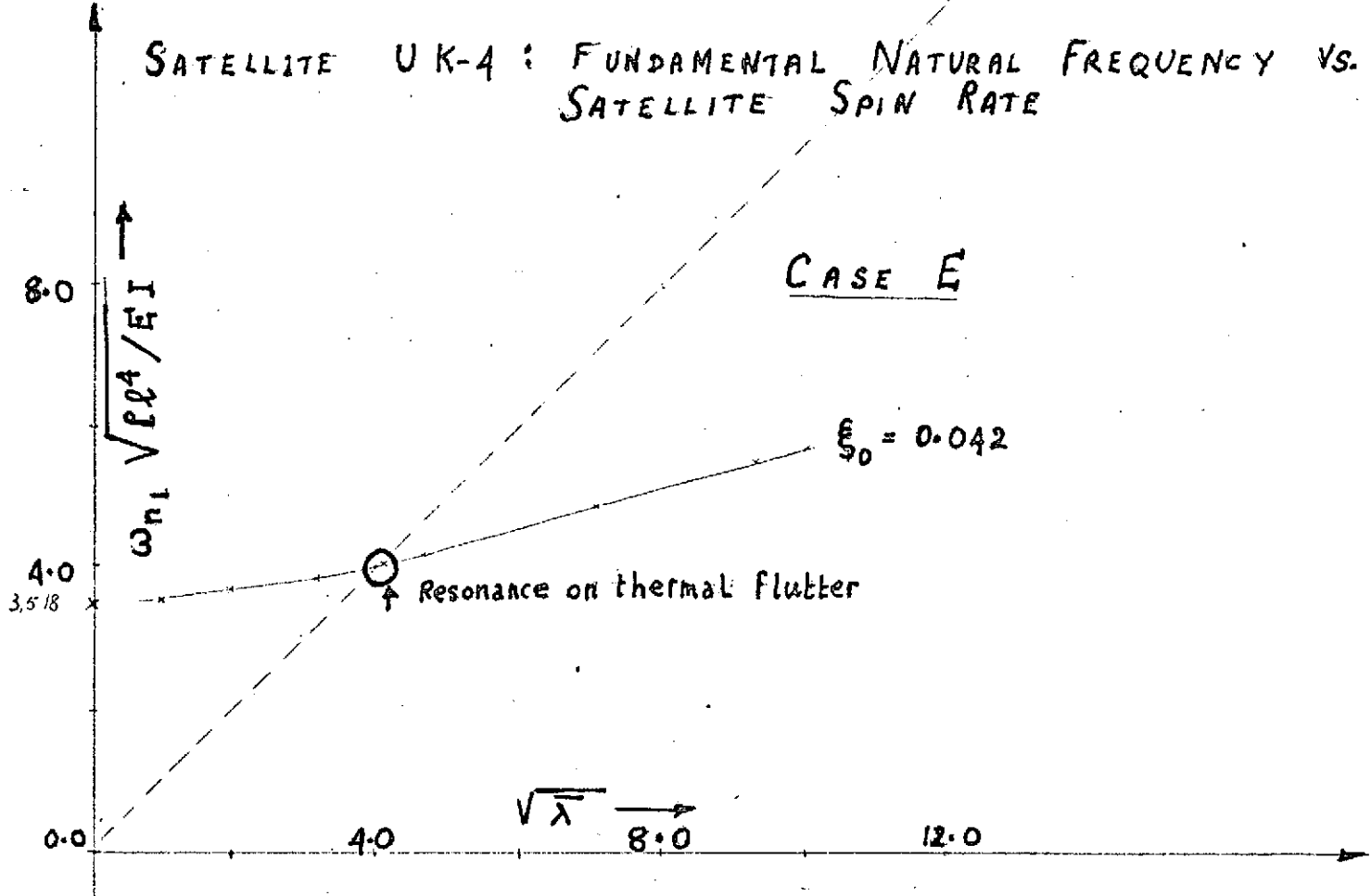


FIG. 3-5. RESONANCE ON THERMAL FLUTTER: UK-4.

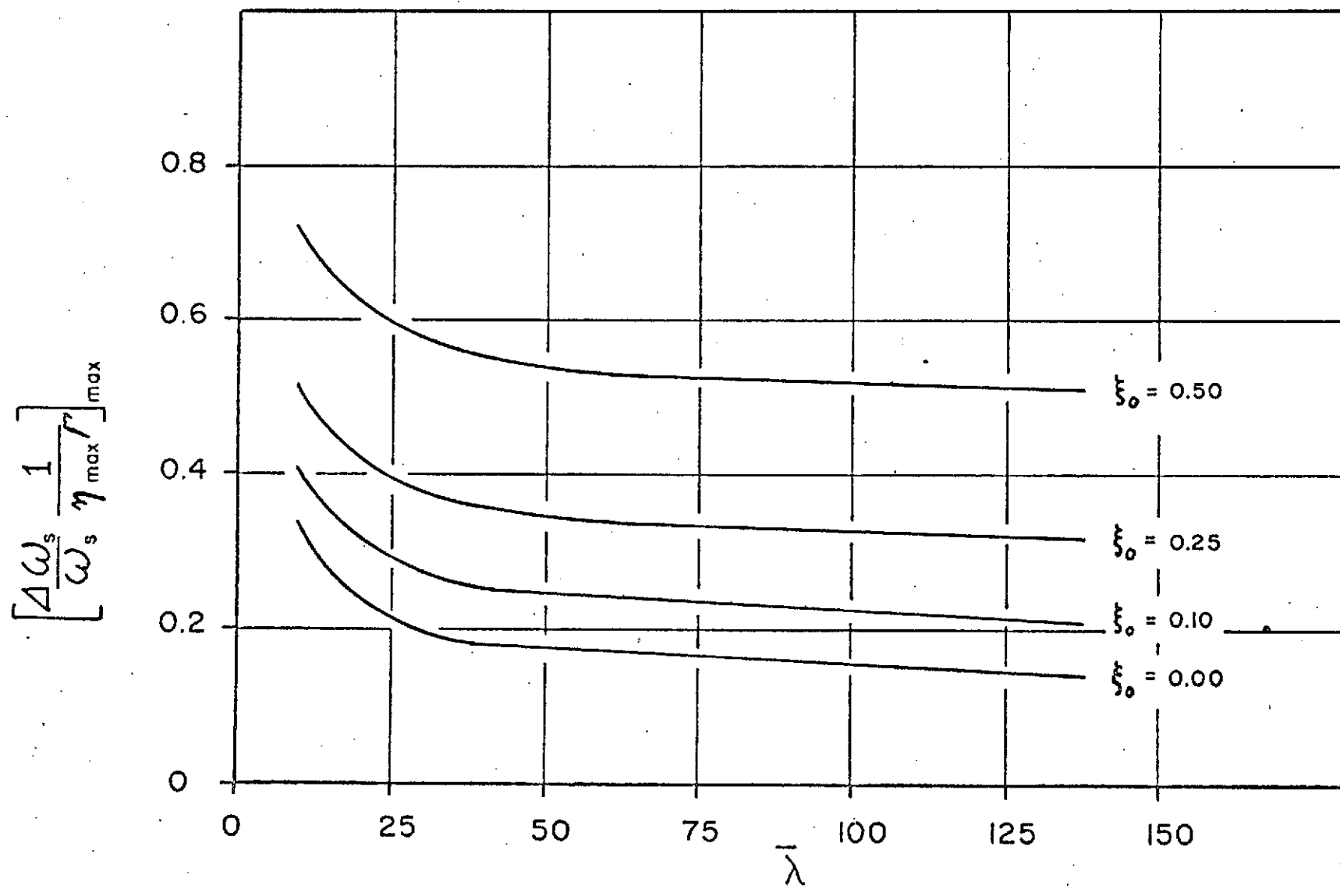


FIG. 3-6  
SPIN VARIATION versus  $\bar{\lambda}$

PROGRAM SIM

LISTING

\$DUP E730MR18, ,PRINT,BCD

@FOR SIM

SUBROUTINE SIM(NDS)

DOUBLE PRECISION MU,XNO,YNO

REAL NU

INTEGER SAM

SIM

C

C

C THIS PROGRAM COMPUTES THE DISPLACEMENT OF THE FREELY VIBRATING  
C ROTATING BOOM AT SPECIFIED STATIONS, STARTING FROM A GIVEN  
C DISPLACEMENT INITIAL CONDITION

C

C IT COMPUTES THE NONDIMENSIONAL SPIN VARIATION AND INDUCED NUTATION  
C ANGLE FOR EITHER THE EQUATORIAL OR MERIDIAN BOOM (SEE NDS BELOW)

C

COMMON/DONE/MU,LAM,SIO,RGAMA,PK,NU,XNO,YNO

DOUBLE PRECISION COR,ME1,ME2

DOUBLE PRECISION P(4),K(4),M(4),L(4),E3(101),E31P(101),E32P(101),  
1E33P(101),E34P(101),E4(101),E41P(101),E42P(101),E43P(101),  
3E44P(101),A,B,C,E,AD,BO,CO,EO,

4SIO,SI

DOUBLE PRECISION EDA(2),EIG(2)

REAL H,NN,LAM

INTEGER I,D,N,Z, NINT,INTER

DOUBLE PRECISION ELSM3(2),ELSM4(2)

DOUBLE PRECISION EMOM3(2),EMOM4(2),ESHR3(2),ESHR4(2),

1RMOM3(2),RMOM4(2),RSHR3(2),RSHR4(2),BPT(101,2),TFAC(2),  
2COFDIST(2,2),ALFA(2), MMX3(101,2),MMX4(101,2),BETA(2),MUI

DIMENSION AA(2,2),BBB(2),CCC(2),GAMA(2),CC2(2)

INTEGER PPP(2),QQQ(2)

DOUBLE PRECISION RTORK,DTORK,EDA2P1,EDA3P1

REAL DLTT,MODE

GAMA(1)=RGAMA

GAMA(2)=0.0

EIG(1)=MU

EIG(2)=0.

EDA(1)=XNO

EDA(2)=YNO

IEND=1

MAXT=27

STP=25.

NR=2

C\*\*\* THIS PROGRAM USES REVERSED INTEGRATION ONLY

WRITE(6,300)

300 FORMAT('OSIMULATION ENTERED')

C NDS = DIRECTION SWITCH

C NDS = 1 IN PLANE, = 0 OUT OF PLANE

C\*\*\* SET IBIG=1 TO READ BIGMODE 1 ONLY

IVAR=1

IBIG=1

IFIRST=1

KK=1

N=1

NINT=100

```

INTER=NINT+1
74 ANFRQ=SQRT(LAM)
      WRITE(6,60) ANFRQ
60 FORMAT(1H , 'NFRQ=SQRT LAM=', F10.5)
99 SI=0.

```

C  
C CLEAR ARRAYS  
C

```
DO 31 I=1,4
```

```
K(I)=0.
```

```
L(I)=0.
```

```
M(I)=0.
```

```
31 P(I)=0.
```

```
DO 1 I=1,101
```

```
E34P(I)=0.
```

```
E44P(I)=0.
```

```
E33P(I)=0.
```

```
E43P(I)=0.
```

```
E32P(I)=0.
```

```
E42P(I)=0.
```

```
E31P(I)=0.
```

```
E41P(I)=0.
```

```
E4(I)=0.
```

```
1 E3(I)=0.
```

```
H=1./FLOAT(NINT)
```

```
D=3
```

```
8 IF(D.EQ.4) GO TO 2
```

```
B0=0.
```

```
E3(1)=1.
```

```
E0=E3(1)
```

```
C0=0.
```

```
A0=0.
```

```
GO TO 3
```

```
2 C0=0.
```

```
E41P(1)=1.
```

```
A0=E41P(1)
```

```
B0=0.
```

```
E0=0.
```

```
3 A=A0
```

```
B=B0
```

```
C=C0
```

```
E=E0
```

```
N=1
```

```
4 I=1
```

```
NN=N
```

```
SI=(NN-1.)*H
```

```
5 K(I)=H*A
```

```
L(I)=H*B
```

```
M(I)=H*C
```

```
MU1=1.+EIG(KK)*EIG(KK)
```

```
IF(NDS.EQ.1) GO TO 40
```

```
MU1=MU1-1.
```

```
40 P(I)=((-SI*SI+2.*SI*(1.+S10))/2.*B
      1+(1.-SI+S10)*A+MU1*E)*LAM*H
```

```

SI=(NN-1.)*H
I=I+1
IF(I.GT.3) GO TO 6
Z=I-1
E=EO+K(Z)/2.
A=AO+L(Z)/2.
B=BO+M(Z)/2.
C=CO+P(Z)/2.
SI=SI+H/2.
GO TO 5
IF(I.GT.4) GO TO 7
E=EO+K(3)
A=AO+L(3)
B=BO+M(3)
C=CO+P(3)
SI=SI+H
GO TO 5
IF(0.EQ.4) GOTO 9
SI=NN*H
Z=N+1
E3(Z)=E3(N)+(K(1)+2.*K(2)+2.*K(3)+K(4))/6.
E31P(Z)=E31P(N)+(L(1)+2.*L(2)+2.*L(3)+L(4))/6.
E32P(Z)=E32P(N)+(M(1)+2.*M(2)+2.*M(3)+M(4))/6.
E33P(Z)=E33P(N)+(P(1)+2.*P(2)+2.*P(3)+P(4))/6.
E34P(Z)=LAM*((S10+1.)*2-(1.-SI+S10)**2)
1*E32P(Z)/2.+((1.-SI+S10)*E31P(Z)+MUL*E3(Z))
E=E3(N+1)
A=E31P(N+1)
B=E32P(N+1)
C=E33P(N+1)
AO=A
BO=B
EO=E
CO=C
N=N+1
IF(N.LT.INTER) GO TO 4
EMOM3(KK)=E3(INTER)
ELSM3(KK)=E32P(1)
RMOM3(KK)=E32P(INTER)
ESHR3(KK)=E33P(1)
RSHR3(KK)=E33P(INTER)
DO 28 I=1,101
  MMX3(I,KK)=E3(I)
  D=4
  GOTO 2
SI=NN*H
Z=N+1
E4(Z)=E4(N)+(K(1)+2.*K(2)+2.*K(3)+K(4))/6.
E41P(Z)=E41P(N)+(L(1)+2.*L(2)+2.*L(3)+L(4))/6.
E42P(Z)=E42P(N)+(M(1)+2.*M(2)+2.*M(3)+M(4))/6.
E43P(Z)=E43P(N)+(P(1)+2.*P(2)+2.*P(3)+P(4))/6.
E44P(Z)=LAM*((S10+1.)*2-(1.-SI+S10)**2)
1*E42P(Z)/2.+((1.-SI+S10)*E41P(Z)+MUL*E4(Z))
E=E4(N+1)

```

A=E41P(N+1)

B=E42P(N+1)

C=E43P(N+1)

EO=E

AO=A

BO=B

CO=C

N=N+1

IF(N.LT.INTER) GO TO 4

EMOM4(KK)=E4(INTER)

ELSM4(KK)=E42P(1)

RMOM4(KK)=E42P(INTER)

ESHR4(KK)=E43P(1)

RSHR4(KK)=E43P(INTER)

DO 29 I=1,101

29 MMX4(I,KK)=E4(I)

94 CONTINUE

ALFA(KK)=EMOM3(KK)/EMOM4(KK)

BETA(KK)=MMX3(1,KK)-ALFA(KK)\*MMX4(1,KK)

GAMA(KK)=EIG(KK)\*SQRT(LAM)

DO 102 LB=1,101

LL=102-LB

102 BPT(LL,KK)=(MMX3(LB,KK)-ALFA(KK)\*MMX4(LB,KK))/BETA(KK)

SUM=0.

DO 216 I=2,101

216 SUM=SUM+(BPT(I,1)+BPT(I-1,1))/2.\*((FLOAT(I)-1.5)\*H+S10)\*H

ME2=SUM

SUM=0.

DO 218 I=2,101

218 SUM=SUM+(BPT(I,1)\*#2+BPT(I-1,1)\*#2)/2.\*H

ME1=SUM

COR=ME2\*ME2/ME1

IF(IFRST.NE.1) GO TO 92

EDA(1)=BPT(51,1)

EDA(2)=BPT(101,1)

92 WRITE(6,98) EDA(1),EDA(2)

98 FORMAT(1H,'INITIAL DISPLACEMENTS',6X,F12.6,3X,F12.6/)

WRITE(6,105) ME1,ME2,COR,NDS

105 FORMAT(1H,'M1=',D12.6,3X,'M2=',D12.6,3X,'COR=',D12.6,13X,'NDS=',I3/)

72 IF(IBIG.NE.1) GO TO 73

GAMA(1)=EIG(1)\*ANFRQ

GAMA(2)=0.

CC2(1)=1.

CC2(2)=0.

ALFA(2)=0.

RMOM3(2)=0.

RSHR3(2)=0.

RSHR4(2)=0.

ELSM3(2)=0.

ELSM4(2)=0.

ESHR3(2)=0.

EIG(2)=0.

```

73 DO 213 I=1,2
213 WRITE(6,214)ALFA(I),I
214 FORMAT(1H , 'ALFA=',012.6,3X,'KK=',I3)
     IF(TBIG>EQ.I) GO TO 109
     DO 104 KK=1,2
     MM=51
     DO 104 LL=1,2

```

C C THESE COEFFICIENTS FIT THE BOOM TO INITIAL DISPLACEMENTS

C C COFDDIS(LL,KK)=BPT(MM,KK)
AA(LL,KK)=COFDDIS(LL,KK)

```
104 MM=MM+50
```

C C GJR IS USED TO INVERT THE COEFFICIENT MATRIX

```

CALL GJR(AA,2,BBB,CCC,PPP,QQQ,$113)
DO 161 I=1,NR
SUMM=0.
DO 160 J=1,NR
160 SUMM=SUMM+AA(I,J)*EDA(J),
CC2(I)=SUMM
161 WRITE(6,162)CC2(I),I
162 FORMAT(1H , 'CC2=',E12.6,3X,'I=',I3)

```

C C MODAL SOLUTION FORM HERE

```

109 FF=0.
FEE=0.
RTORK=0.
DTORK=0.
TINT=0.
DLTT=1.0/(STP*GAMA(1))*2.*3.1416
WRITE(6,50)DLTT
50 FORMAT(1H , 'DLTT=',F10.5/)
SFAC=1./EIG(1)
WRITE(6,131) SFAC
131 FORMAT(1H , 'THE NO. OF ROT CYC PER FUND VIB CYC IS',F10.4/)
DO 122 I=1,MAXT
T=DLTT*FLOAT(I-1)
DO 129 KK=1,2
129 TFAC(KK)=CC2(KK)*COS(GAMA(KK)*T)
EDA2P1=0.
EDA3P1=0.
EDAE2=0.
EDAE3=0.
DO 119 KK=1,2
SUM2=(RMOM3(KK)-ALFA(KK)*RMOM4(KK))*TFAC(KK)
SUM3=(RSHR3(KK)-ALFA(KK)*RSHR4(KK))*TFAC(KK)
SUM6=(ELSM3(KK)-ALFA(KK)*ELSM4(KK))*TFAC(KK)
SUM7=(ESHR3(KK)-ALFA(KK)*ESHR4(KK))*TFAC(KK)
EDAE2=EDAE2+SUM6

```

EDAE3=EDAE3-SUM7  
EDA2P1=EDA2P1+SUM2  
119 EDA3P1=EDA3P1-SUM3  
RTORK=EDA2P1-S10\*EDA3P1  
AVTK=(RTORK+DTORK)/2.  
DTORK=RTORK  
IF(I.NE.1) GO TO 134  
AVTK=0.  
134 TINT=TINT+AVTK\*DLTT/ANFRQ  
FEE=360.\*SFAC\*FLOAT(I-1)/STP  
IF(FEE-360.)140,140,117  
117 FF=FF+1.  
FEE=FEE-360.  
140 IF(I.NE.1) GO TO 44  
WRITE(6,215)T,FEE,FF  
215 FORMAT(1H , 'TIME IN SEC',F9.3,3X,'FEE=',F9.4,3X,'NROT=',F9.4//)  
WRITE(6,130)EDA2P1,EDAE2,EDA3P1,EDAE3  
130 FORMAT(1H , 'ELAS RMOM',D12.6,3X,'TIP MOM',E12.6,3X,  
1'RSHAR=',D12.6,3X,'TIP SHEAR',E12.6//)  
WRITE(6,41)TINT  
41 FORMAT(1H , '1/SQRT(LAM)\*INTEGRAL(M\*DLTT) =',E12.6//)  
44 DO 111 LL=1,101,50  
SUM = 0.  
DO 112 KK=1,2  
MODE=BPT(LL,KK)\*TFAC(KK)  
112 SUM=SUM+MODE  
IF(I.EQ.1) GO TO 114  
IF(IVAR.EQ.1) GO TO 111  
114 WRITE(6,115) SUM,LL  
111 CONTINUE  
115 FORMAT(1H , 'ADA',E12.6,3X,'STATION',I3)  
IF(IVAR.NE.1) GO TO 122  
WRITE(6,121) SUM,TINT,T,I  
122 CONTINUE  
121 FORMAT(1H , 'ENDISP',F12.6,3X,'TINT',E12.6,3X,'T',F9.3,3X,'I',I3)  
120 WRITE(6,568)  
568 FORMAT(1H /)  
GO TO 100  
113 SAM=2  
WRITE(6,116) SAM  
116 FORMAT(1H , 'GJR DUMPED SAM=',I3)  
100 CONTINUE  
GO TO 42  
42 RETURN

C  
END

CARDS IN = 316, CARDS OUT = 0, PAGES OUT = 6

```

SUBROUTINE GUR(A,N,P,Q)
  INTEGER N,P(N),Q(N)
  DIMENSION A(N,N),B(N),C(N)
  EPS=1.*(10.)*-7
101 EPS=EPS/10.
  IF(EPS.LT.10.*-15) GO TO 102
  DO 35 K=1,N
  PIVOT=0.
  DO 5 I=K,N
  DO 5 J=K,N
  IF(ABS(A(I,J)).LE.ABS(PIVOT)) GO TO 5
  PIVOT=A(I,J)
  P(K)=I
  Q(K)=J
5   CONTINUE
  IF(ABS(PIVOT).LE.EPS)GO TO 101
  IF(P(K)-K)6,10,6
6   DO 7 J=1,N
  L=P(K)
  Z=A(L,J)
  A(L,J)=A(K,J)
7   A(K,J)=Z
10  IF(Q(K)-K)11,15,11
11  DO 12 I=1,N
  L=Q(K)
  Z=A(I,L)
  A(I,L)=A(I,K)
12  A(I,K)=Z
15  DO 25 J=1,N
  IF(J-K)20,16,20
16  B(J)=1./PIVOT
  C(J)=1.
  GO TO 22
20  B(J)=-A(K,J)/PIVOT
  C(J)=A(J,K)
22  A(K,J)=0.
  A(J,K)=0.
25  CONTINUE
  DO 30 I=1,N
  DO 30 J=1,N
30  A(I,J)=A(I,J)+C(I)*B(J)
35  CONTINUE
  DO 50 M=1,N
  K=N-M+1
  IF(P(K)-K)40,45,40
40  DO 43 I=1,N
  L=P(K)
  Z=A(I,L)
  A(I,L)=A(I,K)
  A(I,K)=Z
43  CONTINUE
45  IF(Q(K)-K)46,50,46
46  DO 48 J=1,N
  L=Q(K)
  Z=A(L,J)
  A(L,J)=A(K,J)
  A(K,J)=Z
48  CONTINUE
50  CONTINUE
  RETURN
102 WRITE(6,103)
103 FORMAT(21H0 GUR COULD NOT DO IT)
  RETURN 7
END

```

## CHAPTER 4

Simulation of the Motion of The Central Rigid  
Body and its Elastic Appendages

## 4.1 Introduction

In the previous chapters, the problem of determining the modal shapes and frequencies of the rotating structure was examined, and applications were studied in which these modes are utilized.

In the present chapter, equations of motion are written for the generalized coordinates representing the flexible structure and for the angular rates of the central rigid body. A simulation of the spacecraft motion is then possible. Various cases of simulation are examined, and the effect of modal truncation and of nonlinear terms is discussed.

4.2 Modal Equations of Motion: equatorial vibrations (Case "E",  
for equatorial)4.2.1 Constancy of  $\vec{H}$ .

In what follows, it is assumed that the motion of the center of mass of the spacecraft is negligible (or that only antisymmetric motions of the booms are considered) and that the "limited approach" is taken<sup>[4-1]</sup>, i.e. the motion of the spacecraft's center of mass in inertial space can be determined independently of the attitude.

If over the time of interest, i.e. a few tens. of spin periods or so, the torque-impulse due to all environmental attitude perturbing torques (gravity-gradient, solar pressure, magnetic, etc.) can

be considered as negligible, then very sensibly the moment of momentum  $\vec{H}$  about the center of mass remains constant:

$$\vec{H} = \vec{H}(0) = \text{constant vector} \quad (4.2-1)$$

in which  $\vec{H}$  is the value of  $\vec{H}$  at  $t = 0$ .

#### 4.2.2 Representation of the elastic appendages

Consider a particle of a boom, having non-dimensional abscissa  $\xi$ , located along axis  $+x$  in its undeflected position. Its elastic displacement,  $\eta = \frac{w(x)}{\ell}$ , is represented in terms of the modes  $\Phi_j(\xi = \frac{x}{\ell})$

$$\eta_{+x} = \sum_{j=1}^N q_j(\bar{t}) \Phi_j(\xi) \quad (4.2-2)$$

in which the  $q_j$  are non-dimensional amplitudes, dependent on the non-dimensional time  $\bar{t} = \omega_s t$ , with  $\omega_s = \frac{2\pi}{\tau_s}$  the angular spin rate of the satellite in its nominal motion.  $N$  is some positive integer, which specifies the number of terms after which the series is truncated.

We recall that the  $\Phi_j(\xi)$  are orthogonal modes, normalized to unit deflection at the boom's tip, so that

$$\int_{\text{boom}} \Phi_j(\xi) \Phi_k(\xi) = 0 \quad j \neq k \quad (4.2-3)$$

$$m_{1,j} \stackrel{\text{def}}{=} \int_{\text{boom}} \Phi_j^2(\xi) d\xi > 0 \quad j = k \quad (4.2-4)$$

$\xi_1 = \xi + \xi_0$ ;  
both  $m_{1,j}$ ,  $m_{2,j}$  are assumed to be known quantities, determined as in Chapter 2.

#### 4.2.3 Kinetic energy contained in the elastic structure

The total kinetic energy,  $T$ , is made out of two parts: one is independent of the generalized coordinates  $q_j$  and the other one,  $T_1$ , depends on the  $q_j$  and appears as the integral of a density  $\vartheta_{T_1}$ . More specifically (Fig. 4.1)

$$T = \sum_{\text{all particles}} m \frac{\vec{v}^2}{2} \quad (4.2-6)$$

$m$

with  $\vec{v}_m = \vec{\omega} \wedge (\vec{r}_{m,0} + \vec{\delta}) + \dot{\vec{\delta}}$  (4.2-7)

in which  $\vec{\omega}$  is the instantaneous rotation,  $\vec{r}_{m,0}$  is the vector coordinate to  $m$  in its reference position and  $\vec{\delta}$  is the elastic displacement from  $\vec{r}_{m,0}$ .

Computing  $T$ ,

$$T = \sum_{\substack{\text{Rigid} \\ \text{PARTS}}} \frac{m}{2} (\vec{\omega} \wedge \vec{r}_{m,0})^2 + \sum_{\substack{\text{FLEXIBLE} \\ \text{PARTS}}} \left\{ \frac{1}{2} m [(\vec{\omega} \wedge \vec{\delta})^2 + 2(\vec{\omega} \wedge \vec{r}_{m,0}) \cdot (\vec{\omega} \wedge \vec{\delta}) + 2(\vec{\omega} \wedge \vec{r}_{m,0}) \cdot \dot{\vec{\delta}} + 2(\vec{\omega} \wedge \vec{\delta}) \cdot \dot{\vec{\delta}} + \dot{\vec{\delta}}^2] \right\}$$

Now, for small linear displacements of the elastic parts

$$\vec{\delta} = \begin{pmatrix} w_1 \\ w_2 \\ w_3 \end{pmatrix}$$

$$\vec{\omega} \wedge \vec{\delta} = \begin{pmatrix} -w_2 w_3 \\ 0 \\ w_1 w_2 \end{pmatrix}$$

Thus

$$\sum_{\substack{\text{ALL ELASTIC} \\ \text{PARTS}}} \frac{1}{2} m (\vec{\omega} \wedge \vec{\delta})^2 = \sum \frac{1}{2} m (w_z^2 + w_x^2) w^2 \quad (4.2-9)$$

If  $\omega_x, \omega_y, \dot{w}$  are assumed to be of first order of smallness, (4.2-9) is rewritten

$$\sum \frac{1}{2} w^2 (\omega_z^2) + O(\epsilon^4) = \sum \frac{1}{2} w^2 \omega_s^2 + O(\epsilon^3) \quad (4.2-10)$$

in which  $\omega_s$  is the (constant) nominal value of the spin rate.

$$\vec{\omega} \wedge \vec{r}_{m,0} = \begin{pmatrix} 0 \\ \omega_z x_1 \\ -\omega_y x_1 \end{pmatrix}$$

Then

$$\frac{1}{2} \sum_{\substack{\text{ALL} \\ \text{ELASTIC} \\ \text{PARTS}}} 2m (\vec{\omega} \wedge \vec{r}_{m,0}) \cdot (\vec{\omega} \wedge \vec{\delta}) = \sum_m \begin{bmatrix} 0 & \omega_z x & -\omega_y x \end{bmatrix} \begin{bmatrix} -w\omega_z \\ 0 \\ w\omega_y \end{bmatrix} = O(\epsilon^3) \quad (4.2-11)$$

Furthermore,

$$\sum_{\substack{\text{ALL} \\ \text{EL. PARTS}}} \frac{1}{2} m \dot{\vec{\delta}}^2 = \sum \frac{1}{2} m \dot{w}^2 \quad (4.2-12)$$

and

$$\frac{1}{2} \sum_{\substack{\text{ALL} \\ \text{EL. PARTS}}} 2m (\vec{\omega} \wedge \vec{r}_{m,0}) \cdot \dot{\vec{\delta}} = \sum_m \omega_z x_1 \dot{w} \quad (4.2-13)$$

Finally,

$$\frac{1}{2} \sum_{\substack{\text{ALL} \\ \text{EL. PARTS}}} 2m (\vec{\omega} \wedge \vec{\delta}) \cdot \dot{\vec{\delta}} = 0 \quad (4.2-14)$$

Introducing expressions (4.8-10) through (4.2-14) in Equations (4.2-8), we obtain

$$T = T_0 + \frac{1}{2} \int_0^l \rho ds (w^2 \omega_s^2 + \dot{\omega}^2 + 2 \omega_z x_1 \dot{w}) + O(\epsilon^3) \quad (4.2-15)$$

Since the element of curvilinear abscissa,  $ds$ , is related to  $dx$  by

$$ds^2 = dx^2 + dy^2 = dx^2(1 + (\frac{\partial w}{\partial x})^2)$$

or

$$\begin{aligned} ds &= dx(1 + (\frac{\partial w}{\partial x})^2)^{1/2} \\ &= dx(1 + \frac{1}{2}(\frac{\partial w}{\partial x})^2 + \dots) \end{aligned}$$

and

$$dx = ds(1 - \frac{1}{2}(\frac{\partial w}{\partial x})^2 \dots)$$

Therefore, consistent with the order of magnitudes retained explicitly, (4.2-15) can be rewritten with  $x$  instead of  $s$  as the integration variable,

$$T = T_0 + \frac{1}{2} \int_0^l \rho dx (w^2 \omega_s^2 + \dot{\omega}^2 + 2 \omega_z x_1 \dot{w}) + O(\epsilon^3) \quad (4.2-16)$$

The "flexible body" part of  $T_0$ , however, has to include a correction term, since for terms involving

$$\int_0^l x^2 ds = \int_0^l x^2 dx + \frac{1}{2} \int_0^l x^2 (\frac{\partial w}{\partial x})^2 dx$$

i.e. with an integrand of zero-th order of magnitude, we can write

$$\int_0^l x^2 ds = \int_0^{l_{upper}} x^2 dx + \frac{1}{2} \int_0^{l_{upper}} x^2 \left( \frac{\partial w}{\partial x} \right)^2 dx \quad (4.2-17)$$

Neglecting terms of 3<sup>rd</sup> order of smallness,

$$\int_0^l x^2 ds = \int_0^l x^2 dx - l^2 (l - l_{upper}) + \frac{1}{2} \int_0^l x^2 \left( \frac{\partial w}{\partial x} \right)^2 dx \quad (4.2-18)$$

and using (4.2-17),

$$\int_0^l x^2 ds = \int_0^l x^2 dx - \frac{1}{2} \int_0^l (l^2 - x^2) \left( \frac{\partial w}{\partial x} \right)^2 dx \quad (4.2-19)$$

Now, if the integrand is

$$x_1^2 = (x_0 + x)^2 = x^2 + 2x_0 x + x_0^2$$

we obtain

$$\begin{aligned} \int_0^l x_0^2 ds &= x_0^2 l = x_0^2 \int_0^l dx \\ \int_0^l x ds &= \int_0^{l_{upper}} x dx + \frac{1}{2} \int_0^{l_{upper}} x \left( \frac{\partial w}{\partial x} \right)^2 dx \end{aligned}$$

or neglecting terms of third order of smallness

$$\begin{aligned} \int_0^l x ds &= \int_0^l x dx - l(l - l_{upper}) + \frac{1}{2} \int_0^l x \left( \frac{\partial w}{\partial x} \right)^2 dx \\ &= \int_0^l x dx - \frac{1}{2} \int_0^l (l - x) \left( \frac{\partial w}{\partial x} \right)^2 dx \end{aligned}$$

Finally,

$$\int_0^l x_1^2 ds = \int_0^l x_1^2 dx - \frac{1}{2} \int_0^l [(l^2 - x^2) + 2x_0(l - x)] \left( \frac{\partial w}{\partial x} \right)^2 dx$$

Therefore,  $T_0$  is rewritten, with  $\Phi(\vec{\omega})$  the inertia dyadic of the rigidified, undeflected total reference body as

$$T_0 = \frac{1}{2} \vec{\omega} \cdot \vec{\Phi}(\vec{\omega}) - \frac{1}{2} \int_0^l \rho dx \frac{1}{2} \left[ (\ell^2 - x^2) + 2x_0(\ell - x) \right] \left( \frac{\partial w}{\partial x} \right)^2 dx \quad (4.2-20)$$

Collecting (4.2-16) and (4.2-20)

$$\begin{aligned} T = & \frac{1}{2} \vec{\omega} \cdot \vec{\Phi}(\vec{\omega}) + \frac{1}{2} \int_0^l \rho dx \left( w^2 \omega_3 + \dot{w}^2 + 2\omega_z x_i \dot{w} - \frac{1}{2} [(\ell^2 - x^2) \right. \\ & \left. + 2x_0(\ell - x)] \left( \frac{\partial w}{\partial x} \right)^2 \right) dx + O(\epsilon^3) \end{aligned} \quad (4.2-21).$$

#### 4.2.4 Potential energy of the elastic structure

For pure flexure in the (x,y) plane, the potential energy is given by

$$V = \frac{EI}{2} \int_0^l \left( \frac{\partial^2 w}{\partial x^2} \right)^2 dx + O(\epsilon^3)$$

where it is legitimate to use x, instead of s, as the integration variable, to the order of the terms explicitly retained.

#### 4.2.5 Equations of motion for the elastic modes, equatorial vibrations.

##### 4.2.5.1 Equation for the jth coordinate, $q_j$

At this point we introduce the modal representation (4.1-2). For the sake of simplicity, let the bars on  $\bar{t} = [\frac{t}{1/\omega_s}]$ , be dropped. Furthermore, let the energies be non-dimensionalized by

$$\rho \ell^3 \omega_s^2 \quad \text{and the lengths by } \ell$$

Although  $\bar{\omega}_s$ , non-dimensional value of the nominal satellite spin-rate,

is 1, we shall for clarity retain it in the equations.

In non-dimensional form, with  $\cdot$  designating derivatives with respect to  $\bar{t}$ , and  $\xi_1 = \xi + \xi_0$ ,

$$\begin{aligned}\bar{T} &= \frac{1}{\rho l^3 \omega_s^2} (T - \frac{1}{2} \vec{\omega} \cdot \vec{\Phi}(\vec{\omega})) = \frac{1}{2} \int_{\text{beam}} (\dot{\eta}^2 + \eta^2 \bar{\omega}_s^2 + 2 \bar{\omega}_s \dot{\eta} \dot{\xi}_1) d\xi \\ &\quad - \frac{1}{2} [(1-\xi^2) + 2 \xi_0 (1-\xi)] \left( \frac{\partial \eta}{\partial \xi} \right)^2 d\xi\end{aligned}\quad (4.2-22)$$

$$\bar{V} = \frac{1}{2 \bar{\lambda}} \int_{\text{beam}} \left[ \frac{\partial^2 \eta}{\partial \xi^2} \right]^2 d\xi \quad (4.2-23)$$

with  $\bar{\lambda} = \frac{\rho l^4}{EI} \omega_s^2$ , as in Chapter 2.

Now let, with  $t$  the non-dimensional time,

$$\eta = \sum_{j=1}^N q_j(t) \bar{\Phi}_j(\xi)$$

Then

$$\dot{\eta} = \sum_{j=1}^N \dot{q}_j(t) \bar{\Phi}_j$$

$$\eta^2 = \sum_{j=1}^N \sum_{k=1}^N q_j q_k \bar{\Phi}_j \bar{\Phi}_k$$

$$\dot{\eta}^2 = \sum_{j=1}^N \sum_{k=1}^N \dot{q}_j \dot{q}_k \bar{\Phi}_j \bar{\Phi}_k$$

$$\frac{\partial \eta}{\partial \xi} = \sum_{j=1}^N q_j \frac{d \bar{\Phi}_j}{d \xi}$$

$$\left( \frac{\partial \eta}{\partial \xi} \right)^2 = \sum_{j=1}^N \sum_{k=1}^N q_j q_k \frac{d \bar{\Phi}_j}{d \xi} \frac{d \bar{\Phi}_k}{d \xi}$$

Similarly,

$$\left( \frac{\partial^2 \eta}{\partial \xi^2} \right)^2 = \sum_{j=1}^N \sum_{k=1}^N q_j q_k \frac{d^2 \bar{\Phi}_j}{d \xi^2} \frac{d^2 \bar{\Phi}_k}{d \xi^2}$$

Thus, the Lagrangian function is

$$\bar{\mathcal{L}} \equiv \frac{1}{2} \vec{\omega} \cdot \vec{\Phi}(\vec{\omega}) + \bar{T}_i - \bar{V} = \frac{1}{2} \int_{\text{boom}} \sum_{j=1}^N \sum_{k=1}^N \left[ \dot{q}_j \dot{q}_k \bar{\Phi}_j \bar{\Phi}_k + \bar{\omega}_s^2 q_j q_k \bar{\Phi}_j \bar{\Phi}_k + 2 \omega_z \dot{q}_j \xi_j \bar{\Phi}_j \right] - \frac{1}{2} [(1-\xi^2) + 2\xi_0(1-\xi)] q_j q_k \frac{d\phi_j}{d\xi} \frac{d\phi_k}{d\xi} - \frac{1}{\pi} q_j q_k \frac{d^2\phi_j}{d\xi^2} \frac{d^2\phi_k}{d\xi^2} d\xi \quad (4.2-24)$$

Now, for any  $i = 1, 2, \dots$ ,

$$\frac{d}{dt} \left( \frac{\partial \mathcal{L}}{\partial \dot{q}_i} \right) - \frac{\partial \mathcal{L}}{\partial q_i} = 0 \quad (4.2-25)$$

We recall that, as in (4.2-3), (4.2-4), (4.2-5)

$$\int_{\text{boom}} \phi_j \phi_k d\xi = 0 \quad (j \neq k)$$

boom

$$\int_{\text{boom}} \phi_j^2 d\xi \equiv m_{1,j}$$

boom

$$\int_{\text{boom}} \phi_j \xi_1 d\xi \equiv m_{2,j}$$

the  $\phi_j$  having been previously normalized to unit deflection at the boom's tip. Using these relations, and (4.2-25) for  $i = j$ , after defining

$$a_{jk} = a_{kj} \text{ def } \frac{1}{2} \int_{\text{boom}} [(1-\xi^2) + 2\xi_0(1-\xi)] \frac{d\phi_j}{d\xi} \frac{d\phi_k}{d\xi} d\xi \quad (4.2-26)$$

$$b_{jk} = b_{kj} \text{ def } \int_{\text{boom}} \frac{d^2\phi_j}{d\xi^2} \frac{d^2\phi_k}{d\xi^2} d\xi \quad (4.2-27)$$

we obtain, for the  $j$ th modal coordinate

$$m_{1,j} \ddot{q}_j - m_{1,j} \bar{\omega}_s^2 q_j + \sum_{k=1}^N a_{jk} q_k + \frac{1}{\pi} \sum_{k=1}^N b_{jk} q_k = -m_{2,j} \dot{\omega}_z \quad (4.2-28)$$

#### 4.2.5.2 Evaluation of the coefficient of $q_j$

We now evaluate the coefficient of  $q_j$  in (4.2-28), say  $c_j$ ,

$$c_j \stackrel{\text{def}}{=} \frac{1}{\lambda} \sum_{k=1}^N b_{jk} + \sum_{k=1}^N a_{jk} - m_{1,j} \bar{\omega}_s^2 \quad (4.2-29)$$

From Equation (2.2-23), written in terms of  $a_{jk}$ ,  $b_{jk}$ ,

$$\frac{1}{\lambda} b_{jk} + a_{jk} = 0 \quad j \neq k$$

$$\frac{1}{\lambda} b_{jj} + a_{jj} = m_{1,j} (\bar{\omega}_j^2 + \bar{\omega}_s^2) \quad j=k$$

Thus (4.2-28) takes the simple form

$$m_{1,j} \ddot{q}_j + m_{1,j} \bar{\omega}_j^2 q_j = - \frac{m_{2,j}}{m_{1,j}} \dot{\omega}_z$$

or

$$\ddot{q}_j + \bar{\omega}_j^2 q_j = - \frac{m_{2,j}}{m_{1,j}} \dot{\omega}_z \quad (4.2-30)$$

A few remarks should be made regarding (4.2-30). First of all, the modal equations for the  $j^{th}$  coordinate reduce to a harmonic motion, in the case where  $\bar{\omega}_z$  is constant. Second, as has been seen in Chapter 3, the "driving amplitude", measured by the non-dimensional ratio

$$\frac{m_{2,j}}{m_{1,j}}$$

is strongly a function of  $\xi_0$ , and to a lesser extent of  $\lambda$ , Etkin's number. Thirdly, it should be noted that it is only because, for the sake of consistency, the difference of an integral in  $s$  (curvilinear abscissa) and  $x$  was carefully considered when the integrand

was a quantity of zeroth order (as detailed above), that term

$$- m_{1,j} \bar{\omega}_s^2 q_j$$

could finally be cancelled in Equation (4.2-30). Failure to make this distinction leads to having this extra term still present in the final equation and in order to "fall back" on (4.2-30), one has to introduce, rather belatedly, an additional term due to a "rotational potential"<sup>[4-2]</sup>. Finally, if linear distributed damping is introduced, Equation (4.2-30) takes the form

$$\ddot{q}_j + 2\nu\bar{\omega}_j\dot{q}_j + \bar{\omega}_j^2 q_j = - \frac{m_{2,j}}{m_{1,j}} \dot{\omega}_z \quad (4.2-31)$$

whose derivatives are taken with respect to non-dimensional time.

#### 4.3 Modal Equations of Motion: meridional vibrations (Case "M", for meridional)

Without repeating in the same detail the explanations of Section 4.2, we now derive the modal equations in the case of motions parallel to axis-z (meridional vibrations). Only the relevant differences are underlined.

##### 4.3.1 Constancy of $\vec{H}$

In the absence of attitude perturbing torques, the torque-free motion has the integral

$$\vec{H} = \vec{H}_0 \quad (4.3-1)$$

where  $\vec{H}_0$  is the value of the moment of momentum at  $t = 0$ .

##### 4.3.2 Representation of the elastic appendages

The displacement  $\eta(x) = \frac{w(x)}{l}$  of an element of boom located at  $\xi = \frac{x}{l}$  of axis +x in terms of the modes  $\Phi_j(\xi)$  for meridional motions is

$$\eta_{+x} = \sum_{j=1}^N q_j(\bar{t}) \Phi_j(\xi) \quad (4.3-2)$$

Again  $q_j$  are non-dimensional amplitudes, functions of the non-dimensional time  $\bar{t} = \frac{t}{1/\omega_s}$ .  $N$  is positive integer specifying the number of terms after which the series is truncated.

The "meridional" modes are orthogonal

$$\int_{\text{boom}} \phi_j(\xi) \phi_k(\xi) d\xi = 0 \quad j \neq k \quad (4.3-3)$$

and we have defined

$$m_{1,j} \equiv \int_{\text{boom}} \phi_j^2(\xi) d\xi > 0 \quad (4.3-4)$$

$$m_{2,j} \equiv \int_{\text{boom}} \xi_1 \phi_j(\xi) d\xi \quad \text{with } \xi_1 = \xi + \xi_0 \quad (4.3-5)$$

These quantities are known as functions of  $\lambda$ , Etkin's number, and  $\xi_0 = \frac{x_0}{\lambda}$ , hub non-dimensional radius.

#### 4.3.3 Kinetic energy contained in the elastic structure

With the same notations as in Section 4.2.3,

$$T = T_0 \text{ (rigid part + flexible part)} + T_1$$

Now

$$\vec{\delta} = w \vec{I}_z$$

$$\vec{\omega} \wedge \vec{\delta} = \begin{bmatrix} \omega_y w \\ -\omega_z w \\ 0 \end{bmatrix}$$

and  $\sum_{\text{quasi}} \frac{1}{2} m (\vec{\omega} \wedge \vec{\delta})^2 = \sum \frac{1}{2} m w^2 (\omega_x^2 + \omega_y^2) = O(\epsilon^4) \quad (4.3-6)$

Let  $x_1 = x + x_0$ . Then

$$\vec{\omega} \wedge \vec{r}_{m,0} = \begin{pmatrix} 0 \\ \omega_z x_1 \\ -\omega_y x_1 \end{pmatrix}$$

The next terms are

$$\frac{1}{2} \sum_{\substack{\text{ALL} \\ \text{EL. PARTS}}} 2m (\vec{\omega} \wedge \vec{r}_{m,0}) \cdot (\vec{\omega} \wedge \vec{\delta}) = \frac{1}{2} \sum (-2\omega_s \omega_x x_i w) + O(\epsilon^3) \quad (4.3-7)$$

$$\sum_{\substack{\text{ALL EL.} \\ \text{PARTS}}} \frac{1}{2} m \vec{\delta}^2 = \sum \frac{1}{2} m \dot{w}^2 \quad (4.3-8)$$

$$\frac{1}{2} \sum_{\substack{\text{ALL} \\ \text{EL. PARTS}}} 2m (\vec{\omega} \wedge \vec{r}_{m,0}) \cdot \vec{\delta} = -\frac{1}{2} \sum 2m \omega_y x_i \dot{w} \quad (4.3-9)$$

$$\frac{1}{2} \sum_{\substack{\text{ALL} \\ \text{EL. PARTS}}} 2m (\vec{\omega} \wedge \vec{\delta}) \cdot \vec{\delta} = 0 \quad (4.3-10)$$

Introducing expressions (4.3-6) through (4.3-10) into (4.2-8), and since we can substitute  $dx$  for  $ds$  when the integrand is of first order of smallness, or smaller,

$$T = \frac{1}{2} \vec{\omega} \cdot \vec{\omega} + \frac{1}{2} \int_0^l \rho dx (\dot{w}^2 - 2\omega_s \omega_x x_1 w - 2\omega_y x_1 \dot{w} - \frac{1}{2} [(\ell^2 - x^2) + 2x_0(\ell - x)] \left( \frac{\partial w}{\partial x} \right)^2) + O(\epsilon^3) \quad (4.3-12)$$

#### 4.3.4 Potential energy of the elastic structure

For pure flexure in the  $(x, z)$  plane, the potential energy is

$$V = \frac{EI}{2} \int_0^L \left( \frac{\partial^2 w}{\partial x^2} \right)^2 dx + O(\epsilon^3)$$

Again, it is legitimate to use  $x$ , instead of  $s$ , as the integration, to the order of the terms explicitly retained.

#### 4.3.5 Equations of motion: elastic modes, meridional vibrations

##### 5.3.5.1 Equation for the $j$ th coordinate, $q_j$

The kinetic energy,  $T$ , and potential energy,  $V$ , are non-dimensionalized by the quantity  $\rho l^3 \omega_s^2$ . Note that, although  $\bar{\omega}_s$ , non-dimensional value of the nominal satellite spin rate, is 1, it is retained as " $\bar{\omega}_s$ " in the equations. Let  $T_{rb} = \frac{1}{2} \vec{\omega} \cdot \vec{\Phi}(\vec{\omega})$ .

$$\begin{aligned} \bar{T} &\stackrel{\text{def}}{=} \frac{T}{\rho l^3 \omega_s^2} = \frac{T_{rb}}{\rho l^3 \omega_s^2} + \frac{1}{2} \int_{\text{boom}} \left( \dot{\eta}^2 - 2\bar{\omega}_s \bar{\omega}_x \xi_j \dot{\eta} - 2\omega_y \xi_j \dot{\eta} - \frac{1}{2} [(1-\xi^2) \right. \\ &\quad \left. + 2\xi_0 (1-\xi)] \left( \frac{\partial \eta}{\partial \xi} \right)^2 \right) d\xi \\ \bar{V} &\stackrel{\text{def}}{=} \frac{V}{\rho l^3 \omega_s^2} = \frac{1}{2\lambda} \int_{\text{boom}} \left( \frac{\partial^2 \eta}{\partial \xi^2} \right)^2 d\xi \end{aligned}$$

With the same substitutions as in (4.2), we obtain the Lagrangian

$$\begin{aligned} \bar{\mathcal{L}} &= \frac{T_{rb}}{\rho l^3 \omega_s^2} + \frac{1}{2} \int_0^L \sum_{j=1}^N \sum_{k=1}^N \left[ \dot{q}_j \dot{q}_k \dot{\phi}_j \dot{\phi}_k - 2\bar{\omega}_s \bar{\omega}_x \xi_j q_j \dot{\phi}_j - 2\bar{\omega}_y \xi_j q_j \dot{\phi}_j \right. \\ &\quad \left. - \frac{1}{2} [(1-\xi^2) + 2\xi_0 (1-\xi)] q_j q_k \frac{d\phi_j}{d\xi} \frac{d\phi_k}{d\xi} - \frac{1}{\lambda} q_j q_k \frac{d^2 \phi_j}{d\xi^2} \frac{d^2 \phi_k}{d\xi^2} \right] d\xi \end{aligned} \quad (4.3-13)$$

Now define

$$a_{jk} = a_{kj} \stackrel{\text{def}}{=} \frac{1}{2} \int_{\text{boom}} [(1-\xi^2) + 2\xi_0 (1-\xi)] \frac{d\phi_j}{d\xi} \frac{d\phi_k}{d\xi} d\xi$$

$$b_{jk} = b_{kj} \stackrel{\text{def}}{=} \int_{\text{boom}} \frac{d^2 \phi_j}{d\xi^2} \frac{d^2 \phi_k}{d\xi^2} d\xi$$

For modal coordinate  $q_j$ , the Lagrangian equation is, with Equations (4.3-3) through (4.3-5),

$$m_{1,j} \ddot{q}_j + \frac{1}{\lambda} \sum_{k=1}^N b_{jk} + \sum_{k=1}^N a_{jk} = + m_{2,j} (\dot{\bar{\omega}}_y - \bar{\omega}_s \bar{\omega}_x) \quad (4.3-14)$$

#### 4.3.5.2 Evaluation of the coefficient of $q_j$

From Equations (2.3-11, 12), Section 2.23, we obtain

$$\frac{1}{\lambda} b_{jk} + a_{jk} = 0 \quad j \neq k$$

$$\frac{1}{\lambda} b_{jj} + a_{jj} = \bar{\omega}_j^2 m_{1,j} \quad j=k$$

Thus Equation (4.3-14) can be rewritten in the form

$$\ddot{q}_j + \bar{\omega}_j^2 q_j = \frac{m_{2,j}}{m_{1,j}} (\dot{\bar{\omega}}_y - \bar{\omega}_s \bar{\omega}_x) \quad (4.3-15)$$

in which  $\bar{\omega}_j$  is the  $j^{\text{th}}$  eigenfrequency of meridional vibrations, a function of  $\bar{\lambda}$  and  $\xi_0$ .

Again, if linear distributed damping is introduced, the equation of motion becomes

$$\ddot{q}_j + 2v\bar{\omega}_j \dot{q}_j + \bar{\omega}_j^2 q_j = \frac{m_{2,j}}{m_{1,j}} (\dot{\bar{\omega}}_y - \bar{\omega}_s \bar{\omega}_x) \quad (4.3-16)$$

$\frac{m_{2,j}}{m_{1,j}}$  thus appears as a "driving amplitude". As seen in Chapter 2, it is also strongly dependent on  $\xi_0$ , and to a lesser extent on Etkin's number  $\bar{\lambda}$ .

#### 4.4 Equations for the rates: equatorial vibrations (Case "E")

The equation for the time derivatives of the rates are now derived from the constancy of the moment of momentum for the torque-free motion, as given in (4.2-1).

Since, about the center of mass,

$$\dot{\vec{H}} = \vec{H}(0) = \int \vec{r} \wedge \dot{\vec{r}} dm$$

$$\dot{\vec{H}} = \int \vec{r} \wedge \ddot{\vec{r}} dm$$

Computing, with the same notations as in 4.2 and 4.3,

$$\dot{\vec{r}} = \dot{\vec{\delta}} + \vec{\omega} \wedge (\vec{r}_{m,0} + \vec{\delta})$$

$$\ddot{\vec{r}} = \ddot{\vec{\delta}} + 2\vec{\omega} \wedge \dot{\vec{\delta}} + \vec{\omega} \wedge \dot{\vec{r}}_{m,0} + \vec{\omega} \wedge \dot{\vec{\delta}} + \vec{\omega} \wedge (\vec{\omega}_s \wedge \vec{r}_{m,0}) + \vec{\omega} \wedge (\vec{\omega} \wedge \vec{\delta})$$

Let  $\dot{\vec{H}}$  be divided between a part "relating to  $\vec{r}_{m,0}$ ",  $\dot{\vec{H}}_I$ , and a part relating to  $\vec{\delta}$ ,  $\dot{\vec{H}}_{II}$

$$\dot{\vec{H}} = \dot{\vec{H}}_I + \dot{\vec{H}}_{II}$$

and

$$\dot{\vec{H}}_I = \int_{\text{boom}} \vec{r}_{m,0} \wedge \{\vec{\omega} \wedge \dot{\vec{r}}_{m,0} + \vec{\omega} \wedge (\vec{\omega} \wedge \vec{r}_{m,0})\} ds \quad (4.4-1)$$

$$\dot{\vec{H}}_{II} = \int_{\text{boom}} [\vec{r} \wedge \{\ddot{\vec{\delta}} + 2\vec{\omega} \wedge \dot{\vec{\delta}} + \vec{\omega} \wedge \dot{\vec{\delta}} + \vec{\omega} \wedge (\vec{\omega} \wedge \vec{\delta})\} + \vec{\delta} \wedge (\vec{\omega} \wedge \dot{\vec{r}}_{m,0}) + \vec{\delta} (\vec{\omega} \wedge (\vec{\omega} \wedge \vec{r}_{m,0}))] ds \quad (4.4-2)$$

$$+ \vec{\delta} \wedge (\vec{\omega} \wedge \dot{\vec{r}}_{m,0}) + \vec{\delta} (\vec{\omega} \wedge (\vec{\omega} \wedge \vec{r}_{m,0}))] ds$$

Note that as has been seen in Section (4.3) and (4.3)

$$ds = dx(1 + \frac{1}{2}(\frac{\partial w}{\partial x})^2) + \text{higher order terms} \quad (4.4-3)$$

in which the elastic displacement (along +y) is

$$\vec{\delta} = w(x)\vec{i}_y \quad (4.4-4)$$

Therefore, if  $\bar{\omega}_x$ ,  $\bar{\omega}_y$  (normalized to  $\omega_s$ , nominal value of the satellite spin rate) and  $\eta(x) = \frac{w(x)}{\ell}$  are considered to be of first order of smallness ( $O(\varepsilon)$ ), the equations for the rates deduced from (4.4-1) should be written with

$$-\int_{\text{boom}} [\dots] ds = \int_{\text{boom}} [\dots] dx ,$$

for integrands of zeroth order of smallness, or smaller, if only quantities of first-order of smallness, or larger, are retained.

Thus, neglecting terms of order 3 of smallness, or smaller (with  $\int_{\text{boom}} [\dots] ds = \int_{\text{boom}} [\dots] dx$  for an integrand of first order of smallness, or smaller),

$$\dot{(\vec{H}_{II})}_x = \int_{\text{boom}} -x_1 \dot{\omega}_y w dx$$

$$\dot{(\vec{H}_{II})}_y = \int_{\text{boom}} x_1 (-2\omega_x \dot{w} - \dot{\omega}_x w - \omega_y \omega_x w) dx$$

$$\dot{(\vec{H}_{II})}_z = -\int_{\text{boom}} x_1 \ddot{w} dx$$

Now, neglecting terms of order 2 of smallness, or smaller (with  $\int_{\text{boom}} [\dots] ds = \int_{\text{boom}} [\dots] dx$  for an integrand of first order of smallness, or smaller)

$$\dot{(\vec{H}_{II})}_x = \dot{(\vec{H}_{II})}_y = 0$$

in the analysis.

$$\int_{\text{boom}} [\dots] ds = \int_{\text{boom}} [\dots] [1 + \frac{1}{2} (\frac{\partial w}{\partial x})^2] dx , \text{ in a manner similar}$$

to the one used in Section 4.2 and 4.3, if the integrand is of zeroth order of smallness, and if quantities of second order of smallness, or larger, are to be retained in the analysis.

With this qualification in mind, the various terms in the integrand

of (4.4-2) are computed without eliminating smaller terms at this point.

$$\vec{\delta} = w \vec{i}_y$$

$$\vec{\pi} \wedge \dot{\vec{\delta}} = \begin{bmatrix} 0 \\ 0 \\ x_1 \dot{w} \end{bmatrix}$$

$$2 \vec{\omega} \wedge \dot{\vec{\delta}} = 2 \begin{bmatrix} -\omega_{xz} \dot{w} \\ 0 \\ \omega_x \dot{w} \end{bmatrix}$$

$$2 \vec{\pi} \wedge (\vec{\omega} \wedge \dot{\vec{\delta}}) = 2 \begin{bmatrix} \omega_x w \dot{w} \\ -x_1 \omega_x \dot{w} \\ \omega_z w \dot{w} \end{bmatrix}$$

$$\vec{\pi} \wedge (\dot{\vec{\omega}} \wedge \dot{\vec{\delta}}) = \begin{bmatrix} \dot{\omega}_x w^2 \\ -x_1 \dot{\omega}_{xz} w \\ \dot{\omega}_z w^2 \end{bmatrix}$$

$$\vec{\delta} \wedge (\dot{\vec{\omega}} \wedge \vec{\pi}_{m,o}) = \begin{bmatrix} -x_1 \dot{\omega}_y w \\ 0 \\ 0 \end{bmatrix}$$

$$\vec{\delta} \wedge (\vec{\omega} \wedge (\dot{\vec{\omega}} \wedge \vec{\pi}_{m,o})) = \begin{bmatrix} x_1 \omega_x \omega_z w \\ 0 \\ x_1 (\omega_y^2 + \omega_z^2) \omega_z \end{bmatrix}$$

$$\vec{\pi} \wedge (\vec{\omega} \wedge (\dot{\vec{\omega}} \wedge \dot{\vec{\delta}})) = \begin{bmatrix} \omega_z \omega_y w^2 \\ -x_1 \omega_y \omega_z w \\ -x_1 (\omega_x^2 + \omega_z^2) w \end{bmatrix}$$

$$(\vec{H}_{II})_z = \int_{beam} x_1 \ddot{w} dx + O(\epsilon^2)$$

$$\begin{aligned} (\vec{H}_I) &= [ I_z \dot{\omega}_x + (I_z - I_y) \omega_y \omega_z ] \vec{i}_x + [ I_y \dot{\omega}_y + (I_x - I_z) \omega_z \omega_x ] \vec{i}_y \\ &\quad + [ I_x \dot{\omega}_z + (I_y - I_x) \omega_x \omega_y ] \vec{i}_z \end{aligned} \quad (4.4-5)$$

if it can be assumed that  $x$ ,  $y$ ,  $z$  are principal axes of inertia of the total, rigidified spacecraft, of total moments of inertia  $I_x$ ,  $I_y$ ,  $I_z$  about the corresponding axes.

To summarize, we have, to order  $\epsilon$ , the following equations for the rates, in case E,

$$\begin{aligned}\dot{\omega}_x &= - \frac{I_z - I_y}{I_x} \omega_y \omega_s \\ \dot{\omega}_y &= - \frac{I_x - I_z}{I_y} \omega_s \omega_x \\ \dot{\omega}_z + \frac{1}{I_z} \int_{\text{boom}}^{\infty} \ddot{\omega}_x dx &= - \frac{I_y - I_x}{I_z} \omega_x \omega_y \approx 0, \text{ to } O(\epsilon) \quad (4.4-6)\end{aligned}$$

Let the time,  $t$ , be non-dimensionalized as  $\bar{t} = \frac{t}{1/\omega_s}$  (from now on, will designate derivatives with respect to  $\bar{t}$ ); the lengths are non-

dimensionalized by  $\ell$ , length of the boom, and  $\xi = \frac{x}{\ell}$ ,  $\xi_0 = \frac{x_0}{\ell}$ ,  $\eta = \frac{w}{\ell}$ ;  $k_x = \frac{I_x}{I_z}$ ,  $k_y = \frac{I_y}{I_z}$ . We obtain

$$\begin{aligned}\dot{\bar{\omega}}_x &= - \frac{1 - k_y}{k_x} \bar{\omega}_y \\ \dot{\bar{\omega}}_y &= - \frac{k_x - 1}{k_y} \bar{\omega}_x \\ \dot{\bar{\omega}}_z &= - \frac{\ell \ell^3}{I_z} \int_{\text{boom}}^{\infty} \ddot{\eta} \xi_i d\xi \quad (4.4-7)\end{aligned}$$

Using the modal expansion in terms of  $\phi_j(\xi)$ , having eigenfrequencies  $\bar{\omega}_{j,E}$ , with  $\dot{\Phi}_j$  and  $\ddot{\omega}_{j,E}$  functions of  $\bar{\lambda}$  and  $\xi_0$ ,

$$\dot{\bar{\omega}}_z = - \frac{\rho l^3}{I_z} \int_{\text{boom}} \sum_{j=1}^N \ddot{q}_j \phi_j(\xi) \xi_j d\xi \quad (4.4-7)$$

Now, from Equation (4.2-31), with  $\bar{\omega}_j = \bar{\omega}_{j,E}$

$$\ddot{q}_j = - \frac{m_{2,j}}{m_{1,j}} \dot{\bar{\omega}}_z - 2\nu \bar{\omega}_j \dot{q}_j - \bar{\omega}_j^2 q_j$$

Substituting

$$\dot{\bar{\omega}}_z \left( 1 - \frac{\rho l^3}{I_z} \sum_{j=1}^N \frac{m_{2,j}^2}{m_{1,j}} \right) = - \frac{\rho l^3}{I_z} \sum_{j=1}^N [ 2\nu \bar{\omega}_j \dot{q}_j + \bar{\omega}_j^2 q_j ] m_{2,j} \quad (4.4-8)$$

Thus the normalized moment of inertia is apparently reduced from the value 1, due to the flexibility of the boom, by an amount equal to

$$\frac{\rho l^3}{I_z} \sum_{j=1}^N \frac{m_{2,j}^2}{m_{1,j}} \quad (4.4-9)$$

or writing, with  $I_{zh}$  = moment of inertia, about  $z$ , of the central hub,

and

$$\Delta \stackrel{\text{def}}{=} \xi_0^2 + \xi_0 + \frac{1}{3} \quad (4.4-10)$$

$$I_z = I_{zh} + \rho l^3 \Delta \quad (4.4-11)$$

the non-dimensional inertia correction becomes, in Equation (4.4-8),

with  $\Gamma \stackrel{\text{def}}{=} \frac{\rho l^3}{I_{zh}}$ ,

$$- \frac{\Gamma}{1 + \Gamma \Delta} \sum_{j=1}^N \frac{m_{2,j}^2}{m_{1,j}} \quad (4.4-12)$$

and (4.4-8) is rewritten (Rate equations for case E)

$$\begin{aligned}\dot{\bar{\omega}}_x &= - \frac{1-k_y}{k_x} \bar{\omega}_y \\ \dot{\bar{\omega}}_y &= - \frac{k_x-1}{k_y} \bar{\omega}_x\end{aligned}\quad (4.4-13)$$

$$\dot{\bar{\omega}}_z \left( 1 - \frac{\Gamma'}{I + \Gamma' A} \sum_{j=1}^N \frac{m_{2,j}^2}{m_{1,j}} \right) = \frac{\Gamma'}{I + \Gamma' A} \sum_{j=1}^N [2\pi \bar{\omega}_j \dot{q}_j + \bar{\omega}_j^2 q_j] m_{2,j}$$

The stability of the motion, in the presence of equatorial vibrations, as studied in Chapter 5, can be done on the basis of equations

(4.2-25) for the modal coordinates

(4.4-13) for the angular rates

with  $N = 1, 2$  or  $3$ , depending on the number of modes retained in the analysis.

#### 4.5 Equations for the rates: meridional vibrations (Case "M")

##### 4.5.1 Equations for the rates, boom along the direction

Without repeating the development of Section 4.1.1, the components of  $\vec{H}_{II}$ , in expression (4.4-2) are rederived for an elastic displacement  $\vec{\delta}$  parallel to axis-z.

$$\vec{\delta} = w(x) \vec{i}_z$$

$$\vec{\pi} \wedge \vec{\delta} = \begin{bmatrix} 0 \\ -x_1 \dot{w} \\ 0 \end{bmatrix}$$

$$2\vec{\pi} \wedge (\vec{\omega} \wedge \vec{\delta}) = 2 \begin{bmatrix} w_x \dot{w} \ddot{w} \\ w_y \dot{w} \ddot{w} \\ -x_1 w_x \dot{w} \end{bmatrix}$$

$$\vec{\pi} \wedge (\dot{\vec{\omega}} \wedge \vec{\delta}) = \begin{bmatrix} \dot{\omega}_x w^2 \\ \dot{\omega}_y w^2 \\ -x_1 \dot{\omega}_x w \end{bmatrix}$$

$$\vec{\pi} \wedge (\vec{\omega} \wedge (\dot{\vec{\omega}} \wedge \vec{\delta})) = \begin{bmatrix} -\omega_z \omega_y W^2 \\ -\omega_x \omega_z W^2 + x_1 (\omega_x^2 + \omega_y^2) W \\ x_1 \omega_z \omega_y W \end{bmatrix}$$

$$\vec{\delta} \wedge (\dot{\vec{\omega}} \wedge \vec{\pi}_{m,0}) = \begin{bmatrix} x_1 w \dot{\omega}_z \\ 0 \\ 0 \end{bmatrix}$$

$$\vec{\delta} \wedge (\vec{\omega} \wedge (\dot{\vec{\omega}} \wedge \vec{\pi}_{m,0})) = \begin{bmatrix} -x_1 \omega_x \omega_y w \\ -x_1 (\omega_y^2 + \omega_z^2) w \\ 0 \end{bmatrix}$$

Neglecting terms of order 3 of smallness,

$$(\dot{\vec{H}}_{II})_z = \int_{boom} x_1 w \dot{\omega}_z p dx$$

$$(\dot{\vec{H}}_{II})_y = \int_{boom} x_1 (\ddot{w} - \ddot{w}) (\omega_z^2 + \omega_y^2) p dx$$

$$(\dot{\vec{H}}_{II})_x = \int_{boom} x_1 (\omega_z \omega_y w - \omega_x \dot{w} - \dot{\omega}_x w) p dx$$

Neglecting terms of order 2 of smallness,

$$(\dot{\vec{H}}_{II})_x = (\dot{\vec{H}}_{II})_z = 0$$

$$(\dot{\vec{H}}_{II})_y = - \int_{boom} x_1 (\ddot{w} + w \omega_z^2) p dx$$

$$\begin{aligned} (\dot{\vec{H}}_I) &= [I_x \dot{\omega}_x + (I_z - I_y) \omega_y \omega_z] \vec{i}_x + [I_y \dot{\omega}_y + (I_x - I_z) \omega_z \omega_x] \vec{i}_y \\ &\quad + [I_z \dot{\omega}_z + (I_y - I_x) \omega_x \omega_y] \vec{i}_z \end{aligned}$$

with the same assumption as in 4.4

To summarize, we have to order  $\epsilon$ , after non-dimensionalization

of time by  $1/\omega_s$ , and with  $k_x = \frac{I_x}{I_z}$ ,  $k_y = \frac{I_y}{I_z}$ ,

$$\begin{aligned} \dot{\bar{\omega}}_x &= -\frac{1-k_y}{k_x} \bar{\omega}_y \\ \dot{\bar{\omega}}_y &= \frac{k_x}{k_y} - \frac{k_x - 1}{k_y} + \frac{\ell \ell^3}{I_y} \int_{boom} (\ddot{\eta} + \eta) \xi_1 d\xi \quad (4.5-1) \\ \dot{\bar{\omega}}_z &= 0 \end{aligned}$$

In the second of equations (4.5-1),

$$\frac{\rho l^3}{I_y} = \frac{\rho l^3}{I_z k_y} = \frac{1}{k_y} \frac{\Gamma}{1 + \Gamma \Delta}$$

Using the modal expression for  $\eta_M = \sum_{j=1}^N q_j(t) \phi_{jm}(\xi)$ ,  $\phi_j(\xi)$  being the  $j$ th modal shape having associated frequency  $\bar{\omega}_{j,M}$ ,

$$\int_{beam} \sum_{j=1}^N (\ddot{q}_j + q_j) \Phi_j \xi_1 d\xi = \sum_{j=1}^N \ddot{q}_j m_{2,j} + \sum_{j=1}^N q_j m_{2,j}$$

Since, from Equation (4.3-16), with  $\bar{\omega}_s = 1$ ,

$$\ddot{q}_j = -\bar{\omega}_j^2 q_j + \frac{m_{2,j}}{m_{1,j}} (\bar{\omega}_y - \bar{\omega}_x) - 2\nu\bar{\omega}_j \dot{q}_j$$

we obtain in (4.5-1)

$$\ddot{\omega}_x = -\frac{1 - k_y}{k_x} \bar{\omega}_y$$

$$\begin{aligned} \ddot{\omega}_y \left( 1 - \frac{\Gamma}{1 + \Gamma \Delta} \frac{1}{k_y} \sum_{j=1}^N \frac{m_{2,j}^2}{m_{1,j}} \right) &= -\bar{\omega}_x \left( \frac{k_x - 1}{k_y} + \frac{1}{k_y} \frac{\Gamma}{1 + \Gamma \Delta} \sum_{j=1}^N \frac{m_{2,j}^2}{m_{1,j}} \right) \\ &\quad + \frac{\Gamma}{1 + \Gamma \Delta} \frac{1}{k_y} \sum_{j=1}^N m_{2,j} / (1 - \bar{\omega}_j^2) q_j - 2\nu\bar{\omega}_j \dot{q}_j \end{aligned} \quad (4.5-2)$$

$$\dot{\omega}_x = 0$$

Investigation of the stability of the motion in the presence of meridional vibrations, as studied in Chapter 5, will be carried

out on the basis of equations

(4.3-16) for the modal coordinates

(4.5-2) for the angular rates

with  $N = 1, 2$  or  $3$ , depending on the number of modes retained in the analysis. Since so far we have been considering a single boom located along the  $+x$  axis, it is of importance to generalize the analysis to multi-booms configurations. This is done in the following section.

#### 4.6 Generalization to Multiple-Boom Geometry

The equations for the rates and modal coordinates were given, for equatorial vibrations, by Equations (4.4-13) and (4.2-25), respectively, and for meridional vibrations by Equations (4.5-2) and (4.3-16) respectively, in the case of a single boom located along the  $+x$  axis. In the present section, we proceed to generalize the developments to the case of multiple-boom arrangements located in plane  $(x, y)$  (A plane containing axes  $x_p, y_p$ , two principal axes of inertia of the ellipsoid in inertia of the rigidified, total spacecraft) (Fig. 4.1).

In order to allow for various possibilities, the following definitions and notations are used

-  $k_x \stackrel{\text{def}}{=} \frac{I_x}{I_z}$ ,  $k_y \stackrel{\text{def}}{=} \frac{I_y}{I_z}$  are ratios, smaller than one for quasi-

rigid body stability, which relate to principal moments of inertia  $I_x, I_y, I_z$  of the total, rigidified structure.

- given the Etkin's number,  $\bar{\lambda}_k$ , and non-dimensional radius  $\xi_{0,k}$ , for boom "k", the notation :

-  $\phi_{j,k}(\bar{\lambda}_k, \xi_{0,k})$  is used for the  $j^{\text{th}}$  modal shape corresponding to these values of  $\bar{\lambda}$  and  $\xi_0$ . (there is no necessity to distinguish between  $\phi_j$  for the equatorial vibrations as opposed to  $\phi_j$  for meridional vibration, since they are the same)

$$\begin{aligned} m_{2,j,k} &\equiv \int_{\text{boom } k} \xi_{1,k} \Phi_{j,k}(\xi_k) d\xi_k \\ m_{1,j,k} &\equiv \int_{\text{boom } k} \bar{\Phi}_{j,k}^2(\xi_k) d\xi_k \quad \xi_{1,k} \underset{\text{def}}{\equiv} \xi_{0,k} + \xi_k \\ \text{and all } \Phi_{j,k} \text{ are normalized to a unit deflection at the tip.} \end{aligned}$$

-  $\bar{\omega}_{j,k}$ , a function of  $\bar{\lambda}_k$ ,  $\xi_{0,k}$ , for given  $j$ , is the  $j^{\text{th}}$  eigenfrequency for equatorial vibrations. whereas  $\tilde{\omega}_{j,k}$  is the  $j^{\text{th}}$  eigenfrequency for meridional vibrations. For the same pair  $(\lambda_k, \xi_{0,k})$ , we have from Equation

$$\bar{\omega}_{j,k}^2 + 1 = \tilde{\omega}_{j,k}^2 \quad (\text{all } j, k)$$

-  $q_{j,k}$  is the  $j^{\text{th}}$  modal coordinate (of type E, or M depending on which equations contain it) for boom  $k$ .

-  $\zeta_k$  is the angle between the boom's undeflected position (an axis normal to  $Z_p \equiv z$ , thus contained in plane  $x_p, y_p$ ) and axis  $x_p$  of the ellipsoid of inertia.

$$\Gamma_k \equiv \frac{(\ell l^3)_k}{(I_{z,k})_k}; \Delta_k \equiv \frac{1}{3} + \xi_{0,k} + \xi_{0,k}^2$$

#### 4.6.1 2 pairs of booms at right angle, along two principal axes of inertia

In this case, we assume that booms  $(+x, -x)$  are aligned on  $x_p$ , principal axis of inertia, and that booms  $(+y, -y)$  are normal to

( $+x$ ,  $-x$ ), thus aligned on principal axis of inertia  $y_p$  (Fig. 4-1).

In order to generalize the previously obtained equations for the modal coordinates and angular rates, we observe that in these equations,

$(x, y, z)$  are a r.h.s. system, with

+y in case E  
BOOM ALONG +x, deflection q along  
+z in case M

Now consider the boom along -x. Equations analogous to these derived for the +x boom will apply, substituting .

for the expression

axis x axis -x

axis y                    axis -y

axis z axis -z

$q_x$  along z       $q_{-x}$  along z

since  $(-x, -y, -z)$  is a direct system. The deflection  $q_{-x}$ , along  $-y$  (i.e. in case E), will be measured, for the sake of convenience, along axis  $+y$ , in the same manner as  $q_{+x}$  is measured. Therefore, in the analogous equations, written for case E, substitute

for the expression

$$q_{+x} \text{ along } +y \quad -q_{-x} \text{ along } +y \quad (4.6-1)$$

Similarly, the substitutions needed are, in the following cases:

boom along +y axis Substitute

for	the expression
axis x	axis y
axis y	axis -x
axis z	axis z
$q_{+x}$ along z	$q_{-y}$ along z
$q_{+x}$ along +y	$-q_y$ along +x

(4.6-2)

boom along -y axis Substitute

for	the expression
axis x	axis -y
axis y	axis x
axis z	axis z
$q_{+x}$ along z	$q_{-y}$ along z
$q_{+x}$ along y	$q_{-y}$ along +z

(4.6-3)

Effecting these substitutions in Equations (4.4-13) and (4.2-31), we

obtain

#### Equatorial vibrations (case E)

It should be recalled that  $\bar{\omega}_{j,k}$  refers to "E" type, jth eigenfrequency of boom "k". Although this is not done explicitly, the 'v' could be subscripted to account for different damping ratios in the various booms.

#### Rates

Booms -x, +y, -y: the equations for  $\dot{\omega}_x$ ,  $\dot{\omega}_y$  in (4.4-13) remain unchanged.

The equations for  $\dot{\omega}_z$ , in (4.4-13), read

-x boom:

$$\dot{\bar{\omega}}_x \left( 1 - \frac{\Gamma_x}{1 + \Gamma_x \Delta_x} \sum_{j=1}^N \frac{m_{2,j,-x}^2}{m_{1,j,-x}} \right) = - \frac{\Gamma_x}{1 + \Gamma_x \Delta_x} \sum_{j=1}^N \left( 2\nu \bar{\omega}_{j,-x} \dot{q}_{j,-x} + \bar{\omega}_{j,-x}^2 q_{j,-x} \right)$$

+y boom:

$$\dot{\bar{\omega}}_z \left( 1 - \frac{\Gamma_y}{1 + \Gamma_y \Delta_y} \sum_{j=1}^N \frac{m_{2,j,y}^2}{m_{1,j,y}} \right) = - \frac{\Gamma_y}{1 + \Gamma_y \Delta_y} \sum_{j=1}^N \left( 2\nu \bar{\omega}_{j,y} \dot{q}_{j,y} + \bar{\omega}_{j,y}^2 q_{j,y} \right) \quad (4.6-4)$$

-y boom:

$$\dot{\bar{\omega}}_z \left( 1 - \frac{\Gamma_y}{1 + \Gamma_y \Delta_y} \sum_{j=1}^N \frac{m_{2,j,-y}^2}{m_{1,j,-y}} \right) = \frac{\Gamma_y}{1 + \Gamma_y \Delta_y} \sum_{j=1}^N \left( 2\nu \bar{\omega}_{j,-y} \dot{q}_{j,-y} + \bar{\omega}_{j,-y}^2 q_{j,-y} \right)$$

Modal Coordinates:-x boom:

$$\ddot{q}_{j,-x} + 2\nu \bar{\omega}_{j,-x} \dot{q}_{j,-x} + \bar{\omega}_{j,-x}^2 q_{j,-x} = \frac{m_{2,j,-x}}{m_{1,j,-x}} \dot{\bar{\omega}}_z \quad (4.6-5)$$

+y boom:

$$\ddot{q}_{j,y} + 2\nu \bar{\omega}_{j,y} \dot{q}_{j,y} + \bar{\omega}_{j,y}^2 q_{j,y} = \frac{m_{2,j,y}}{m_{1,j,y}} \dot{\bar{\omega}}_z$$

-y boom:

$$\ddot{q}_{j,-y} + 2\nu \bar{\omega}_{j,-y} \dot{q}_{j,-y} + \bar{\omega}_{j,-y}^2 q_{j,-y} = - \frac{m_{2,j,-y}}{m_{1,j,-y}} \dot{\bar{\omega}}_z$$

Meridional vibrations (case M)

Again,  $\bar{\omega}_{j,k}$  refers to "M" type, jth eigenfrequency of boom "k", and although this is not explicitly done, the  $\nu$ 's could be subscripted to account for different damping ration in the various booms.

Rates

Booms -x, +y, -y: the equation for  $\dot{\bar{\omega}}_z$  remains unchanged, in (4.5-2)

The equations for  $\dot{\bar{\omega}}_x$ ,  $\dot{\bar{\omega}}_y$  read, with  $b_k \equiv \frac{\Gamma_k}{1 + \Gamma_k \Delta_k}$ ;  $k = +x, -x, +y, -y$  (4.5-2)

-x boom:

$$\dot{\bar{\omega}}_x = - \frac{1 - k_y}{k_x} \bar{\omega}_y$$

$$\begin{aligned} \dot{\bar{\omega}}_y \left( 1 - \frac{b_x}{k_y} \sum_{j=1}^N \frac{m_{2,j,-x}^2}{m_{1,j,-x}} \right) &= -\bar{\omega}_x \left( \frac{k_x - 1}{k_y} + b_x \frac{1}{k_y} \sum_{j=1}^N \frac{m_{2,j,x}^2}{m_{1,j,-x}} \right) \\ &\quad - \frac{b_x}{k_y} \sum_{j=1}^N m_{2,j,-x}^2 \left\{ (1 - \bar{\omega}_{j,-x}^2) q_{j,-x} - 2\nu \bar{\omega}_{j,-x} \dot{q}_{j,-x} \right\} \end{aligned}$$

+y boom.

$$\ddot{\omega}_x \left( 1 - b_y \frac{1}{k_x} \sum_{j=1}^N \frac{m_{2,j,y}^2}{m_{1,j,y}} \right) = -\bar{\omega}_y \left( \frac{1-k_y}{k_x} - \frac{1}{k_x} b_y \sum_{j=1}^N \frac{m_{2,j,y}^2}{m_{1,j,y}} \right)$$

$$- b_y \frac{1}{k_x} \sum_{j=1}^N m_{2,j,y} \left\{ (1-\bar{\omega}_{j,y}^2) q_{j,y} - 2\nu \bar{\omega}_{j,y} \dot{q}_{j,y} \right\}$$

$$\ddot{\omega}_y = - \frac{k_x - 1}{k_y} \bar{\omega}_x$$

-y boom.

$$\ddot{\omega}_x \left( 1 - \frac{b-y}{k_x} \sum_{j=1}^N \frac{m_{2,j,-y}^2}{m_{1,j,-y}} \right) = -\bar{\omega}_y \left( \frac{1-k_y}{k_x} - \frac{b-y}{k_x} \sum_{j=1}^N \frac{m_{2,j,-y}^2}{m_{1,j,-y}} \right)$$

$$+ \frac{b-y}{k_x} \sum_{j=1}^N m_{2,j,-y} \left\{ (1-\bar{\omega}_{j,-y}^2) q_{j,-y} - 2\nu \bar{\omega}_{j,-y} \dot{q}_{j,-y} \right\}$$

$$\ddot{\omega}_y = - \frac{k_x - 1}{k_y} \bar{\omega}_x$$

(4.6-6)

Modal Coordinates:-x boom:

$$\ddot{q}_{j,-x} + 2\rho \bar{\omega}_{j,x} \dot{q}_{j,-x} + \bar{\omega}_{j,x}^2 q_{j,-x} = -\frac{m_{2,j,-x}}{m_{1,j,-x}} (\ddot{\omega}_y - \bar{\omega}_x) \quad (4.6-6)$$

+y boom:

$$\ddot{q}_{j,y} + 2\rho \bar{\omega}_{j,y} \dot{q}_{j,y} + \bar{\omega}_{j,y}^2 q_{j,y} = -\frac{m_{2,j,y}}{m_{1,j,y}} (\ddot{\omega}_x + \bar{\omega}_y) \quad (4.6-7)$$

-y boom:

$$\ddot{q}_{j,-y} + 2\rho \bar{\omega}_{j,-y} \dot{q}_{j,-y} + \bar{\omega}_{j,-y}^2 q_{j,-y} = -\frac{m_{2,j,-y}}{m_{1,j,-y}} (\ddot{\omega}_x + \bar{\omega}_y) \quad (4.6-7)$$

## 4.6.1.1 The Four Different booms

Let

$$b_k \stackrel{\text{def}}{=} \frac{(\rho l^3)_k}{I_z} \quad r_k = \frac{(\rho l^3)_k}{(I_z h)_k} \quad \Delta_k = \frac{1}{3} + \xi_{o,k} + \xi_{o,k}^2$$

The equations of motion become

Equatorial vibrations (case E):Rates  $k = +x, -x, +y, -y ; j = 1, 2, \dots, N$ 

$$\dot{\bar{\omega}}_x = -\frac{k_y}{k_x} \bar{\omega}_y$$

$$\dot{\bar{\omega}}_y = -\frac{k_x - 1}{k_y} \bar{\omega}_x$$

$$\ddot{\omega}_z \left( 1 - \sum_k b_k \sum_{j=1}^N \frac{m_{2,j,k}^2}{m_{1,j,k}} \right) = \sum_{j=1}^N \left[ b_x \left[ 2\nu \bar{\omega}_{j,x} \dot{q}_{j,x} + \bar{\omega}_{j,x}^2 q_{j,x} \right] - b_{-x} \left[ 2\nu \bar{\omega}_{j,-x} \dot{q}_{j,-x} \right. \right. \\ \left. \left. + \bar{\omega}_{j,-x}^2 q_{j,-x} \right] - \sum_{j=1}^N \left[ b_y \left[ 2\nu \bar{\omega}_{j,y} \dot{q}_{j,y} + \bar{\omega}_{j,y}^2 q_{j,y} \right] - b_{-y} \left[ 2\nu \bar{\omega}_{j,-y} \dot{q}_{j,-y} + \bar{\omega}_{j,-y}^2 q_{j,-y} \right] \right] \right] \\ (4.6-8)$$

Modal coordinates:For  $j = 1, 2, \dots, N; k = +x, -y$ 

$$\ddot{q}_{j,k} + 2\nu \bar{\omega}_{j,k} \dot{q}_{j,k} + \bar{\omega}_{j,k}^2 q_{j,k} = - \frac{m_{2,j,k}}{m_{1,j,k}} \ddot{\omega}_z \\ (4.6-9)$$

For  $j = 1, 2, \dots, N; k = -x, +y$ 

$$\ddot{q}_{j,k} + 2\nu \bar{\omega}_{j,k} \dot{q}_{j,k} + \bar{\omega}_{j,k}^2 q_{j,k} = \frac{m_{2,j,k}}{m_{1,j,k}} \ddot{\omega}_z$$

Meridional vibrations (case M)Rates: With  $k$  taking the values indicated;  $j = 1, 2, \dots, N;$ 

$$\ddot{\omega}_x \left( 1 - \frac{1}{k_x} \sum_{k=+y, -y} b_k \sum_{j=1}^N \frac{m_{2,j,k}^2}{m_{1,j,k}} \right) = -\bar{\omega}_y \left( \frac{1-k_y}{k_x} - \frac{1}{k_x} \sum_{k=+y, -y} b_k \sum_{j=1}^N \frac{m_{2,j,k}}{m_{1,j,k}} \right) \\ - \frac{1}{k_x} \left[ b_y \sum_{j=1}^N m_{2,j,y} \left\{ (1-\bar{\omega}_{j,y}^2) q_{j,y} - 2\nu \bar{\omega}_{j,y} \dot{q}_{j,y} \right\} \right. \\ \left. - b_{-y} \sum_{j=1}^N m_{2,j,-y} \left\{ (1-\bar{\omega}_{j,-y}^2) q_{j,-y} - 2\nu \bar{\omega}_{j,-y} \dot{q}_{j,-y} \right\} \right] \\ (4.6-10)$$

$$\ddot{\omega}_y \left( 1 - \frac{1}{k_y} \sum_{k=+x, -x} b_k \sum_{j=1}^N \frac{m_{2,j,k}^2}{m_{1,j,k}} \right) = -\bar{\omega}_x \left( \frac{k_x-1}{k_y} + \frac{1}{k_y} \sum_{k=+x, -x} b_k \sum_{j=1}^N \frac{m_{2,j,k}}{m_{1,j,k}} \right) \\ + \frac{1}{k_y} \left[ b_x \sum_{j=1}^N m_{2,j,x} \left\{ (1-\bar{\omega}_{j,x}^2) q_{j,x} - 2\nu \bar{\omega}_{j,x} \dot{q}_{j,x} \right\} \right. \\ \left. - b_{-x} \sum_{j=1}^N m_{2,j,-x} \left\{ (1-\bar{\omega}_{j,-x}^2) q_{j,-x} - 2\nu \bar{\omega}_{j,-x} \dot{q}_{j,-x} \right\} \right] \\ \ddot{\omega}_z = 0 \\ (4.6-10)$$

Modal coordinates

For  $j = 1, 2, \dots, N; k = +x, -x, +y, -y;$

$$\begin{aligned}
 \ddot{q}_{j,k} + 2\nu\bar{\omega}_{j,k}\dot{q}_{j,k} + \bar{\omega}_j^2 q_{j,k} &= \frac{m_{2,j,k}}{m_{1,j,k}} (\dot{\bar{\omega}}_y - \bar{\omega}_x) & k = x \\
 \text{or} \\
 &= -\frac{m_{2,j,k}}{m_{1,j,k}} (\dot{\bar{\omega}}_y - \bar{\omega}_x) & k = -x \\
 &= -\frac{m_{2,j,k}}{m_{1,j,k}} (\dot{\bar{\omega}}_x + \bar{\omega}_y) & k = y \quad (4.6-11) \\
 &= \frac{m_{2,j,k}}{m_{1,j,k}} (\dot{\bar{\omega}}_x + \bar{\omega}_y) & k = -y
 \end{aligned}$$

4.6.1.8 Aligned booms identical; different booms along (+x, +y).

Equations (4.6-8) and (4.6-9), or (4.6-10) and (4.6-11) are simplified, in view of the relations

$$\begin{aligned}
 \Gamma_x &= \Gamma_{-x}; \xi_{o,x} = \xi_{o,-x}; \Delta_x = \Delta_{-x}; b_x = b_{-x}; \bar{\omega}_{j,x} = \bar{\omega}_{j,-x}; m_{2,j,x} = m_{2,j,-x}; m_{1,j,x} = m_{1,j,-x} \\
 \text{and similar ones for subscripts } y, -y. & \quad (4.6-12)
 \end{aligned}$$

Equatorial case:

Rates: With  $j = 1, 2, \dots, N;$

$$\dot{\bar{\omega}}_x = -\frac{1-k_y}{k_x} \bar{\omega}_y$$

$$\dot{\bar{\omega}}_y = -\frac{k_x-1}{k_y} \bar{\omega}_x$$

$$\dot{\bar{\omega}}_z = \left(1 - 2b_x \sum_{j=1}^N \frac{m_{2,j,x}^2}{m_{1,j,x}} - 2b_y \sum_{j=1}^N \frac{m_{2,j,y}^2}{m_{1,j,y}}\right) = b_x \sum_{j=1}^N m_{2,j,x} \left[ (2\nu\bar{\omega}_{j,x} \dot{q}_{j,x}) \right. \quad (4.6-13)$$

$$\left. + \bar{\omega}_{j,x}^2 q_{j,x} \right] - \left( 2\nu\bar{\omega}_{j,x} \dot{q}_{j,-x} + \bar{\omega}_{j,x}^2 q_{j,-x} \right) - b_y \sum_{j=1}^N m_{2,j,y} \left[ (2\nu\bar{\omega}_{j,y} \dot{q}_{j,y}) + \bar{\omega}_{j,y}^2 q_{j,y} \right] - \left( 2\nu\bar{\omega}_{j,y} \dot{q}_{j,-y} + \bar{\omega}_{j,y}^2 q_{j,-y} \right) \quad (4.6-13)$$

Modal coordinates:

Same as (4.6-9), with Equations (4.6-12). (4.6-14)

Meridional case:

Rates: With  $j = 1, 2, \dots, N$ ;

$$\begin{aligned} \dot{\bar{\omega}}_x & \left( 1 - \frac{2}{k_x} b_y \sum_{j=1}^N \frac{m_{2,j,y}^2}{m_{1,j,y}} \right) = -\bar{\omega}_y \left( \frac{1-k_y}{k_x} - \frac{2}{k_x} \sum_{j=1}^N \frac{m_{2,j,y}^2}{m_{1,j,y}} \right) \\ & - \frac{1}{k_x} b_y \sum_{j=1}^N m_{2,j,y} \left\{ \left[ (1-\bar{\omega}_y^2) q_{j,y} + 2\nu \bar{\omega}_y \dot{q}_{j,y} \right] - \left[ (1-\bar{\omega}_y^2) q_{j,-y} + 2\nu \bar{\omega}_y \dot{q}_{j,-y} \right] \right\} \\ \dot{\bar{\omega}}_y & \left( 1 - \frac{2}{k_y} b_x \sum_{j=1}^N \frac{m_{2,j,x}^2}{m_{1,j,x}} \right) = -\bar{\omega}_x \left( \frac{k_x-1}{k_y} + \frac{2}{k_y} b_x \sum_{j=1}^N \frac{m_{2,j,x}^2}{m_{1,j,x}} \right) \\ & + \frac{1}{k_y} b_x \sum_{j=1}^N m_{2,j,x} \left\{ \left[ (1-\bar{\omega}_{j,x}^2) q_{j,x} + 2\nu \bar{\omega}_{j,x} \dot{q}_{j,x} \right] - \left[ (1-\bar{\omega}_{j,x}^2) q_{j,-x} + 2\nu \bar{\omega}_{j,x} \dot{q}_{j,-x} \right] \right\} \quad (4.6-15) \\ \dot{\bar{\omega}}_z & = 0 \end{aligned}$$

Modal coordinates:

Same as (4.6-11), with Equations (4.6-12)

(4.6-16)

4.6.1.3 Identical booms along  $x, -x, y, -y$ 

In this case, we can use in common for all booms, the notations

$$\bar{\omega}_j, m_{1,j}, m_{2,j}, \Gamma, \Delta, \xi_0, b$$

Thus Equations (4.6-15) and (4.6-16) are simplified as follows:

Equatorial case:

Rates: With  $j = 1, 2, \dots, N$ ;

$$\begin{aligned} \dot{\bar{\omega}}_x & = -\frac{1-k_y}{k_x} \bar{\omega}_y \\ \dot{\bar{\omega}}_y & = -\frac{k_x-1}{k_y} \bar{\omega}_x \\ \dot{\bar{\omega}}_z & \left( 1 - 4b \sum_{j=1}^N \frac{m_{2,j}^2}{m_{1,j}} \right) = 2b \sum_{j=1}^N m_{2,j} \left[ \bar{\omega}_j^2 (q_{j,x} + q_{j,-y} - q_{j,-x} - q_{j,y}) \right. \\ & \left. + 2\nu \bar{\omega}_j (\dot{q}_{j,x} + \dot{q}_{j,-y} - \dot{q}_{j,-x} - \dot{q}_{j,y}) \right] \quad (4.6-17) \end{aligned}$$

Modal coordinates: With  $j = 1, 2, \dots, N$ ;

$$\begin{aligned}\ddot{q}_{j,x} + 2\nu\bar{\omega}_j \dot{q}_{j,x} + \bar{\omega}_j^2 q_{j,x} &= -\frac{m_{2,j}}{m_{1,j}} \frac{\ddot{\omega}_z}{\bar{\omega}_z} \\ \ddot{q}_{j,-x} + 2\nu\bar{\omega}_j \dot{q}_{j,-x} + \bar{\omega}_j^2 q_{j,-x} &= \frac{m_{2,j}}{m_{1,j}} \frac{\ddot{\omega}_z}{\bar{\omega}_z} \\ \ddot{q}_{j,y} + 2\nu\bar{\omega}_j \dot{q}_{j,y} + \bar{\omega}_j^2 q_{j,y} &= \frac{m_{2,j}}{m_{1,j}} \frac{\ddot{\omega}_z}{\bar{\omega}_z} \\ \ddot{q}_{j,-y} + 2\nu\bar{\omega}_j \dot{q}_{j,-y} + \bar{\omega}_j^2 q_{j,-y} &= -\frac{m_{2,j}}{m_{1,j}} \frac{\ddot{\omega}_z}{\bar{\omega}_z}\end{aligned}\quad (4.6-18)$$

Meridional case:

Rates: With  $j = 1, 2, \dots, N$ ;

$$\begin{aligned}\ddot{\omega}_x \left( 1 - \frac{2}{k_x} b \sum_{j=1}^N \frac{m_{2,j}^2}{m_{1,j}} \right) &= -\bar{\omega}_y \left( \frac{1-k_y}{k_x} - \frac{2}{k_x} b \sum_{j=1}^N \frac{m_{2,j}^2}{m_{1,j}} \right) \\ &\quad - \frac{1}{k_x} b \sum_{j=1}^N m_{2,j} \left\{ (1-\bar{\omega}_j^2)(q_{j,y} - q_{j,-y}) - 2\nu\bar{\omega}_j (\dot{q}_{j,y} - \dot{q}_{j,-y}) \right\} \\ \ddot{\omega}_x \left( 1 - \frac{2}{k_y} b \sum_{j=1}^N \frac{m_{2,j}^2}{m_{1,j}} \right) &= -\bar{\omega}_x \left( \frac{k_x-1}{k_y} + \frac{2}{k_y} b \sum_{j=1}^N \frac{m_{2,j}^2}{m_{1,j}} \right) \\ &\quad + \frac{1}{k_y} b \sum_{j=1}^N m_{2,j} \left\{ (1-\bar{\omega}_j^2)(q_{j,x} - q_{j,-x}) - 2\nu\bar{\omega}_j (\dot{q}_{j,x} - \dot{q}_{j,-x}) \right\} \\ \ddot{\omega}_z &= 0\end{aligned}\quad (4.6-19)$$

Modes: With  $j = 1, 2, \dots, N$ ;  $k = +x, -x, +y, -y$

$$\begin{aligned}\ddot{q}_{j,k} + 2\nu\bar{\omega}_j \dot{q}_{j,k} + \bar{\omega}_j^2 q_{j,k} &= \frac{m_{2,j}}{m_{1,j}} (\ddot{\omega}_y - \bar{\omega}_x) \quad k=x \\ &\text{or} \\ &= \frac{m_{2,j}}{m_{1,j}} (\ddot{\omega}_y - \bar{\omega}_x) \quad k=-x \\ &\text{or} \\ &= -\frac{m_{2,j}}{m_{1,j}} (\ddot{\omega}_x + \bar{\omega}_y) \quad k=y \\ &\text{or} \\ &= \frac{m_{2,j}}{m_{1,j}} (\ddot{\omega}_x + \bar{\omega}_y) \quad k=-y\end{aligned}\quad (4.6-20)$$

An alternate form of the equations for the rates has been used in the computer programs described in Chapter 5.

Let

$$K_{hx} \stackrel{\text{def}}{=} \frac{I_{z, \text{hub}}}{I_{x, \text{hub}}}$$

$$K_{hy} \stackrel{\text{def}}{=} \frac{I_{z, \text{hub}}}{I_{y, \text{hub}}}$$

Assume furthermore that the motion is antisymmetric, i.e.  $\dot{q} = -\dot{q}_x$ ,

$\dot{q}_y = -\dot{q}_y$ : Then

$$k_x = \frac{I_x}{I_z} = \frac{I_{x, \text{hub}} + 2 \Delta \rho l^3}{I_{z, \text{hub}} + 4 \Delta \rho l^3} = \frac{\frac{1}{K_{hx}} + 2 \Gamma \Delta}{1 + 4 \Gamma \Delta}$$

$$k_y = \frac{I_y}{I_z} = \frac{\frac{1}{K_{hy}} + 2 \Gamma \Delta}{1 + 4 \Gamma \Delta}$$

and the rates, as given in (4.6-17) and (4.6-19), respectively, can be rewritten:

Case E:

$$\dot{\bar{\omega}}_x = - \frac{\frac{1}{K_{hx}} + 2 \Gamma \Delta}{\frac{1}{K_{hy}} + 2 \Gamma \Delta} \bar{\omega}_y \quad (4.6-21)$$

$$\dot{\bar{\omega}}_y = - \frac{\frac{1}{K_{hx}} + 2 \Gamma \Delta - 1}{\frac{1}{K_{hy}} + 2 \Gamma \Delta} \bar{\omega}_x$$

$$\dot{\bar{\omega}}_z = - \frac{2 \Gamma \left[ \sum_{j=1}^n m_{2,j} [\bar{\omega}_j^2 (\dot{q}_y - \dot{q}_x) + 2 \nu \bar{\omega}_j (\dot{q}_y - \dot{q}_x)] \right]}{1 + 4 \Gamma \left( \Delta - \sum_{j=1}^n \frac{m_{2,j}^2}{m_{1,j}} \right)}$$

Case M:

$$\begin{aligned}\dot{\bar{\omega}}_x &= - \frac{[1 - \frac{1}{K_{hx}} + 2\Gamma(\Delta - \sum_{d=1}^N \frac{m_{2,d}^2}{m_{1,d}}) + 2\Gamma \sum_{j=1}^N m_{2,j} [(\bar{\omega}_j^2)q_{j,y} - 2\nu\bar{\omega}_j \dot{q}_{j,y}]]}{\frac{1}{K_{hy}} - 1 - 2\Gamma(\Delta - \sum_{d=1}^N \frac{m_{2,d}^2}{m_{1,d}}) - 2\Gamma \sum_{j=1}^N m_{2,j} [(\bar{\omega}_j^2)q_{j,x} - 2\nu\bar{\omega}_j \dot{q}_{j,x}]} \\ \dot{\bar{\omega}}_y &= - \frac{\frac{1}{K_{hx}} - 1 - 2\Gamma(\Delta - \sum_{d=1}^N \frac{m_{2,d}^2}{m_{1,d}}) - 2\Gamma \sum_{j=1}^N m_{2,j} [(\bar{\omega}_j^2)q_{j,x} - 2\nu\bar{\omega}_j \dot{q}_{j,x}]}{\frac{1}{K_{hy}} + 2\Gamma(\Delta - \sum_{d=1}^N \frac{m_{2,d}^2}{m_{1,d}})} \\ \dot{\bar{\omega}}_z &= 0\end{aligned}\quad (4.6-22)$$

If furthermore, the transverse moments of inertia of the hub are equal, i.e.

$$I_{x,\text{hub}} = I_{y,\text{hub}}$$

$$K_h = K_{hx} = K_{hy}$$

the above equations for the rates simplify to

Case E:

$$\begin{aligned}\dot{\bar{\omega}}_x &= - \frac{\frac{1}{K_h} + 2\Gamma\Delta}{\frac{1}{K_h} + 2\Gamma\Delta - 1} \bar{\omega}_y \\ \dot{\bar{\omega}}_y &= - \frac{\frac{1}{K_h} + 2\Gamma\Delta - 1}{\frac{1}{K_h} + 2\Gamma\Delta} \bar{\omega}_x \\ \dot{\bar{\omega}}_z &= - \frac{\frac{1}{K_h} + 2\Gamma\Delta \left[ \sum_{d=1}^N m_{2,d} [\bar{\omega}_d^2 (q_{j,y} - q_{j,x}) + 2\nu\bar{\omega}_d (\dot{q}_{j,y} - \dot{q}_{j,x})] \right]}{1 + 4\Gamma \left( \Delta - \sum_{d=1}^N \frac{m_{2,d}^2}{m_{1,d}} \right)}\end{aligned}\quad (4.6-23)$$

Case M:

$$\begin{aligned}\dot{\bar{\omega}}_x &= - \frac{1 - \frac{1}{K_h} + 2\Gamma \left( \Delta - \sum_{d=1}^N \frac{m_{2,d}^2}{m_{1,d}} \right) + 2\Gamma \sum_{j=1}^N m_{2,j} [(\bar{\omega}_j^2)q_{j,y} - 2\nu\bar{\omega}_j \dot{q}_{j,y}]}{\frac{1}{K_h} + 2\Gamma \left( \Delta - \sum_{d=1}^N \frac{m_{2,d}^2}{m_{1,d}} \right)} \\ \dot{\bar{\omega}}_y &= - \frac{\frac{1}{K_h} - 1 - 2\Gamma \left( \Delta - \sum_{d=1}^N \frac{m_{2,d}^2}{m_{1,d}} \right) - 2\Gamma \sum_{j=1}^N m_{2,j} [(\bar{\omega}_j^2)q_{j,x} - 2\nu\bar{\omega}_j \dot{q}_{j,x}]}{\frac{1}{K_h} + 2\Gamma \left( \Delta - \sum_{d=1}^N \frac{m_{2,d}^2}{m_{1,d}} \right)}\end{aligned}\quad (4.6-24)$$

4.6.2 "B" booms in  $x, y$  plane, necessarily along principal axes of inertia.

The booms are all contained in plane  $x, y$ , with  $x, y$  as two transverse axes of inertia of the rigidified structure, and are normal to  $z_p$ , satellite spin axis. With the notations introduced in the beginning of Section 4.6,  $\zeta_k$  is the angle between the axis of the boom and axis  $x$ .

Let  $q_{j,k}$  be the  $j$ th modal coordinate of boom  $k$ . The equations for the modal coordinates and the rates, written in Sections 4.2 to 4.5 for the "+x boom", along a principal axis of inertia, will be modified as follows:

#### 4.6.2.1 +x boom "k"; angle $\zeta_k$ with $x_p$

##### Equatorial case.

##### Modal coordinate:

$$\ddot{q}_{j,k} + 2\nu \bar{\omega}_{j,k} \dot{q}_{j,k} + \bar{\omega}_j^2 q_{j,k} = - \frac{m_{2,j,k}}{m_{1,j,k}} \frac{\dot{\omega}_z}{\omega_z} \quad (4.6-25)$$

Rates:  $X \equiv x_p, Y \equiv y_p, Z \equiv z_p$

$$\begin{aligned} \dot{\omega}_X &= - \frac{1-k_y}{k_X} \bar{\omega}_Y \\ \dot{\omega}_Y &= - \frac{k_X - 1}{k_Y} \bar{\omega}_X \end{aligned} \quad (4.6-26)$$

$$\dot{\omega}_{\zeta} \left( 1 - \frac{(\rho l^3)_k}{I_{\zeta}} \sum_{j=1}^N \frac{m_{2,j,k}^2}{m_{1,j,k}} \right) = \frac{(\rho l^3)_k}{I_{\zeta}} \sum_{j=1}^N m_{2,j,k} [2\nu \bar{\omega}_{j,k} \dot{q}_{j,k} + \bar{\omega}_{j,k}^2 q_{j,k}]$$

##### Meridional case

$$\ddot{q}_{j,k} + 2\nu \bar{\omega}_{j,k} \dot{q}_{j,k} + \bar{\omega}_j^2 q_{j,k} = - \frac{m_{2,j,k}}{m_{1,j,k}} \left( \frac{\dot{\omega}_X}{\omega_X} \sin \zeta_k + \frac{\dot{\omega}_Y}{\omega_Y} \cos \zeta_k - \bar{\omega}_X \cos \zeta_k - \bar{\omega}_Y \sin \zeta_k \right) \quad (4.6-27)$$

since  $\dot{\bar{\omega}}_y$  in (4.3-16) becomes  $-\ddot{\bar{\omega}}_x \sin \xi_k + \dot{\bar{\omega}}_y \cos \xi_k$

$\dot{\bar{\omega}}_x$  in (4.3-16) becomes  $\ddot{\bar{\omega}}_x \cos \xi_k + \dot{\bar{\omega}}_y \sin \xi_k$

### Rates:

In the case of a "+x" boom, Equation (4.5-1) shows that the vibrations parallel to the z-axis generate a torque along the direction normal to "+x", i.e. "+y" having projections:

$$\begin{aligned} (\rho l^3)_k \int_{\text{boom}, k} (\ddot{\gamma} + \gamma) \xi_j d\xi &\times (-\sin \xi_k) && \text{ALONG } x \\ (\rho l^3)_k \int_{\text{boom}, k} (\ddot{\gamma} + \gamma) \xi_j d\xi &\times (\cos \xi_k) && \text{ALONG } y \end{aligned}$$

The equations for the rates will read, before dividing by  $I_x$ ,  $I_y$  respectively,

$$\begin{aligned} I_x \dot{\bar{\omega}}_x + (I_z - I_y) \bar{\omega}_y &= (\rho l^3)_k (-\sin \xi_k) \sum_{j=1}^N m_{2,j,k} [(1 - \bar{\omega}_{j,k}^2) q_{j,k} - 2\nu \bar{\omega}_{j,k} \dot{q}_{j,k}] \\ &+ (\rho l^3)_k (-\sin \xi_k) \sum_{j=1}^N \frac{m_{2,j,k}^2}{m_{1,j,k}} (-\dot{\bar{\omega}}_x \sin \xi_k + \dot{\bar{\omega}}_y \cos \xi_k - \bar{\omega}_x \cos \xi_k - \bar{\omega}_y \sin \xi_k) \\ I_y \dot{\bar{\omega}}_y + (I_x - I_z) \bar{\omega}_x &= (\rho l^3)_k (\cos \xi_k) \sum_{j=1}^N m_{2,j,k} [(1 - \bar{\omega}_{j,k}^2) q_{j,k} \\ &- 2\nu \bar{\omega}_{j,k} \dot{q}_{j,k}] + (\rho l^3)_k (\cos \xi_k) \sum_{j=1}^N \frac{m_{2,j,k}^2}{m_{1,j,k}} (-\dot{\bar{\omega}}_x \sin \xi_k + \dot{\bar{\omega}}_y \cos \xi_k - \bar{\omega}_x \cos \xi_k \\ &- \bar{\omega}_y \sin \xi_k) \\ \dot{\bar{\omega}}_z &= 0 \end{aligned} \quad (4.6-28)$$

Now define the following coefficients

$$A_{11} \underset{\text{def}}{=} I_X - (\rho l^3)_k \sin^2 \xi_k \sum_{j=1}^N \frac{m_{2,j,k}^2}{m_{1,j,k}}$$

$$A_{12} \underset{\text{def}}{=} (\rho l^3)_k \sin \xi_k \cos \xi_k \sum_{j=1}^N \frac{m_{2,j,k}^2}{m_{1,j,k}}$$

$$A_{21} \underset{\text{def}}{=} (\rho l^3)_k \sin \xi_k \cos \xi_k \sum_{j=1}^N \frac{m_{2,j,k}^2}{m_{1,j,k}}$$

$$A_{22} \underset{\text{def}}{=} I_Y - (\rho l^3)_k \cos^2 \xi_k \sum_{j=1}^N \frac{m_{2,j,k}^2}{m_{1,j,k}}$$

$$\alpha_{11} \underset{\text{def}}{=} \frac{A_{11}}{I_X}$$

$$\alpha_{12} \underset{\text{def}}{=} \frac{A_{12}}{I_X}$$

$$\alpha_{21} \underset{\text{def}}{=} \frac{A_{21}}{I_Y}$$

$$\alpha_{22} \underset{\text{def}}{=} \frac{A_{22}}{I_Y}$$

Let

$$\begin{aligned} f_{1,k} &\stackrel{\text{def}}{=} \frac{(\rho l^3)_k}{I_x} (-\sin \xi_k) \sum_{j=1}^N \left\{ m_{2,j,k} \left[ \left( 1 - \bar{\omega}_{j,k}^2 \right) q_{j,k} - 2\nu \bar{\omega}_{j,k} \dot{q}_{j,k} \right] \right. \\ &\quad \left. + \frac{m_{2,j,k}^2}{m_{1,j,k}} \left( -\bar{\omega}_x \cos \xi_k - \bar{\omega}_y \sin \xi_k \right) \right\} \\ f_{2,k} &\stackrel{\text{def}}{=} \frac{(\rho l^3)_k}{I_y} (\cos \xi_k) \sum_{j=1}^N \left\{ m_{2,j,k} \left[ \left( 1 - \bar{\omega}_{j,k}^2 \right) q_{j,k} - 2\nu \bar{\omega}_{j,k} \dot{q}_{j,k} \right] \right. \\ &\quad \left. + \frac{m_{2,j,k}^2}{m_{1,j,k}} \left( -\bar{\omega}_x \cos \xi_k - \bar{\omega}_y \sin \xi_k \right) \right\} \end{aligned}$$

System (4.6-28) is rewritten

$$a_{11} \ddot{\omega}_x + a_{12} \ddot{\omega}_y = f_{1,k}$$

$$a_{21} \ddot{\omega}_x + a_{22} \ddot{\omega}_y = f_{2,k}$$

$$\text{Let } D_k = a_{11}a_{22} - a_{21}a_{12} = 1 - (\rho l^3)_k \left( \frac{\sin^2 \xi_k}{I_x} + \frac{\cos^2 \xi_k}{I_y} \right) \sum_{j=1}^N \frac{m_{2,j,k}^2}{m_{1,j,k}}$$

Then the equations for the rates are

$$\begin{aligned} \frac{\ddot{\omega}_x}{D_k} &= \frac{a_{22} f_{1,k} - a_{12} f_{2,k}}{D_k} \\ \frac{\ddot{\omega}_y}{D_k} &= \frac{a_{11} f_{2,k} - a_{21} f_{1,k}}{D_k} \\ \ddot{\omega}_z &= 0 \end{aligned} \tag{4.6-29}$$

4.6.2.2 General case: "B" booms, making angles  $\xi_k$  ( $k = 1, \dots, B$ )

with  $x_p$ .

Equations (4.6-28) will, in the general case of B booms, at angles  $\xi_k$  ( $k = 1, \dots, B$ ), have r.h. sides with sums over k, in

addition to the summation over  $j$ . Important note: all modal displacements are referred to the  $+z$  axis (case M) or to the normal "y<sub>k</sub>" to the boom "x<sub>k</sub>" (in case E) such that  $(x_k, y_k, z)$  is a direct system.

### Equatorial case:

#### Modal coordinates:

$$\ddot{q}_{j,k} + 2\nu \bar{\omega}_{j,k} \dot{q}_{j,k} + \bar{\omega}_{j,k}^2 q_{j,k} = - \frac{m_{2,j,k}}{m_{1,j,k}} \dot{\omega}_z \quad (4.6-30)$$

in which expression (4.6-31) is substituted.

#### Rates:

$$\dot{\omega}_x = - \frac{1-k_y}{k_x} \bar{\omega}_y \quad (4.6-31)$$

$$\dot{\omega}_y = - \frac{k_x - 1}{k_y} \bar{\omega}_x$$

$$\dot{\omega}_z \left( 1 - \frac{1}{I_z} \sum_{k=1}^B (\rho l^3)_k \sum_{j=1}^N \frac{m_{2,j,k}^2}{m_{1,j,k}} \right) = \frac{1}{I_z} \sum_{k=1}^B \left\{ (\rho l^3)_k \sum_{j=1}^N m_{3,j,k} \left[ 2\nu \bar{\omega}_{j,k} \dot{q}_{j,k} + \bar{\omega}_{j,k}^2 q_{j,k} \right] \right\}$$

### Meridional case:

#### Modal coordinates:

$$\ddot{q}_{j,k} + 2\nu \bar{\omega}_{j,k} \dot{q}_{j,k} + \bar{\omega}_{j,k}^2 q_{j,k} = \frac{m_{2,j,k}}{m_{1,j,k}} \left( -\bar{\omega}_x \sin \xi_k + \bar{\omega}_y \cos \xi_k - \bar{\omega}_x \cos \xi_k - \bar{\omega}_y \sin \xi_k \right) \quad (4.6-32)$$

in which expression (4.6-33) is substituted

Defining

$$c_{11} \stackrel{\text{def}}{=} 1 - \sum_{k=1}^B \frac{(P l^3)_k}{I_X} \sin^2 \xi_k \sum_{j=1}^N \frac{m_{2,j,k}^2}{m_{1,j,k}}$$

$$c_{12} \stackrel{\text{def}}{=} \sum_{k=1}^B \frac{(P l^3)_k}{I_X} \sin \xi_k \cos \xi_k \sum_{j=1}^N \frac{m_{2,j,k}^2}{m_{1,j,k}}$$

$$c_{21} \stackrel{\text{def}}{=} \sum_{k=1}^B \frac{(P l^3)_k}{I_Y} \sin \xi_k \cos \xi_k \sum_{j=1}^N \frac{m_{2,j,k}^2}{m_{1,j,k}}$$

$$c_{22} \stackrel{\text{def}}{=} 1 - \sum_{k=1}^B \frac{(P l^3)_k}{I_Y} \cos^2 \xi_k \sum_{j=1}^N \frac{m_{2,j,k}^2}{m_{1,j,k}}$$

$$D \stackrel{\text{def}}{=} c_{11} c_{22} - c_{21} c_{12}$$

$$= 1 - \sum_{k=1}^B \frac{(P l^3)_k}{I_X} \left( \frac{\sin^2 \xi_k}{I_X} + \frac{\cos^2 \xi_k}{I_Y} \right) \sum_{j=1}^N \frac{m_{2,j,k}^2}{m_{1,j,k}}$$

$$\begin{aligned} f_1 &\stackrel{\text{def}}{=} \sum_{k=1}^B \frac{(P l^3)_k}{I_X} \left( -\sin \xi_k \sum_{j=1}^N m_{2,j,k} [(-\bar{\omega}_j^2) q_{j,k} - 2\bar{\omega}_j \dot{q}_{j,k}] \right. \\ &\quad \left. + \frac{m_{2,j,k}^2}{m_{1,j,k}} (-\bar{\omega}_X \cos \xi_k - \bar{\omega}_Y \sin \xi_k) \right) \end{aligned}$$

$$\begin{aligned} f_2 &\stackrel{\text{def}}{=} \sum_{k=1}^B \frac{(P l^3)_k}{I_X} (\cos \xi_k) \sum_{j=1}^N m_{2,j,k} [(-\bar{\omega}_j^2) q_{j,k} - 2\bar{\omega}_j \dot{q}_{j,k}] \\ &\quad + \frac{m_{2,j,k}^2}{m_{1,j,k}} (-\bar{\omega}_X \cos \xi_k - \bar{\omega}_Y \sin \xi_k) \end{aligned}$$

we obtain the equations

$$\begin{aligned} \dot{\bar{\omega}}_x &= \frac{c_{22} f_1 - c_{12} f_2}{D} \\ \dot{\bar{\omega}}_y &= \frac{c_{11} f_2 - c_{21} f_1}{D} \\ \dot{\bar{\omega}}_z &= 0 \end{aligned} \tag{4.6-33}$$

The above formulation is the most general that will be considered in this work.

4.6.3 System considering meridional and equatorial vibrations simultaneously. (B booms in  $X, Y$  plane, not necessarily along a principal axis of inertia).

In the Lagrangian formulation, for an elastic displacement

$$\vec{w}_{\text{total}} = w_E(x) \vec{i}_y + w_M(x) \vec{i}_z$$

$$V = \sum_{\substack{\text{ALL} \\ \text{Booms}}} \frac{EI}{2} \int_{\text{Boom}} \left[ \left( \frac{\partial^2 w_E}{\partial x^2} \right)^2 + \left( \frac{\partial^2 w_M}{\partial x^2} \right)^2 \right] ds + O(\epsilon^3)$$

and the kinetic energy is, if  $\eta_E = \frac{w_E}{\ell_k}$ ,  $\eta_M = \frac{w_M}{\ell_k}$ , etc.,

$$\begin{aligned} T = & T_{\text{Body}} + \frac{1}{2} \sum_{\substack{\text{ALL} \\ \text{Booms}}} \left( \rho l^3 \right)_k^b \omega_s^2 \int_{\text{Boom}} \left( \dot{\eta}_{E,k}^2 + \dot{\eta}_{M,k}^2 + \ddot{\eta}_{E,k}^2 \right. \\ & + 2 \bar{\omega}_z \dot{\xi}_{E,k} \dot{\eta}_{E,k} - 2 \bar{\omega}_x \dot{\xi}_{E,k} \eta_{M,k} - 2 \bar{\omega}_y \dot{\xi}_{M,k} \dot{\eta}_{M,k} - \frac{1}{2} [(1-\xi^2) \\ & \left. + 2 \xi_0 (1-\xi)] \left[ \left( \frac{\partial \eta_{M,k}}{\partial \xi} \right)^2 + \left( \frac{\partial \eta_{E,k}}{\partial \xi} \right)^2 \right] \right) d\xi \end{aligned}$$

It can readily be seen that when  $\eta_E$ ,  $\eta_M$  are expanded in their modes  $\phi(\bar{\lambda}, \xi_0)$ , with associated frequencies  $\bar{\omega}_{j,h}$ ,  $\bar{\omega}_{j,k}$ , the corresponding modal equations for

$$\begin{matrix} q_{j,k} \\ E \\ M \end{matrix} \quad \begin{matrix} q_{j,k} \\ E \\ M \end{matrix}$$

are uncoupled. For "E", only  $\dot{\bar{\omega}}_z$  will appear in the r.h. side, and this quantity is a function of the  $q_{j,k}$  only. For "M", only  $\dot{\bar{\omega}}_x$ ,  $\dot{\bar{\omega}}_y$ ,  $\dot{\bar{\omega}}_x$ ,  $\dot{\bar{\omega}}_y$  will appear in the r.h. sides, and these quantities are functions of the  $q_{j,k}$ . Hence, in the total system,

- the two first equations of (4.6-33) are those for  $\dot{\bar{\omega}}_x$ ,  $\dot{\bar{\omega}}_y$

- the last equation of (4.6-31) is the one for  $\dot{\omega}_z$
- the modal coordinate equations for  $q_{j,k}^M$  are given by  
(4.6-32)
- the modal coordinate equations for  $q_{j,k}^E$  are given by  
(4.6-30)

#### 4.7 Conclusion

The equations of motion of the spinning spacecraft having flexible appendages have been derived in a rather general case, using the modes of the rotating structure at the nominal spin rate, and for a central hub of non-zero radius. They were found to be in agreement with some other published results<sup>[4-3]</sup> in the limit case of a central body of zero radius, and can be used with profit in the numerical simulation of flexible spacecraft motions.

REFERENCES - Chapter 4

- [4-1] BELETSKII, V.: Motion of an Artificial Satellite About Its Center of Mass. (Translated from Russian). Published for NASA and NSF, Israel Program for Scientific Translations, Jerusalem, 1966 (NASA TT F-429).
- [4-2] RAKOWSKI, J.E.: "A Study of the Attitude Dynamics of a Spin-Stabilized Satellite Having Flexible Appendages," Ph.D. Thesis, Mech. Engrg., Carnegie-Mellon University, December 1970.
- [4-3] HUGHES, P.C. and FUNG, J.C.: "Liapunov Stability of Spinning Satellites with Long Flexible Appendages." Celestial Mechanics, 4, 295-308, 1971.

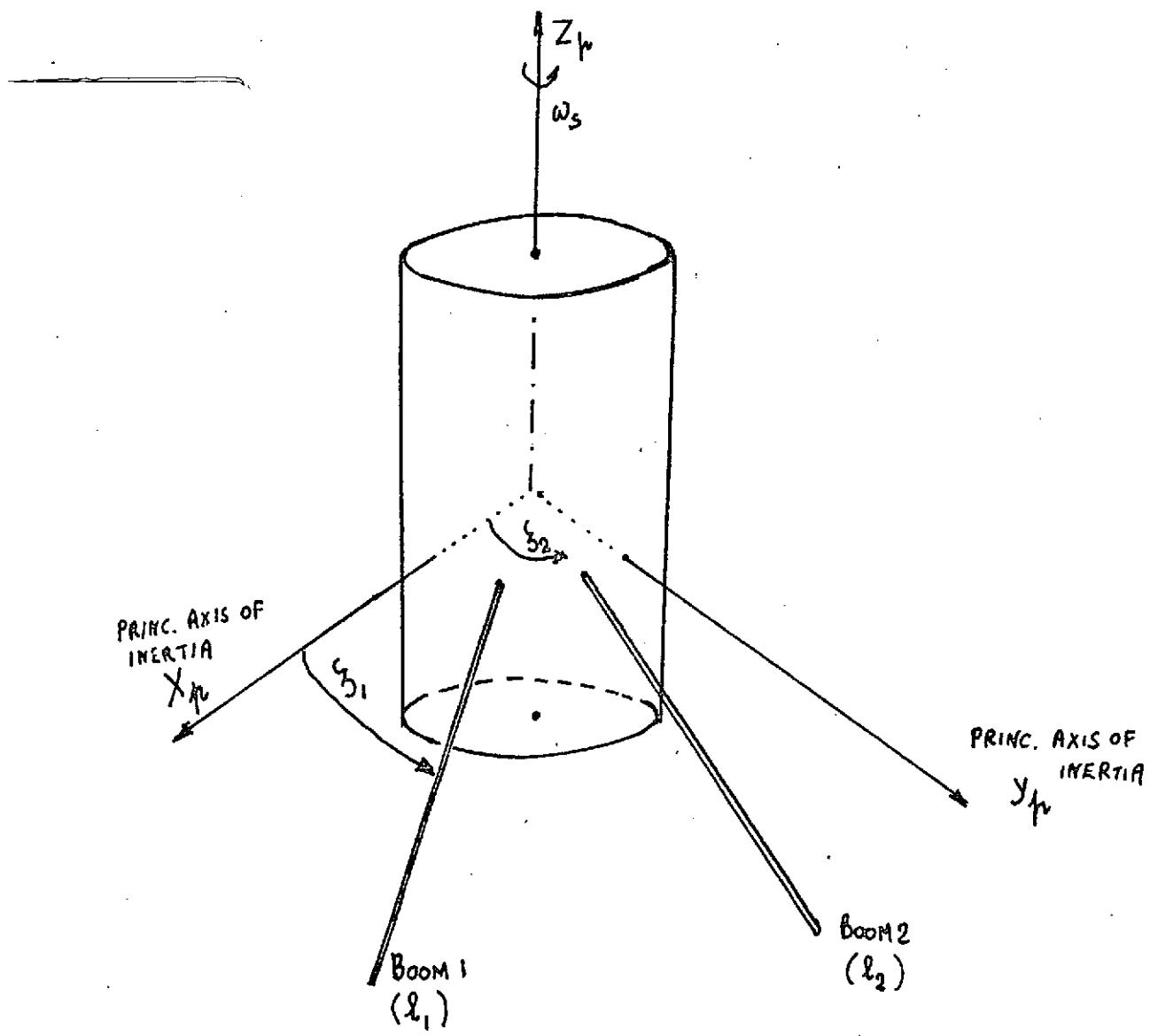


FIG. 4-1 MULTI-BOOM GEOMETRY

## CHAPTER 5

Simulation of the Satellite AttitudeMotion and Stability Studies

## 5.1 Motivation

In the present chapter, we present a simulation study of the evolution with time of the satellite attitude, from which stability charts can be obtained for use by the satellite designer. Of particular interest is the "nutational divergence" phenomenon, in which the satellite, although stable if it were "quasi-rigid", exhibits a steadily increasing nutation angle. Its spin axis thus drifts away from the invariant angular momentum vector, on which it is assumed to be aligned initially. This instability is due only to the dissipative motion of the elastic appendage.

To this effect, a set of computer programs, "FLEXAT", has been developed which numerically integrates the equations of motion and prints or graphically outputs the variables of interest. This program quite markedly differs from earlier versions we have used in the work, as will be explained later. The version given here accommodates three modes of the rotating structure and a dissymmetric central body, and since it permits an easy visualization of the qualitative features of the attitude motion, it should appeal to the satellite project engineer.

## 5.2 A Package for the Simulation of the Spacecraft with Flexible Appendages.

## 5.2.1 Generalities

FLEXAT is a set of programs, written in FORTRAN V, which were

mostly run on the UNIVAC 1108 at Carnegie-Mellon University. It is composed of the following parts:

- a) A short "MAIN" program calling on the relevant SUBROUTINES.
- b) A subroutine CASEM 2 called upon to study the stability of the meridional vibrations. This subroutine internally calls on its own subroutine RATES, which computes the angular rates  $\dot{\omega}_x$ ,  $\dot{\omega}_y$ ,  $\dot{\omega}_z$ .
- c) A subroutine CASEE 2 called upon to simulate the equatorial vibrations. Again, this subroutine internally calls on its own subroutine RATES, which computes the angular rates  $\dot{\bar{\omega}}_x$ ,  $\dot{\bar{\omega}}_y$ . In particular, this subroutine can be used to simulate the nutational divergence occurring when the GMI (greater moment of inertia) rule is violated, for the rigidified body.
- d) A subroutine SEARCH (NDS) called by the MAIN program and yielding the eigenfrequencies  $\bar{\omega}_j$  (up to  $j=3$ , if required) of the rotating structure, corresponding to the specified values of  $\bar{\lambda}$ ,  $\xi_0$ . This subroutine, for the essential part, is the same as that described in Section 2.4.
- e) A subroutine PLOT, called internally in either CASEM 2 or CASEE 2, giving a graphical output of the evolution with time of the satellite nutation angle, over a number of satellite spin periods (generally taken to be 10 to 20).

Each of these parts is now discussed in more detail.

### 5.2.2 Program MAIN

In this program, COMMON, DIMENSION etc. are given. Then the "unchanging parameters" are specified by cards. The listing given at the end of this chapter, for example, specifies

NSKPI : skip the printing of 60% of the results if desired (NSKP = 1) else NSKPI = 1; all results plotted in both cases  
 NDRU=NSUP=3: include 3 modal coordinates for each boom.  
 XN $\phi$ (1)=0.05: the "x-boom" and the "-x-boom" have modal deflections (1st mode) equal to  $\pm 0.05$  times the length of the boom  
 XN $\phi$ (2) ... YN $\phi$ (3): the "x-boom" and the "y-boom" have zero modal deflections, for the 2nd and 3rd modes.  
 NU(1) NU(3)=0.05: same damping ratio on the 3 modes  
 CASE = 'M' : meridional vibrations  
 SIO = 0 : value of  $\xi_0$   
 LAM = 10 : value of  $\bar{\lambda}$   
 MGIV : a switch. If equal to 1, the eigenfrequencies  $\bar{\omega}_j$  and  $m_{1,j}, m_{2,j}$  are given as data (they are assumed to be known from a previous study, or from a table). If equal to 0, the  $\bar{\omega}_j$  and the other quantities will be obtained "on line" by calling SEARCH(1) (in case E) or SEARCH (0) (in case M)  
 GAM :  $\Gamma$  in the developments of Chapter 4.  
 PKX,PKY : ratios  $K_{px} = I_{z,hub}/I_{x,hub}$ ;  $K_{py} = I_{z,hub}/I_{y,hub}$ . These measure dissymmetry of the ellipsoid of inertia of the central body.  
 PREC : the integration interval in time is equal to  $\frac{\tau_{\text{spin}}}{75}$  or  $\frac{2\pi/\omega_j}{75}$  (with  $j = \text{PREC}$ ) whichever the smaller.  
 It has been found sufficient to take PREC = 1.

MAXP : maximum number of such periods (defined under PREC) to be considered.

MODES : 3 (should be the same as NGRU, NSUP). Three modes are retained.

### 5.2.3 Subroutine SEARCH (NDS)

This subroutine has already been described in Chapter 2. It obtains  $\bar{\omega}_j$  in the relevant case (E or M) for  $j = 1, 2, \dots, \text{NSUP}$ . Note that

- a) NDS is an argument given in MAIN (0 for case M; 1 for case E)
- b) SEARCH is bypassed if MGIV = 1, i.e. if the eigenfrequencies in the case of interest are externally given, other than completed on line.

### 5.2.4 Subroutines CASEM2, CASEE2

This subroutine, fed with the  $\bar{\omega}_j$ ,  $m_{1,j}$ ,  $m_{2,j}$  values obtained from data or computed in SEARCH, proceeds to integrate equations (2.2-8) or (2.3-5), as the case may be, if MGIV = 0, and bypasses the procedure if MGIV = 1.

It then proceeds to compute the quantity

$$\sum_{j=1}^{\text{NSUP}} \frac{m_{2,j}^2}{m_{1,j}}$$

The equations which are integrated are those for

$$q_{x,j}, q_{y,j}, \bar{\omega}_x, \bar{\omega}_y, \bar{\omega}_z$$

The system is thus of order  $4 \text{NSUP} + 3$ . The rates are computed in an internal subroutine "RATES". Antisymmetric vibrations are assumed, so that  $q_{x,j} = -q_{-x,j}$ ;  $q_{y,j} = -q_{-y,j}$ . The four booms are assumed to have

the same geometric and structural properties (thus same  $\xi_0$ ,  $\bar{\lambda}$ ,  $\Gamma$ ,  $\rho l^3$ ), to be along the principal axes of inertia of the rigidified structure ( $\zeta_k = 0, \pi$  for the x-booms,  $\zeta_k = \frac{\pi}{2}, \frac{3\pi}{2}$  for the y-boom, in Chapter 4). The ellipsoid of inertia need not be of revolution ( $K_{px} \neq K_{py}$ ). Thus the relevant equations have been written as equations

(4.6-20) and (4.6-24) for program CASEM2

(4.6-18) and (4.6-23) for program CASEE2

Different assumptions (booms of different length, structural properties) could easily be considered by the user, for any special application, after a rather simple rewrite of the equations, as given in Chapter 4, or a suitable distinction between " $\Gamma_x$ ", " $\Gamma_y$ ", ... etc. rather than the common " $\Gamma$ "... adopted here.

The method of integration is RUNGE-KUTTA with fixed step , the latter being computed in the program as some function of the spin period or of the vibration period of the jth mode, as precised in 5.2.2. under "PREC".

The output consists of a print of the case data, of the quantities NSUP  $\sum_{j=1}^{NSUP} \frac{m_{2,j}^2}{m_{1,j}}$ ;  $\Delta$ ,  $v_1$ ,  $v_2$ ,  $v_3$ ;  $\bar{\omega}_j$ ,  $m_{1,j}$ ,  $m_{2,j}$  ( $j=1, \dots, NSUP$ );  $H$  initial =  $\frac{|\vec{H}_0|}{I_{zh}}$  (assuming  $\vec{H}_0$  and z are initially aligned); then tables giving

$q_{x,1}$	$q_{y,1}$	$q_{x,2}$	$q_{y,2}$	$q_{x,3}$	$q_{y,3}$	$\bar{\omega}_x$	$\theta$	STEP
(angle of nutation, degrees)								

There exists an option to skip the printing of the first 60% of the results over the time interval considered, which makes sense if one is only interested at looking at the long-term behavior.

#### 5.2.5 Subroutine PL0T

The PLOT routine graphically presents the results of the above computation. PLOT is internal to CASEM2 or CASEE2, as the case may be.

### 5.3 Results from simulation study, using FLEXAT

#### 5.3.1 Comparison between the present and some previous results

As compared to the approach previously taken by J. Rakowski and the present author<sup>[5-1,5-2]</sup>, the equations used in the present simulation do not include "extra" non-linear terms such as  $q_x^2$ ,  $q_y^2$ ,  $\omega_x \omega_y \dots$  Including these terms, although they appear in the derivations of Chapter 4, did not seem fully consistent with writing the contributions to the kinetic and elastic energy with some terms of order 3 of smallness neglected (such would be the case, for instance, if  $\int \{ \dots \} dx = \int \{ \dots \} ds$ , with the integrand of first order of smallness).

However, strictly for the sake of comparison, the stability boundaries, derived as explained in 5.3.2, were compared in a large number of cases using, on one hand, the equation with the extra non-linear terms, and on the other hand the equations obtained in Chapter 4.

In no cases were the differences of much significance. All were well within the sampling interval ( $K_p \pm .016$ ).

### 5.3.2 Parametrization of the stability chart

Following the notation adopted earlier [5-1,5-2], it is proposed to define a stability chart as follows, in the symmetric case

$(K_{px} = K_{py} = K_p)$  (See Fig. 5.1)

- abscissa:  $K_p = \frac{I_{p,hub}}{I_{z,hub}}$ , a measure of the asymmetry of the ellipsoid of inertia of the central body.

- ordinate:  $\Gamma = \frac{\rho l^3}{I_{z,h}}$ , a measure of the relative importance of the inertia of a boom ( $\frac{1}{3} \rho l^3$ , if  $\xi_0 = 0$ ), and the inertia of the hub. All things being equal, small booms of small mass will give small values of  $\Gamma$ .

- parameter of the plane:

$\xi_0$  = fixed non-dimensional radius of the hub (referred to the booms length)

- parameters of the curves:

$\bar{\lambda} = \frac{\pi l^4}{EI} \omega_s^2 \div \left( \frac{\omega_s}{\omega_c} \right)^2$ , a ratio of centrifugal to elastic forces, large for high spin rates or very flexible booms ( $E$ ,  $I$  small;  $\rho l^4$  large)

Thus  $\bar{\lambda}$  = constant curves will be drawn on the  $(K_p, \Gamma)$  plane, for  $\xi_0$  = constant, corresponding to the observed limit of stability, i.e. a point, at given  $\Gamma$ ,  $\xi_0$ ,  $\bar{\lambda}$ , such that any slight increase in  $K_p$  causes stability of the observed motion, the nutation angle tending asymptotically to zero; whereas to the left of it (decreasing  $K_p$ ), the motion is observed to be unstable, the nutation angle steadily increasing with time.

In the asymmetric case, one more degree of freedom exists, and the chart will draw  $\bar{\lambda}$  = constant curves, corresponding to the observed

limit of stability, for given  $\xi_0$ ,  $K_{py}$ , in a  $(\Gamma, K_{px})$  plane of representation.

### 5.3.3 The GMI rule

As described in [5-3], a rigid body undergoing a torque-free motion about its center of mass, but having internal energy dissipation, has a stable spinning motion only about its maximum axis of inertia, i.e. if

$$\frac{I_z}{I_x} \text{ and } \frac{I_z}{I_y} > 1 \quad (5.3-1)$$

If one of these ratios was one, there would be no preferred axis of rotation about which the satellite would spin after an initial nutation has been removed by energy dissipation. Condition (5.3-1) is commonly referred to as the GMI rule (or greatest moment of inertia rule).

In the stability chart, planes described above, condition (5-1) will be represented, in the symmetrical case

$$I_x = I_y = I_p$$

by a locus of equation

$$2\Gamma\Delta > \frac{1}{K_p} - 1 \quad (5.3-2)$$

or

$$2\Gamma\left(\frac{1}{3} + \xi_0 + \xi_0^2\right) > \frac{1}{K_p} - 1 \quad (5.3-3)$$

These curves will, whatever the value of  $\xi_0$ , tend to the common point

$$\Gamma \rightarrow 0 \quad K_p \rightarrow 1$$

which they should not include. This corresponds to the case where the satellite has no flexible appendages ( $\rho l^3 \rightarrow 0$ ) and a spherical ellipsoid of inertia. The curves are shifted to the left as  $\xi_0$  in-

creases (Fig. 5.1). Their  $\bar{\lambda}$  parameter is  $\bar{\lambda} = 0$ .

### Conclusion

For the stability of the satellite with perfectly rigid appendages, and of the satellite with flexible appendages in the presence of equatorial vibrations (as explained in 5.3.4), the greatest moment of inertia rule

$$I_z > I_x, I_y$$

should be satisfied for the total, rigidified satellite. On the  $(\Gamma, K_p)$  stability charts, the design point

$$(\Gamma, K_p)$$

for given

$$\xi_0, \bar{\lambda}$$

should be to the right (i.e. in the region not including the origin) of the Quasi-Rigid (QR) locus given by Equation (5-3).

### 5.3.4 Stability with equatorial vibrations

Stability in the presence of equatorial vibrations, was found to be equivalent to quasi-rigid body stability. The stability condition for case E is thus the same as the Q.R. body condition given in Equation (5.3-3). This result is in good agreement with Hughes and Fung<sup>[5-4]</sup> analysis in the case where  $\xi_0 = 0$ . Two examples are given in Fig. 5-2 and 5-3.

#### 5.3.5.1 Stability charts (case M), using three-mode analysis

Using the FLEXAT program with subroutine CASEM2, and retaining the three modes in the simulation, figures such as 5-4 to 5.7 can be pro-

duced. Each of them corresponds to the same value of  $\Gamma = 10$  and  $\xi_0 = 0.1$ . For  $\bar{\lambda} = 100$ , two values of  $K_p$  are considered corresponding to a slightly unstable or a slightly stable condition (Fig. 5.4, 5.6). The same applies to a higher  $\bar{\lambda}$  case ( $\bar{\lambda} = 1,000$ ) (Fig. 5.6, 5.7)

The final results of the three-mode stability analysis in the presence of meridional vibrations are summarized on charts 5-8, 5-9, 5-10 for values of  $\bar{\lambda} = 0$  (Quasi-rigid body case) to  $\bar{\lambda} = 10,000$ , and for  $\xi_0 = 0, 0.1, 0.25$ .

IMPORTANT NOTE: When using program FLEXAT, with subroutines SEARCH and CASEM2, for  $\bar{\lambda} \gtrsim 5,000$ , the values of the relevant frequency and modal quantities:

$$\bar{\omega}_{j,M}, m_{1,j}, m_{2,j} \quad (5.3-4)$$

should be given as input data, using option MGIV = 1, or described in Section 5.2.2. Quantities (5.3-4) cannot be obtained on line using program SEARCH DP, for such high values of  $\bar{\lambda}$ . They have been obtained using a multiple precision version (OS-MP or NP-package) of SEARCH, which is rather time-consuming and should be run only to set up tables such as in Section 2.8, for interpolation purposes.

### 5.3.5.2 Effect of higher modes, and of modal truncation

As the tables in Section 2.8 show, the effect of higher order modes ( $j = 2,3$ ) on the motion parameters is as follows:

a) 
$$\sum_{d=1}^{NSUP} m_{2,d}^2 / m_{1,j}$$

For small values of  $\bar{\lambda}$ , the changes of this sum by increasing NSUP from 1 to 2,3 is at most 2.5% for  $\xi_0 = 0$ , and 9% for  $\xi_0 = 0.25$ .

For large values of  $\bar{\lambda}$  ( $\bar{\lambda} = 5,000$ ), the corresponding changes are 0.03% for  $\xi_0 = 0$ , and 0.5% for  $\xi_0 = 0.25$ .

b)  $\frac{m_{2,j}}{m_{1,j}}$  (amplitude in r.h. side of jth modal equation)

It can be seen that this ratio is at most 25% (for  $j = 2$ ) of the value corresponding to  $j = 1$ , when  $j$  is increased to 2,3 .

c)  $m_{2,j}$  (amplitude of some terms in the r.h. side of the rate equations).

The same comments apply to  $m_{2,j}$ .

To assess the effect of higher modes qualitatively, it should be remembered that, when non-dimensionalized by  $\omega_z$ ,

$$\bar{\omega}_{j,M} > 1 \quad j = 1, \dots, NSUP$$

and the forcing frequency (precision frequency in body-fixed axes)

on the terms would be, for  $|q_x|, |q_y| \ll 1$ ,

$$\bar{\omega}_{F, eq} \approx \frac{\frac{1}{K_F} + 2\Gamma(\Delta - \frac{m_2^2}{m_1})}{\frac{1}{K_F} + 2\Gamma(\Delta - \frac{m_2^2}{m_1})} < 1$$

as opposed to

$$\bar{\omega}_{F, rigid} = \frac{\frac{1}{K_F} + 2\Gamma\Delta}{\frac{1}{K_F} + 2\Gamma\Delta} < 1$$

for a quasi-rigid body.

Note that  $\frac{m_2^2}{m_1}$  is always smaller than  $\Delta$ . Typically, for

$$\xi_0 = 0.1 \quad \Delta = 0.443$$

$$\frac{m_2^2}{m_1} = 0.419 \text{ for } \bar{\lambda} = 0; 0.430 \text{ for } \bar{\lambda} = 100; 0.437 \text{ for } \bar{\lambda} = 1,000.$$

Therefore, in an approximate sense, it can be said that angular rates  $\bar{\omega}_F$  will not appreciably excite modes 2,3,... which are larger than  $\bar{\omega}_1$  by a factor of several units at least.

With these observations in mind, we now discuss the conclusions of a detailed study of the effect of modal truncation on the stability charts ( $\Gamma$ ,  $K_p$ ; constant  $\bar{\lambda}$ ,  $\xi_0$ ).

It was indeed observed in the simulation that higher modes never developed to amplitudes of more than a few % of the amplitudes of the first mode, assuming i.e. which can be considered as "normal" for the initial deflection, namely close to the shape of the first mode  $\Phi_1(\xi)$ .

Within the accuracy retained in establishing the stability charts ( $K_p \pm 0.015$ ), no noticeable difference could be reported between the stability chart determined here on the basis of three modal coordinates for each boom, and that we obtained on the basis of a single modal coordinate. Seiling times, however, were larger.

The results of the 3-mode analysis, using program FLEXAT, are summarized in Figures 5.8, 5.9, 5.10.

### 5.3.5.3 Effect of some higher order terms

As was mentioned in 5.1, there was a lack of consistency in retaining some non-linear terms of order 2 in the equations and neglecting some others. Equations (4.6-20) and (4.6-24) were used in the present stability simulation. It should be noted that little difference resulted in the stability charts. The angles of nutation, however, are

computed here by

$$\theta = \text{nutation angle} = \arcsin \left( \frac{\sqrt{H_x^2 + H_y^2}}{H_{\text{tot}}} \right) = O(\epsilon)$$

and since they involve quantities of first order of smallness, should be accurate, whereas the use of formula

$$\cos \theta = \frac{H_z}{H_{\text{tot}}} = 1 - O(\epsilon^2)$$

will see  $\theta$  critically effected by terms of  $O(\epsilon^2)$ , none of which should then have been neglected.

#### 5.3.5.4 Parametric studies for $I_x \neq I_y$ (Ellipsoid of inertia not of revolution)

With the particular geometry considered here,

$I_y < I_x < I_z$  implies that

$$I_{y,\text{hub}} < I_{x,\text{hub}}$$

or  $K_{py} > K_{px}$

A set of parameters is chosen, namely

$$\xi_0, \bar{\lambda}, \Gamma, \text{ number of modes.}$$

In the  $(K_{py}, K_{px})$  plane, the bisectrix of the first quadrant,  $K_{px} = K_{py}$ , will correspond to the symmetric case,

$$K_{px} = K_{py} = K_p$$

and the limit of stability  $K_{p*}$ , such that  $K_p > K_{p*}$  will ensure stability of the motion, was found previously. Furthermore, in order to satisfy the GMI rule, we must have

$$K_{px} \text{ and } K_{py} > \frac{1}{1+2\Gamma\Delta}$$

In order to determine the parameter region to be studied with program FLEXAT, it is useful to note that

$$-1 < \frac{I_{zh} - I_{yh}}{I_{xh}} < 1$$

or  $\frac{1}{K_{py}} - \frac{1}{K_{px}} < 1$

and  $\frac{1}{K_{py}} + \frac{1}{K_{px}} > 1$

Similarly, from

$$-1 < \frac{I_{zh} - I_{xh}}{I_{yh}} < 1$$

$$\frac{1}{K_{px}} - \frac{1}{K_{py}} < 1$$

This is most conveniently represented on a  $(1/K_{px}, 1/K_{py})$  plane. (Fig. 5.11). Thus, if

$$X_* = \frac{1}{K_{px}} \quad Y_* = \frac{1}{K_{py}}$$

the admissible domain of study is bounded by

$$Y_* - X_* < 1 \quad X_* < 1 + 2\Gamma\Delta$$

$$Y_* + X_* > 1 \quad Y_* < 1 + 2\Gamma\Delta$$

$$X_* - Y_* < 1$$

$$X_* > 0 \quad Y_* > 0$$

In particular, for a constant ratio of  $\frac{K_{px}}{K_{py}}$  (or  $\frac{I_{yh}}{I_{xh}}$ ), the limits are shown by circles on Fig. 5.11.

#### 5.4 Conclusions

A program has been developed for stability studies and simulation of the nutational motion of a spinning satellite with flexible appendages. The results of this program can be used with profit in the preliminary attitude design, to ascertain stability, determine the importance of structural damping and study the rate at which nutation is generated or removed from the system.

REFERENCES - Chapter 5

- [5-1] Rakowski, J.E. and Renard, M.L.: "A Study of the Nutational Behavior of a Flexible Spinning Satellite Using Natural Frequencies and Modes of the Rotating Structure," Paper 70-1046, AAS/AIAA Astrodynamics Conference. Santa Barbara, August 1970.
- [5-2] Rakowski, J.E.: "A Study of the Attitude Dynamics of a Spin-Stabilized Satellite having Flexible Appendages," Ph.D. Thesis, Mechanical Engineering, Carnegie-Mellon University, December 1970.
- [5-3] Thomson, W.T.: Space Dynamics, John Wiley Ed., 1963.
- [5-4] Hughes, P.C. and Fung, J.C.: "Liapunov Stability of Spinning Satellites with Long Flexible Appendages." Celestial Mechanics, 4, 295-308, 1971.

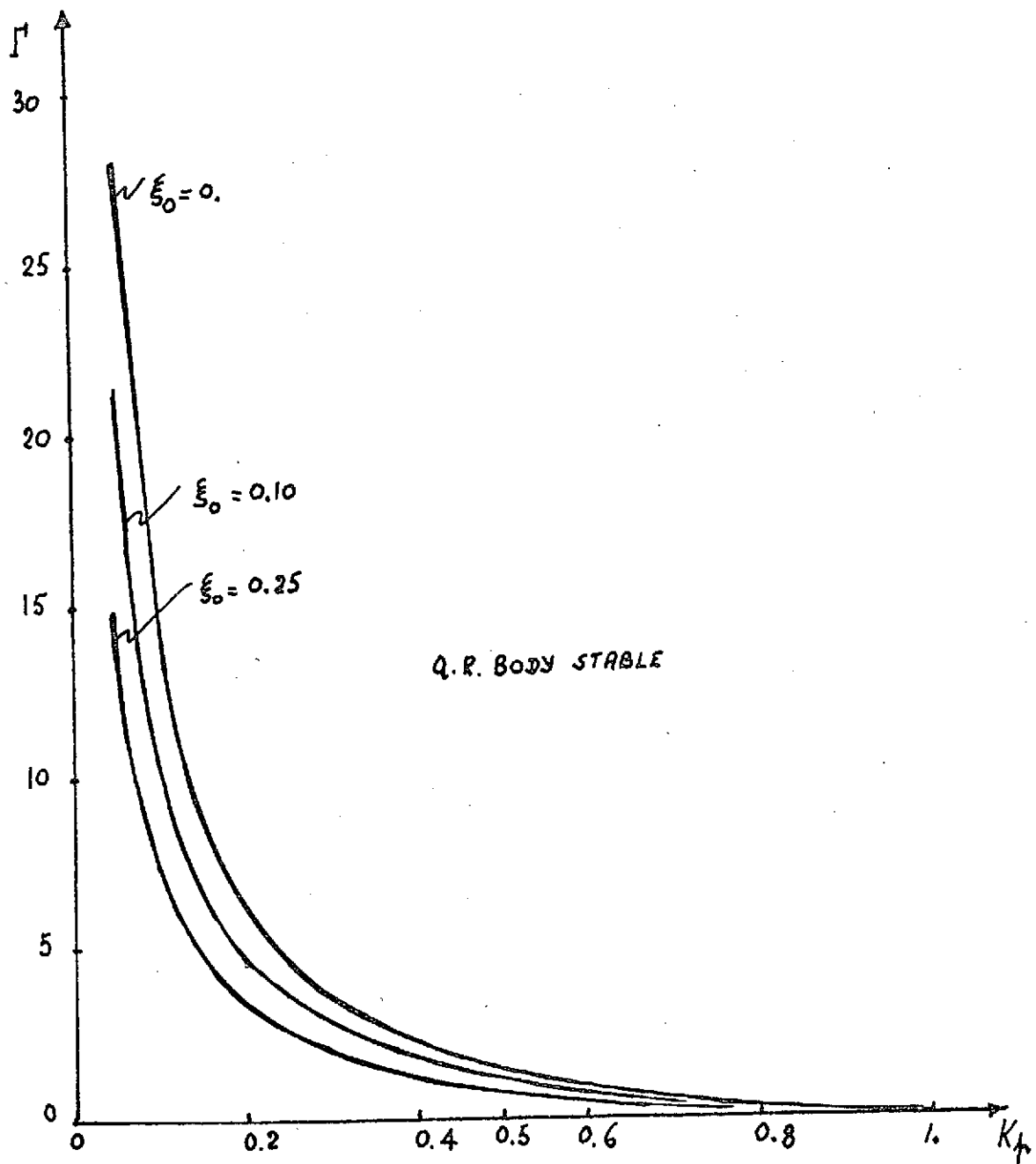


FIG. 5-1. QUASI-RIGID BODY STABILITY

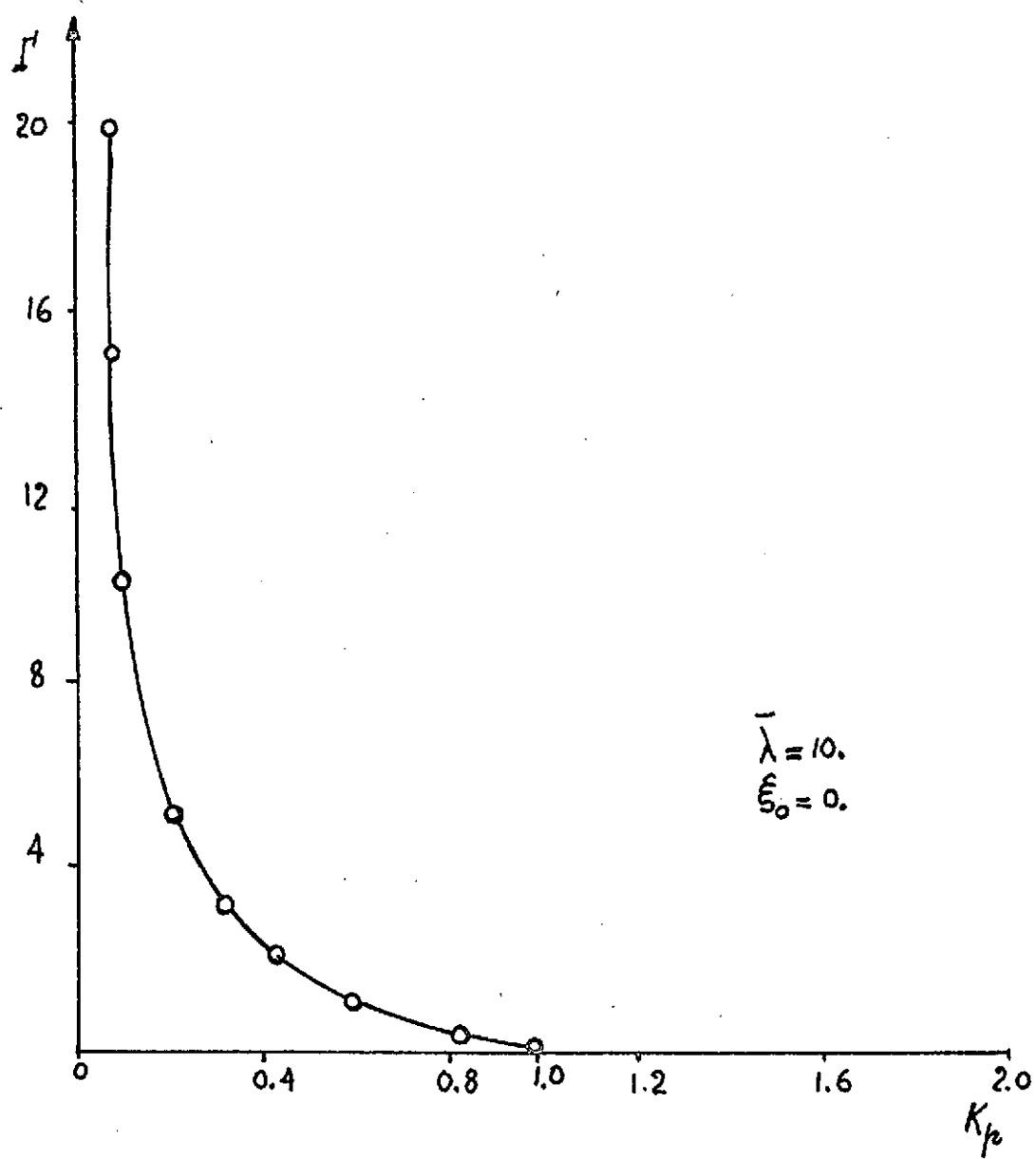


FIG. 5-2. Stability chart. Case E.

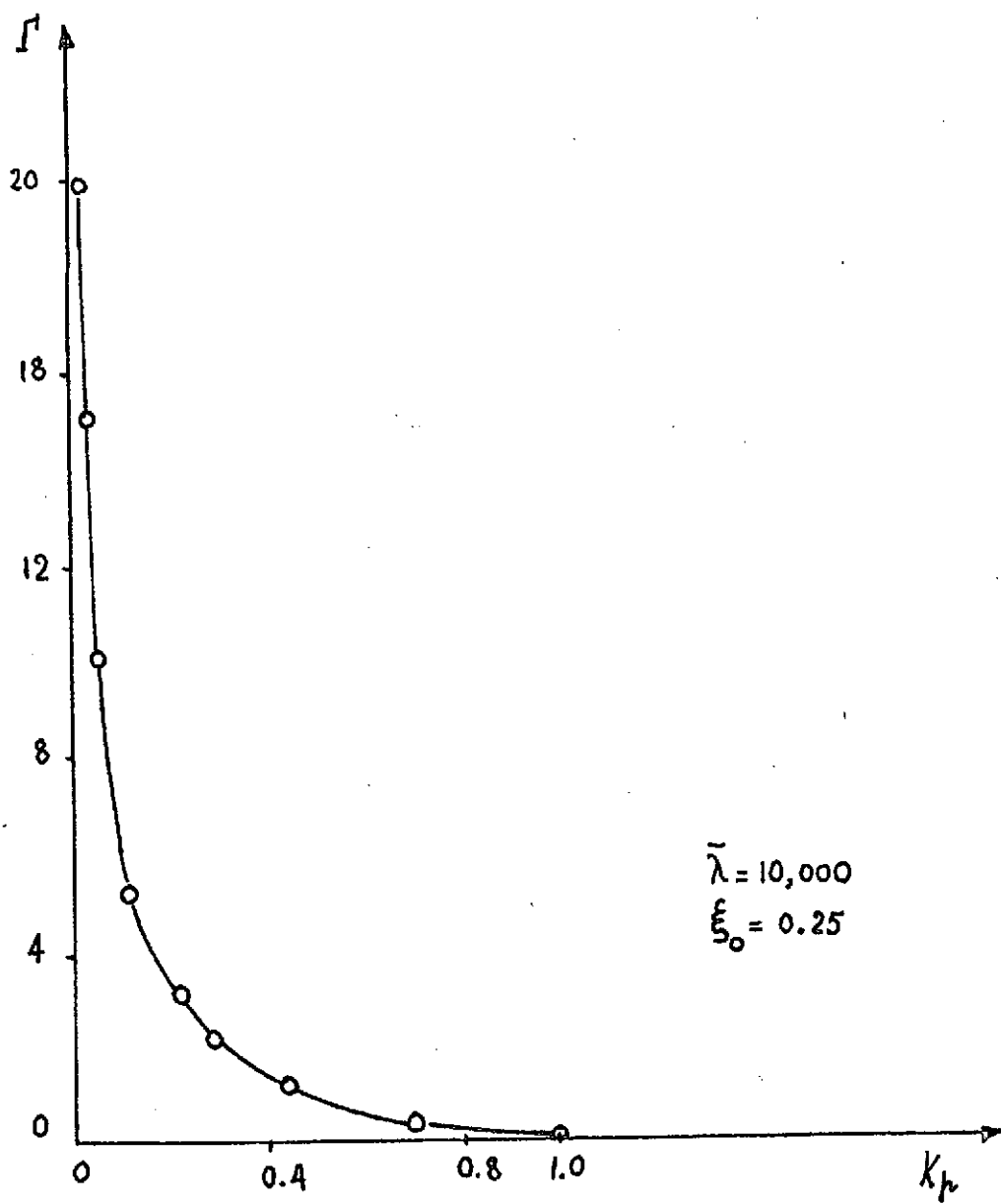


FIG. 5 -3. Stability chart. Case E.

## PLOT OF INITIATION ANGLE IN DEGREES VS N FOR

LAMBDA= 100.

SI-ZERO= .10

GAMA= 10.000

PKX= .2200

PKY= .2200

PREC= 1

MAXP= 15

MODES= 3

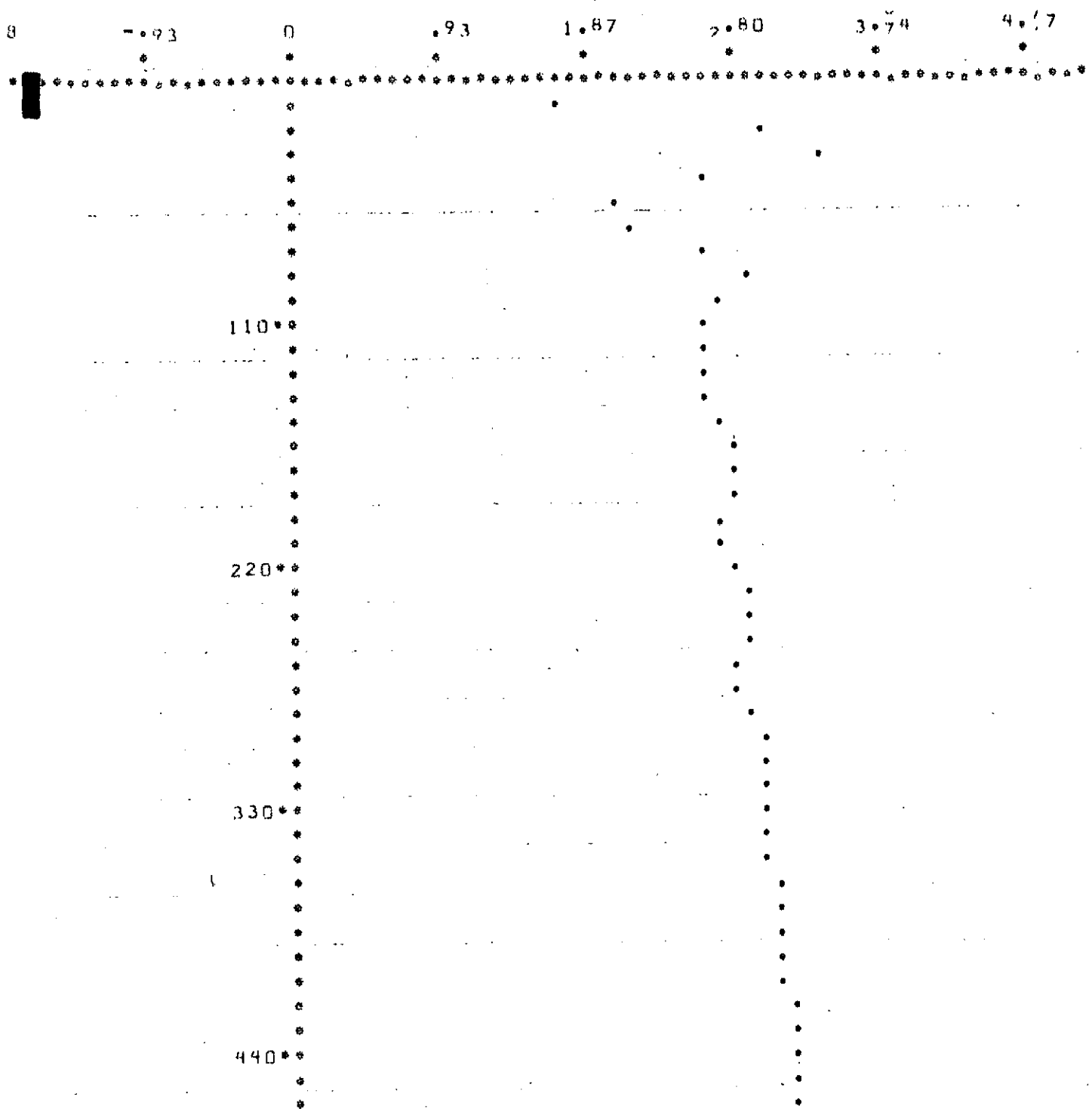


FIG. 5-4

550 \*\*

660 \*\*

770 \*\*

880 \*\*

990 \*\*

1100 \*\*

FIG.5-4  
(Continued)

PLOT OF NUTATION ANGLE IN DEGREES VS N FOR  
LAMBDA = 100.  
SI-ZERO = .10  
GAMA = 10.000  
PKX = .2800  
PKY = .2800  
PREC = 1  
MAXP = 15  
NODES = 3

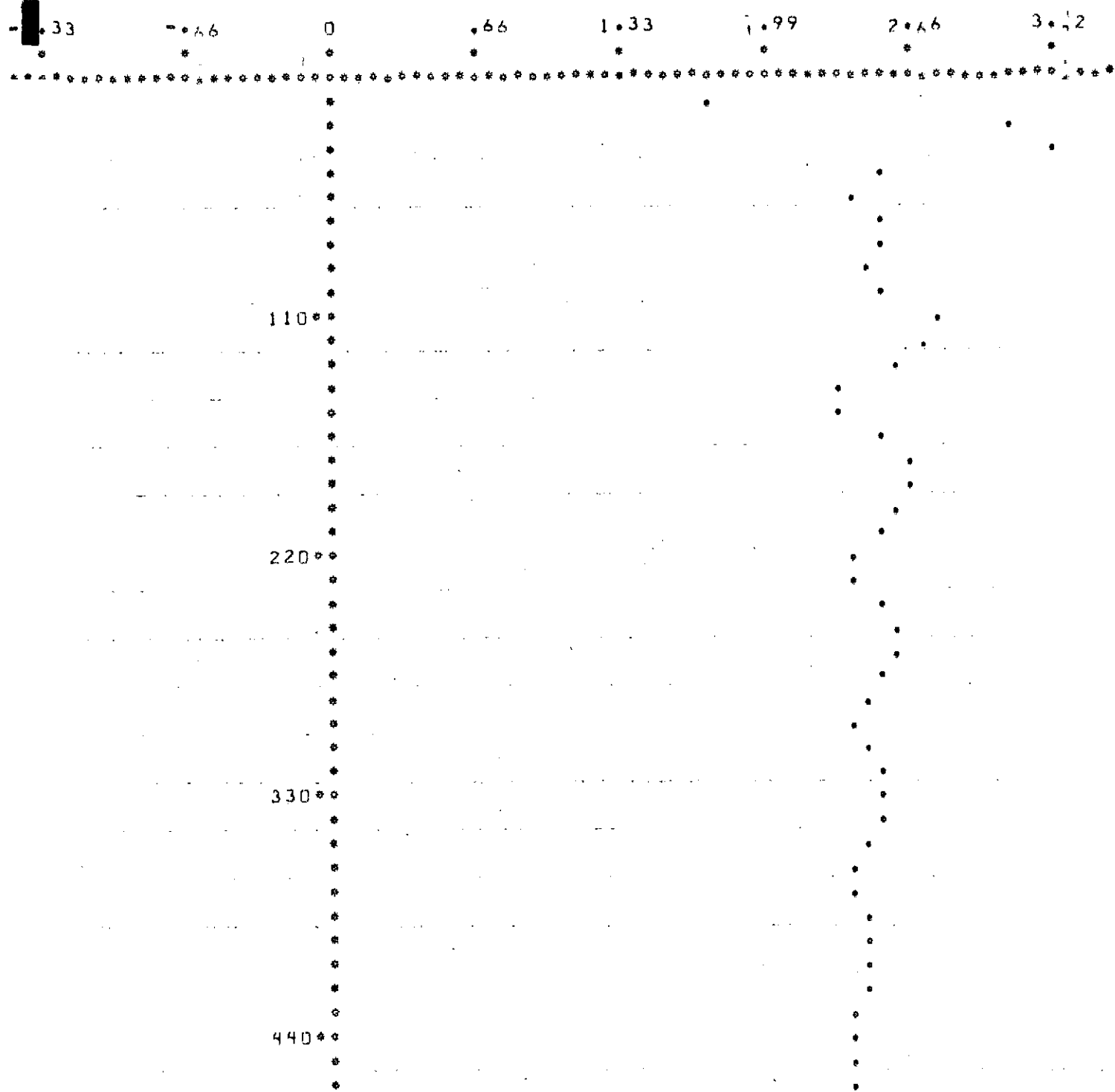


FIG. 5-5

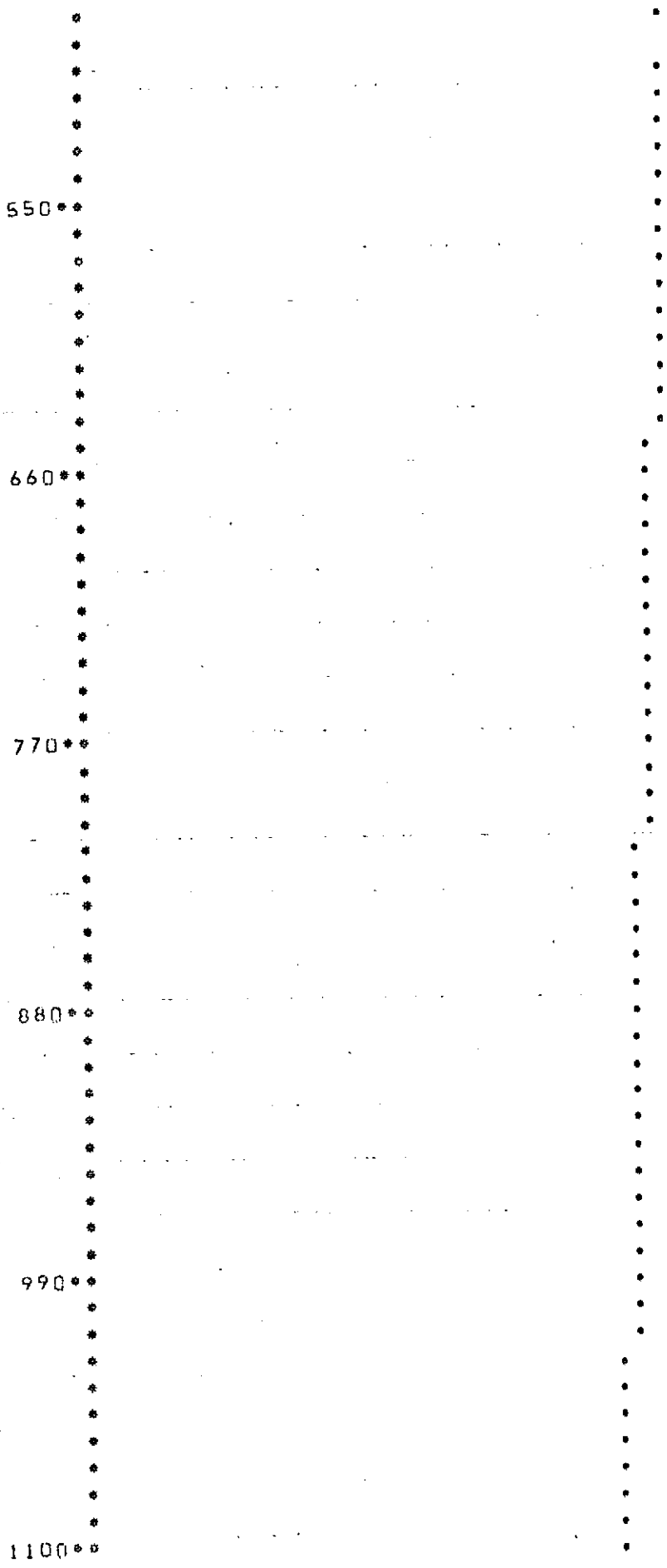


FIG. 5-5  
(Continued)

## PLOT OF NUTATION ANGLE IN DEGREES VS N FOR

LAMBDA= 1000.  
SI-ZERO= .10  
GAMA= 10.000  
PKX= .3500  
PKY= .3500  
.PREC= 1  
MAXP= 15  
MODES= 3

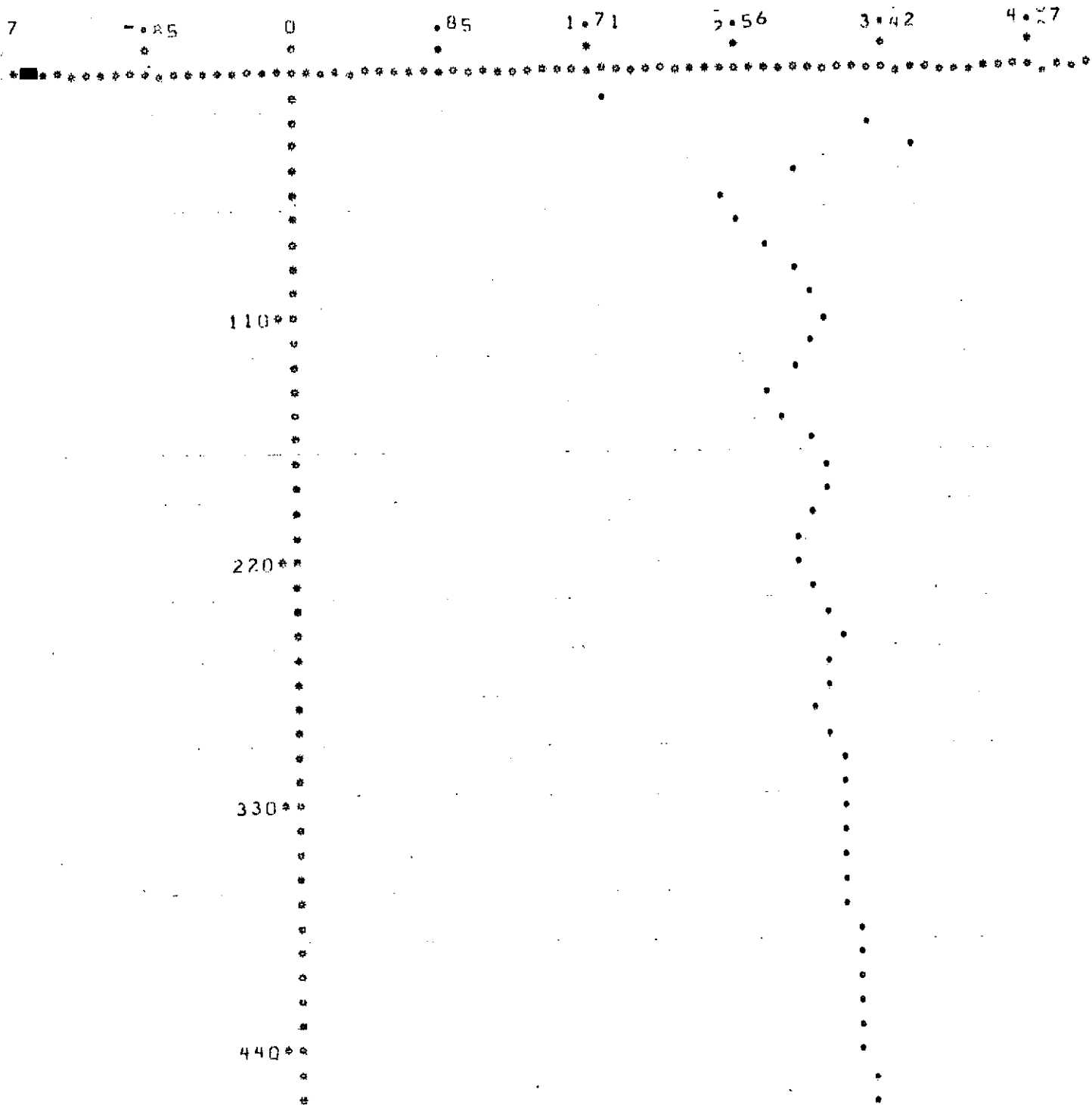


FIG. 5-6

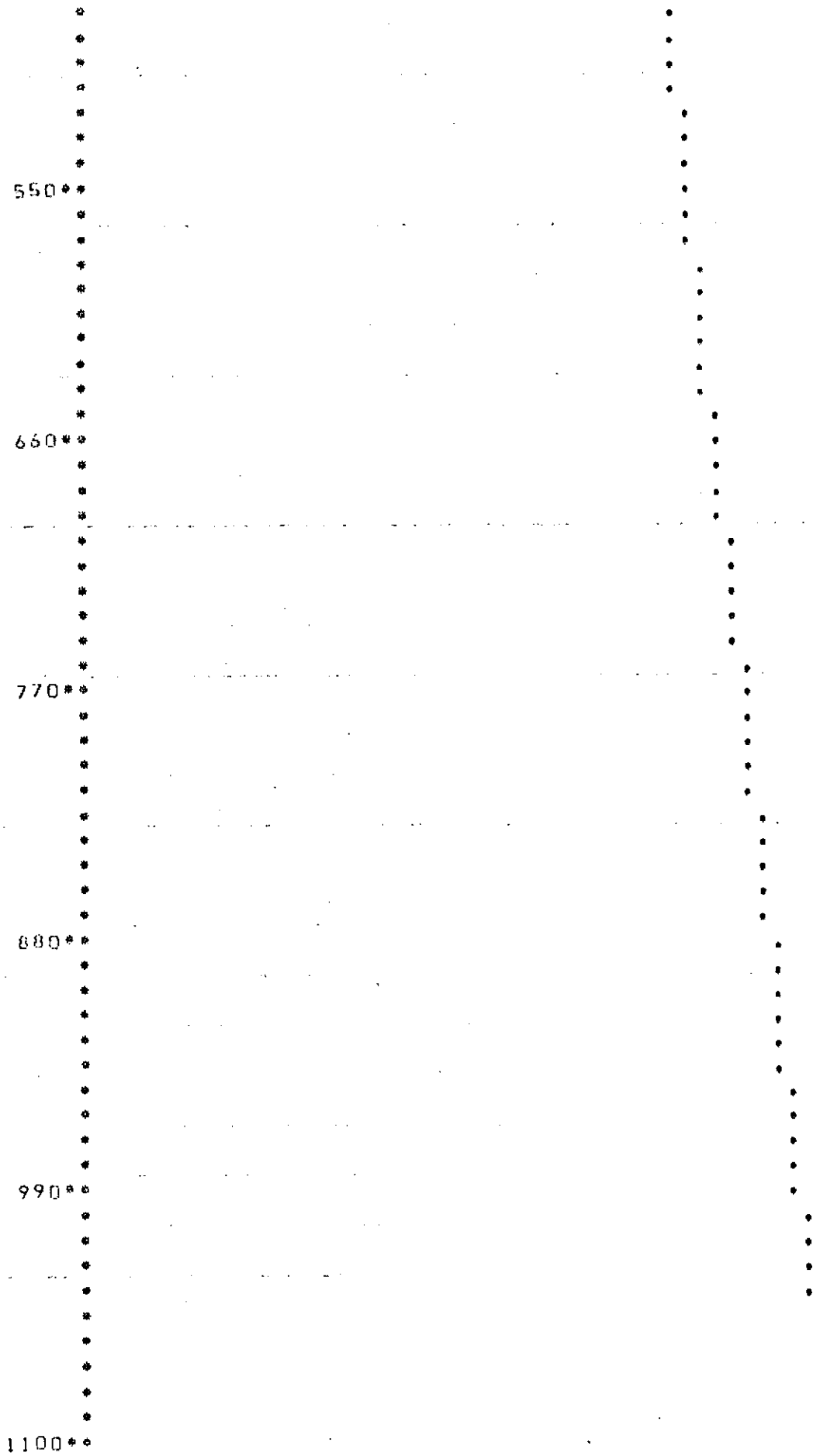


FIG. 5-6  
(Continued)

PLOT OF NUTATION ANGLE IN DEGREES VS N FOR  
LAMBDA= 1000.  
SI-ZERO= .10  
GAMA= 10.000  
PKX= .4000  
PKY= .4000  
PREC= 1  
MAXP= 15  
MODES= 3

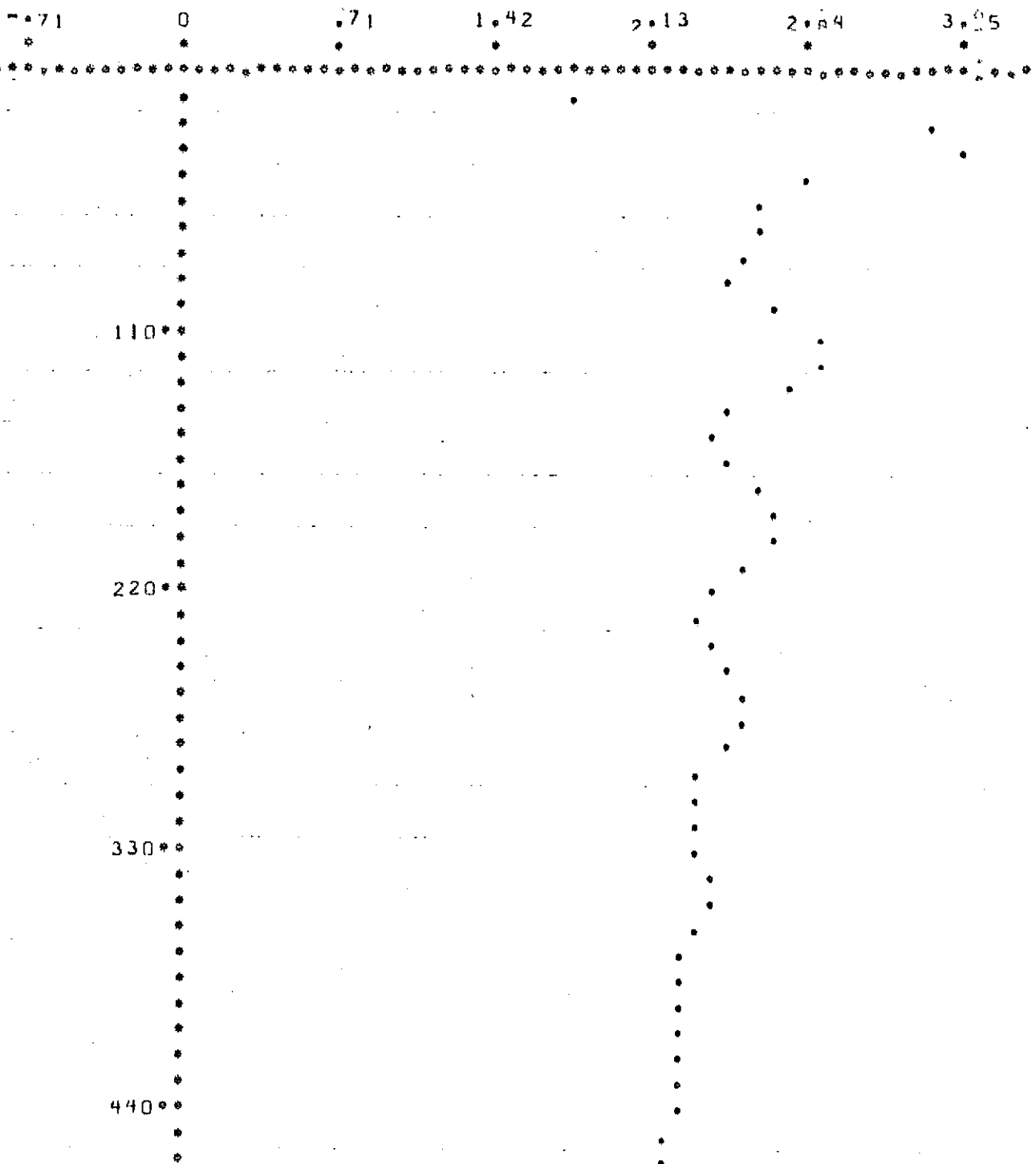


FIG.5-7

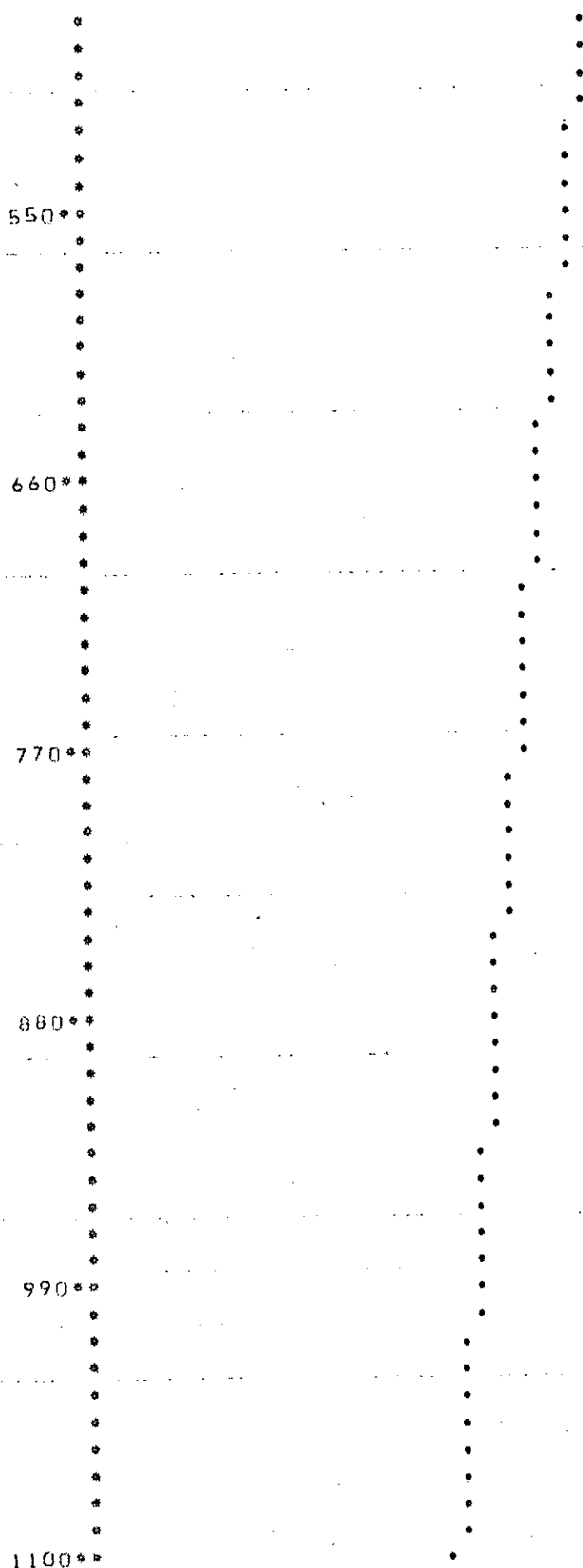


FIG. 5-7  
(Continued)

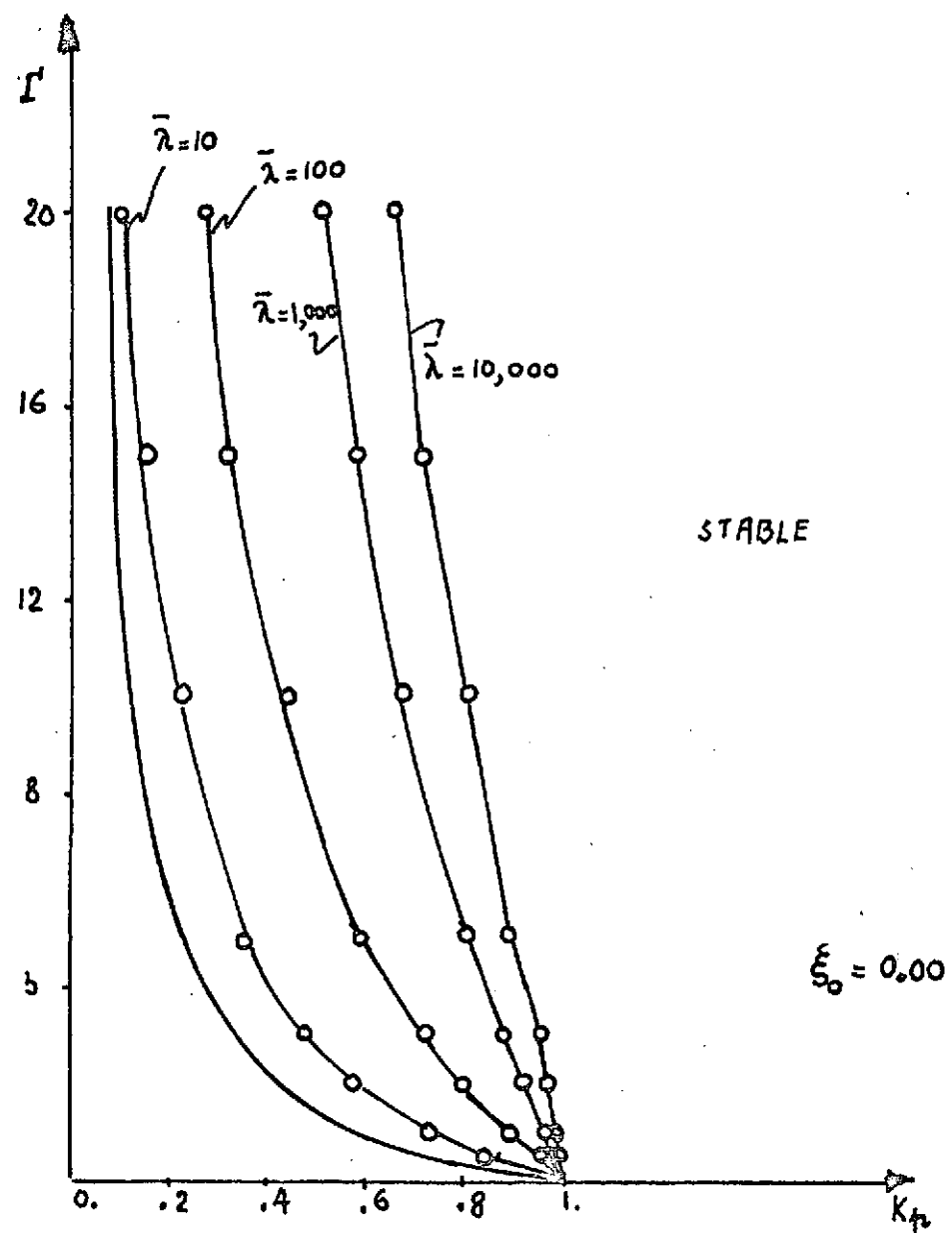


FIG. 5.8 Stability Diagram. Case M. 3 Modes.

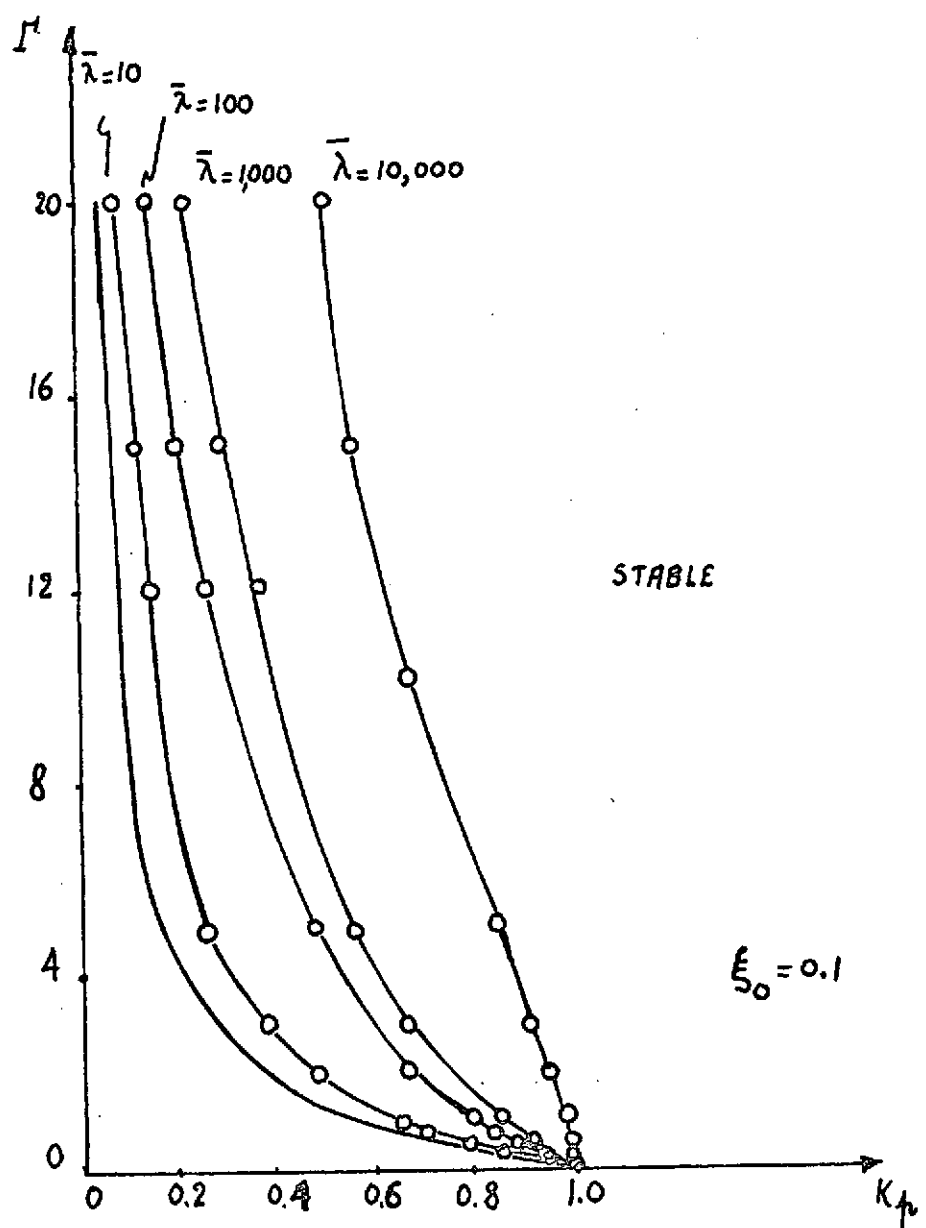


FIG. 5.9 Stability Diagram.. Case M. 3 Modes.

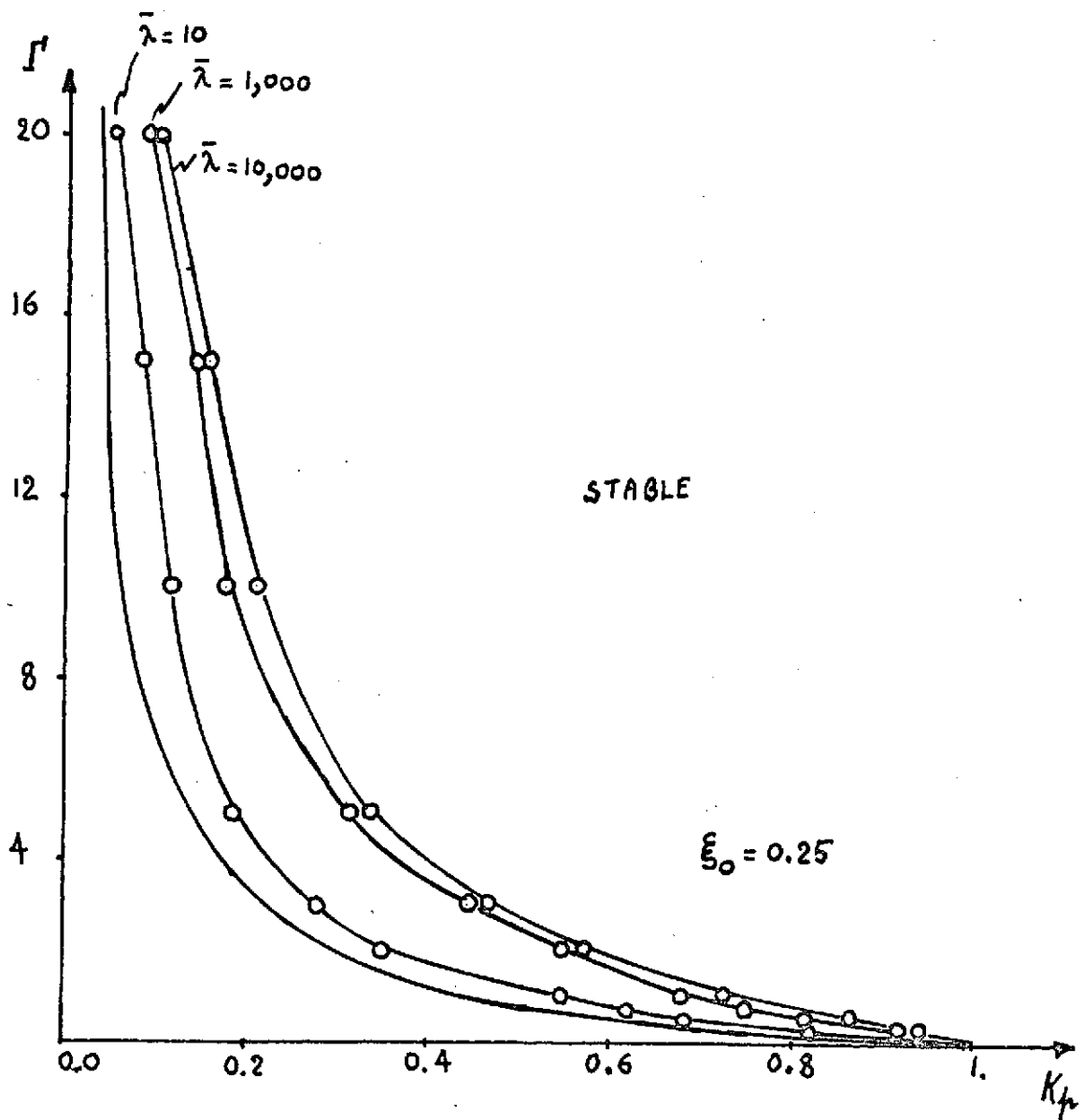


FIG. 5-10. Stability Diagram, Case M. 3 Modes.

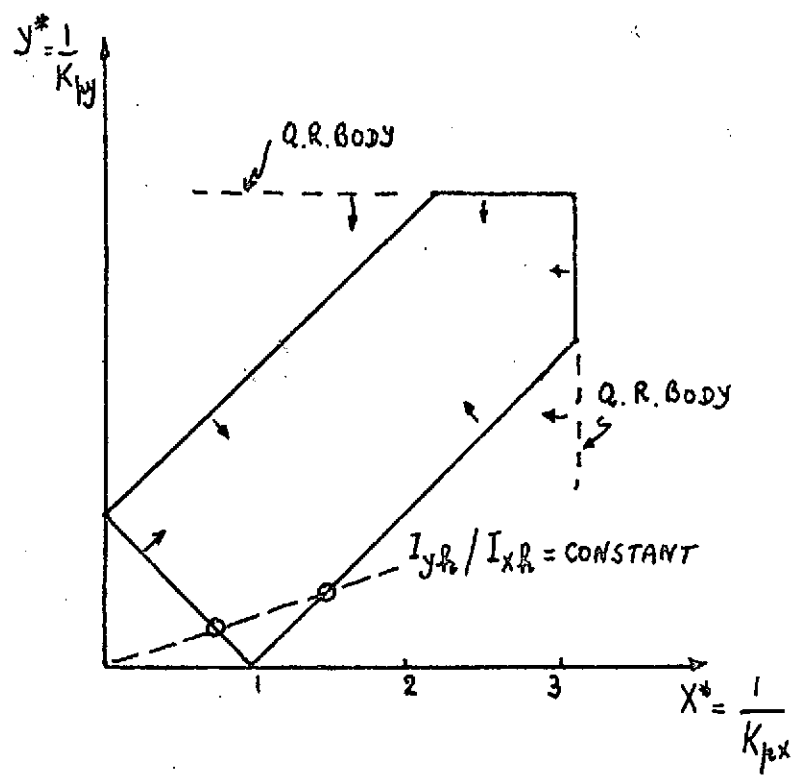


FIG. 5-11.  $X^*, Y^*$  DIAGRAM.

## (Case2)

THIS IS THE MAIN PROGRAM WHICH INPUTS DATA AND CALLS THE SUBPROGRAMS  
DOUBLE PRECISION XNO(3),YNO(3),OMU(3),S10  
REAL LAM,NU,PXK,PKY,GAMA  
INTEGER PREC,CASE  
DIMENSION NU(3)  
COMMON/ONE/GAMA,PXK,PKY,XNO,YNO,NU  
COMMON/LEN/LAM,S10  
COMMON/ZEN/OMU  
COMMON/THREE/MODES  
COMMON/THIRD/NSUP  
COMMON/FOUR/IQ,LM,NORD  
COMMON/SIX/MAXP,PREC  
COMMON/EDIT/NSKP,MTIV  
EQUIVALENCE(CASE,IQ)  
DATA/LM/1HM  
NSKP=0 SKIP NO PRINTING,PLOT ALL  
NSKP=1 SKIP 60 PERCENT OF PRINT,INITIALLY,PLOT ALL  
NSKP=0

## UNCHANGING PARAMETERS

NORD=3  
NSUP=3  
MODES=3  
NU(1)=0.05  
NU(2)=0.05  
NU(3)=0.05  
XNO(1)=.02  
XNO(2)=0.  
XNO(3)=0.  
YNO(1)=-.02  
YNO(2)=0.  
YNO(3)=0.  
PREC=1  
MAXP=15

C MGIV=1 MEANS MODAL QUANTITIES ARE INPUT DATA  
C MGIV=0  
C IF(MGIV.EQ.0) GO TO 10  
C INSERT VALUES OF OMEGA-J,AM1-J,AM2-J HERE IF MGIV=1  
C AS MANY CARDS NEEDED AS THREE TIMES NUMBER OF MODES  
10 CONTINUE  
CASE=1M1  
LM=1000.  
S10=0.1  
IZ=1  
IF(IQ.EQ.LM) IZ=0  
CALL SEARCH(IZ)  
GAMA=10.  
PKX=0.4  
PKY=0.4  
CALL CASEM2  
PKy=0.35  
PKY=0.35  
CALL CASEM2  
LM=100.  
S10=0.1  
IZ=1  
IF(IQ.EQ.LM) IZ=0  
CALL SEARCH(IZ)  
PKX=0.22  
PKY=0.22  
CALL CASEM2  
PKX=0.28  
PKY=0.28  
CALL CASEM2  
STOP  
END

## SUBROUTINE SEARCH(NDS)

C THIS PROGRAM FINDS THE FIRST THREE EIGENVALUES (MU) FOR THE ROTATING  
C BOOM IN EITHER EQUATORIAL OR MERIDION FLEXURE  
C IT WILL COMPUTE THESE ACCURATELY FOR VALUES OF LAMDA UP TO  
C APPROXIMATELY 5000.

```
DOUBLE PRECISION P(4),K(4),M(4),L(4),E3(101),E31P(101),E32P(101),
1FE34,DECID,IVAL,HY,PHOM3,EMOM4,ESHR3,ESHR4,FEPRV,
1E33P(101),E34P(101),E41P(101),E42P(101),E43P(101),
3E44P(101),A,B,C,E,A0,B0,C0,E0,MU1,MU,EPSE,EPSC,LAS,LASS,
4 DLT,UP,DOWN,S10,SI
DIMENSION OMU(3)
REAL H,NN,LAM,NATRQ
INTEGER I,D,N,Z, NINT,INTER,AL,R,U,NOR,KKK
COMMON/ZEN/OMU
COMMON/THIRD/NSUP
COMMON/LEN/LAM,S10
```

C SET NORP = 1 FOR REVERSED INTEGRATION (TIP TO ROOT)

NDS = DIRECTION SWITCH

WHEN NDS = 1, SEARCH FOR EQUATORIAL ROOTS,

WHEN NDS = 0, SEARCH FOR MERIDION ROOTS

```
16 IF(NDS.EQ.1)WRITE(6,16)
17 IF(NDS.EQ.0)D1WRITE(6,17)
FORMAT(*EQUATORIAL CASE*//)
17 FORMAT(*MERIDIONAL CASE*//)
21 WRITE(6,21) LAM,S10,NSUP
21 FORMAT(1H ,*LAM=*,F12.6,3X,*S10=*,D0.3,3X,*NSUP=*,1S,/)
KKK=1
R=0
U=1
FE34=0.
MU=1.0D-6
EPSB=1.0D-14
W=0
FEPRV=0.
EPSR=1D-**4=14
NORP=1
NOR=1
N=1
DLT=1.
LA=0
NINT=TUU
INTER=NINT+1
ANFRQ=SQRT(LAM)
5n WRITE(6,50) ANFRQ
5n FORMAT(1H ,*NFRQ=SQRT(LAM=*,F10.5)
5n 786 JL=1,NSUP
99 SI=0.
IVAL=FE34
IJ=0
DO 31 I=1,4
  K(I)=0.
  L(I)=0.
  M(I)=0.
  P(I)=0.
  DO 1 I=1,101
    E34P(I)=0.
    E44P(I)=0.
    E33P(I)=0.
    E43P(I)=0.
    E32P(I)=0.
```

```

E42P(1)=0.
E31P(1)=0.
E41P(1)=0.
E4(1)=0.
E3(1)=0.
H=1./FLOAT(NINT)

```

### SET INITIAL CONDITIONS ON THE S3 AND S4 SOLUTIONS

```

D=3
1F(D+E9+4) GO TO 2
E0=0.
B0=0.
1F(NOPT+GT+0) GO TO 12
E32P(1)=1.
A0=E32P(1)
GO TO 13
E3(1)=1.
E0=E3(1)
C0=0.
A0=0.
GO TO 3
A0=0.
C0=0.
1F(NOPT+Gr+0) GO TO 14
E43P(1)=1.
C0=E43P(1)
GO TO 15
14 E41P(1)=1.
A0=E41P(1)
B0=0.
E0=0.
A=A0
B=B0
C=C0
E=E0

```

### BEGIN RUNGA KUTTA INTEGRATION

```

N=1
I=1
NN=N
SI=(NN-1)*H
K(1)=H*A
L(1)=H*B
M(1)=H*C
MU1=1.+MU*MU
1F(NDS+EQ+1) GO TO 40
MU1=MU1*1.
P(1)=L(1)+SI*S1+2.*SI0*(I+-SI))/2.*+- (SI+SI0)*A+MU1*E+LAM*H
1F(NOPT+GT+0) P(1)=L(1)+SI*S1+2.*SI0*(I+-SI0))/2.*0
I+(1.-SI+SI0)*A+MU1*E+LAM*H
SI=(NN-1+)*H
I=I+1
1F(I>GT+3) GO TO 6
Z=I-1
E=EO+K(Z)/2.
A=A0+L(Z)/2.

```

```

B=0+H(2)/2.
C=C0+P(Z)/2.
SI=SI+H/2.
GO TO 5
IF(I>GT+4) GO TO 7
E=E0+K(3)
A=A0+L(3)
B=B0+M(3)
C=C0+P(3)
SI=SI+H
GO TO 5
IF(D>E4+4) GOTO 9
SI=NN+H
Z=i+1
E3(Z)=E3(N)+(K(1)+2.*K(2)+2.*K(3)+K(4))/6.
E31P(Z)=E31P(N)+(L(1)+2.*L(2)+2.*L(3)+L(4))/6.
E32P(Z)=E32P(N)+(M(1)+2.*M(2)+2.*M(3)+M(4))/6.
E33P(Z)=E33P(N)+(P(1)+2.*P(2)+2.*P(3)+P(4))/6.
E34P(Z)=LAN*((SI0+i)*2-(SI+SI0)*2)*E32P(Z)/2.
1*(SI+SI0)*E31P(Z)+M01*E3(Z))
IF(NOPT>0) E34P(Z)=LAN*((SI0+i)*2-(1.-SI+SI0)*2)
1*E32P(Z)/2+(1.-SI+SI0)*E31P(Z)+M01*E3(Z))
E=E3(N+1)
A=E31P(N+1)
B=E32P(N+1)
C=E33P(N+1)
E0=E
A0=A
B0=B
C0=C
N=i+1
IF(N<LT+INTER) GO TO 4
EMOM3=E32P(INTER)
ESHRR3=E33P(INTER)
IF(NOPT>0) EMOM3=E3(INTER)
IF(NOPT>0) ESHRR3=E31P(INTER)
D=4
GO TO 8
SI=NN+H
Z=i+1
E4(Z)=E4(N)+(K(1)+2.*K(2)+2.*K(3)+K(4))/6.
E41P(Z)=E41P(N)+(L(1)+2.*L(2)+2.*L(3)+L(4))/6.
E42P(Z)=E42P(N)+(M(1)+2.*M(2)+2.*M(3)+M(4))/6.
E43P(Z)=E43P(N)+(P(1)+2.*P(2)+2.*P(3)+P(4))/6.
E44P(Z)=LAN*((SI0+i)*2-(SI+SI0)*2)*E42P(Z)/2.
1*(SI+SI0)*E41P(Z)+M01*E4(Z))
IF(NOPT>0) E44P(Z)=LAN*((SI0+i)*2-(1.-SI+SI0)*2)
1*E42P(Z)/2+(1.-SI+SI0)*E41P(Z)+M01*E4(Z))
E=E4(N+1)
A=E41P(N+1)
B=E42P(N+1)
C=E43P(N+1)
E0=E
A0=A
B0=B
C0=C
N=i+1
IF(N<LT+INTER) GO TO 4

```

```

E40H4=E42H(INTER)
E5HR4=E43H(INTER)
IF(NOPT.GT.0) E40H4=E4(INTER)
IF(NOPT.GT.0) E5HR4=E41H(INTER)

```

RUNGA KUTTA FINISHED  
NOW BEGIN LINEAR INTERPOLATION  
FE34 IS THE VALUE OF THE DETERMINANT (S3 AND S4)

```

FE34=EMOM3*ESHN4+ESHR3*EMOM4
IF(R.EQ.1) GO TO S1
IF(U.EQ.1) GO TO S0
IF(FE34*DECID)52,51,5a
DECID=FE34
LAS=MU
LASS=LAS
WRITE(6,85)FC34,MU,U
FORMAT(1H ,*FE34*,D12.6,5X,*MU=*,D12.6,5X,*U=*,I3)
MU=MU+DLT
U=U+1
GO TO 99
52 UP=IU
DOWN=LAS
HY=FE34
TVAL=FE34
51 IF(ABS(FE34).LE.EPSR) GO TO 53
IF(ABS(DECID).LE.EPSD) GO TO 92
R=1
IF(FE34*DECID)55,51,56
55 UP=MU
DU=DOWN-(DOWN-UP)*DECID/(DECID*FE34)
KKK=KKK+
EPSC=ABS(LAS(MU)-ABS(LASS))
IF(EPS<LT*MU*10**-4)GO TO 1n
LASS=MU
GO TO 58
56 DOWN=MU
DECID=FE34
MU=DOWN-(DOWN-UP)*DECID/(DECID*HY)
KKK=KKK+
EPSC=ABS(LAS(MU)-ABS(LASS))
IF(EPS<LT*MU*10**-4)GO TO 1n
LASS=MU
58 FE1=ABS(FEPRV)-ABS(FE34)
IF(ABS(FE1).GT.1.0D-14)GOTO A2
IA=IA+1
IF(IA.LT.5) GO TO 82
WRITE(6,83)FE34
FORMAT(1H ,*STUCK ON THIS FE34*,D12.6)
IA=0
FEPRV=0.
GO TO 53
82 FEPRV=FE34
GO TO 99
42 WRITE(6,43)DECID
43 FORMAT(1H ,*NO GOOD DECID=*,D12.6)
GO TO 53
1n WRITE(6,1)) FE34,MU

```

```
11 FORMAT(1HO,*MU CONVERGED FE34=*,D24.18,3X,*MU=r,D12.6)
53 NATERQ=MU*SQR(LAM)
      WRITE(6,54) FE34,MU,LAM,NATERQ,R
      MU(JL)=MU
54 FORMAT(1HO,*FE34=*,D12.6,5X,*MU=*,D12.6,5X,*LAM=*,F12.6,
      15X,*NATERQ=*,E12.6,5X,*R=*,13)
      WRITE(6,56) DLT,NOR
56 FORMAT(1HO,*DLT=*,D9*3,5X,*NOR=*,13)
      NOR=NOR+1
      R=q
      U=1
      KKK=1
      MU=MU+DLT
786 CONTINUE
2      RETURN
END.
```

ELATION: NO DIAGNOSTICS.

EG	0002 D 000204	DELTA	0002 D 000204	DELTA	0000 R 000014	DPV
HV	0002 D 000074	OV	0000 D 006437	E	0000 D 001631	EMOM3
E0	0000 D 000473	E3	0000 D 001005	E31P	0000 D 001317	E32P
34P	0000 D 004447	E4	0000 D 004761	F41P	0000 D 005273	E42P
44P	0003 R 000060	GAMA	0003 R 000000	GAMA	0002 D 000206	GAMA2
H	0000 R 006520	HSQ	0002 I 000210	I	0002 I 000210	I
NJPS	0000 007365	INJPS	0000 I 000005	INTER	0000 I 006473	IR
KF	0000 I 006463	J1	0000 I 006601	J2	0000 I 007077	J1
LAM	0000 I 006601	KMAX	0000 I 007102	K1	0000 D 006463	L
LAX	0007 I 000000	MAXP	0000 R 006537	L1NE	0000 I 006472	LL
TK	0000 D 001641	MNX3	0007 I 000000	MAXP	0012 I 000001	MGIV
MODES	0005 I 000000	MODES	0000 D 002153	MNX4	0000 I 006467	MODE
T	0006 I 000001	N	0000 D 006524	NU	0000 D 006453	MU
N	0000 I 006466	NOPT	0006 I 000001	N	0000 I 006466	NPS
NSUP	0011 I 000000	NSUP	0000 I 006513	NP	0000 I 006474	NPI
I	0000 R 006521	OMXY	0003 n00005	NU	0003 R 000017	NU
MU	0000 R 006507	OMXO	0002 R 000217	OMEGA	0002 R 000217	OMEGA
OMZDG	0000 R 006506	OMZO	0000 R 006504	OMXO	0000 R 006510	OMYDO
P1	0003 R 000001	PKX	0000 D 000433	P	0000 R 006477	PER
REC	0007 R 000001	PREC	0003 R 000001	PKX	0003 R 000002	PKY
S10	0004 D 000001	S10	0000 D 000467	PY	0000 R 006715	SAVE
UN2	0002 D 000211	UN2	0000 R 006464	S10R	0000 D 000431	SM
XO	0003 D 000003	XO	0002 D 000000	V	0002 D 000000	V
YO	0003 D 000041	YNO	0002 D 000200	XI	0002 D 000200	XI
ZKI			0002 D 000202	YI	0002 D 000202	YI

### SUBROUTINE CASEM2

CASEM2 SIMULATES THE NUTATIONAL MOTION OF THE FLEXIBLE SPIN-STABILIZED SATELLITE WITH BOOMS IN MERIDION-VIBRATION, GIVEN A SET OF 2 I.C.'S ON THE BOOMS AND 3 INITIAL ANGULAR RATES AND THEIR DERIVITIVES  
 MODIFIED VERSION USES THE FIRST THREE MODES IN THE SIMULATION AND USES THE EQUATIONS WITH FIRST ORDER TERMS RETAINED  
 THE OUTPUT CONSISTS OF TRANSVERSE RATES, BOOM TIP DISPLACEMENTS, VARIATIONS ON ANGULAR MOMENTUM AND MECHANICAL ENERGY AND THE NUTATION ANGLE IN DEGREES

```

DIMENSION DHU(3)
COMMON/V,DV,C0H,AM2,X1,Y1,DELTA,GAMA2,I,UN2,OMEGA
COMMON/ZONE/GAMA,PKX,PKY,XNO,YNO,NU
COMMON/LEN/LAN,S10
COMMON/THREE/MODES
COMMON/FIVE/NK,N,CA
COMMON/SIX/MAXP,PREC
COMMON/ZEN/OMU
COMMON/THIRD/NSUP
COMMON/EDIT/NSUP,MGIV
INTEGER PREC
REAL NN,LAM,NU
INTEGER MAXP,KMAX,HZ,I,D,N,Z,WINT,ITER
DIMENSION NH(3),DAM1(3),DAM2(3),DMU(3)
DOUBLE PRECISION V(10,3),DV(10,3),
  DOUBLE PRECISION C0H,GAMA2,DELTA,X1,Y1,ZKI
  
```

```

DOUBLE PRECISION XND0(3),YND0(3)
DOUBLE PRECISION AM1(3),AM2(3),A1M(3),A2M(3)
DOUBLE PRECISION UN2(3),AM21(3),XND(3),YND(3)
DOUBLE PRECISION AK(7,4+3),CC(7,3),DW(3),ACX(3)
DOUBLE PRECISION ACY(3),SM
DOUBLE PRECISION P(4),K(4),L(4),E3(101),E31P(101),E32P(101),
              MMX3(101),MMX4(101),BPT(101,3),
TE33P(101),E34P(101),E4(101),E41P(101),E42P(101),E43P(101),
TE44P(101),A,B,C,E,A0,B0,C0,E0,MU1,MU(3),ST0,S1
DO 711 J1=1,NSUP
711 MU(J1)=0.0
      ST0=ST0
      WRITE(6,347)
347 FORMAT(1H,*CASE M           PROGRAM VERSION FIRST ORDER *+/)
C
C   SET PARAMETERS TO CONTROL SIMULATION
C   SET NOPT=1 FOR REVERSED INTEGRATION
C   NDS = DIRECTION SWITCH
C   NDS = 1 IN PLANE, = 0 OUT OF PLANE
C
      NOPT=1
      NDS=0
      NIINT=100
      INTER=NINT+
      WRITE(6,95) LAM,S10R,GAMA,PKX,PKY,PREC,MAXP,MODES
95    FORMAT(1H,*LAMRDA=*,F6+0+1H,*XI-ZERO=*,F4+2+1H,*GAMA=*,F7+3,/
             X1H,*PKX=*,F6+4+1H,*PKY=*,F6+4/
             X     1H,*PREC=*,I2+1H,*MAXP=*,I3+1H,*MODES=*,I2//)
      IF(MGIV.EQ.1) GO TO 340
      DO 34 MODE=1,MODES
99    SI=0.
      N=1
      H=.ZFLOAT(NINT)
C
C   CLEAR ARRAYS
C
      DO 31 I=1,4
      K(I)=0.
      L(I)=0.
      M(I)=0.
31    P(I)=0.
      DO 1 I=1,101
      E34P(I)=0.
      E44P(I)=0.
      E33P(I)=0.
      E43P(I)=0.
      E32P(I)=0.
      E42P(I)=0.
      E31P(I)=0.
      E41P(I)=0.
      E4(I)=0.
1     E3(I)=0.
C
C   THIS SECTION COMPUTES THE FIRST MODE SHAPE AND THEN THE MODE SHAPE
C   PARAMETERS MU1 AND MU2 FOR CASE M
C
      D=3
8     IF(D.EQ.4) GO TO 2

```

```

E0=0.
B0=0.
IF(NOPT.GT.0) GO TO 12
E32P(1)=1,
B0=E32P(1)
GO TO 13
12 E3(1)=1.
E0=E3(1)
13 C0=0.
B0=0.
GO TO 3
2 A0=0.
C0=0.
IF(NOPT.GT.0) GO TO 14
E43P(1)=1.
C0=E43P(1)
GO TO 15
14 E41P(1)=1.
A0=E41P(1)
15 B0=0.
E0=0.
3 K=A0
B=B0
C=C0
E=E0
N=1
4 I=1
NN=N
SI=(NN-1)*H
5 K(1)=H*A
L(1)=H*B
M(1)=H*C
MU1=1+MU(MODE)+MU(00DE)
IF(NDS.EQ.1) GO TO 40
MU1=MU1-1.
40 P(1)=((1.-SI*SI+2.*SI0*(1.-SI))/2.+R-(SI+SI0)*A+HUI*E)*LAM*H
IF(NOPT.GT.0) P(1)=(-SI*SI+2.*SI*(1.+SI0))/2.*B
I+(1.-SI+SI0)*A+MU1*E)*LAM*H
SI=(NN-1)*H
I=I+1
IF(I.GT.3) GO TO 6
Z=I-1
E=E0+K(Z)/2.
A=A0+L(Z)/2.
B=B0+M(Z)/2.
C=C0+P(Z)/2.
SI=SI+H/2.
GO TO 5
6 IF(I.GT.4) GO TO 7
E=E0+K(3)
A=A0+L(3)
B=B0+M(3)
C=C0+P(3)
SI=SI+H
GO TO 5
7 IF(D.EQ.4) GOTO 9
SI=MN*H
Z=I+1

```

```

E3(Z)=E3(N)+(K(1)+2.*K(2)+2.*K(3)+K(4))/6.
E31P(Z)=E31P(N)+(L(1)+2.*L(2)+2.*L(3)+L(4))/6.
E32P(Z)=E32P(N)+(M(1)+2.*M(2)+2.*M(3)+M(4))/6.
E33P(Z)=E33P(N)+(P(1)+2.*P(2)+2.*P(3)+P(4))/6.
E34P(Z)=LAM*((S10+1)**2-(S1+S10)**2)*E32P(Z)/2.
1*(S1+S10)*E31P(Z)+MU1*E3(Z))
IF(NOPT.GT.0) E34P(Z)=LAM*((S10+1)**2-(1.-S1+S10)**2)
1*E32P(Z)/2+(1.-S1+S10)*E31P(Z)+HUI*E3(Z))
E=F3(N+1)
A=E31P(N+1)
B=E32P(N+1)
C=E33P(N+1)
E0=E
AO=A
BO=B
CO=C
N=N+1
IF(N.LT.INTER) GO TO 4
EMOM3=E32P(INTER)
IF(NOPT.GT.0) EMOM3=E3(INTER)
DO 30 I=1,INTER
30 MMX3(I)=E3(I)
D=4
GO TO 8
9 SI=NN*H
Z=N+1
E4(Z)=E4(N)+(K(1)+2.*K(2)+2.*K(3)+K(4))/6.
E41P(Z)=E41P(N)+(L(1)+2.*L(2)+2.*L(3)+L(4))/6.
E42P(Z)=E42P(N)+(M(1)+2.*M(2)+2.*M(3)+M(4))/6.
E43P(Z)=E43P(N)+(P(1)+2.*P(2)+2.*P(3)+P(4))/6.
E44P(Z)=LAM*((S10+1)**2-(S1+S10)**2)*E42P(Z)/2.
1*(S1+S10)*E41P(Z)+MU1*E4(Z))
IF(NOPT.GT.0) E44P(Z)=LAM*((S10+1)**2-(1.-S1+S10)**2)
1*E42P(Z)/2+(1.-S1+S10)*E41P(Z)+MU1*E4(Z))
E=E4(N+1)
A=E41P(N+1)
B=E42P(N+1)
C=E43P(N+1)
E0=F
AO=A
BO=B
CO=C
N=N+1
IF(N.LT.INTER) GO TO 4
EMOM4=E42P(INTER)
IF(NOPT.GT.0) EMOM4=E4(INTER)
DO 32 I=1,INTER
32 MMX4(I)=E4(I)
ALFA=EMOM3/EMOM4
BETA=MMX3(1)-ALFA*MMX4(1)
IF(NOPT.GT.0) BETA=MMX3(1)-ALFA*MMX4(1)
DO 102 LL=1,101
LL=LB
IF(NOPT.GT.0) LL=102-LB
102 BPT(LL,MODE)=(MMX3(LB)-ALFA*MMX4(LB))/BETA
SM=0.
DO 216 I=2,101
216 SM=(BPT(I,MODE)+BPT(I-1,MODE))/2.+(FLOAT(I)-1.*S1+H+S10)*H

```

AM2(MODE)=SH

SM=0.

DO 218 I=2,101

SM=SM+BPRT(I,MODE)\*BPRT(I,MODE)+BPRT(I-1,MODE)\*BPRT(I-1,MODE))/2\*H

AM1(MODE)=SH

34 CONTINUE

END OF MODE SHAPE AND MODE PARAMETER CALCULATION

ALL VARIABLES ARE NON-DIMENSIONAL

NP IS THE STEP DUMMY

NPI IS THE INTERNALLY CALCULATED PRINT INTERVAL

KMAX IS THE NUMBER OF SEGMENTS IN THE SMALLEST PERIOD

NX DETERMINES HOW MUCH OF THE SIMULATION IS PRINTED OUT

GAMA=RHO\*L\*\*3/3-HUB-2

COR=SUM OVER N MODES OF M2 SQUARED OVER H1

340 CONTINUE

KMAX=75

IR=MU(PREC)

IF (PREC.NE.1) NPI=NPI\*IR

BFRQ=NU(PREC)

PFAC=1./FLOAT(KMAX)

PER=B\*\*ATAN(1.)

IF (BFRQ.GT.1.) PER=PER/MU(PREC)

H=PER\*PFAC

MK=MAXP\*KMAX

IF (PREC.NE.1) MK=MAXP\*KMAX\*IR

NX=.6\*MK

NPI=(MK-NX)/60

COR=0.

DO 202 JW=1,MODES

AM21(JW)=AM2(JW)/AM1(JW)

A1M1(JW)=2.\*AM1(JW)

A2M2(JW)=2.\*AM2(JW)

202 COR=COR+AM2(JW)\*AM21(JW)

DELTA=S10\*S10+S10+.3333333

DDELTA=DELTA

DCOR=COR

WRITE(6,97) DCOR,DDELTA,NU

FORMAT(1H , 'COR=' , E11.5/1H , 'DELTA=' , E 9.5/1H , 'NU=' , E10.4/1H ,  
X 'NU2=' , E10.4/1H , 'NU3=' , E10.4//1)

DO 203 JW=1,MODES

DAM1(JW)=AM1(JW)

DAM2(JW)=AM2(JW)

DMU(JW)=MU(JW)

UN2(JW)=2.\*NU(JW)\*NU(JW)

WRITE(6,400) JW,DRHOU(JW),JW,DAM1(JW),JW,DAM2(JW)

400 FORMAT(1H , 'NU' , 11, '=' , E11.5,SX , 11, '=' , E11.5,SX ,

X 'NU2' , 11, '=' , E11.5/1)

203 CONTINUE

DO 406 JW=1,MODES

PW(JW)=MU(JW)\*NU(JW)

GAMA2=2.\*GAMA

ZK1=1.+2.\*GAMA2\*DELTA

X1=1./PKX

Y1=1./PKY

36 DEFINE INITIAL CONDITIONS

```

OMX0=0.
OMY0=0.
OMZ0=1.
OMEGA=1.
OMXDO=0.
OMYDO=0.
OMZDO=0.
THESE 1.C. ALIGN Z-AXIS ON H-VECTOR
DO 404 JW=1,NODES
OMX0=OMX0+GAMA2*OMZ0*XNO(JW)/(X1+2*GAMA*DELTA)
404 OMY0=OMY0+GAMA2*OMZ0*YNO(JW)/(Y1+2*GAMA*DELTA)
DO 405 JW=1,3
XND0(JW)=0.
YNDO(JW)=0.
V(1,JW)=XND0(JW)
V(2,JW)=YNDO(JW)
V(3,JW)=XND0(JW)
405 V(4,JW)=YNDO(JW)
V(5,1)=OMX0
V(6,1)=OMY0
V(7,1)=OMZ0
V(8,1)=OMXDO
V(9,1)=OMYDO
V(10,1)=OMZDO
DO 98 J=1,10
DO 98 JW=1,NODES
98 DV(J,JW)=V(J,JW)
N=1
NP=1
98 I=1
50 CONTINUE

```

## RUNGE KUTTA INTEGRATION

```

DO 407 JW=1,NODES
ACX(JW)=-UN2(JW)*DV(3,JW)-DV(1,JW)*PW(JW)-AM21(JW)*
X (OMEGA*DVA5,1+DV(9,1))
ACY(JW)=-UN2(JW)*DV(4,JW)-DV(2,JW)*PW(JW)-AM21(JW)*
X (OMEGA*DVA6,1+DV(8,1))
AK(1,1,JW)=H*DVA(3,JW)
AK(2,1,JW)=H*DVA(4,JW)
AK(3,1,JW)=H*ACX(JW)
407 AK(4,1,JW)=H*ACY(JW)
AK(5,1,1)=H*DVA(6,1)
AK(6,1,1)=H*DVA(9,1)
AK(7,1,1)=H*DVA(10,1)
I=I+1
IF(I.GT.3) GO TO 60
Z=I-1
DO 91 J=1,7
DO 91 JW=1,NODES
91 DV(J,JW)=V(J,JW)+AK(J,Z,JW)/2.
CALL RATES
GO TO 50
60 IF(I.GT.4) GO TO 90
DO 10 J=1,7
DO 10 JW=1,NODES

```

```

10 DV(J,JW)=V(J,JW)+AK(J,J,JW)
CALL RATES
GO TO 50
90 DO 11 J=1,7
DO 11 JW=1,MODES
CC(J,JW)=AK(J+1,JW)+2.*(AK(J+2,JW)+AK(J+3,JW))+AK(J+4,JW)
Y(J,JW)=V(J,JW)+CC(J,JW)/6.
DO 89 J=1,7
DO 89 JW=1,MODES
89 DV(J,JW)=V(J,JW)
CALL RATES

```

RUNGE KUTTA FINISHED

NOW CALCULATE OUTPUT VARIABLES

```

IF(NPNE+1) GO TO 41
COMPUTE COMPONENTS OF H-VECTOR IN BODY-FIXED AXES
AMX=V(5,1)*(X1+GAMA2*DELTAT)
AMY=V(6,1)*(Y1+GAMA2*DELTAT)
DO 451 KF=1,NSUP
AMY=AMX+AMZ(KF)*(V(4,KF)-V(7,KF)*V(1,KF))*GAMA2
451 AMY=AMY-AM2(KF)*(V(3,KF)+V(7,KF)*V(2,KF))*GAMA2
AMZ=ZKI*V(7,1)
HSQ=AMX*AMX+AMY*AMY+AMZ*AMZ
HSQ=SQRT(HSQ)
OHXY=AMX*AMX+AMY*AMY
OHXY=SQRT(OHXY)
PI=3.141592
DEG=180./PI
CA=DEG*ASIN(OHXY/HSQ)
IF(NSKP.EQ.0) GO TO 427
IF(N.GT.1 .AND. U.LT.NX) GO TO 41
427 CONTINUE
IF(N.NE.1) GO TO 29
*WRITE(6,33) HSQ
33 FORMAT(1H ,INITIAL H#=,E12.6)
*WRITE(6,94)
94 FORMAT(//1H , QX MODE1 QY MODE1 QX MODE2 QY MODE2
      XQX MODE3 QY MODE3 OMEGA_X C ANG N/,/)
29 CONTINUE
IF(NPNE+1) GO TO 41

```

WRITE OUTPUT VARIABLES

```

*WRITE(6,22)V(1,1),V(2,1),V(1,2),V(2,2),V(1,3),V(2,3),V(5,1),
1CA,N
22 FORMAT(1H ,6(D15.5,IX), D12.6,1X,F11.6,1X,15)
41 NP=NP+1
IF(NP.EQ.1) NP=1
CALL PLOT
N=N+1
IF(N.GT.NKE) RETURN
GO TO 88

```

SUBROUTINE RATES

THIS ROUTINE CALCULATES THE DERIVATIVES OF THE ANGULAR RATES

```

COMMON V,DV,COR,AM2,X1,Y1,DELTA,GAM2,I,UN2,OMEGA
COMMON/ZEN/OMU
COMMON/THREE/MODES
COMMON/THIRD/NSUP
DIMENSION OMU(3)
DOUBLE PRECISION V(10,3),DV(1n,3),COR,AM2(3),
X UN2(3),GAMA2,DELTA,X1,Y1,BU(3),AUX1,AUX2
DO 711 JI=1,NSUP
711 HU(JI)=OMU(JI)
AUX1 = -1.0/(X1+GAMA2*(DELTA-COR))
DV(8,1)=AUX1*(1.0-Y1+GAMA2*(DELTA-COR))+OMEGA*Dv(6,1)
AUX2 = -1.0/(Y1+GAMA2*(DELTA-COR))
DV(9,1)=AUX2*(X1-1.0-GAMA2*(DELTA-COR))+OMEGA*Dv(5,1)
DV(10,1)=0.0
DO 12 J=1,MODES
DV(8,1)=DV(8,1)+AUX1*GAMA2*AM2(J)*DV(2,J)*(OMEGA*OMEGA-
X HU(J)*HU(J))-UN2(J)*DV(4,J)
DV(9,1)=DV(9,1)+AUX2*GAMA2*AM2(J)*DV(1,J)*(OMEGA*OMEGA-
X HU(J)*HU(J))-UN2(J)*DV(3,J)
12 CONTINUE
IF(I.LE.4) RETURN
V(8,1)=DV(8,1)
V(9,1)=DV(9,1)
V(10,1)=DV(10,1)
RETURN

```

```

SUBROUTINE PLOT
THIS SUBROUTINE PLOTS ROTATION ANGLE VS N
COMMON/ONE/GAMA,PKX,PKY,XNO,YNO,NU
COMMON/LEN/LAN,S10
COMMON/THREE/MODES
COMMON/FIVE/MK,N,CA
COMMON/SIX/MAXP,PREC
DOUBLE PRECISION S10
REAL MAX,LAN,LINE
DIMENSION SAVE(100),LINE(110),AP(5),AN(5)
DATA BLANK,STAR,DOT/1H ,1H*,1H*/,
IF(M.NE.1) GO TO 2
N1=(MK+50)/100
DO 1 J1=1,100
1 SAVE(J1)=0.
J1=0
MAX=0.
LINE=0.
SIOR=S10
2 IF(N/N1.NE.0) GO TO 3
J1=J1+1
SAVE(J1)=CA
IF(ABS(CA).GT.MAX) MAX=ABS(CA)
3 IF(N.NE.MK) RETURN
WRITE(6,4)
4 FORMAT(1H,*PLOT OF ROTATION ANGLE IN DEGREES VS N FOR *)
WRITE(6,95) LAN,SIOR,GAMA,PKX,PKY,PREC,MAXP,MODES
95 FORMAT(1H ,*LAURDA=*,F6.0/1H ,*SI=ZERO=*,F4.2/1H ,*GAMA=*,F7.3,/
X1H ,*PKX=*,F6.4/1H ,*PKY=*,F4.8/
X 1H ,*PREC=*,12/1H ,*MAXP=*,14/1H ,*MODES=*,12//1)

```

```

A1=MAX/50.
DO 6 I1=1,5
AN(I1)=A1*(60+10.*I1)
6 AP(6-I1)=-AN(I1)
I1=0
WRITE(6,7) AN,I1,AP
7 FORMAT(1H ,14X,5(F6.2,4X),3X,I1,2X,G(5X,F5.2))
DO 8 J1=1,110
LINE(J1)=BLANK
8 IF((J1+4)/10*10.EQ.(J1+4)) LINE(J1)=STAR
WRITE(6,9) LINE
9 FORMAT(1H ,12X,10A1)
DO 10 J1=1,110
LINE(J1)=STAR
WRITE(6,9) LINE
DO 11 J1=1,110
LINE(J1)=BLANK
DO 13 K1=1,100
J1=SAVE(K1)/A1*56*5
LINE(56)=STAR
IF(K1/10*10.NE.K1) GO TO 12
LINE(55)=STAR
12 LINE(J1)=DOT
WRITE(6,9) LINE
IF(K1/10*10.NE.K1) GO TO 15
IF(J1.GE.50.AND.J1.LE.54) GO TO 15
M1=N1*K1
WRITE(6,14) M1
14 FORMAT(1H+,6IX,1S)
15 LINE(J1)=BLANK
13 LINE(55)=BLANK
RETURN
END

```

INITIATION: NO DIAGNOSTICS.

## CHAPTER 6

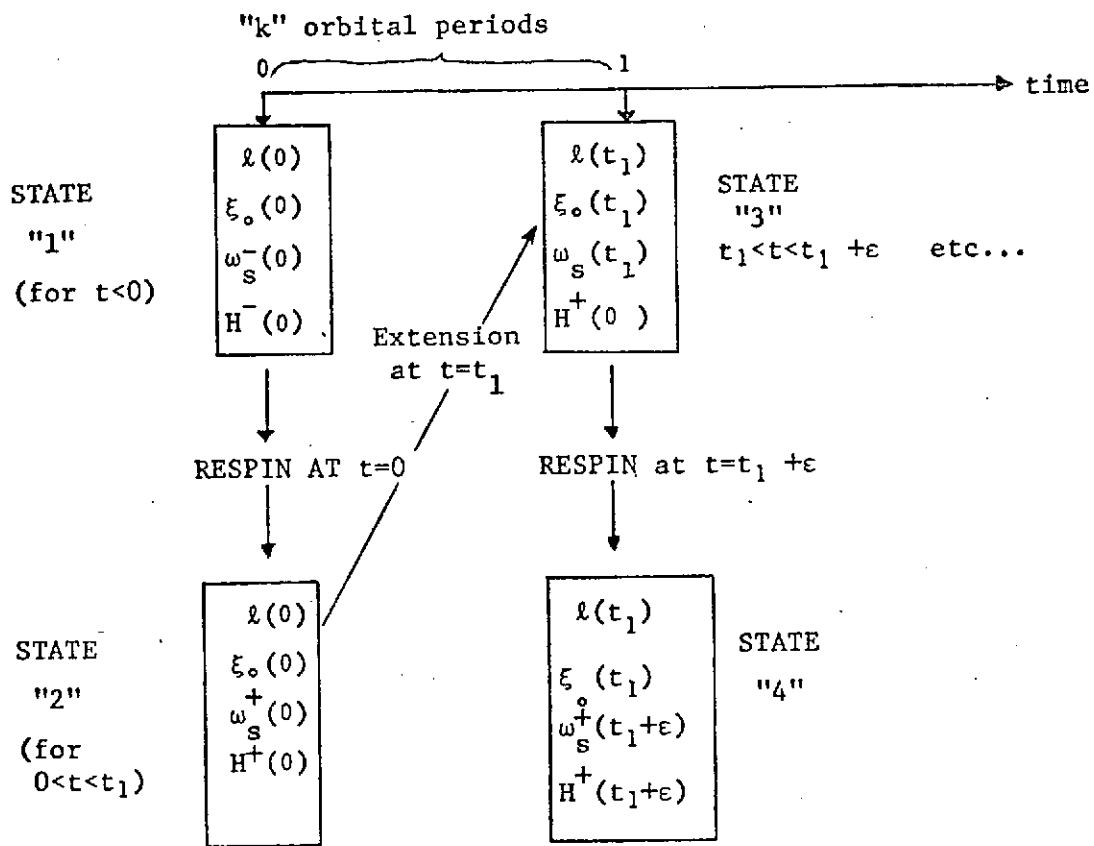
Other Topics

The present chapter contains a short note on the use of the stability charts in deployment dynamics, and two bibliographical reports on passive nutation damping devices.

## 6.1 Stability charts and deployment dynamics

## 6.1.1 Dynamic parameters during deployment

A deployment phase such as the one for IMP-I may be summarized as follows, if  $H$ ,  $\ell$ ,  $\xi_0$ ,  $\omega_s$  designate the angular momentum, length of booms, non-dimensional radius of the hub ( $\frac{x_0}{\ell}$ ), and spin rate  $\omega_s$  - or +



We define a "state" as a set of values  $\ell$ ,  $\xi_0$ ,  $\omega_s$ ,  $H$ . If non-dimensional variables are used, let

$$H_0 \stackrel{\equiv}{=} H(\ell=0) = I_{zh} \omega_s$$

$$h(\text{any state}) \underset{\text{def}}{\equiv} \frac{H(\text{any state})}{H_0} \quad h(\ell=0) = 1$$

$$\omega_s(0^-) \underset{\text{def}}{\equiv} \omega_{s0}$$

Thus

$$h = \frac{I_z \omega_s}{H_0} = \frac{(1 + 4\Gamma\Delta) I_{zh}}{I_{zh} \omega_{s0}} = (1 + 4\Gamma(\xi_0^2 + \xi_0 + \frac{1}{3})) \frac{\omega_s}{\omega_{s(0)}} \quad (1)$$

with

$$\Gamma = \frac{\rho l^3}{I_{z,h}}$$

$$\Delta = \xi_0^2 + \xi_0 + \frac{1}{3}$$

$I_{z,h}$  = moment of inertia of central hub about "z".

$\rho$  = linear density of boom

In view of these definitions, an extension maneuver at  $t$  corresponds to

$$h(t+0) = h(t-0)$$

$$\ell(t+0) = \ell(t-0) + \Delta\ell$$

$$\frac{\omega_s(t+0)}{\omega_s(t-0)} = \frac{(1 + 4\Gamma\Delta)t+0}{(1 + 4\Gamma\Delta)t+0}$$

in which  $\Delta\ell$  is specified.

A respin maneuver at  $t$  will give

$$h(t+0) = h(t-0) + (1 + 4\Gamma(\xi_0^2 + \xi_0 + \frac{1}{3}))_{t+0} \frac{\omega_s(t+0) - \omega_s(t-0)}{\omega_{s(0)}}$$

$$(1 + 4\Gamma(\xi_0^2 + \xi_0 + \frac{1}{3}))_{t+0} = (1 + 4\Gamma(\xi_0^2 + \xi_0 + \frac{1}{3}))_{t-0}$$

in which  $\delta\omega_s(t) = \omega_s(t+0) - \omega_s(t-0)$  is specified.

For a satellite of given hub ( $x_0$ ,  $I_{zh}$  specified)

$$\xi_0 = \frac{x_0}{l} = x_0 \cdot \left( \frac{\rho}{I_{zh}} \right)^{1/3} = \frac{x_0 \rho^{1/3}}{I_{zh}^{1/3}} \frac{1}{l^{1/3}} = \bar{s} \frac{1}{l^{1/3}} \quad (2)$$

with  $\bar{s}$  a fixed non-dimensional number def  $\bar{s} \equiv \frac{x_0 \rho^{1/3}}{I_{zh}^{1/3}}$

Now, substituting (2) for  $\xi_0$  in Equation (1)

$$\omega_s = \omega_{s0} [1 + 4\Gamma(\bar{s}^2 \Gamma^{-2/3} + \bar{s} \Gamma^{-1/3} + \frac{1}{3})]^{-1/2} h$$

If  $\underline{l}$  is specified in any state,

$$\Gamma = \frac{\rho \underline{l}^3}{I_{z,h}}$$

can be computed.

To that state there corresponds an Etkin's number

$$\bar{\lambda} = \frac{\rho \underline{l}^4}{EI} \omega_s^2 = \frac{\rho \underline{l}^4 \omega_{s0}^2}{EI x_0^4} x_0^4 [1 + 4(\bar{s} \Gamma^{1/3} + \bar{s} \Gamma^{2/3} + \frac{1}{3} \Gamma)]^{-2} h^2$$

The quantity  $\frac{\rho x_0^4}{EI}$  is specified for a given design. Let  $\bar{R}$  be the non-dimensional quantity

$$\begin{aligned} \bar{R} &\stackrel{\text{def}}{=} \left( \frac{\omega_{s0}}{\omega_*} \right)^2 \\ \omega_*^2 &\stackrel{\text{def}}{=} \frac{EI}{l x_0^4} \end{aligned}$$

Then

$$\begin{aligned} \bar{\lambda} &= \bar{R} \xi_0^{-1} \left[ 1 + 4 \left( \bar{s}^2 \Gamma^{1/3} + \bar{s} \Gamma^{2/3} + \frac{1}{3} \Gamma \right) \right]^{-2} h^2 \\ &= \frac{\bar{R}}{\bar{s}^4} \Gamma^{4/3} \left[ 1 + 4 \left( \bar{s}^2 \Gamma^{1/3} + \bar{s} \Gamma^{2/3} + \frac{1}{3} \Gamma \right) \right]^{-2} h^2 \quad (3) \end{aligned}$$

(2) and (3) thus give  $\xi_0$ ,  $\bar{\lambda}$  during the "states" of deployment as functions of boom's length and angular momentum. In these relations,  $\bar{R}/\omega_{s0}$  and  $\bar{s}$  are fixed for any given design.

### 6.1.2 Stability during deployment

The determination of the stability during deployment will thus proceed as follows:

a)  $\bar{R}/\omega_{s_0}$  is computed (a fixed quantity), then  $\bar{K}$  for  $\omega_{s_0}$  given.

b)  $\bar{S}$ , a fixed quantity, is computed;

given the state  $\omega_s$ ,  $\ell$ ,  $\xi_0$  and  $H$  for some  $t$ :

c) compute  $h$ ;

d) compute  $\Gamma(\cdot)$ ;

e) compute  $\Delta(\xi_0)$ ;

using the relevant formulae for either respin or

extension maneuver

f) compute  $\bar{\lambda}$  from (3);

g) determine the stability of the corresponding  $(K_p, \Gamma)$  point

on the stability chart corresponding to the computed

values of  $\bar{\lambda}$  and  $\xi_0$ , using program FLEXAT of Chapter 5.

C<sup>3</sup>

**6.2 A SURVEY OF PASSIVE  
NUTATION DAMPING TECHNIQUES**

Prepared by

William O. Keksz

## I. Introduction

In this paper, several methods of passive nutation damping are surveyed. In a review of rigid body dynamics, conditions of stability are presented. Ball, pendulum, and fluid dampers are surveyed, among others, along with effects of magnetic and gravitational torques and structural hysteresis energy dissipation. Finally, a few active and semipassive systems are mentioned in the way of comparison.

$A, B, C$	Moments of inertia about $x, y, z$ axes
$D, E, F$	Products of inertia for $xy, xz, yz$ planes
$x, y, z$	Body-fixed axes, $z$ along spin axis
$X, Y, Z$	Inertial axes, $Z$ along $\vec{H}$
$\vec{\omega}$	Total angular velocity
$p, q, r$	Components of $\vec{\omega}$ along $x, y, z$ axes
$(\cdot)$	$d(\cdot)/dt$
$\vec{H}$	Angular momentum
$q_i$	Generalized coordinates
$L_{qi}$	Moment in direction of $q_i$
$\varphi, \theta, \psi$	Euler's angles
$\dot{\varphi}$	Precession rate
$\dot{\psi}$	Spin rate
$\dot{\theta}$	Nutation angle
$\gamma$	Magnetic or structural hysteresis factor
$\omega_T$	$(p^2 + r^2) =$ component of $\vec{\omega}$ in $xy$ plane
$\lambda$	$(C - A)/\Lambda$
$\Omega$	$\lambda r =$ forcing frequency
$i$	$(-1)^{1/2}$
$\hat{i}, \hat{j}, \hat{k}$	Unit vectors along $x, y, z$
$M$	Mass of main body
$m$	Damper mass
$s$	Radius of gyration

Other symbols are defined throughout the text as needed.

### III. Review of Rigid Body Dynamics [33]

#### A. Definitions

##### 1. Euler's Angles

If  $X, Y, Z$  is fixed in space and  $x, y, z$  is the body fixed system, we define the Euler Angles  $\psi$ ,  $\theta$ , and  $\varphi$  in Fig. II-1. The spin axis is along  $z$ , and:

$$\dot{\psi} = \text{precession rate}$$

$$\dot{\theta} = \text{nutation angle}$$

$$\dot{\varphi} = \text{spin rate}$$

The unit vectors  $\hat{i}, \hat{j}, \hat{k}$  lie along  $x, y, z$ .

We have:

$$\begin{bmatrix} X \\ Y \\ Z \end{bmatrix} = \begin{bmatrix} (\cos \varphi \cos \psi - \sin \varphi \cos \theta \sin \psi) \\ (\cos \varphi \sin \psi + \sin \varphi \cos \theta \cos \psi) \\ (\sin \theta \sin \varphi) \end{bmatrix}$$

$$\begin{bmatrix} x \\ y \\ z \end{bmatrix} = \begin{bmatrix} (-\sin \varphi \cos \psi - \sin \psi \cos \theta \cos \varphi) & (\sin \theta \sin \psi) \\ (-\sin \varphi \sin \psi + \cos \varphi \cos \theta \cos \psi) & (-\sin \theta \cos \psi) \\ (\sin \theta \cos \psi) & (\cos \theta) \end{bmatrix} \begin{bmatrix} X \\ Y \\ Z \end{bmatrix}$$

##### 2. Angular Velocity

If  $\vec{\omega} = \omega_x \hat{i} + \omega_y \hat{j} + \omega_z \hat{k}$  is the total angular velocity of the body, then:

$$\begin{bmatrix} \omega_x \\ \omega_y \\ \omega_z \end{bmatrix} = \begin{bmatrix} (\sin \theta \sin \varphi) & (0) & (\cos \varphi) \\ (\sin \theta \cos \varphi) & (0) & (-\sin \varphi) \\ (\cos \theta) & (1) & (0) \end{bmatrix} \begin{bmatrix} \dot{\psi} \\ \dot{\varphi} \\ \dot{\theta} \end{bmatrix}$$

Note that  $r$  is not the spin rate.

In most cases, the linear velocity of the center of mass is ignored for damper analysis.

### 3. Angular Momentum

$$\vec{H} = \begin{bmatrix} \hat{i}\hat{A} & -\hat{j}\hat{B}' & -\hat{k}\hat{C}' \\ -\hat{j}\hat{A}' & \hat{j}\hat{B} & -\hat{k}\hat{F}' \\ -\hat{k}\hat{A}' & -\hat{k}\hat{F}' & \hat{k}\hat{C} \end{bmatrix} \cdot \vec{\omega}$$

The above is the angular momentum in x,y,z. For most cases, we can ignore the external torques produced by electromagnetic fields and gravitational gradients. Thus  $\vec{H}$  is constant in inertial space (X,Y,Z), and thus we can align the Z axis along  $\vec{H}$ . If x,y,z are aligned along the principle axes of the body,  $D',E',F' = 0$ , and:  $\vec{H} = Ap\hat{i} + Bq\hat{j} + Cr\hat{k}$  where p,q,r are the  $\omega_x, \omega_y, \omega_z$  for alignment with the principle axes.

### 4. Kinetic Energy

The kinetic energy of the body is:

$$T = \frac{1}{2}(A\omega_x^2 + B\omega_y^2 + C\omega_z^2) - D\omega_x\omega_y - E\omega_x\omega_z - F\omega_y\omega_z$$

and for the principle axes:

$$T = \frac{1}{2}(Ap^2 + Bq^2 + Cr^2)$$

### 5. Euler's Equations

Here Euler's Equations are presented only for a principle axis x,y,z:

$$L_1 = Ap + qr(C-B)$$

$$L_2 = Bq + pr(A-C)$$

$$L_3 = Cr + pq(B-A)$$

where  $L_1, L_2$ , and  $L_3$  are the extornal moments about the corresponding principle axes; here they will usually be zero.

## 6. Poinsot Ellipsoid

For a rigid body,  $T = \text{constant}$ , and thus:

$$\frac{\vec{\omega} \cdot \vec{H}}{H} = \frac{2T}{H} = Q$$

This must be the component of  $\vec{\omega}$  along  $\vec{H}$  and  $Z$ . If both sides of the energy relationship are divided by  $T$ , we get:

$$1 = \frac{p^2}{2T/A} + \frac{q^2}{2T/B} + \frac{r^2}{2T/C}$$

This is the Poinsot ellipsoid. If a plane is placed perpendicular to  $\vec{H}$  a distance  $Q$  from the center of this ellipsoid, we see the Poinsot ellipsoid rolls on the plane (called the invariant plane), without slipping. The contact point is the tip of  $\vec{\omega}$  (Fig.II-2). The curve traced out by the contact point on the plane is the herpolhode, and that on the ellipsoid is the polhode.

## 7. Body and Space Cones (Axisymmetric Body)

From the above we see that  $\vec{\omega}$  sweeps out a surface in both the  $x,y,z$  and  $X,Y,Z$  frames. If  $\theta = 0$  and we have an axisymmetric body ( $A=B$ ) then these are both right circular cones. From the relations between  $p,q,r$  and  $\dot{\psi}, \dot{\phi}, \dot{\varphi}$  substituted into the Euler moment equations, we have:

$$\dot{\psi} = \frac{C \dot{\varphi}}{(A-C)\cos\theta}$$

(a)  $C > A$ :  $\dot{\psi}$  and  $\dot{\varphi}$  are opposite in sign, and this is known as retrograde precession.

(b)  $C < A$ :  $\dot{\psi}$  and  $\dot{\varphi}$  have the same sign, and this is known as direct or posigrade precession.

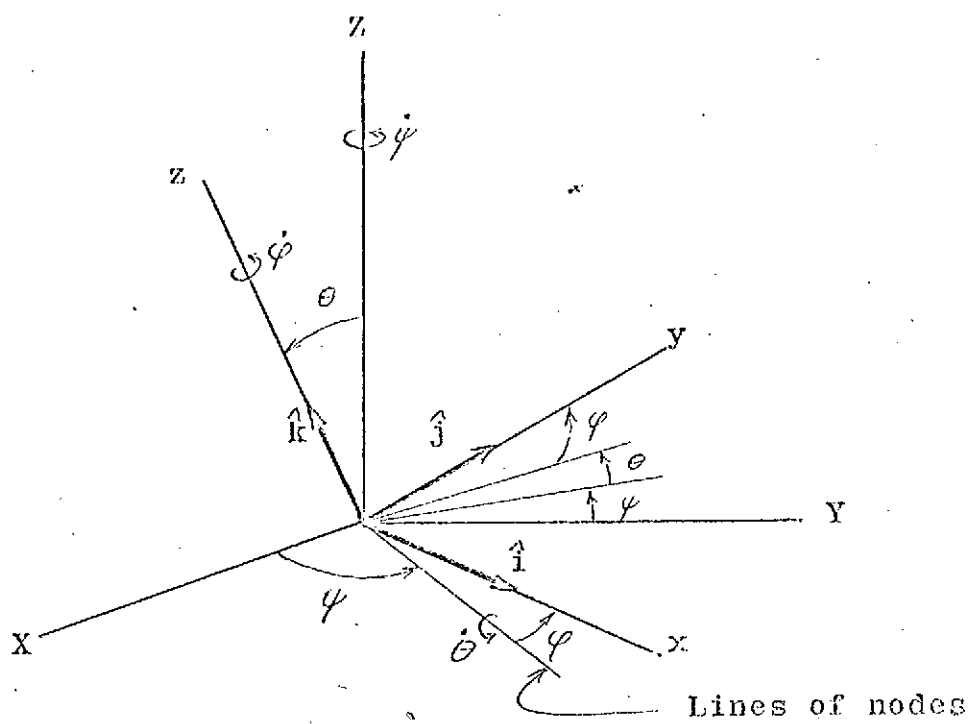


Fig. III-1: Euler's angles.

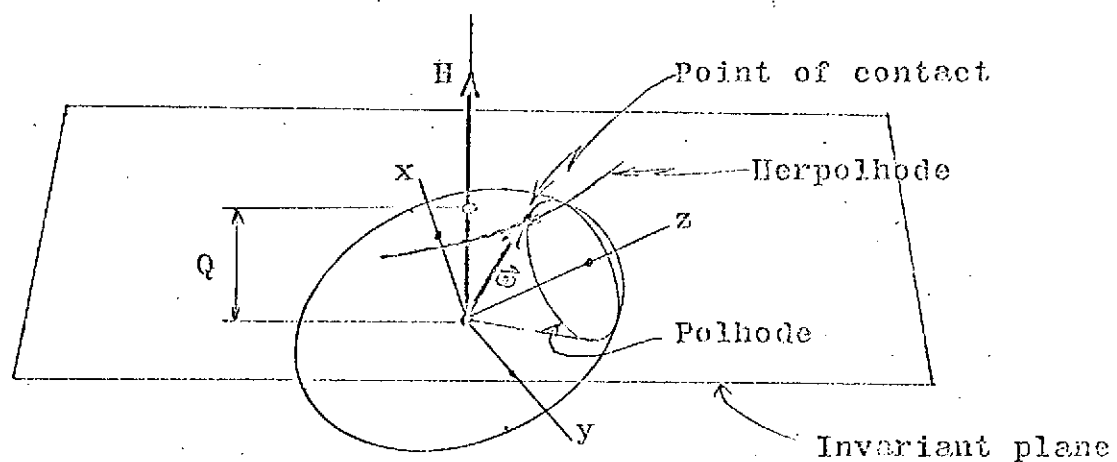
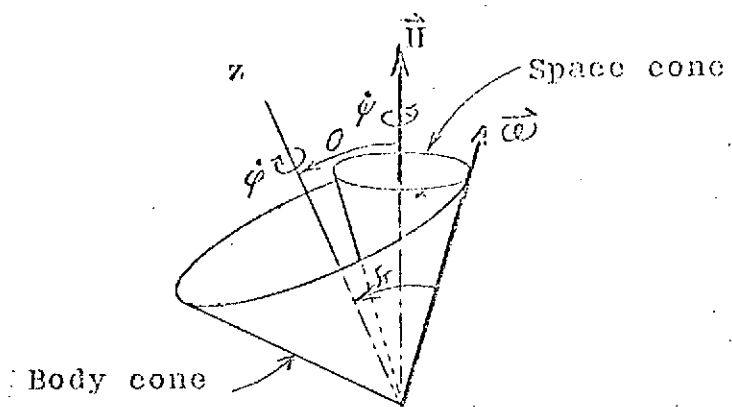
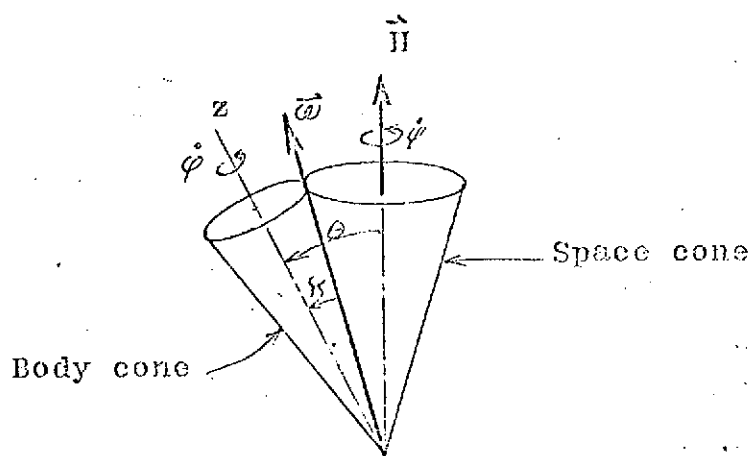


Fig. III-2: Poinsot ellipsoid.



(a) Retrograde precession;  $C > A$ .



(b) Direct precession;  $C < A$ .

Fig. III-3: Precession of body cone rolling on space cone.  $\vec{\omega}$  is along the line of contact.

The body cone rolling on the space cone for each of these cases is illustrated in Fig. III-3. The angle between  $\vec{\varphi}$  and  $\vec{\omega}$  is  $\kappa$ :

$$\tan \kappa = (p^2 + q^2)^{1/2}/r = \omega_T/r$$

where  $\omega_T$  is the component of  $\vec{\omega}$  lying in the x,y plane. The angle between  $\vec{\varphi}$  and  $\vec{H}$  is  $\theta$ :

$$\tan \theta = (A/C)/(\omega_T/r)$$

By substituting  $\alpha = [(C-A)/A]r = \lambda r$  into the Euler equations, we have:

$$\ddot{p} + \Omega q = 0 \rightarrow \ddot{p} = -\Omega q$$

$$\ddot{q} - \Omega p = 0$$

$$\text{Thus } \ddot{p} + \Omega^2 p = 0$$

$$\text{and } p = p_0 \cos \Omega t + (\dot{p}_0/\Omega) \sin \Omega t$$

$$q = p_0 \sin \Omega t - (\dot{p}_0/\Omega) \cos \Omega t$$

These last imply that  $\omega_T = (p^2 + q^2)^{1/2}$  rotates about the z axis at the rate  $\Omega$ .

By using a complex analysis, Ames and Murnaghan show that [1]:

$$\omega_T = \left[ \frac{H^2 - 2CT}{A(A-C)} \right]^{1/2} e^{int}$$

#### 8. A Note on Unsymmetrical Bodies

The relations for  $\vec{\omega}$  are given by Thomson for the case  $A > B > C$  and  $H^2 \geq 2TB$ , a body spinning about its axis of least inertia [33a]:

$$p = \left[ \frac{H^2 - 2TC}{A(A-C)} \right]^{1/2} \operatorname{cn} f(t - t_0)$$

$$q = \left[ \frac{H^2 - 2TC}{B(B - C)} \right]^{\frac{1}{2}} \sin f(t - t_0)$$

$$r = - \left[ \frac{2TA - H^2}{C(A - C)} \right]^{\frac{1}{2}} \operatorname{dn} f(t - t_0)$$

$$\text{where } f = \left[ \frac{(B - C)(2TA - H^2)}{ABC} \right]^{\frac{1}{2}}$$

and the modulus of the elliptic functions is:

$$k = \left[ \frac{(A - B)}{(B - C)} \cdot \frac{(H^2 - 2TC)}{(2TA - H^2)} \right]^{\frac{1}{2}}$$

This results in spin about the z axis with a superimposed wobble, with a  $\theta_{\max}$  and  $\theta_{\min}$ :

$$\cos^2 \theta_{\max} = C(2TB - H^2) / (B - C)H^2$$

$$\cos^2 \theta_{\min} = C(2TA - H^2) / (A - C)H^2$$

## B. Miscellaneous Concepts

### 1. Stability of a Rigid Body

For a rigid body, T is a constant. If we let the initial condition be:

$$p = p_1 + \epsilon$$

$q, r$  small

where  $\epsilon$  is small, we can differentiate the Euler equations and substitute for  $p, q, r$  and  $\dot{p}, \dot{q}, \dot{r}$ . Then:

$$\ddot{q} + p_1^2 q(A - B)(A - C)/BC = 0$$

$$\ddot{r} + p_1^2 r(A - B)(A - C)/BC = 0$$

These are stable only if  $(A - B)$  and  $(A - C)$  are of the same sign. Thus they are unstable only if A is the intermediate rotational inertia.

### 2. Energy and Stability

In a real spacecraft, there is always an energy loss

due to flexure of nonrigid parts, magnetic hysteresis, etc. Thus we have  $\dot{T} < 0$ .

For an axisymmetric body, we have:

$$2T = A\omega_T^2 + Cr^2$$

$$H^2 = A^2\omega_T^2 + C^2r^2$$

Since  $Cr = H \cos \theta$ :

$$H^2 - 2TA = \cos^2 \theta H^2(C - A)/C$$

$$\text{or } T = H^2 [1 - \cos^2 \theta (C - A)/C]/2A$$

Since there are no external torques,  $H$  is constant, and

$$\begin{aligned}\dot{T} &= [H^2(C - A)/AC](\sin \theta \cos \theta)\dot{\theta} \\ &= (H^2\lambda/C)(\sin \theta \cos \theta)\dot{\theta}\end{aligned}$$

Thus, for decreasing  $T$ ,  $\theta$  decreases only if  $C > A$ , and the satellite is spinning about its axis of maximum inertia. This is the stable condition. For a prolate body, there must be an energy input for stability, which implies an active nutation control.

The change in energy required to stabilize a precessing body can easily be found. The desired energy state is:

$$T_f = \frac{1}{2}Cr_f^2$$

where the subscript f denotes final condition. Since  $H^2$  is constant [36]:

$$H^2 = A^2\omega_T^2 + C^2r^2 = C^2r_f^2 = H_f^2$$

$$\text{Then } r_f^2 = (A/C)\omega_T^2 + r^2$$

$$\text{Thus } \Delta T = |T - T_f| = |\frac{1}{2}A(1 - A/C)\omega_T^2|$$

For an oblate body ( $A < C$ ), this is the precessional energy, the amount to be removed; for a prolate body, it is the amount to be added.

$$\text{Also } \omega_T = (r - \Omega) \tan \theta = (C/A) r \tan \theta$$

### III. Passive Dampers

Unless stated otherwise, the satellite will be assumed axisymmetric about the z (spin) axis,  $A = B$ , and oblate ( $A < C$ ) for the below.

#### A. Ball-type [4, 24, 36].

##### 1. Mounted in the Meridian Plane

This type was first used in Telstar and later in ESRO II. These consist of a ball allowed to roll inside a circular cross section curved tube which is filled with a gas. Two are used, diametrically opposed, to maintain symmetry, and mounted in a plane through the spin axis. Energy dissipation comes about through viscous friction between the ball and gas, rolling friction between the ball and tube wall, and collision of the ball with the tube end, the latter only at large nutation angles.

Such a system is shown in Fig. III-1. According to Yu, the rotational motion of the ball (of radius  $a$ ) is given:

$$(2/5)ma^2(\ddot{\theta}r/r) = ka - N$$

where  $k$  is the friction force at the contact point, and  $N$  the rolling friction torque.  $N$  is approximately an order of magnitude smaller than the viscous term. Neglecting  $N$  and assuming  $\theta$  small, the motion of the ball

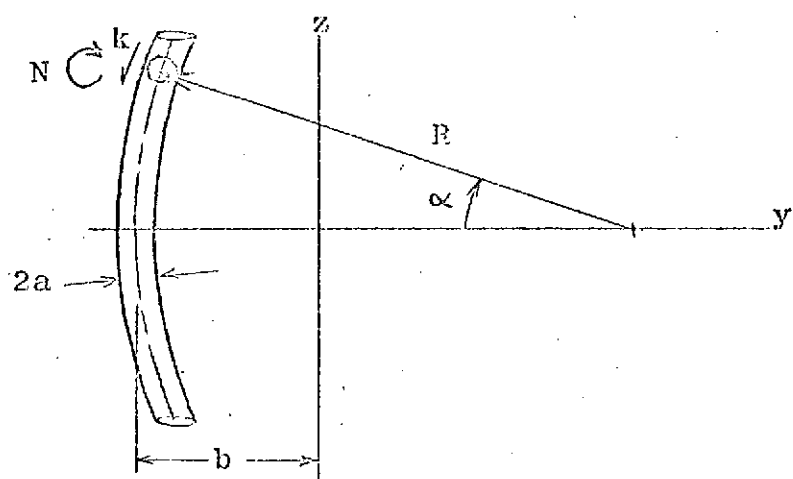
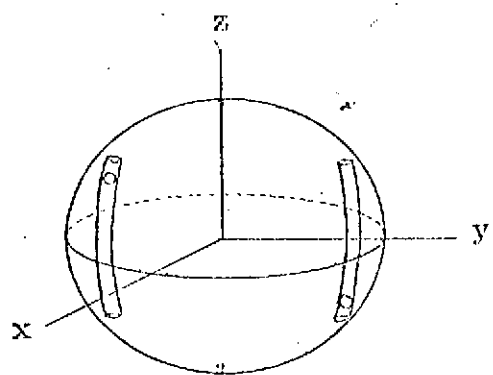


Fig. III-1: Ball-type damper mounted in  
meridien plane.

is described by:

$$\ddot{\theta} + (5c/7m)\dot{\theta} + (5br^2/7R)\theta \approx (5b/7R)\cos\Omega t$$

where  $c$  is the coefficient of viscous friction. The time average rate of energy dissipation is, for viscous friction:

$$\bar{dT}_v/dt = T_v \Omega / 2\pi = -cR^2\Omega^2\dot{\theta}_0^2/2$$

$$\text{where } \dot{\theta}_0 = \theta(1 - \Omega^2/r^2) \left[ (1 - \Omega^2/P^2)^2 + 4n^2\Omega^2/P^4 \right]^{-1/2}$$

$$n = 5c/14m$$

and  $P = (5br^2/7R)^{1/2}$  is the natural frequency, the square root of the  $\propto$  coefficient.

We end up with an exponential damping:

$$\theta = \theta_0 e^{-t/\tau}$$

$$\text{and } \tau = \frac{5c[(1 - \Omega^2/P^2)^2 + 4n^2\Omega^2/P^4]}{7nmR^2\lambda (\lambda + 1)^2(1 - \lambda)^2}$$

If rolling friction dissipation is included:

$$\bar{dT}_r/dt = 2FR\dot{\theta}_0 |\Omega|/\pi$$

where  $F$  is the rolling friction, and:

$$\theta = (\theta_0 + \mu)e^{-t/\tau'} - \mu$$

$$\tau' = \tau \ln \left[ (1 + \theta_0/\mu) / (1 + \theta_0/\mu e) \right]$$

Numerical computations show that  $\mu$  is substantially less than one degree. Thus the viscous-only results can be used if  $\theta_0$  is somewhat greater than one degree.

The damping time can be greatly reduced by designing a resonant system, making  $P = \Omega$ . Then:

$$R_{res} = 5b/7\lambda^2$$

The time constant is then:

$$\gamma_{\text{res}} = 28nC \lambda' m b^2 (\lambda + 1)^2 r^2 (1 - \lambda)^2$$

A resonant damper could not be used in Telstar because  $\lambda$  was close to zero and room had to be made for an electronics package, preventing a small value of  $b$ .

It is possible to conceive of dampers using straight tubes or tubes concave outward. It is easily seen, however, that the equilibrium position for the ball during nutation would be at the ends of the tubes, and the final spin axis would not coincide with that of the satellite without the balls.

The parameters for Telstar were  $A/C = .95$ ,  $\dot{\phi} = 20-180$  rpm,  $R = 15$  ft,  $m = 0.0021$  slug,  $a = 0.242$  in (tungsten for its large density),  $c = 0.00193$  lb-sec/ft (neon for its high viscosity). The theoretical damping time was calculated to be a maximum of about three minutes.

Note that a gas of low viscosity should be used for a tuned (resonant) damper, as  $n$ , proportional to  $c$ , appears in the numerator of the expression for  $\gamma_{\text{res}}$ .

The problems in this analysis are due to the assumed small  $\theta$  and linearization of the equations. G.T. Kosyuk devised a ground test of a model supported at its center of gravity which showed that the experimental  $\gamma$  was about four times that calculated using the mean value of the transverse inertia moments, and nine times that using the minimum value. Taking these fac-

tors into account, the  $\gamma$  for Telstar was calculated to be no more than thirty minutes.

## 2. Mounted in a Plane Parallel to the Equatorial

Two of this type were mounted in FR-I, and one in the HEOS spacecraft, which also used a liquid damper.

If  $h$  is the distance from the damper plane to the center of gravity, Routh criteria applied to the Euler equations indicate that  $b/R < 1 - mh^2/A$  is necessary for stability. Also, optimum damping (minimum  $\gamma$ ) is given by a viscous friction coefficient of:

$$c_{opt} = mR^2r[14mh^2(\lambda + 1)^3/5A\lambda]^{1/2}$$

This results in:

$$\gamma_{opt} = (1/r)[56A\lambda/mh^2(\lambda + 1)^3]^{1/2}$$

Experimental results agree well with the theoretical. For two dampers and  $\lambda = 0.61$ ,  $h = 0.15m$ ,  $R = 0.2m$ ,  $r = 0.2$  rad/sec, and 250 gm give a maximum  $\gamma$  of 120 sec for reasonable  $\theta$ . The experimental result was 130 sec. With all parameters equal, the efficiency ratio of the equatorial to meridian damper is  $[(1 + \lambda)/(1 - \lambda)]^2$ .

## B. TEAM Damper [24, 25]

The TEAM damper, used in Tiros, is essentially the same in concept as the meridian-mounted ball damper. A small mass fitted with rollers is allowed to run along a curved monorail (Fig. III-2). The difference lies in that there is no fluid involved, so only rolling friction exists. From the ball damper analysis, it can be

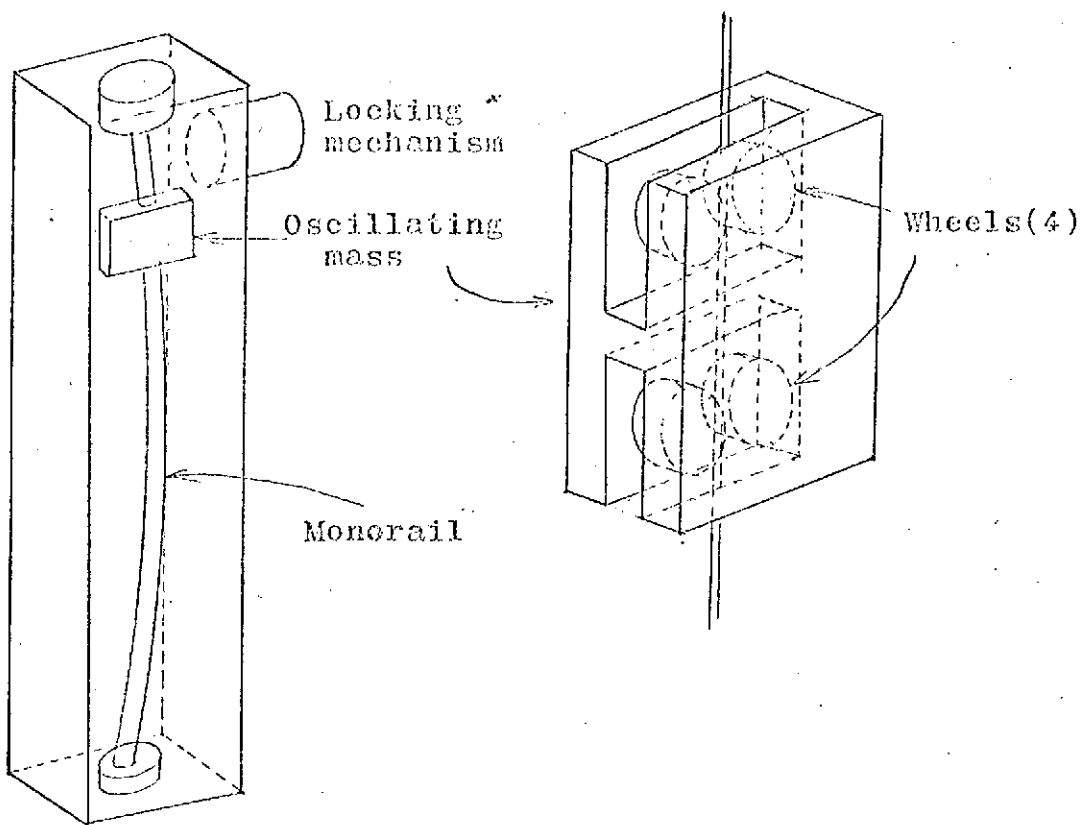


Fig. III-3: Tiros TEAM damper.

seen that this would behave well only at small  $\theta$ .

For Tiros, the damper mass was about 0.001 of the total satellite mass, and assured a  $\theta$  of less than 0.5 degrees. The time to damp from 2.5 to 0.5 degrees was about one minute. It was chosen because tests showed that the tube radius  $R$  of the ball damper would be greater than the track radius of TEAM. Also, it was found that the ball damper required an A/C not less than  $1.6(\lambda \neq 0.375)$ , where A/C for Tiros was 1.45 ( $\lambda = 0.31$ ).

C. Pendulum Damper  
1. Spin Axis Pivoted

The motion for a satellite with a pendulum pivoted on the spin axis, and moving in a plane perpendicular to the axis was described by Cartwright, Massingill, and Trueblood [6]. The driving frequency of the pendulum is the frequency of the acceleration due to nutation,  $\Omega = \lambda r$ . Without friction the pendulum would oscillate in synchronism opposite  $\vec{\omega}_T$  at  $\Omega$ , as in Fig.III-3a. However, if the pivot exerts a frictional torque, the pendulum lags behind this position by an angle  $\delta$  (Fig.III-3b). The resulting torque on the axisymmetric main body causes the damping. As this lag angle increases, so does the damping, producing the convex portion of Fig.III-3b, and called the "nutation synchronous" mode.

When  $\delta$  reaches 90 degrees, however, the pendulum is no longer in sync with  $\vec{\omega}_T$ , but is driven toward synchronism with  $r$ . This is a decreasing-rate decay with

a superimposed convergent oscillation. It would be desirable to make the transition between the two modes at as small a  $\theta$  as possible.

If the mass is assumed small so that the  $\vec{\omega}_p$  rotates precisely at the nutation rate  $(\lambda + 1)r = \Omega + r$  in inertial space, and  $\Omega$  small, we have:

$$\dot{\theta} = (mlh/\Lambda)(\lambda + 1)r \sin \alpha$$

$$\ddot{\theta} + (c_p/m)\dot{\alpha} + (h/\ell)(\lambda + 1)r^2\theta \sin \alpha = -(c_p/m)\lambda r$$

where  $\alpha$  is the angle between the  $x$  axis and  $\vec{\omega}_p$ , assumed approximately equal to  $\delta$ . Also,  $c_p$  is the friction coefficient of the relative velocity between the pendulum and main body.

Computer analysis has shown that the  $\dot{\alpha}$  term can be neglected. To find the time and nutation angle at transition between modes, we set  $\alpha = \pi/2$  and integrate the above equations. Thus:

$$\theta_* = -c_p(\ell/mlr)\lambda/(1 + \lambda)^2$$

$$t_* = [(c_0^2 - \theta_*^2)/c_p\ell^2](c/2\lambda)$$

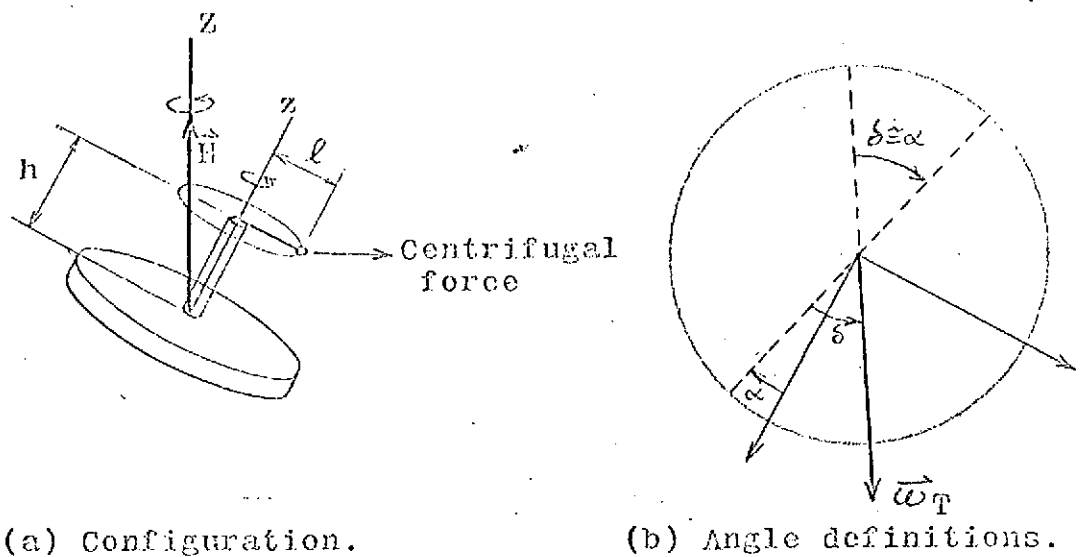
Numerical integration of exact equations show that the first equation overestimates  $\theta_*$  by as much as a factor of 2, and the second underestimates  $t_*$  by as much as a factor of 2. Also, for these equations to be valid,  $\alpha$  must be near zero at time  $t = 0$ ; thus:

$$ml^2 \ll c\theta_0^2(\lambda/c)/(1 - \lambda/c)$$

is a necessary condition for their validity.

Because of its nonsymmetry, there will be a small final nutation angle when only one damper is used:

$$\theta_f \approx (mlh/c)(\lambda + 1)/\lambda$$



(a) Configuration.

(b) Angle definitions.

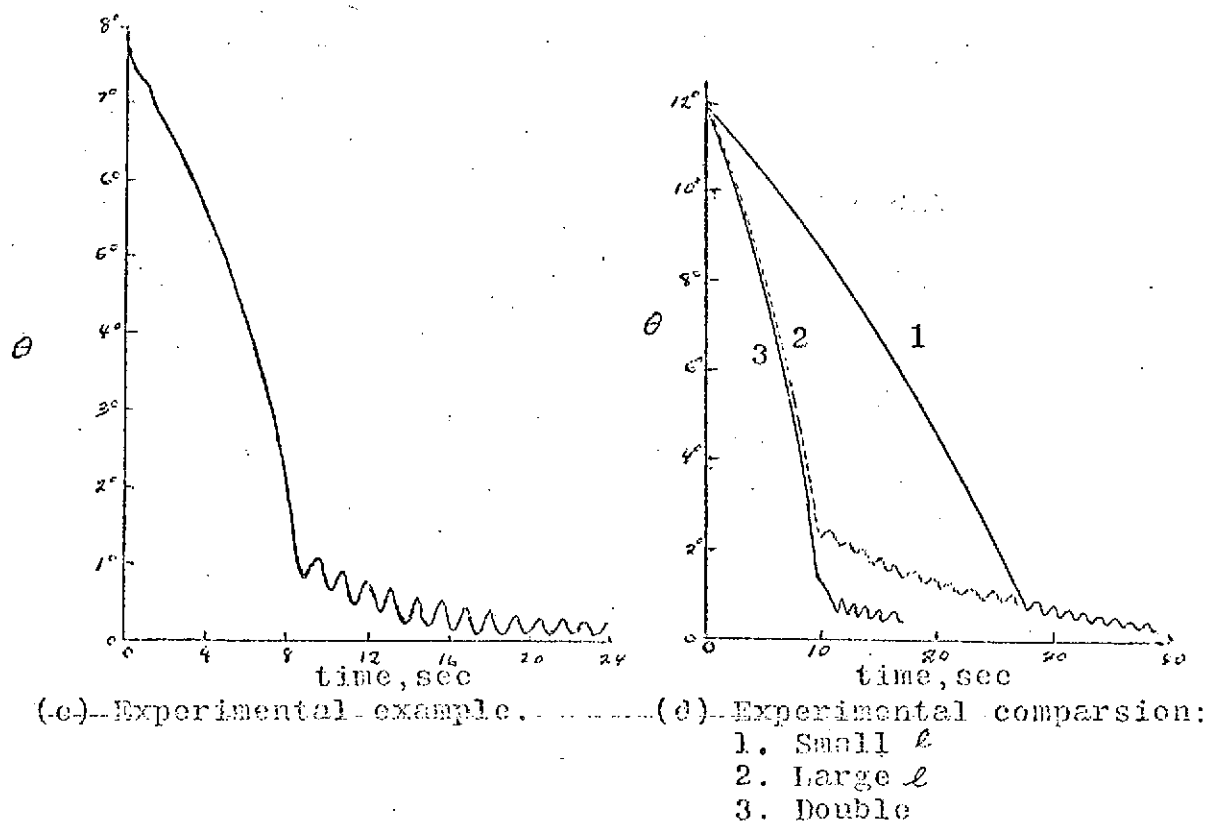


Fig. III-3: Axially-mounted pendulum.

If  $c_p$  is large,  $t_*$  decreases but  $\theta_*$  increases. If  $c_p$  is an increasing function of velocity, there will be strong damping at the beginning. As the relative velocity decreases, so does  $c_p$ , and the damper-main body system is decoupled enough to delay transition.

Another improvement would be to use two pendulums of different radii. Experimental results show these to act independently, the long one damping quickly at large  $\theta$  (Fig.III-3d), the short at small  $\theta$ .

## 2. Pivoted Away From the Spin Axis

The problem of a pendulum moving in a plane perpendicular to the spin axis and pivoted at a point away from the axis have been studied by Haseltine [16, 17] and Newkirk, Haseltine, and Pratt [23].

If  $\gamma$  is the rotation required to reach a point on the body, the kinetic energy of the system is [23]:

$$T = \frac{1}{2} [C\dot{\varphi}^2 + A\omega_p^2 + \bar{m}(\dot{\varphi} \times \mathbf{r}_m)^2]$$

where  $\dot{\varphi} = \mathbf{r} + \dot{\gamma}$

$$\bar{m} = Mm/(M + m)$$

and  $\mathbf{r}_m$  is the distance from the center-of-gravity to the damper mass.

Using a set of modified Lagrangian equations:  
 $d(\partial T / \partial \dot{q}_i) / dt = L_{q_i}$

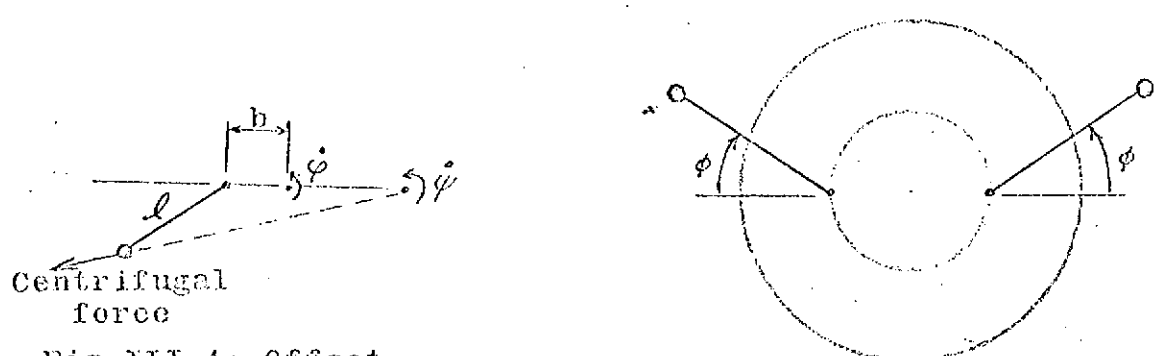
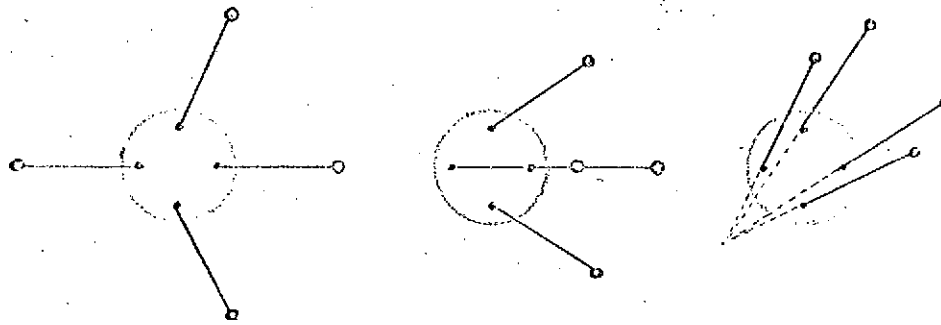


Fig. III-4: Offset.

(a) Off-design equilibrium  
for two offset pendulums.



(b) Off-design equilibrium for four  
pendulums.

Fig. III-5: Offset pendulum dampers.

in which all the  $L_{qi}$  are zero except:

$$L_\theta = -c_p \dot{\varphi}$$

The following equations result:

$$\ddot{\varphi} = -(c_p/\Lambda)(\ddot{x} - r)$$

$$\begin{aligned}\dot{r} &= \bar{A}c_p(\ddot{x} - r)/(\bar{A}\bar{C} - \bar{D}^2) \\ &\quad + \bar{C}\bar{D} \omega p/(\bar{A}\bar{C} - \bar{D}^2) + pq\end{aligned}$$

$$\begin{aligned}\dot{q} &= -pr + \bar{C}\bar{C}\bar{k}p/(\bar{A}\bar{C} - \bar{D}^2) \\ &\quad + \bar{D}c_p(\ddot{\varphi} - r)/(\bar{A}\bar{C} - \bar{D}^2)\end{aligned}$$

$$\begin{aligned}\dot{p} &= (\bar{A} - \bar{C})qr/(\bar{A} + \bar{C}) \\ &\quad + \bar{C}\bar{k}q/(\bar{A} + \bar{C}) - \bar{D}(r^2 - q^2)/(\bar{A} + \bar{C})\end{aligned}$$

where  $\bar{A} = A + \bar{m}y^2$

$$\bar{C} = \bar{m}h^2$$

$$\bar{D} = \bar{m}hy$$

and  $y$  is the  $y$  coordinate of the mass. No small angle assumptions have been made. If however,  $\theta$  and  $m$  are small,  $\ddot{\varphi}$  constant, and other limiting assumptions are made:

$$\begin{aligned}\ddot{S} &= -c_p(\ddot{S} - \ddot{\varphi})/\bar{C} \\ &\quad + (\bar{C}\bar{D}/2\bar{A}\bar{C})\ddot{\varphi}(\bar{U}e^{-iS} + \bar{U}e^{iS})\end{aligned}$$

$$\ddot{U} - i(C/\Lambda)\ddot{\varphi}U = -(D/\Lambda)\dot{S}^2 e^{iS}$$

where  $S = \varphi + \varphi'$

$$\dot{S} \approx r$$

$$U = \sin \theta (\cos \varphi + i \sin \varphi)$$

thus  $|U| = \sin \theta \approx \theta$ .

Three different solutions were tried for this set of equations:

(a) The stable solution in which the damper does not rotate relative to the main body. Then  $|U| \approx \theta_0 = \text{constant}$ .

(b) "Slow damping" in which the damper has a small oscillation about a fixed point on the body, resulting in:

$$\theta = \theta_0 e^{-t/\tau}$$

$$\tau = \left\{ \frac{2(c - A)\Lambda \bar{C}^2 \left[ (c_p/\bar{C})^2 + (c - A)^2 \bar{\varphi}^2 / \bar{C}^2 \right]}{c \bar{D}^2 \bar{\varphi} c_p} \right\}$$

(c) "Fast damping" in which the damper rotates at the nutation frequency  $\Omega_r/\Lambda$ . This solution is good only when  $\theta$  is not small:

$$\theta^2 = \theta_0^2 - [2c_p(c - A)/CA - 2\pi \bar{D}^2 C \bar{\varphi} / \Lambda^3] t$$

The advantage of offsetting the pivot point from the axis is that it would appear that the pendulum will align itself radially outward from the pivot. Then a counterweight could be mounted from the equilibrium position to preserve the symmetry of the satellite, with no residual wobble. An alternate is to employ two diametrically opposed pendulums (Fig. III-4).

For a pendulum offset a distance  $b$  and of arm length  $\ell$ , the frequency is:

$$\frac{\omega}{2\pi} \sqrt{\frac{b}{\ell} + \frac{hC}{\ell A} \tan\theta}$$

For resonance:

$$\ell \approx [b + (\lambda + 1)h\theta]/\lambda^2 \rightarrow b/\lambda^2$$

assuming  $\omega = r$ , for small  $\theta$ . If  $\lambda$  is only slightly greater than zero,  $\ell$  can be large. A solution is to use a pendulum of radius of gyration  $s$ . Then:

$$\ell = [b + (\lambda + 1)h\theta]/\lambda^2(1 + s^2/\ell^2)$$

Haseltine [16] has shown that, when:

$$(\ell/b)[mh^2/(C - A) - (m/M)] > \frac{1}{2}$$

The angle between the two dampers will not be 180 degrees in the steady state (Fig.III-5a). Then:

$\cos\phi$  = lesser of one or  $b(C - A)/2mh^2\ell$  and the apparent wobble angle is approximately  $(2mh\ell \sin\phi)/(C - A)$ .

Haseltine also studied the motion with four identical pendulums mounted 90 degrees apart. Again, experimental results showed possible equilibrium positions resulting in a residual wobble (Fig.III-5b).

## D. Liquid Dampers

### 1. Spin Axis Concentric

The use of an annulus partially filled with a dense, high viscosity liquid, usually mercury, has proven very popular; it was first used in Syncor and the Explorer series [24]. The basic theory was laid out by Carrier and Miles [5] for laminar flow. The equations of motion for the body are similar to those for the pendulum, since both systems are circularly constrained. The dimensions of the system are given in Fig. III-6. For small  $\theta$ , it was assumed that the liquid was in contact with the entire outer surface of the annulus. The rate at which energy is dissipated throughout the fluid is, if  $\rho$  is the density:

$$\dot{T} = -\rho \nu \iiint (\vec{v} \times \vec{v})^2 dV$$

where  $\vec{v}$  is the fluid velocity,  $\nu$  is the kinematic viscosity, and  $dV$  is a differential element volume. Assuming the irrotational component of velocity cannot contribute to the integral:

$$\dot{T} = -8^{1/2} \pi dR^2 \rho (\dot{\phi} h \theta)^2 |\dot{\phi}| n_*^2 |G| / |\Delta|^2$$

$$\text{where } n_* = (1 + \lambda)^2 (1 - a_* / R)^2$$

$$G = (i\dot{\phi} R^2 / \nu)^{1/2}$$

$$\Delta = (n_* - n)G + (n_* + n)$$

$$n = 1 + 2\lambda - \lambda^2$$

This results in a time constant of decay for  $\theta$  of:

$$\tau = \Gamma \Delta / dR^2 \rho |\dot{\phi}|$$

$$\text{and } \Gamma = \frac{\lambda [(n_* - n)^2 |G|^2 + 2^{1/2} (n_*^2 - n^2) |G| + (n_* + n)^2]}{32^{1/2} \nu (\lambda + 1) n_*^2 |G|}$$

This is at a minimum in the neighborhood of  $n_s = n$ . Then:

$$\Gamma_{\min} = \lambda/8^{1/2}\pi(\lambda + 1)|G|$$

and, if  $a_s/R \ll 1$ :

$$a_s \approx R[\lambda^2/(1 + \lambda)^2 + 1/2^{1/2}|G|]$$

is the resonant condition. The variation in thickness of  $a_s$  has been assumed small.

For large  $\theta$ , the fluid completely fills the cross section of the annulus over an angle  $\Theta$  (Fig.III-7).

The energy dissipation is then:

$$\dot{T} = -4|\dot{\psi}|^2 \cdot 5 R^3 \rho \nu^{1/2} (a + d) \Theta^{1/2}$$

The time constant for large  $\theta$  is:

$$\gamma = A |\dot{\psi}| \theta^2 / 8 |\dot{\psi}| (|\dot{\psi}| \nu)^{1/2} R^3 \rho (a + d) \Theta^{1/2}$$

For  $R = 10$  cm,  $h = 10$  cm,  $d = 0.25$  cm,  $a_s = 0.05$  cm,  $A = 1.3$  kg  $\sim$  m<sup>2</sup>,  $\lambda = 1/3$ ,  $\omega = 12$  rad/sec,  $\rho = 13.6$  gm/cc, and  $\nu = 10^{-3}$  cm<sup>2</sup>/sec give a damping time of 14 sec for small  $\theta$ . If a resonant damper were designed,  $a_s$  would be 0.637 cm and  $\gamma = 0.00044$  sec.

The large  $\theta$  result for the above parameters and  $\theta_0 = 1/6$ ,  $\Theta = 5$ , and  $(a + d) = 1/2$  cm gives  $\gamma = 200$  sec. However, the Reynolds number is past critical for these, and the increased friction would reduce  $\gamma$  to about 70 sec.

The above would indicate that it would be desirable to design the damper for resonance. However, a study by Fitzgibbon and Smith [35] show that significant energy can be stored in the surface waves on the fluid

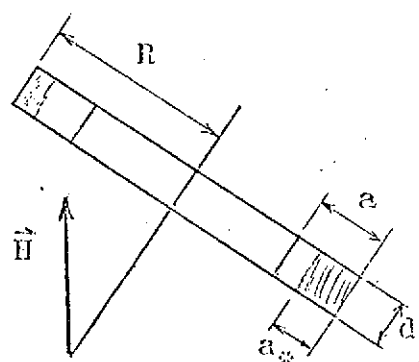


Fig.III-6: Damper parameters.

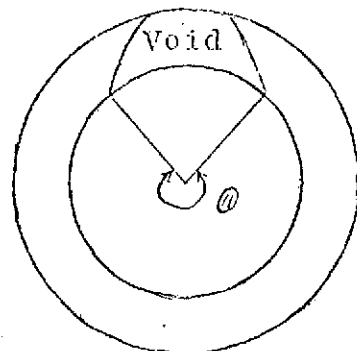


Fig.III-7: Large .

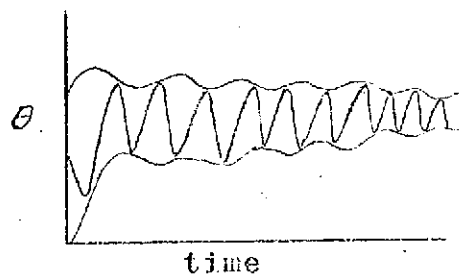


Fig.III-8: Wobble near resonance.

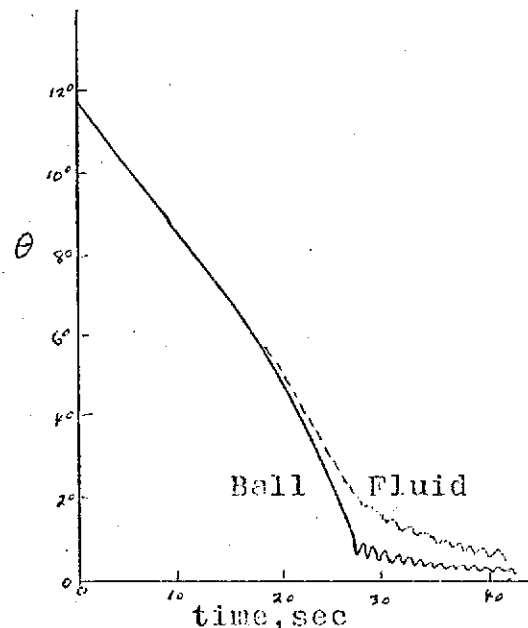


Fig.III-9: Experimental comparison of ball &amp; fluid dampers of equal mass.

near resonance, with the result that energy is traded back and forth between liquid and rigid body. This can result if the damper mass is as little as 2% of the main body, resulting in a history of  $\theta$  as shown in Fig.III-8 [21]. This can be overcome by damping the wave motion by the use of baffles, filling the void with a light liquid such as alcohol, or using enough damping fluid so that the void is small and the waves impact the inner surface of the damper. Also, damper masses are usually much smaller than 2% of the main body weight.

The advantage of this configuration is that it assures symmetry in the steady state, with no apparent residual wobble, as is the case with single, and some multiple, pendulums. A comparison of a fluid damper and single spin axis pivoted pendulum damper of equal mass from experimental results is shown in Fig.III-9[6].

The HEOS used a spin axis concentric mercury and alcohol damper for small  $\theta$ , less than half a degree, and one equatorial ball damper for fast damping at larger  $\theta$ .

## 2. Unsymmetrically Mounted

Ayache and Lynch analized toroidal and rectangular dampers of circular cross section and a U-shaped resonant damper mounted in planes parallel to the spin axis [2] in terms of a frictional coupling factor  $f_{Ds}$  inversely proportional to the time constant. Only the

results are presented here. This is for small  $\Omega$  only, the spacecraft nearly despun. Most of the stabilization is due to a flywheel on the spin axis.

For a toroidal damper as described in Fig.III-10a:

$$f_{DS} = \frac{1}{2} A_{\text{imag}} i / \left[ (1 - K)^2 + K^2 |A|^2 + 2K(1 - K) A_{\text{real}} \right]$$

$$\text{where } A = 2J_1(\beta_0) / \beta_0 J_0(\beta_0)$$

$$\beta_0 = a_t (\Omega/\nu)^{1/2} \quad K = (r/\Omega)^2 (\pi - \frac{1}{2}\theta)/\pi$$

$J_0, J_1$  = Bessel functions of order zero and one, respectively.

This is plotted vs.  $a_t (\Omega/\nu)^{1/2}$  for various bubble sizes in Fig. III-10b, where  $a_t$  is the tube inside radius.

The rectangular damper has a frictional coupling factor  $(1 - w^2)$  that of the toroidal, where (Fig.III-10c):

$$w = (a - b)/(a + b)$$

This means a greater time constant.

For the U-shaped damper (Fig.III-11):

$$f_{DS} = \frac{1}{2} \text{ imag} \left[ \frac{2A - (K_* A_*/A_t)(1 - A)}{2 - 2K_*(1 - A)} \right]$$

$$\text{where } K_* = 2(A_t/A_*) (r/\Omega)^2 \ell_s / \ell$$

$$A_* = (v_t + \dot{\Psi}) / J_0(\beta_0)$$

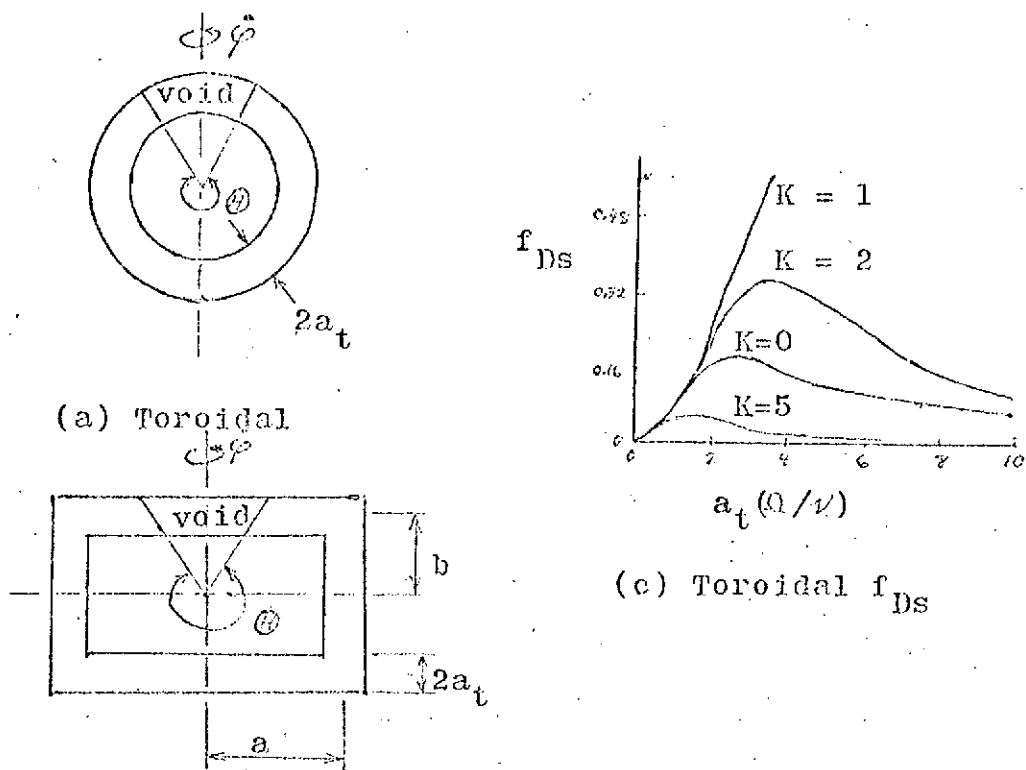


Fig. III-10: Toroidal and rectangular liquid dampers mounted along transverse axis.

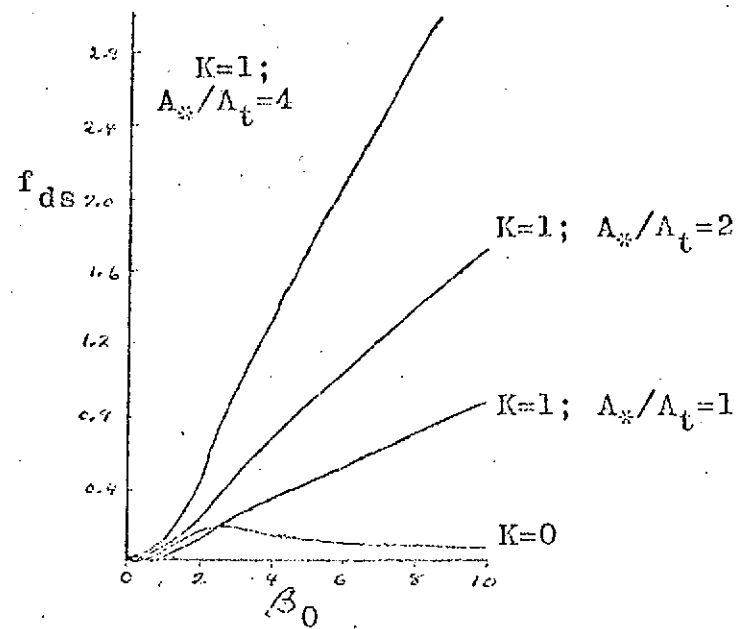
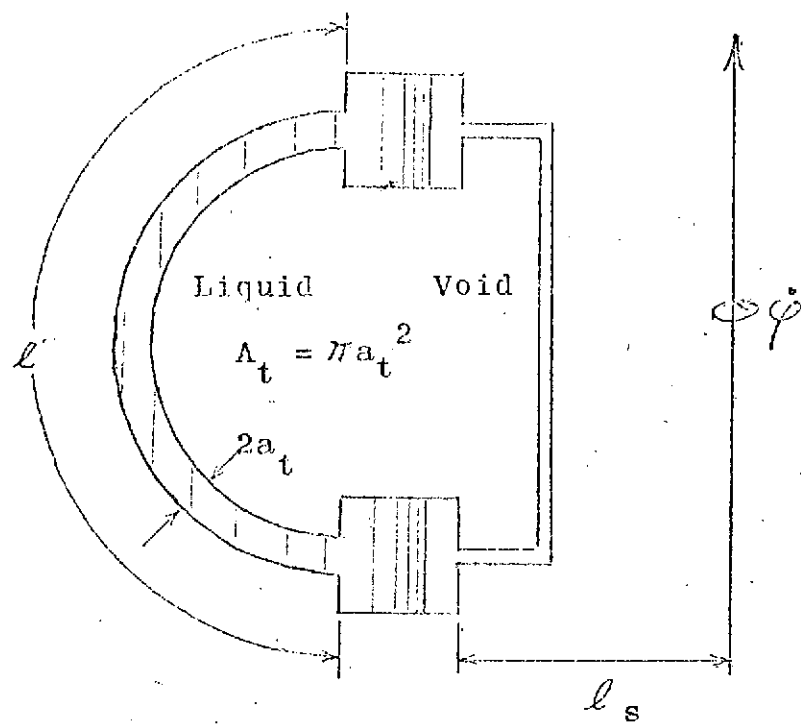


Fig. III-11: U-shaped liquid damper.

$v_t$  = velocity of the tube wall

$$\Psi = (N - v_t c_*) / (-i\Omega^2) \beta$$

$$c_* = \beta r_*^2 \ell / \ell_s$$

$$N = (2c_*/a_v^2) \int_0^{a_v} vr_* dr_*$$

$r_*$  = radial distance from tube center

#### E. Disk Type [26]

In this, a disk is mounted on a ball and socket at the center of gravity. For best results, the friction should be small. To my knowledge, this type has only been used in a test model by Perkel.

When the entire body is spinning smoothly and then disturbed, the disk damps down more quickly than the main body. For small friction, the damper plane is perpendicular to the precession cone axis. Up to a point, greater friction causes faster damping. The limit is when stiction occurs, freezing the damper.

The damping is exponential:

$$\theta = \theta_0 e^{-t/\gamma}$$

$$\gamma^{-1} = \frac{\theta_{1D}}{\theta_0} \frac{c_D}{\Lambda} \left[ 1 - \frac{c_A D}{c_D A} \right] r \left[ 1 - \left( \frac{\theta_{1D}}{\theta_0} \right)^2 \right]^{\frac{1}{2}}$$

where  $c_D$ ,  $\Lambda_D$  = polar and transverse moments of inertia of the damper

$\theta_{1D}$  = initial angle between  $\vec{n}$  and disk axis.

If the angle between the disk and body axes is small,  $r$  may be approximated by  $H/C$ .

The stiction problem can be overcome by using a lubricated bearing. The viscous friction constant for minimum  $\gamma$  is:

$$K_0 = C_D(1 - CA_D/C_D A)(\lambda + 1)r/\lambda.$$

#### F. Mass-Spring Systems

##### 1. Perpendicular to Spin Axis

Wadleigh, Galloway, and Mathur have treated a spring-mass system mounted on and perpendicular to the spin axis [35]. If  $K$  is the spring constant,  $c$  the damping, and  $\omega_n$  the natural frequency:

$$\dot{r} = 0$$

$$\dot{p} + \Omega q = 0$$

$$\dot{q} - \Omega p = 2(c/c_c)(\omega_n^{mh}/\Lambda)\dot{x} - (Kh/\Lambda)x = 0$$

$$x\ddot{x} + 2(c/c_c)\omega_n\dot{x} - (q^2 + r^2 - \omega_n^2)x + hr\dot{p} + h\dot{q} = 0$$

$$\omega_n = (K/m)^{1/2} \text{ and } c_c = 2/(Km)^{1/2}$$

If it is assumed that the sinusoidal character of the spinning body is not affected:

$$p = p_0 \exp(-F_* t/2) \cos \Omega t$$

where  $F_*$  is the Rayleigh dissipation function:

$$F_*/2 = \frac{mh^2(c/c_c)\omega_n\lambda(\lambda + 1)(1 + \lambda^2)}{\Lambda \left[ (\omega_n/r)^2 - 1 - \lambda^2 \right]^2 + 4(c/c_c)^2(\omega_n/r)^2\lambda^2}$$

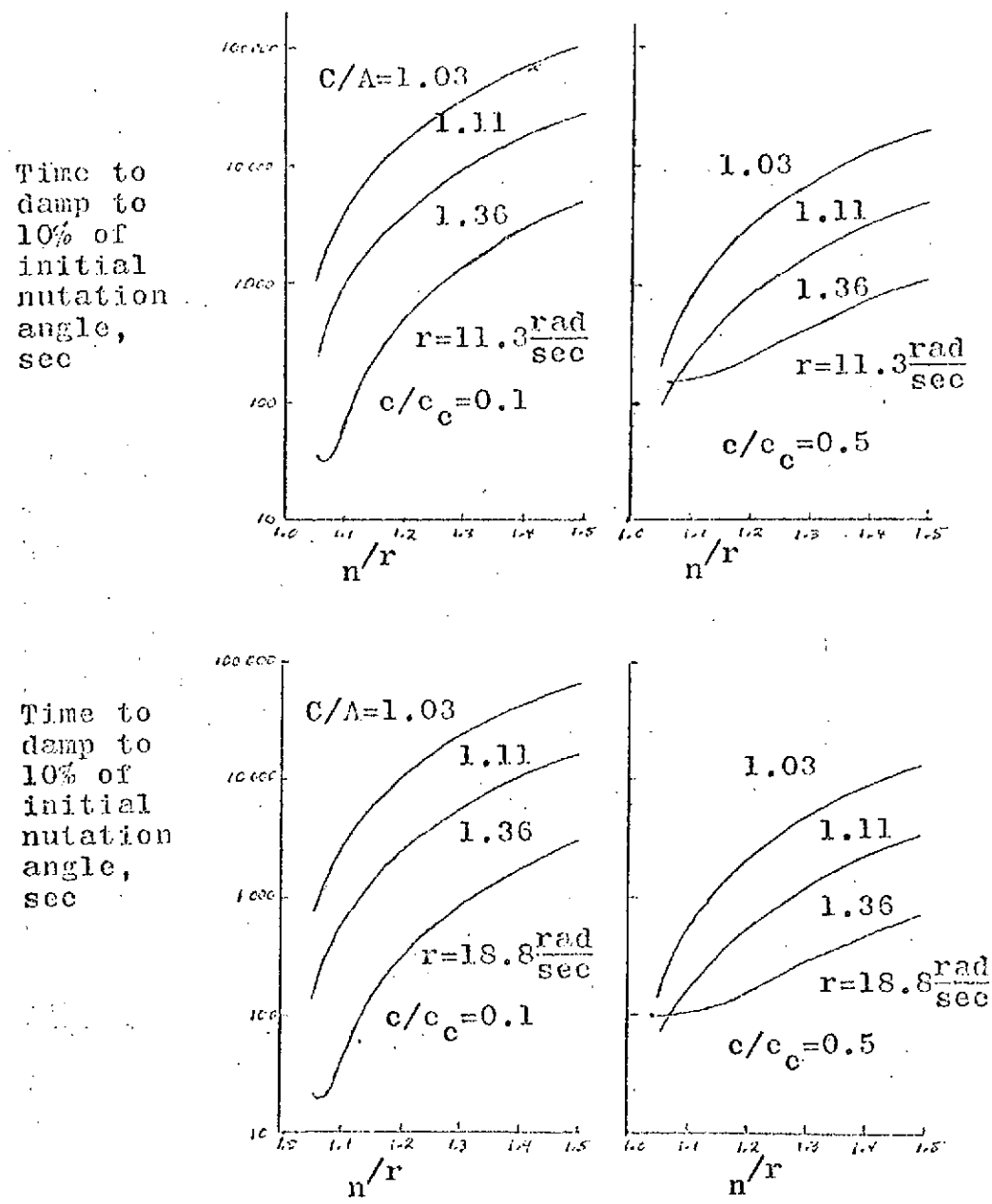


Fig. III-12: Performance of mass-spring dampers mounted on and perpendicular to the spin axis.

The maximum amplitude of the mass oscillation is:

$$x_{\max} = q_0 b(r + \Omega) / 2(c/c_e)\omega_n \Omega$$

Finally, the nutation angle is expressed:

$$\theta^2 = [q_0/(r + \Omega)]^2 \left| \exp \left[ -F_* t/2 + i(r + \Omega)t \right] - 1 \right|^2$$

Because this system will be slightly asymmetric, this converges to an apparent wobble angle of  $q_0/(r + \Omega)$ .

In a laboratory test, with  $\omega_n \approx 3 \text{ cps}$ ,  $c/c_e \approx 0.5$ ,  $\omega_n/r \approx 1.1$ ,  $mh^2/A = 0.00135$ , and an initial spin of 3 cps, all nutation damped out in 6 sec. See Fig. III-12.

## 2. Parallel to Spin Axis

Such a damper is inherently unbalanced. The nutation angle is a decreasing exponential with a superimposed convergent oscillation. Again, however, the apparent residual wobble is small [21]. The damper is not on the spin axis.

## G. Spherical

A pendulum pivoted in a ball and socket and immersed in a fluid was mounted on the despun portion of OSO [9]. However, it will work for a single body satellite for  $C/A > 1$ .

If  $p_* = (c/\Lambda)\dot{\varphi}$  and  $c$  is the damping constant of the fluid:

$$\gamma = \frac{1}{2}Ac/h^2 m^2 p_*^2$$

For resonance:

$$(c/\Lambda)\dot{\varphi} = 1.745(TI_d)^{1/2}/(m\ell^3 + 2.467m\ell s^2)^{1/2}$$

where  $\ell$  is the pendulum length,  $I_d$  is the diametral moment of inertia of the pendulum wire, and  $s$  is the transverse radius of gyration of the bob.

For OSO, there was no evidence of nutation for 8000 orbital passes.

#### H. Mass-Drum System

This is another system devised by Perkel [26], and consists of two masses strung on wires which are wrapped around a drum. The drum is connected to the main body concentric with the spin axis by a torsional spring-damper system. When nutation occurs, there is a restoring torque due to the relative deflection of the wires in addition to energy dissipation in the dampers. Fig.III-13.

Experimental work on a lab model indicated this system was capable of damping the nutation of a prolate body. Of course, if the cables were long enough, the actual polar inertia moment could be greater than that of the prolate main body alone, possibly greater than the transverse moment of inertia.

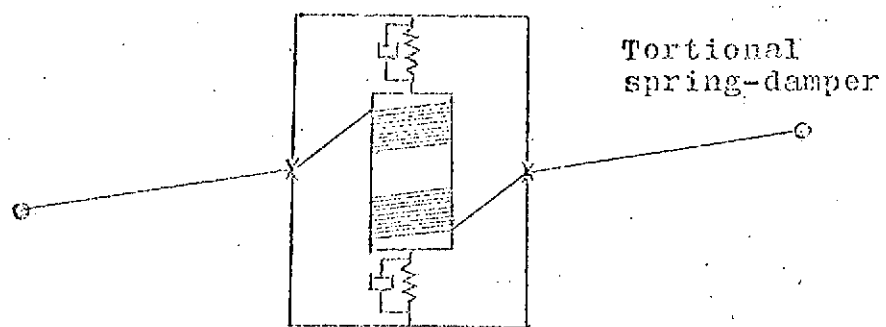


Fig. III-13: Mass-drum nutation damper and spin rate control.

Another possibility along these lines would be to dispense with the drum, mounting masses on damped springs on the outside of the spacecraft, opposite each other. In this case there would be no direct coupling of the motion of the two dampers.

### I. Magnetic Damping

One method is used to align the spin axis of a spacecraft along the local external magnetic field. A strong, permanent magnet is mounted in the spacecraft along the axis. This method was used in TRANSIT 1B and 2A. The spin had to be reduced to below 0.1 rps. Otherwise, the oblate spacecraft could have overcome the magnetic torque and assumed an attitude fixed in space [13].

Energy dissipation also comes about through eddy currents and magnetic hysteresis. If a rod is rotating about a transverse axis perpendicular to the external field, the component of the field along the rod is a function of time, and thus there must be an induced current. This eddy current causes heat to be radiated due to the resistance of the members. For a spacecraft of polar moment C, n number of permeable rods of volume V and diameter D, and spinning perpendicular to the local field initially at  $\omega_0$ :

$$\omega = \omega_0 \exp [(-k_e / 4\pi^2 C) t]$$

$$k_e = 6.25 \pi^2 \sigma_e n \rho_e^{-1} (B_m^2) e V D^2 \times 10^{-11} \text{ erg-sec}$$

where  $\sigma_e$  = separation effect due to distance between rods ( $\sigma_e = 1$  for  $\infty$ )

$\rho_s$  = resistivity of rod (ohm-cm)

$(B_m^2)_e$  = average of square of maximum flux density over entire length of rod for one orbit (gauss<sup>2</sup>).

Hysteresis damping is due to the friction between the magnetic domains in the spacecraft. This results in a linear damping.

Note that in all of the above, there are external torques, and angular momentum is not conserved. Since there are energy losses, however, they can be applied to nutation damping. The latter two methods will generally cause energy loss no matter what the orientation of the satellite is intended to be, fixed in space.

In general, the magnetic torques are disturbances that must be overcome by other nutation dampers, and thus are beneficial only for spin removal and alignment with the local magnetic field.

#### J. Gravity Gradient

---

As in the above, this can be used for nutation damping only when the spin is very low, and the spin axis (always a prolate body in this case) oriented toward earth. For this type of spacecraft, no spin is usually desired along this axis. In satellites

not meant to be gravity gradient stabilized, it is a disturbance to be overcome by the nutation damper [20,32].

According to Thomson, the torque on a satellite with spin axis perpendicular to the orbital plane is:

$$L = 3\omega_*^2(A + C)\theta_e$$

where  $\theta_e$  = deviation of spin axis from normal to orbital plane towards earth (small)

$\omega_*$  = orbital angular velocity

and L is about the axis tangent to the orbit. Conditions for stability are defined in terms of:

$$b/2\omega_*^2 = \frac{1}{2}[-5\lambda - (1 - \lambda)^2] + (\dot{\varphi}_1/\omega_*)(\lambda + 1)\lambda$$

$$-\frac{1}{2}(\dot{\varphi}_1/\omega_*)^2(\lambda + 1)^2$$

$$c/\omega_*^4 = 4\lambda^2 + 5(\dot{\varphi}_1/\omega_*)\lambda(\lambda + 1) + (\dot{\varphi}_1/\omega_*)^2(\lambda + 1)^2$$

$\dot{\varphi}_1$  = spin relative to the tangent to the orbit

For stability:  $b^2/2\omega_*^2 < 0$

$$c^2/\omega_*^4 > 0$$

$$(b/2\omega_*^2)^2 > c/\omega_*^2$$

## K. Structural Energy Dissipation

No structure is perfectly rigid, and the accelerations on a precessing spacecraft will cause energy loss through mechanical hysteresis. Usually, however, part or parts of the spacecraft can be considered rigid with energy dissipation only from the relatively flexible parts, such as antennae or solar panels. Two examples have been worked by Thomson [31, 33].

We have already shown that, for no external torques:

$$\dot{T} = (H^2 \lambda / C) (\sin \theta \cos \theta) \dot{\theta}$$

for an axisymmetric body. The energy loss per cycle of stress per unit volume is:

$$\gamma \sigma^2 / 2E$$

where E is Young's modulus,  $\sigma$  the normal stress, and  $\gamma$  the hysteresis factor. Integrating this over the whole structure, for period of stress oscillation  $t_0$ :

$$\int (\gamma \sigma^2 / 2Et_0) dV = \dot{T}$$

Considering an arbitrary point on the spacecraft at coordinates  $(x, y)$ , we can compute the acceleration at that point, which is the excitation. If  $\dot{\theta}$  is comparatively small:

$$\begin{aligned} \vec{\omega} &= (\dot{\psi} \sin \theta \sin \varphi) \hat{i} + (\dot{\psi} \sin \theta \cos \varphi) \hat{j} \\ &\quad + (\dot{\varphi} + \dot{\psi} \cos \theta) \hat{k} \end{aligned}$$

$$\vec{\ddot{\omega}} = \dot{\varphi} \dot{\psi} \sin \theta (\cos \varphi \hat{i} - \sin \varphi \hat{j})$$

Note that  $(x, z)$  does define an arbitrary point in the spacecraft, not restricted to one plane, because of the axisymmetry. If the relative motion of the points on the spacecraft can be considered small, the acceleration at a point is:

$$\vec{a} = \vec{\omega} \times (\vec{\omega} \times \vec{x}) + \dot{\vec{\omega}} \times \vec{x}$$

$$\text{where } \vec{x} = x\hat{i} + z\hat{k}.$$

For an example, let us assume that the elastic part of a spacecraft serves only the function of energy dissipation, and the deflections cause no changes in the inertia. The satellite in Fig.III-14 consists of two disks, each of inertia  $C_1$  and  $A_1$ , and mass  $M_1$ , connected by a flexible tube of radius  $x_1$  and length  $2\ell$ . The gyroscopic moment required by each disk is:

$$L_g = C_1(\dot{\phi} + \dot{\psi} \cos\theta) \dot{\psi} \sin\theta - A_1 \dot{\psi}^2 \sin\theta \cos\theta$$

$$\text{and } C = 2C_1$$

$$A \approx 2(A_1 + M_1 \ell^2)$$

$$\text{Then } L_g = M_1 \ell^2 \dot{\psi}^2 \sin\theta \cos\theta$$

The moment distribution is linear:

$$L_z = L_g z / \ell$$

and thus the maximum stress is:

$$\sigma = L_z x_1 / I$$

where  $I$  is the cross-sectional moment of inertia of the tube. Substituting these into the energy dissipation equation:

$$\begin{aligned} \dot{\theta} &= (\mathcal{J}/24\pi E)(M_1 \ell^2 x_1 / I)^2 (v/c) (C/I)^4 \omega_0^3 \sin\theta \cos^2\theta \\ &= K \sin\theta \cos^2\theta \end{aligned}$$

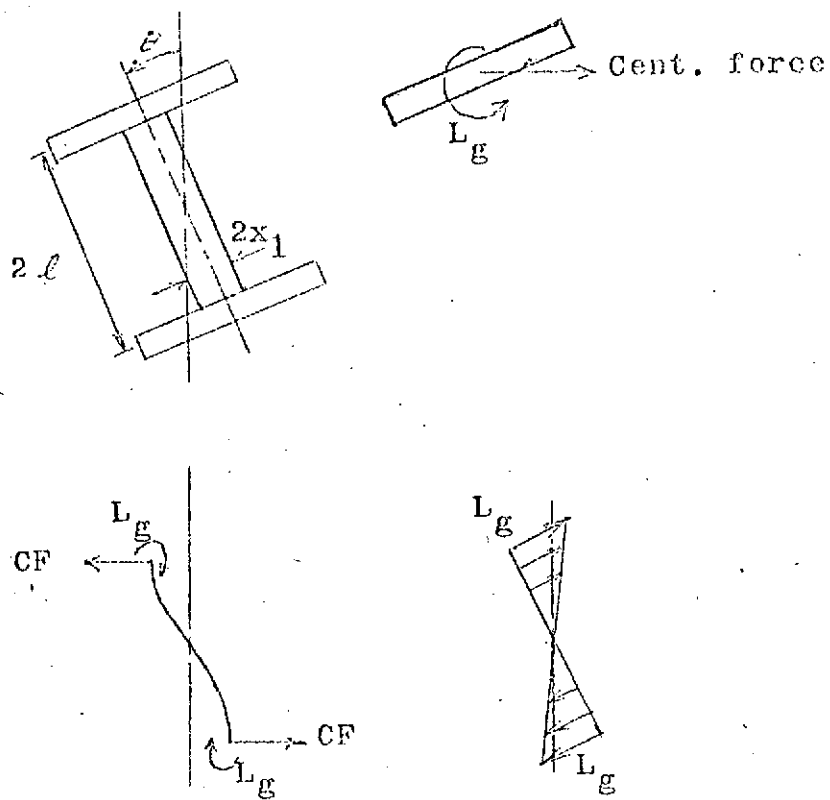


Fig. III-14: Structural energy dissipation example.

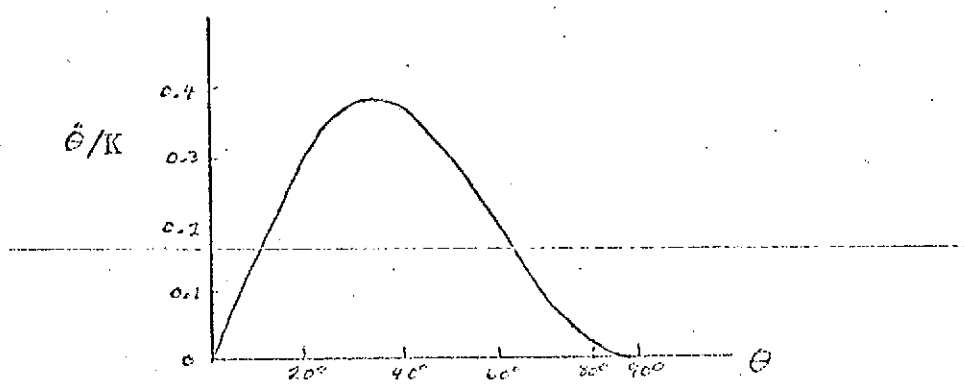


Fig. III-15: Variation in rate of tumbling.

This is shown in Fig.III-15.  $V$  is the volume of the stressed material and  $\omega_0$  the initial angular velocity.

If  $\Lambda \gg C$ , such as for a missile:

$$\ddot{a} = 2\omega_0^2 x(C/\Lambda) \sin\theta \cos\theta \sin\varphi \hat{k} = a_w \hat{k}$$

If we consider the inertia of the deflected members, resonance is observed. Fig.III-16 shows a cylindrical spacecraft of radius  $R$ , with four beams of length  $\ell$ . If the elastic deformations  $w(\xi, t)$  are assumed small and in the  $z$  direction only:

$$EI \frac{\partial^4 w}{\partial \xi^4} + \frac{m}{\ell} \frac{\partial^2 w}{\partial t^2} = a_w \frac{m}{\ell}$$

where  $m$  and  $I$  are the mass and cross-sectional moments of inertia for the beams. This gives:

$$\dot{\theta} = K_* \sin\theta \cos^2\theta / [(1 - \gamma^2 \cos^2\theta)^2 + (\gamma/2\pi)^2]$$

$$K_* = 16 C m \gamma (\alpha_1 \beta_1 R + 1)^2 \omega_0^3 / \pi \Lambda^2 \beta_1^4 \ell^2 \Omega_1^2$$

$$\gamma = (1 - C/\Lambda) \omega_0 / \Omega$$

$\Omega_1$  = first natural frequency of beams

Also,  $\alpha_1$  and  $\beta_1$  are tabulated in [37]. This is shown graphically in Fig.III-17, which clearly shows resonance effects. The envelope of this curve is the same shape as the curve in Fig.III-15.

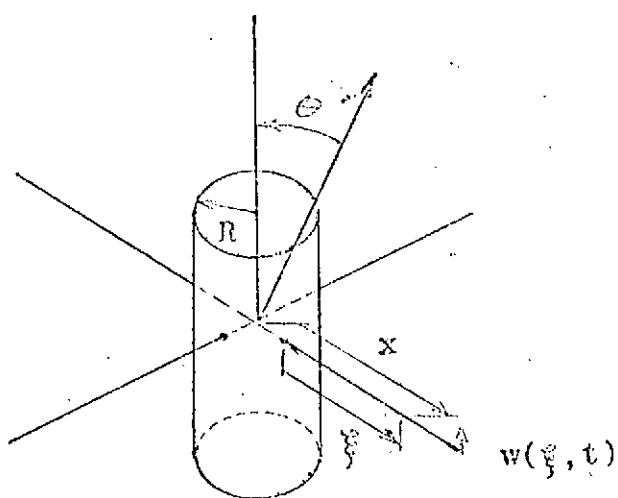


Fig. III-16: Satellite with four elastic beams.

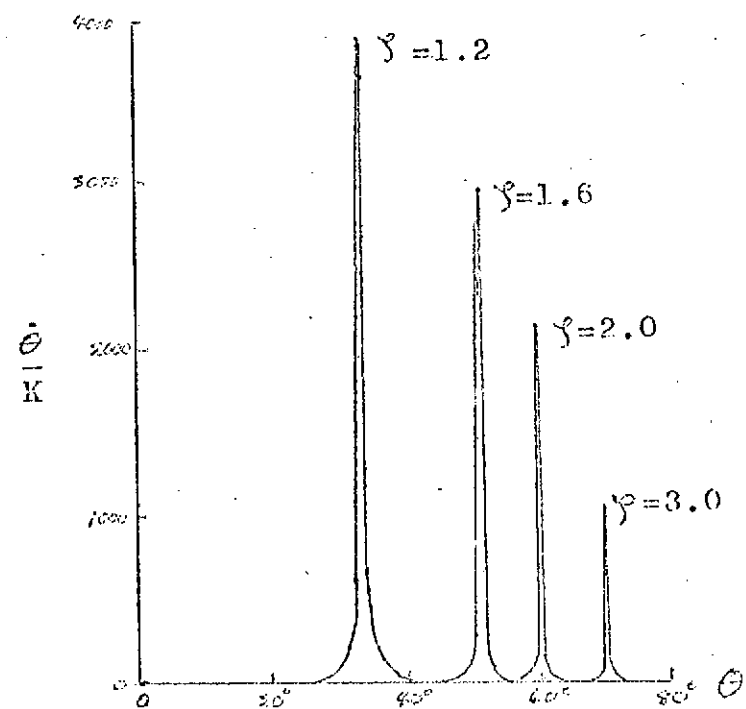


Fig. III-17: Resonance effects.

#### IV. Semipassive and Active Systems

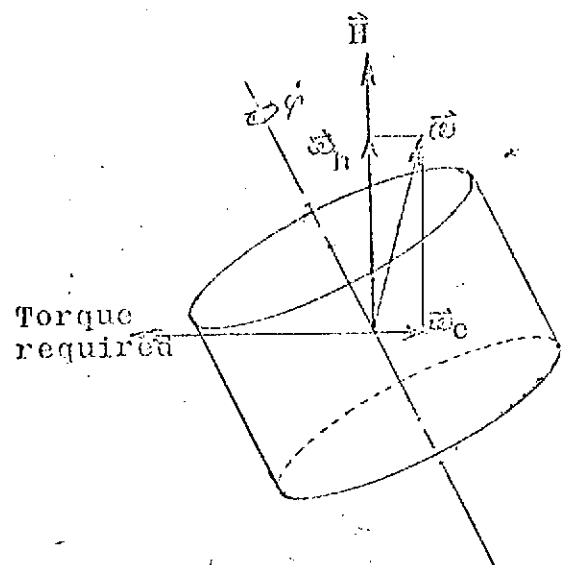
Such systems will be mentioned here only in passing. Active systems have energy sources activated either by on-board sensing equipment or ground command. Semipassive have energy sources that either remain constant or react naturally to attitude changes.

##### A. Oscillating Mass

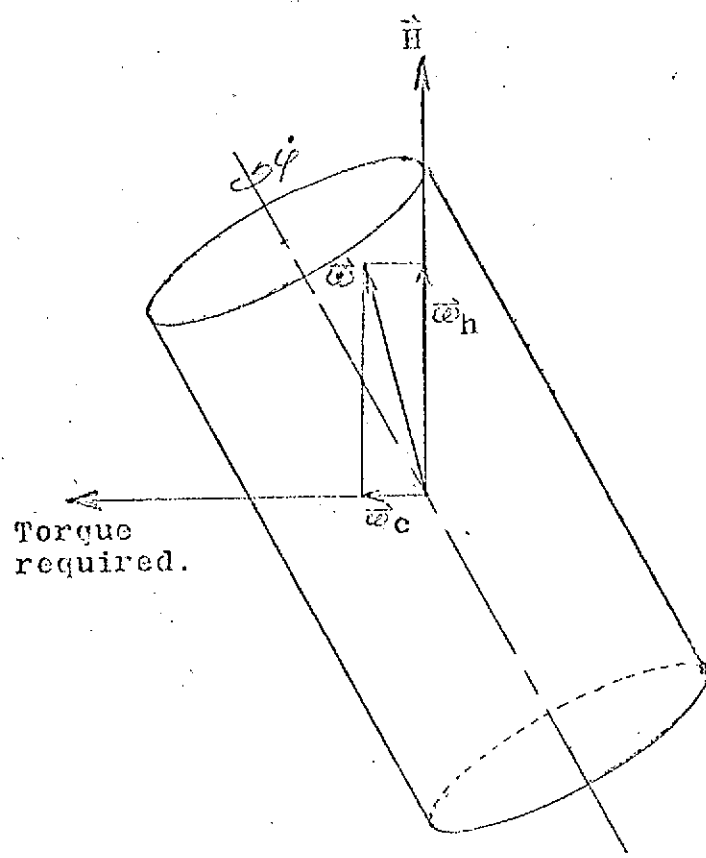
This was proposed by Kane and Sobala [19]. Two masses, diametrically opposed, are forced to oscillate back and forth along the spin axis at constant frequency. The spin axis (axis of symmetry) is normal to the orbital plane. This is capable of maintaining attitude at very low spin rates.

##### B. Dual Spin

The general reasoning behind dual spin spacecraft with despun dampers was most recently outlined by Tonkin [34]. Fig. IV-1 shows the position of  $\vec{\omega}$  relative to  $\vec{H}$  for oblate and prolate bodies. We have  $\omega_h$  and  $\omega_c$  as the components of  $\vec{\omega}$  parallel and normal to  $\vec{H}$ , respectively. Note that the  $\omega_c$  in each case is opposite in sign. An internal torque to reduce nutation must be of zero average value ( $\vec{H}$  conserved) and remove energy for oblate bodies or inject it for prolate. The first requirement means that the required torque is



(a) Oblate spacecraft.



(b) Prolate spacecraft.

Fig. III-1: Torques required for damping.

normal to  $\vec{H}$  and spinning with  $\dot{\varphi}$  in inertial space. Since power is the scalar product of torque and angular velocity, the torque required must be opposite  $\omega_c$  for oblate bodies and of the same sense as  $\omega_c$  for prolate bodies.

The torques produced by a damper dissipate energy, thus the component normal to  $\vec{H}$  is opposite  $\omega_c$ . There is also a component along the spin axis, thus changing the spin of the body upon which the damper is mounted. If the damper is despun, the motor must compensate for this speed differential. This is the source of energy injection for the prolate body. Several references are presented in the bibliography.

### C. Magnetic

As was shown before, eddy currents induced by the earth's magnetic field can cause torques on a spacecraft. This can be overcome by supplying a torquing coil whose axis is normal to the spin axis with a current 180 degrees out of phase with the externally induced EMF [14]. The spin axis can be oriented by another coil whose axis is parallel to the spin axis. The current in this is switched on and off, and the torque being a sinusoid while on, to give zero average torque on one transverse axis, and a resultant torque on the other.

#### D. Jet Pulse

Another method of supplying torque is to activate a single attitude motor aligned parallel with the spin axis. The pulsing is controlled by an on-board nutation sensor, firing when the motor is inside the body cone [15].

V. Bibliography

1. Ames, J., and Murnaghan, F., Theoretical Mechanics, Dover Publications, Inc., N.Y., N.Y., 1929, p.217.
2. Aysche, K., and Lynch, R., "Analyses of the Performance of Liquid Dampers for Nutation in Spacecraft," Journal of Spacecraft and Rockets, 6; 12, Dec. 1969, p.1385.
3. Bainum, P., Fueschel, P., and Mackison, D., "Motion and Stability of a Dual-Spin Satellite with Nutation Damping," Journal of Spacecraft and Rockets, 7;6, June 1970, p. 690.
4. Barbier, Y., Reynaud, P., and De Samiville, B., "Development of a Family of Ball-Type Nutation Dampers," Bendix Technical Journal, v1, Spring 1968, p.99.
5. Carrier, G., and Miles, J., "On the Annular Damper for a Freely Precessing Gyroscope," Journal of Applied Mechanics, v27, June 1960, p.237.
6. Cartwright, W., Massingill, E., Trueblood, R., "Circular Constraint Nutation Dampers," AIAA Journal, 1;6, June 1963, p.1375.
7. Cloutier, G., "Nutation Damper Instability on Spin-Stabilized Spacecraft," AIAA Journal, 7;11, Nov. 1969, p. 2110.

8. Cole, R., Ekstrand, M., and O'Neill, M., "Attitude Control of Rotating Satellites," ARS Journal, Oct. 1961, p.1447.
9. Craig, B., "Nutation Damper for OSO," Astronautics and Aerospace Engineering, Dec. 1963, p.50.
10. De Bra, D., "Principles and Developments in Passive Attitude Control," Recent Developments in Space Flight Mechanics, American Astronautical Society, Washington, D.C., 1966, p.159.
11. Diemel, R., Mechanics of the Gyroscope, The Macmillan Co., N.Y., N.Y., 1929, p.68.
12. De Lisle, J., Ogletree, E., and Hildebrandt, B., "The Application of Gyrostabilizers to Orbiting Vehicles," Torques and Attitude Sensing in Earth Satellites, Academic Press Inc., N.Y., N.Y., 1964, p.31.
13. Fischell, R., "Magnetic Damping of the Angular Motions of Earth Satellites," ARS Journal, Sept. 1961, p.1210.
14. Grasshoff, L., "A Method for Controlling the Attitude of a Spin-Stabilized Satellite," ARS Journal, May 1961, p. 646.
15. Grasshoff, L., "An Onboard, Closed-Loop, Nutation Control System for a Spin-Stabilized Spacecraft," Journal of Spacecraft and Rockets, May 1968, p.530.

16. Haseltine, W., "Passive Damping of Wobbling Satellites: General Stability Theory and Example," Journal of the Aerospace Sciences, v29, May 1962, p.543.
17. Haseltine, W., "Nutation Damping Rates for a Spinning Satellite," Aerospace Engineering, 21;3, March 1962, p.10.
18. Hughes, W., "Nutational Stability of Multi-Body Spin-Stabilized Satellites," Royal Aircraft Establishment Technical Report 67009, Jan., 1967.
19. Kane, T., and Sqbala, D., "A New Method for Attitude Stabilization," AIAA Journal, 1;6, June 1963, p.1365.
20. Kane, R., Marsh, E., and Wilson, W., "Letter to the Editor," The Journal of the Astronautical Sciences, Sept. 1962, p.108.
21. Kuebler, M., "Gyroscopic Motion of an Unsymmetrical Satellite Under No External Forces," NASA-TN-D-596, July 1960.
22. Landon, V., and Stewart, B., "Nutational Stability of an axisymmetric Body Containing a Rotor," Journal of Spacecraft and Rockets, Nov.-Dec. 1964, p.682.
23. Newkirk, H., Haseltine, W., and Pratt, "Stability of Rotating Space Vehicles," Proceedings of the IRE, April 1960, p.743.

24. Nord-Aviation, "Etude sur la Comparaison d' Amortisseurs de Nutation," AE-940-030, Dec. 1965.
25. Perkel, H., "Tires I Spin Stabilization," Astronautics, June 1960, p.38.
26. Perkel, H., "Space Vehicle Attitude Problems," Advances in Astronautical Science, Vol. 4, Plenum Press, Inc., N.Y., N.Y., 1958, p.173.
27. Reiter, G., and Thomson, W., "Rotational Motion of Passive Space Vehicles," Torques and Attitude Sensing in Earth Satellites, Academic Press Inc., N.Y., N.Y., 1964, p.1.
28. Roberson, R., "Torques on a Satellite Vehicle From Internal Moving Parts," Journal of Applied Mechanics, June 1958, p.196.
29. Schnapf, A., "Tires I,II, and III - Design and Performance," Aerospace Engineering, 21; 6, June 1962, p.34.
30. Sen, A., "Stability of a Dual-Spin Satellite with a Four-Mass Nutation Damper," AIAA Journal, 8; 4, Apr. 1970, p.822.
31. Thomson, W., and Reiter, G., "Attitude Drift of Space Vehicles," 7; 2, The Journal of the Astronautical Sciences, 7; 2, Feb. 1960, p.29.

32. Thomson, W., "Spin Stabilization of Attitude Against Gravity Torque," The Journal of the Astronautical Sciences, 9; 1, 1962, p.31.
33. Thomson, W., Introduction to Space Dynamics, John Wiley & Sons, Inc., 1963.
- 33a. Thomson, W., and Reiter, G., "Motion of an Asymmetric Spinning Body with Internal Dissipation," AIAA Journal, 1; 6, June 1963, p.1429.
34. Tonkin, S., "Despun Nutation Dampers on Spinning Satellites," JBIS, v.23, Oct. 1970, p.661.
35. Fitzgibbon, D., and Smith, W., "Final Report on Study of Viscous Liquid Passive Wobble Dampers for Spinning Satellites," Space Technology Laboratories Report EM-11-14, June 1961.
36. Colombo, G., "On the Motion of Explorer XI Around its Center of Mass," Torques and Attitude Sensing in Earth Satellites, Academic Press Inc., N.Y., N.Y., 1964, p.175.
37. Leon, H., "Spin Dynamics of Rockets and Space Vehicles in Vacuum," Technical Report TR-59-0000-0078, Space Technology Laboratories, Inc., Sept. 1959.

6.3 EFFECTS OF A TOROIDAL  
LIQUID NUTATION DAMPER MOUNTED ON A TRANSVERSE  
AXIS OF AN AXISYMMETRIC SINGLE-SPIN SATELLITE

Prepared by

William O. Keksz

## ABSTRACT

In this paper, an attempt is made to discover the parameters relevant to the performance of a toroidal liquid nutation damper mounted with its axis along a transverse axis of a single-spin satellite. Small initial values of the nutation angle ( $\leq 12^0$ ) were assumed. By describing dissipation of energy by the fluid, a time constant for the nutation angle is found as a function of a Bessel function of complex argument.

## NOMENCLATURE

a	Small radius of torus
$a_*$	Radial coordinate within torus
A	Function of $a_*$ only
C	Constant
H	Magnitude of angular momentum of satellite
$\hat{i}_x, \hat{i}_y$	Unit vectors along transverse axes of satellite
$\hat{i}_z$	Unit vector along spin axis
$I_t, I_t, I_z$	Moments of inertia with respect to transverse and spin axes, respectively
j	$(-1)^{1/2}$
$J_0$	Bessel function of order zero
K	Kinetic energy of satellite
q	Argument of Bessel function = $a_*(j\dot{\phi}/\nu)^{1/2}$
$r_t$	Large radius of torus
S	Surface area of control volume
t	Time
T	Function of time only
v	Fluid velocity
$v_a$	Fluid velocity at wall ( $a_* = a$ )
$v_2$	Complex fluid velocity for two dampers
V	Volume

W	Work done on fluid
$\omega$	Angular velocity
$\psi$	Precession angle
$\varphi$	Spin angle
$\rho$	Fluid density
$\mu$	Absolute viscosity
$\nu$	Kinematic viscosity
$\tau$	Shear stress in fluid
$(\cdot)$	Time derivative except for T
$(\cdot)'$	Derivative for A and T
$ (\cdot) $	Magnitude of complex ( )
$\theta$	Angle of nutation

The minimum energy condition for a spinning axisymmetric body is when the angular velocity is aligned with the axis of maximum inertia. When there are no external torques, the magnitude of the angular momentum,

$$H = (I_t^2(\omega_x^2 + \omega_y^2) + I_z^2\omega_z^2)^{1/2},$$

is constant. Values for  $\omega_x$  and  $\omega_y$  exist when the nutation angle is not zero. Here we have assumed the momentum of the damper to be small. We also have

$$2K = I_t(\omega_x^2 + \omega_y^2) + I_z\omega_z^2$$

as twice the kinetic energy, again assuming the motion of the damper small. If the nutation angle decreases slowly, we have the angular velocity in the satellite frame given by

$$\vec{\omega} = \hat{i}_x(\dot{\psi} \sin\theta \sin\varphi) + \hat{i}_y(\dot{\psi} \sin\theta \cos\varphi) + \hat{i}_z(\dot{\varphi} + \dot{\psi} \cos\theta),$$

and the precession speed,

$$\dot{\psi} = I_z\omega_z/I_t \cos\theta = H/I_t.$$

Combining these equations gives

$$H^2 - 2KI_t = (H^2/I_z)(I_z - I_t)\cos^2\theta.$$

If there is energy dissipation, as with a damper,  $H$  remains constant while  $K$  decreases. Thus (5),

$$K = (H^2/I_t I_z)(I_z - I_t)(\sin\theta \cos\theta)\dot{\theta}.$$

With a liquid damper, energy dissipation occurs because of viscous effects, being represented by the time rate of work done on the fluid by the wall of its container (2),

$$\begin{aligned}\dot{W} &= \int_S \vec{\tau} \cdot \vec{v} \, dS \\ &= \frac{d}{dt} \int_V \frac{v^2}{2} \rho \, dV \\ &= -\dot{K}\end{aligned}$$

The damper is illustrated in Fig.1. From the above, it is seen that the velocity distribution of the liquid must be found. Assuming that  $a \ll r_t$ , the velocity of the tube wall relative to the liquid is given by  $v_a = r_t \omega_x$ , or

$$v_a = r_t \dot{\psi} \sin\theta \sin\varphi.$$

It is assumed that the velocity will be entirely tangential to the torus, and pressure variations due to centrifugal body forces are small. Thus the fluid momentum differential vector equation (for a particular  $\theta$ ),

$$\rho \partial v / \partial t = -\vec{\nabla} P + \mu \nabla^2 \vec{v},$$

becomes  $\rho \partial v / \partial t = \mu \nabla^2 \vec{v}$ ,

or, introducing the kinematic viscosity  $\nu = \mu / \rho$ ,

$$\partial v / \partial t = \nu \nabla^2 v.$$

In cylindrical coordinates, this is

$$\frac{\partial v}{\partial t} = \frac{\nu}{a_*} \frac{\partial}{\partial a_*} (a_* \frac{\partial v}{\partial a_*}).$$

Assuming that the solution is a product of a function A of  $a_*$  only, and T of t only, we have

$$AT' = T(a_* A')'/a_*,$$

$$\text{or } a_* AT' = T(A' + a_* A'').$$

If transients due to initial conditions are considered to damp out quickly, the time function will be in phase with  $v_a$ . Thus we let  $T = \sin \varphi$ . Then,

$$a_* A' \dot{\varphi} \cos \varphi = \nu \sin \varphi (A' + a_* A'').$$

Rearranging terms result in

$$a_* A'' + A' - (\dot{\varphi}/\nu) \cot \varphi a_* A = 0,$$

which is rather difficult to solve. The coefficient in the third term is a function of time; it cannot be averaged over one revolution for  $\varphi$  to give a constant, for  $\cot \varphi$  has values of infinity.

A simpler model may be had by assuming we have another damper, identical to the first, mounted on the y axis. Then we can represent the rotation of the transverse component of the angular velocity vector using complex variables. Since

$$\omega_x = \dot{\varphi} \sin \theta \sin \varphi,$$

$$\omega_y = \dot{\varphi} \sin \theta \cos \varphi,$$

$$\text{and } e^{-j\varphi} = \cos\varphi - j \sin\varphi ,$$

the velocity component in the xy plane can be described by a phasor,

$$j\omega_x - \omega_y = -\omega_{xy} e^{-j\varphi} ,$$

$$\text{where } \omega_{xy} = (\omega_x^2 + \omega_y^2)^{\frac{1}{2}}$$

$$= \dot{\varphi} \sin\theta$$

is the phasor magnitude.

Since we now have the term  $e^{-j\varphi}$  as the excitation, we let this be equal to  $T_2$ . Then,

$$T_2' = -j\dot{\varphi} e^{-j\varphi} = -j\dot{\varphi} T_2 ,$$

and the equation for the fluid velocity position dependent function A becomes

$$a_* A'' + A' + (j\dot{\varphi}/\nu) a_* A = 0 ,$$

$$\text{or } a_*^2 A'' + a_* A' + (j\dot{\varphi}/\nu) a_*^2 A = 0 .$$

This is a complex Bessel equation, the solution of which is (1)

$$A = C J_0(q) ,$$

$$\text{where } q = a_* (j\dot{\varphi}/\nu)^{\frac{1}{2}}$$

and C is a constant, which may be found by examining the velocity at the wall, which is given by

$$v_{a2} = -r_t \omega_{xy} e^{-j\varphi} .$$

If we define A at  $a_* = a$  as  $J_0(q_a)$  where

$$q_a = a(j\dot{\varphi}/\nu)^{1/2}$$

$$\text{then } C = r_t \omega_{xy} / J_0(q_a)$$

Thus we have

$$v_2 = AT_2 = r_t \omega_{xy} (J_0(q)/J_0(q_a)) e^{-j\varphi}$$

Using this expression in the integral for work done on the fluid will result in a complex function. This would represent two energy flows for dissipation, ninety degrees out of phase with each other. Averaged over one revolution for  $\varphi$ , the work done could be represented by the magnitude of the complex work. Also at this point we can say that this is twice the energy dissipation rate for a single damper. Thus for the single damper,

$$\begin{aligned} \dot{W} &= \frac{1}{2} |\dot{W}_2| \\ &= \frac{\rho d}{dt} \int_V \frac{1}{2} \rho |v_2|^2 dV_2 \\ &= \frac{\rho}{4} \frac{d}{dt} \int_V |r_t \omega_{xy} (J_0(q)/J_0(q_a)) e^{-j\varphi}|^2 dV_2 \\ &= \frac{\rho r_t^2 \omega_{xy}^2 \dot{\varphi}}{4 |J_0(q_a)|^2} \int_0^a |J_0(q) e^{-j\varphi}|^2 (4\pi r_t)(2\pi a_*) da_* \\ &= 2\rho r_t^3 \omega_{xy}^2 \pi^2 \dot{\varphi} |e^{-j\varphi}/J_0(q_a)|^2 \int_0^a |J_0(q)|^2 a_* da_* . \end{aligned}$$

At any instant,

$$|e^{-j\varphi}|^2 = \cos^2 \varphi + \sin^2 \varphi = 1$$

Making this substitution, we have

$$\dot{W} = 2\varphi r_t^3 \omega_{xy}^2 \pi^2 \dot{\varphi} |J_0(q_a)|^{-2} \int_0^a |J_0(q)|^2 a_* da_* .$$

For a given value of  $\theta$ , we have

$$\dot{\varphi} = I_z \dot{\psi} / (I_t - I_z) \cos \theta$$

$$\text{and } \omega_z = \dot{\varphi} + \dot{\psi} \cos \theta .$$

$$\begin{aligned} \text{Thus } \omega_z &= \dot{\varphi} + I_z \dot{\psi} / (I_t - I_z) \\ &= \dot{\varphi} (1 + I_z / (I_t - I_z)) \\ &= \dot{\varphi} I_t / (I_t - I_z) . \end{aligned}$$

Also, again for a particular  $\theta$  with  $\dot{\theta}$  small,

$$\tan \theta = I_t \omega_{xy} / I_z \omega_z .$$

Rearranging terms gives

$$\omega_{xy} = \omega_z (I_z / I_t) \tan \theta .$$

Substituting the relation between  $\omega_z$  and  $\dot{\varphi}$ , we have

$$\omega_{xy} = \dot{\varphi} (I_z \tan \theta) / (I_t - I_z) .$$

If we assume no external torques and the momentum of the damper relative to the satellite main body small, the Euler equations for the satellite are

$$0 = I_t \dot{\omega}_x + (I_z - I_t) \omega_y \omega_z ,$$

$$0 = I_t \dot{\omega}_y - (I_z - I_t) \omega_x \omega_z ,$$

$$\text{and } 0 = I_z \dot{\omega}_z .$$

Thus we can take  $\omega_z$  constant during the damping action, and therefore  $\dot{\phi}$ ,  $\psi$ , and  $\omega_{xy}$  may also be held constant. Note that this requires that  $H_x$  and  $H_y$  be small compared to  $H_z$ , thus meaning  $\theta$  is small ( $< 12^\circ$ ); therefore

$$\sin \theta \approx \theta ,$$

$$\cos \theta \approx 1 ,$$

$$\text{and } \tan \theta \approx \theta .$$

The equation for  $\omega_{xy}$  is then

$$\omega_{xy} = \dot{\phi} \theta I_z / (I_t - I_z) ,$$

and substituting this into the expression for  $\dot{W}$ ,

$$\dot{W} \approx \frac{2\varphi r_y^3 \pi^2 \dot{\phi}^3 I_z^2 \theta^2}{(I_t - I_z)^2 |J_0(q_a)|^2} \int_0^a |J_0(q)|^2 a_* da_* .$$

Also, the equation for  $\dot{K}$  becomes

$$\dot{K} \approx (H^2 / I_t I_z) (I_z - I_t) \theta \dot{\theta} .$$

But, for small  $\theta$ ,

$$H \approx I_z \omega_z = \dot{\phi} I_t I_z / (I_t - I_z) .$$

$$\begin{aligned} \text{Thus } \dot{K} &\approx \left[ \frac{I_t I_z}{I_t - I_z} \right]^2 \left[ \frac{I_z - I_t}{I_t I_z} \right] \theta \dot{\theta} \\ &= \dot{\phi}^2 \theta \dot{\theta} I_t I_z / (I_t - I_z) . \end{aligned}$$

Setting  $\dot{W} = -\dot{K}$ , we have

$$-\dot{\theta} I_t = \frac{2\varphi r_t^3 \pi^2 I_z \theta \dot{\phi}}{(I_t - I_z) |J_0(q_a)|^2} \int_0^a |J_0(q)|^2 a_* da_* ,$$

$$\text{or } \dot{\Theta} + \left[ \frac{2\varphi r_t^3 \pi^2 I_z \dot{\varphi}}{I_t(I_t - I_z) |J_0(q_a)|^2} \int_0^a |J_0(q)|^2 a_* da_* \right] \Theta = 0$$

The term in brackets is almost constant for small nutation angles, and is thus the inverse of the time constant for a decreasing exponential solution. Thus

$$\Theta = \Theta_0 \exp(-t/t_c)$$

$$\text{where } t_c^{-1} = \frac{2\varphi r_t^3 \pi^2 I_z \dot{\varphi}}{I_t(I_t - I_z) |J_0(q_a)|^2} \int_0^a |J_0(q)|^2 a_* da_*$$

and  $\Theta_0$  is the initial nutation angle. This may also be expressed using the approximation for angular momentum by

$$t_c^{-1} = (2\varphi r_t^3 \pi^2 H / I_t)^2 |J_0(q_a)|^2 \int_0^a |J_0(q)|^2 a_* da_*$$

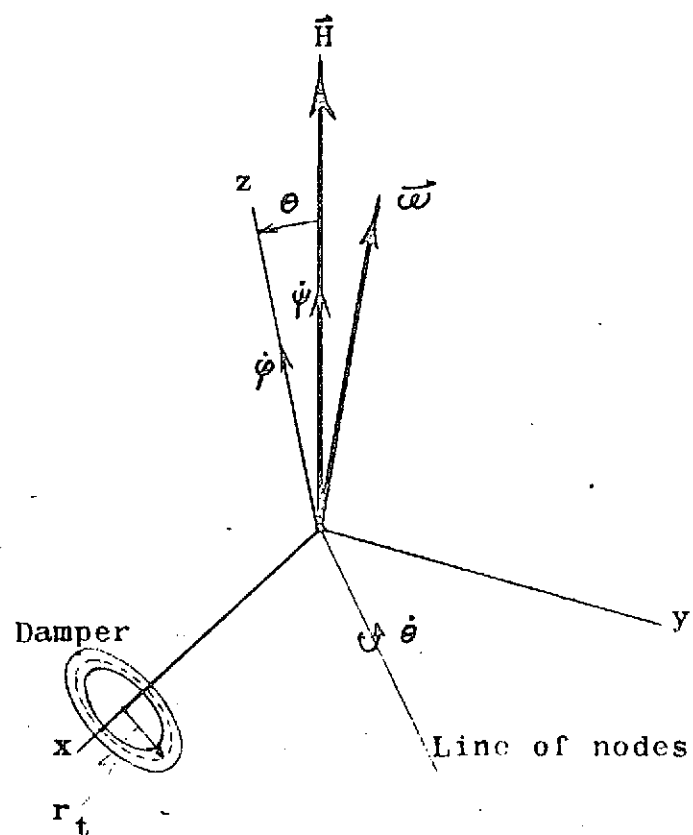


Fig. 1. Positioning of damper.

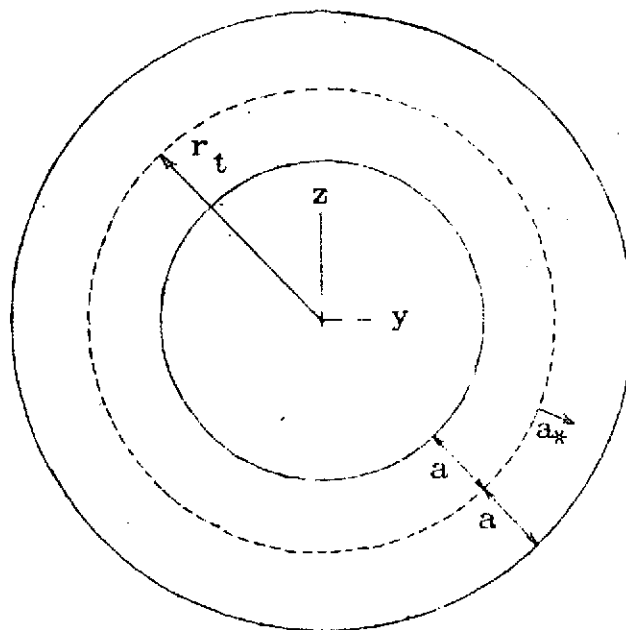


Fig. 2. Coordinates within damper. Not to scale,  
as actually  $r_t \gg a$ .

## CONCLUSION

The above is valid for small initial nutation angles for an axisymmetric single-spin satellite. Values for complex Bessel functions may be found in references 3 and 4. However, these are good only for Bessel functions in which the magnitude of the complex argument  $q$  is less than ten. However, the best liquid for use in the damper is mercury because of its high density; its kinematic viscosity is  $(0.5)10^{-6}$  ft<sup>2</sup>/sec at 75°F. Since  $q$  is inversely proportional to the square root of  $\nu$ , its magnitude will be on the order of  $10^2$  or  $10^3$  for reasonable values of  $\dot{\phi}$ . Bessel functions for complex arguments of these magnitudes have not been tabulated, and must be calculated.

## BIBLIOGRAPHY

1. Ayache, K., and R. Lynch, "Analyses of the Performance of Liquid Dampers for Nutation in Spacecraft," Journal of Spacecraft and Rockets, v.6, n.9, Dec. 1969, pp.1385-1389.
2. Hansen, A.G., Fluid Mechanics, Wiley, New York, 1967, p.124.
3. Jahnke, E., and F. Emide, Tables of Functions, 4th. ed., Dover, New York, 1945, p.266.
4. Mathematical Tables Project, National Bureau of Standards, Table of the Bessel Functions  $J_0(z)$  and  $J_1(z)$  for Complex Arguments, Columbia University Press, New York, 1943, pp.182-201.
5. Thomson, W.T., Introduction to Space Dynamics, Wiley, New York, 1961.

## CHAPTER 7

General Conclusions

As a result of the present study, equations of motion and computer programs have been developed for analyzing the motion of a spin-stabilized spacecraft having long, flexible appendages. Stability charts were derived, or can be redrawn with the desired accuracy for any particular set of design parameters. Simulation graphs of variables of interest are readily obtainable on line using program FLEXAT. Finally, applications to actual satellites, such as UK-4 and IMP-I have been considered.